Universidad de La Laguna
Oficina de Sede Electrónica
Entrada
Nº registro: 2021/90989
Nº reg. oficina: OF002/2021/89977
Fecha: 03/09/2021 12:24:13

UNIVERSIDAD Ð LA LAGUNA
Departamento de Astrofísica

Universidad de La Laguna

Cross-correlation between cosmic microwave background anisotropies and future galaxy surveys

Memoria que presenta
D. José Ramón Bermejo Climent
para optar al grado de
Doctor en Astrofísica.

Director y Tutor: José Alberto Rubiño Martín
Co-director: Fabio Finelli

Año académico 2020/21

INAF OAS BOLOGNA

Este documento incorpora firma electrónica, y es copia auténtica de un documento electrónico archivado por la ULL según la Ley 39/2015.
Su autenticidad puede ser contrastada en la siguiente dirección https://sede.ull.es/validacion/

Identificador del documento: 3764923 Código de verificación: JHlWnlbn

Firmado por:	JOSE RAMON BERMEJO CLIMENT *UNIVERSIDAD DE LA LAGUNA*	Fecha: 01/09/2021 17:41:12
	José Alberto Rubiño Martín *UNIVERSIDAD DE LA LAGUNA*	01/09/2021 17:49:44
	FABIO FINELLI *UNIVERSIDAD DE LA LAGUNA*	02/09/2021 14:12:21

Universidad de La Laguna
Oficina de Sede Electrónica
Entrada
Nº registro: 2021/90989
Nº reg. oficina: OF002/2021/89977
Fecha: 03/09/2021 12:24:13

The work leading to the original results of this thesis and to writing of this thesis have been obtained at IASF Bologna in 2017 and subsequently at OAS Bologna with the financial support of a 4 year INAF fellowship under the INAF - IAC agreement.

Este documento incorpora firma electrónica, y es copia auténtica de un documento electrónico archivado por la ULL según la Ley 39/2015.
Su autenticidad puede ser contrastada en la siguiente dirección https://sede.ull.es/validacion/

Identificador del documento: 3764923 Código de verificación: JHlWnlbn

Firmado por:	JOSE RAMON BERMEJO CLIMENT *UNIVERSIDAD DE LA LAGUNA*	Fecha: 01/09/2021 17:41:12
	José Alberto Rubiño Martín *UNIVERSIDAD DE LA LAGUNA*	01/09/2021 17:49:44
	FABIO FINELLI *UNIVERSIDAD DE LA LAGUNA*	02/09/2021 14:12:21

Universidad de La Laguna
Oficina de Sede Electrónica
Entrada
Nº registro: 2021/90989
Nº reg. oficina: OF002/2021/89977
Fecha: 03/09/2021 12:24:13

Resumen

El Fondo Cósmico de Microondas (FCM) es una imagen del universo temprano ($z \sim 1100$). En los últimos años, varios experimentos han conseguido restringir los parámetros del modelo concordante ΛCDM a partir de un análisis estadístico de las anisotropías del FCM. Por otra parte, varios cartografiados de galaxias medirán la distribución tridimensional de la componente de materia oscura del Universo con una sensibilidad y cobertura sin precedentes. Esta es una herramienta complementaria al FCM, ya que traza la evolución del universo a bajo redshift.

La combinación de las dos pruebas romperá degeneraciones entre parámetros que permanecen cuando se utilizan o bien el FCM o la estructura a gran escala de manera aislada. Además, las contribuciones a las anisotropías del FCM a lo largo de la línea de visión -las llamadas anisotropías secundarias- están correlacionadas con el crecimiento de las perturbaciones a bajo redshift. Por tanto, disponemos de información relevante además de la simple combinación del FCM y las pruebas de estructura a gran escala proporcionadas por los cartografiados de galaxias: la correlación cruzada entre el FCM y los trazadores de la estructura a gran escala, como el número de cuentas de galaxias o el efecto lente débil. En esta tesis, estudiamos la capacidad de la correlación cruzada entre FCM y estructura a gran escala para restringir parámetros cosmológicos, por sí sola o en combinación con el FCM y la estructura a gran escala, mediante datos simulados y herramientas estadísticas, y en la perspectiva de futuros cartografiados cosmológicos.

En primer lugar, exploramos las capacidades del cociente de efecto lente entre las correlaciones cruzadas del efecto lente del FCM con el número de cuentas galaxias, y del efecto lente de galaxias con el número de cuentas de galaxias; un estimador que bajo ciertas aproximaciones es

Este documento incorpora firma electrónica, y es copia auténtica de un documento electrónico archivado por la ULL según la Ley 39/2015.
Su autenticidad puede ser contrastada en la siguiente dirección https://sede.ull.es/validacion/

Identificador del documento: 3764923 Código de verificación: JHlWnlbn

Firmado por:	JOSE RAMON BERMEJO CLIMENT *UNIVERSIDAD DE LA LAGUNA*	Fecha: 01/09/2021 17:41:12
	José Alberto Rubiño Martín *UNIVERSIDAD DE LA LAGUNA*	01/09/2021 17:49:44
	FABIO FINELLI *UNIVERSIDAD DE LA LAGUNA*	02/09/2021 14:12:21

Universidad de La Laguna
Oficina de Sede Electrónica
Entrada
Nº registro: 2021/90989
Nº reg. oficina: OF002/2021/89977
Fecha: 03/09/2021 12:24:13

independiente de ciertas incertidumbres astrofísicas como el bias de las galaxias y de los multipolos. Predecimos una medición de este cociente con un error en torno al 1-2%, usando Euclid y futuros experimentos de FCM para el efecto lente. Además, evaluamos el impacto en el cociente de la inclusión de las contribuciones de relatividad general en el número de cuentas de galaxias. Hallamos que la magnificación por efecto lente provoca una dependencia de los multipolos que no es despreciable para futuros cartografiados de galaxias, y proponemos un nuevo estimador para tener este efecto en cuenta. En el nuevo formalismo, predecimos mediante una aproximación de matriz Fisher la capacidad del cociente de efecto lente para restringir parámetros cosmológicos cuando es combinado con la información del FCM. Encontramos que, para modelos extendidos, añadir el cociente puede mejorar los errores en los parámetros de estado de la energía oscura y en la densidad de curvatura.

Después, estudiamos la importancia global de la correlación cruzada entre el FCM y la estructura a gran escala mediante una aproximación 2D tomográfica en el espacio angular para el análisis conjunto del FCM y el número de cuentas de galaxias. Para ello, calculamos mediante una aproximación de matriz Fisher conjunta los errores en parámetros de varios modelos cosmológicos extendidos, incluyendo la parametrización de una ecuación de estado de la energía oscura que depende del redshift, física de neutrinos y parámetros relacionados con el Universo primordial. Encontramos que la inclusión de la correlación cruzada puede mejorar la figura de mérito de la energía oscura hasta un factor ~ 2. Predecimos una detección de la masa del neutrino con un grado de significación superior a 3σ mediante la combinación de los experimentos CMB-S4 y SPHEREx, sólo con el análisis de escalas cuasi-lineales. También predecimos la medida del parámetro local de no Gaussianidad primordial $f_{\rm NL}$ con una incertidumbre en torno a $\sim 1-2$ mediante la combinación del FCM con futuros cartografiados en el radio continuo como SKA. Nuestra metodología es también aplicada a modelos de posibles rasgos causados por desviaciones de una ley de potencias para el espectro de potencias primordial. Encontramos que la correlación cruzada es útil para ayudar a restringir estos modelos, en particular para cartografiados con gran cobertura en redshift como los de radio continuo. Como siguiente paso, extendemos este análisis conjunto bidimensional a la inclusión del efecto lente débil de galaxias como prueba adicional y presentamos los resultados para la combinación de la likelihood completa de Euclid con el FCM.

Este documento incorpora firma electrónica, y es copia auténtica de un documento electrónico archivado por la ULL según la Ley 39/2015.
Su autenticidad puede ser contrastada en la siguiente dirección https://sede.ull.es/validacion/

Identificador del documento: 3764923 Código de verificación: JHlWnlbn

Firmado por:	JOSE RAMON BERMEJO CLIMENT *UNIVERSIDAD DE LA LAGUNA*	Fecha: 01/09/2021 17:41:12
	José Alberto Rubiño Martín *UNIVERSIDAD DE LA LAGUNA*	01/09/2021 17:49:44
	FABIO FINELLI *UNIVERSIDAD DE LA LAGUNA*	02/09/2021 14:12:21

Universidad de La Laguna
Oficina de Sede Electrónica
Entrada
Nº registro: 2021/90989
Nº reg. oficina: OF002/2021/89977
Fecha: 03/09/2021 12:24:13

Abstract

The cosmic microwave background (CMB) is a snapshot of the Universe at early times ($z \sim 1100$). In the recent years, several experiments have provided constraints on the concordance ΛCDM model from a statistical analysis of the CMB anisotropies. On the other hand, many galaxy surveys will measure the 3D distribution of the dark matter component of the Universe with unprecedented sensitivity and sky coverage. This is a complementary probe to the CMB, since it traces the evolution of the Universe at low redshift.

The addition of the two probes will break degeneracies in the parameters which are left when using either CMB or large scale structure (LSS). Moreover, the contributions to the CMB anisotropies along the line-of-sight -the so-called secondary CMB anisotropies- are correlated with the growth of perturbations at low redshift. Therefore, we have an important information in addition to the simple combination of the CMB with large scale structure (LSS) probes from galaxy surveys: the cross-correlation between the CMB and LSS probes, such as galaxy number counts and weak lensing. In this thesis, we study the capability of the CMB-LSS cross-correlation for constraining cosmological parameters alone or in combination with the CMB and LSS, using mock data and statistical methodologies, in the perspective of upcoming and future cosmological surveys.

First, we explore the capabilities of the lensing ratio between the CMB lensing - galaxy clustering and weak lensing - galaxy clustering cross-correlations, an estimator that under certain approximations is independent on some astrophysical uncertainties such as the galaxy bias and on the multipoles. We forecast a measurement of this ratio with an error around 1-2% using Euclid and future CMB lensing experiments. Furthermore, we evaluate the impact on this ratio of the inclusion of general relativity

Este documento incorpora firma electrónica, y es copia auténtica de un documento electrónico archivado por la ULL según la Ley 39/2015.
Su autenticidad puede ser contrastada en la siguiente dirección https://sede.ull.es/validacion/

Identificador del documento: 3764923 Código de verificación: JHlWnlbn

Firmado por:	JOSE RAMON BERMEJO CLIMENT *UNIVERSIDAD DE LA LAGUNA*	Fecha: 01/09/2021 17:41:12
	José Alberto Rubiño Martín *UNIVERSIDAD DE LA LAGUNA*	01/09/2021 17:49:44
	FABIO FINELLI *UNIVERSIDAD DE LA LAGUNA*	02/09/2021 14:12:21

Universidad de La Laguna
Oficina de Sede Electrónica
Entrada
Nº registro: 2021/90989
Nº reg. oficina: OF002/2021/89977
Fecha: 03/09/2021 12:24:13

contributions to the galaxy number counts. We find that accounting for the lensing magnification contribution induces a multipole dependence of the ratio that will not be negligible for future surveys, and propose a new estimator in order to take it into account. With the new formalism, we forecast by a Fisher matrix approach the capability of the lensing ratio for constraining cosmological parameters when it is added to the CMB information. We find that in extended cosmological models the lensing ratio can improve the errors on the dark energy parameters of state and on the curvature density.

We have also investigated the global importance of the CMB - LSS cross-correlation in a 2D tomographic approach for a joint analysis CMB and galaxy number counts in the angular space. For this, we compute by a Fisher matrix approach the joint constraints on many extended cosmological models, including the dark energy parametrization for a redshift dependent equation of state, neutrino physics and primordial Universe parameters. We find that the inclusion of cross-correlation can improve the dark energy figure of merit up to a factor ~ 2. We forecast a detection of the neutrino mass with $\gtrsim 3\sigma$ significance by combining CMB-S4 with SPHEREx, just by the analysis of quasi-linear scales. We also predict the measurement of the primordial local non-Gaussianity parameter $f_{\rm NL}$ with an uncertaintiy $\sim$1-2 by combining the CMB with future radio continuum surveys such as SKA. Our methodology is then applied to models of features caused by deviations from a power law primordial power spectrum. We find that the cross-correlation is useful for helping to constrain these models, in particular for surveys with large redshift coverage such as the radio continuum ones. As a further step, we extend the analysis to the inclusion of weak lensing as additional probe and present the results for the combination of the full Euclid likelihood with the CMB.

Este documento incorpora firma electrónica, y es copia auténtica de un documento electrónico archivado por la ULL según la Ley 39/2015.
Su autenticidad puede ser contrastada en la siguiente dirección https://sede.ull.es/validacion/

Identificador del documento: 3764923 Código de verificación: JHlWnlbn

Firmado por:	JOSE RAMON BERMEJO CLIMENT *UNIVERSIDAD DE LA LAGUNA*	Fecha: 01/09/2021 17:41:12
	José Alberto Rubiño Martín *UNIVERSIDAD DE LA LAGUNA*	01/09/2021 17:49:44
	FABIO FINELLI *UNIVERSIDAD DE LA LAGUNA*	02/09/2021 14:12:21

Universidad de La Laguna
Oficina de Sede Electrónica
Entrada
Nº registro: 2021/90989
Nº reg. oficina: OF002/2021/89977
Fecha: 03/09/2021 12:24:13

Contents

Resumen **iii**

Abstract **v**

Introduction **1**

1 Cosmology and its open problems **5**
1.1 The Big Bang standard cosmological model 5
1.1.1 The Friedmann-Robertson-Walker metric 6
1.1.2 Cosmological equations of motion 7
1.2 Problems of the Big Bang and cosmic inflation 9
1.2.1 The horizon problem 9
1.2.2 The flatness problem 10
1.2.3 The magnetic monopole problem 10
1.2.4 Perturbations 10
1.2.5 Cosmic inflation 10
1.3 General relativistic perturbations 12
1.3.1 Metric perturbations 13
1.3.2 Energy-momentum tensor perturbations 13
1.3.3 Evolution of perturbations 15
1.4 The ΛCDM concordance model 17
1.4.1 Parameters 17
1.4.2 Tensions between current cosmological data 18

2 Cosmological observations **23**
2.1 The cosmic microwave background 23
2.1.1 Temperature anisotropies 24

Este documento incorpora firma electrónica, y es copia auténtica de un documento electrónico archivado por la ULL según la Ley 39/2015.
Su autenticidad puede ser contrastada en la siguiente dirección https://sede.ull.es/validacion/

Identificador del documento: 3764923 Código de verificación: JHlWnlbn

Firmado por: JOSE RAMON BERMEJO CLIMENT — Fecha: 01/09/2021 17:41:12
UNIVERSIDAD DE LA LAGUNA

José Alberto Rubiño Martín — 01/09/2021 17:49:44
UNIVERSIDAD DE LA LAGUNA

FABIO FINELLI — 02/09/2021 14:12:21
UNIVERSIDAD DE LA LAGUNA

Universidad de La Laguna
Oficina de Sede Electrónica
Entrada
Nº registro: 2021/90989
Nº reg. oficina: OF002/2021/89977
Fecha: 03/09/2021 12:24:13

2.1.2 Polarization anisotropies . . . 26
2.1.3 CMB lensing . . . 27
2.2 Large scale structure tracers and their cross-correlations . 28
2.2.1 Galaxy number counts . . . 28
2.2.2 Galaxy weak lensing . . . 31

3 Including CMB-LSS cross-correlation in future surveys 33
3.1 CMB surveys . . . 33
3.1.1 *Planck* . . . 34
3.1.2 Simons Observatory . . . 35
3.1.3 LiteBIRD . . . 35
3.1.4 CMB-S4 . . . 35
3.1.5 Concepts of future space missions . . . 36
3.2 Future galaxy surveys . . . 36
3.2.1 Euclid surveys . . . 38
3.2.2 Vera C. Rubin Observatory . . . 38
3.2.3 SPHEREx . . . 40
3.2.4 Radio continuum galaxy surveys . . . 41
3.3 Signal-to-noise analysis . . . 41
3.4 Impact of RSD and general relativity contributions . . . 46

4 Lensing ratios with future galaxy surveys 51
4.1 Formalism . . . 54
4.2 Data and specifications . . . 55
4.2.1 Galaxy lenses . . . 55
4.2.2 Galaxy shear sources . . . 56
4.2.3 CMB lensing source . . . 57
4.3 Cosmographic lensing ratio measurements . . . 58
4.3.1 The cosmographic ratio limit . . . 58
4.3.2 Forecasts for future experiments . . . 61
4.4 A generalized lensing ratio estimator . . . 64
4.4.1 Inclusion of RSD and lensing magnification . . . 64
4.4.2 Signal-to-noise analysis . . . 66
4.5 Cosmological parameter constraints . . . 68

5 A 2D tomographic approach to CMB and galaxy clustering 75
5.1 Fisher formalism for cosmological parameter forecasts . . 76
5.2 Constraints on ΛCDM and extensions . . . 77

Este documento incorpora firma electrónica, y es copia auténtica de un documento electrónico archivado por la ULL según la Ley 39/2015.
Su autenticidad puede ser contrastada en la siguiente dirección https://sede.ull.es/validacion/

Identificador del documento: 3764923 Código de verificación: JHlWnlbn

Firmado por: JOSE RAMON BERMEJO CLIMENT — Fecha: 01/09/2021 17:41:12
UNIVERSIDAD DE LA LAGUNA

José Alberto Rubiño Martín — 01/09/2021 17:49:44
UNIVERSIDAD DE LA LAGUNA

FABIO FINELLI — 02/09/2021 14:12:21
UNIVERSIDAD DE LA LAGUNA

Universidad de La Laguna
Oficina de Sede Electrónica
Entrada
Nº registro: 2021/90989
Nº reg. oficina: OF002/2021/89977
Fecha: 03/09/2021 12:24:13

5.2.1 Cosmological models 77
5.2.2 Joint forecasts on cosmological parameters 79
5.3 Constraints on primordial features 89
5.3.1 Deviations from a power law primordial power spectrum 89
5.3.2 Impact on the angular power spectra 92
5.3.3 Joint forecasts on features parameters 93
5.4 Outlook 96
5.4.1 Scale-dependent bias induced by massive neutrinos 97
5.4.2 Inclusion of weak lensing 100
5.5 Full Euclid × CMB joint analysis 103

Conclusions **107**

A Tables of cosmological parameter constraints **111**

Publication list **121**

Bibliography **123**

Acknowledgements **143**

Este documento incorpora firma electrónica, y es copia auténtica de un documento electrónico archivado por la ULL según la Ley 39/2015.
Su autenticidad puede ser contrastada en la siguiente dirección https://sede.ull.es/validacion/

Identificador del documento: 3764923 Código de verificación: JHlWnlbn

Firmado por: JOSE RAMON BERMEJO CLIMENT — Fecha: 01/09/2021 17:41:12
UNIVERSIDAD DE LA LAGUNA

José Alberto Rubiño Martín — 01/09/2021 17:49:44
UNIVERSIDAD DE LA LAGUNA

FABIO FINELLI — 02/09/2021 14:12:21
UNIVERSIDAD DE LA LAGUNA

Universidad de La Laguna
Oficina de Sede Electrónica
Entrada
Nº registro: 2021/90989
Nº reg. oficina: OF002/2021/89977
Fecha: 03/09/2021 12:24:13

Este documento incorpora firma electrónica, y es copia auténtica de un documento electrónico archivado por la ULL según la Ley 39/2015.
Su autenticidad puede ser contrastada en la siguiente dirección https://sede.ull.es/validacion/

Identificador del documento: 3764923 Código de verificación: JHlWnlbn

Firmado por:	JOSE RAMON BERMEJO CLIMENT *UNIVERSIDAD DE LA LAGUNA*	Fecha: 01/09/2021 17:41:12
	José Alberto Rubiño Martín *UNIVERSIDAD DE LA LAGUNA*	01/09/2021 17:49:44
	FABIO FINELLI *UNIVERSIDAD DE LA LAGUNA*	02/09/2021 14:12:21

Universidad de La Laguna
Oficina de Sede Electrónica
Entrada
Nº registro: 2021/90989
Nº reg. oficina: OF002/2021/89977
Fecha: 03/09/2021 12:24:13

Introduction

In the past two decades, several experiments in cosmology have taken place with the aim of understanding the origin, composition and evolution of our Universe. Since the discovery of the accelerated expansion of the Universe in the late 1990s by Saul Perlmutter, Adam Riess and Brian Schmidt, awarded with the Physics Nobel prize in 2011, an effort has been done in order to answer the open questions in cosmology, and our knowledge has improved thanks to the available datasets from cosmological surveys, entering in the era of the so-called precision cosmology.

The cosmic microwave background (CMB) is a relic radiation from the Big Bang that provides a snapshot of the Universe at early times. In 1990, the NASA satellite COBE measured for the first time the anisotropies in the temperature field. More recently, these anisotropies have been studied with a higher detail thanks to space missions such as WMAP and *Planck*. In the upcoming years, a next generation of CMB experiments dedicated to polarization will improve the sensitivity of the measurements.

In this decade, several galaxy surveys are planned with the goal of tracing the large scale structure (LSS) of the Universe. These experiments provide information about the late evolution of the Universe, covering the final stages of the dark matter evolution and the period dominated by dark energy.

The ΛCDM concordance model assumes that the dark energy equation of state corresponds to a cosmological constant. From the current datasets there are no deviations from this model that are statistically favoured. However, some tensions on the values of certain parameters such as the Hubble constant H_0 and S_8 have been found in the last years. The combination of low redshift observations with the CMB will allow us to constrain with better accuracy the parameters of extensions to the ΛCDM model.

Este documento incorpora firma electrónica, y es copia auténtica de un documento electrónico archivado por la ULL según la Ley 39/2015.
Su autenticidad puede ser contrastada en la siguiente dirección https://sede.ull.es/validacion/

Identificador del documento: 3764923 Código de verificación: JHlWnlbn

Firmado por:	JOSE RAMON BERMEJO CLIMENT *UNIVERSIDAD DE LA LAGUNA*	Fecha: 01/09/2021 17:41:12
	José Alberto Rubiño Martín *UNIVERSIDAD DE LA LAGUNA*	01/09/2021 17:49:44
	FABIO FINELLI *UNIVERSIDAD DE LA LAGUNA*	02/09/2021 14:12:21

Universidad de La Laguna
Oficina de Sede Electrónica
Entrada
Nº registro: 2021/90989
Nº reg. oficina: OF002/2021/89977
Fecha: 03/09/2021 12:24:13

Further, beyond the combination of these two kinds of datasets, we will be able to obtain extra information from their cross-correlation.

The cross-correlation between the cosmic microwave background anisotropies and matter tracers carries important cosmological information. First, the cross-correlation of CMB temperature with the galaxy density field traces the Integrated Sachs-Wolfe (ISW) effect, which encodes the nature of dark energy. Further, the cross-correlation of matter tracers with CMB lensing, which will have a larger significance, has been found to be a useful probe for constraining the neutrino mass, the amplitude of fluctuations σ_8 and primordial non-Gaussianities. In this thesis, we investigate with simulated data for future cosmological surveys the amount of information that can be obtained from these cross-correlations and study their capability for helping to constrain many extended models in a combination of CMB and LSS probes.

This thesis is organized as follows:

- In Chapter 1 we review the status of cosmology and its open problems and questions. We introduce the standard Big Bang theory and describe the basics of inflation, which is developed to solve the standard Big Bang problems. We then review the perturbation theory in a general relativistic framework and present the ΛCDM model, describing also its tensions between current cosmological data.
- In Chapter 2 we review the formalism for describing the cosmological observations that we consider in this thesis. First, we introduce the treatment in terms of spherical harmonics of the cosmic microwave background anisotropies for the temperature, polarization and lensing fields. Then, we use also the formalism of the 2D angular space to describe two of the main matter tracers: galaxy clustering and weak lensing, and we introduce their cross-correlations with the CMB fields.
- In Chapter 3 we describe the characteristics and specifications of the CMB and galaxy surveys that we consider in this thesis. We then use the mock likelihoods expected for these surveys for estimating by a signal-to-noise approach the amount of information contained in the CMB temperature-galaxy clustering and CMB lensing-galaxy clustering cross-correlations, and discuss also on the impact of the contributions from redshift space distortions (RSD) and general relativity effects to the galaxy number counts auto and cross spectra.

Este documento incorpora firma electrónica, y es copia auténtica de un documento electrónico archivado por la ULL según la Ley 39/2015.
Su autenticidad puede ser contrastada en la siguiente dirección https://sede.ull.es/validacion/

Identificador del documento: 3764923 Código de verificación: JHlWnlbn

Firmado por: JOSE RAMON BERMEJO CLIMENT — Fecha: 01/09/2021 17:41:12
UNIVERSIDAD DE LA LAGUNA

José Alberto Rubiño Martín — 01/09/2021 17:49:44
UNIVERSIDAD DE LA LAGUNA

FABIO FINELLI — 02/09/2021 14:12:21
UNIVERSIDAD DE LA LAGUNA

Universidad de La Laguna
Oficina de Sede Electrónica
Entrada
Nº registro: 2021/90989
Nº reg. oficina: OF002/2021/89977
Fecha: 03/09/2021 12:24:13

- In Chapter 4 we perform forecasts for the lensing ratio, an estimator that accounts for the ratio between the CMB lensing-galaxy clustering and the galaxy lensing-galaxy clustering cross-correlations. We perform forecasts for many CMB surveys and Euclid for the background and foreground of galaxies, and show how including the contribution from lensing magnification to the galaxy number counts affects the multipole dependence and signal-to-noise of this estimator. Then, we compute by a Fisher matrix approach how the addition of this ratio to the CMB information can improve the constraints on extended cosmological models.
- In Chapter 5 we present a methodology for estimating the joint constraints on cosmological parameters by a 2D tomographic approach to the CMB and galaxy clustering, including all the probes and their cross-correlations. We first show how the cross-correlation can improve the constraints on extensions of the ΛCDM model such as a dark energy redshift-dependent parametrization, the neutrino mass and the primordial local non-Gaussianity. We then apply the same methodology to obtain constraints on features in the primordial power spectra originated by some inflationary models. We also present an outlook of possible extensions of this methodology such as the addition of the galaxy weak lensing, and show the constraints by the combination of the CMB with the full Euclid likelihood.

Finally, we summarize our conclusions.

Este documento incorpora firma electrónica, y es copia auténtica de un documento electrónico archivado por la ULL según la Ley 39/2015.
Su autenticidad puede ser contrastada en la siguiente dirección https://sede.ull.es/validacion/

Identificador del documento: 3764923 Código de verificación: JHlWnlbn

Firmado por:	JOSE RAMON BERMEJO CLIMENT *UNIVERSIDAD DE LA LAGUNA*	Fecha: 01/09/2021 17:41:12
	José Alberto Rubiño Martín *UNIVERSIDAD DE LA LAGUNA*	01/09/2021 17:49:44
	FABIO FINELLI *UNIVERSIDAD DE LA LAGUNA*	02/09/2021 14:12:21

Universidad de La Laguna
Oficina de Sede Electrónica
Entrada
Nº registro: 2021/90989
Nº reg. oficina: OF002/2021/89977
Fecha: 03/09/2021 12:24:13

Este documento incorpora firma electrónica, y es copia auténtica de un documento electrónico archivado por la ULL según la Ley 39/2015.
Su autenticidad puede ser contrastada en la siguiente dirección https://sede.ull.es/validacion/

Identificador del documento: 3764923 Código de verificación: JHlWnlbn

Firmado por:	JOSE RAMON BERMEJO CLIMENT *UNIVERSIDAD DE LA LAGUNA*	Fecha: 01/09/2021 17:41:12
	José Alberto Rubiño Martín *UNIVERSIDAD DE LA LAGUNA*	01/09/2021 17:49:44
	FABIO FINELLI *UNIVERSIDAD DE LA LAGUNA*	02/09/2021 14:12:21

Universidad de La Laguna
Oficina de Sede Electrónica
Entrada
Nº registro: 2021/90989
Nº reg. oficina: OF002/2021/89977
Fecha: 03/09/2021 12:24:13

1

Cosmology and its open problems

The aim of cosmology is to understand the composition and properties of our Universe as well as its evolution and origin.

In the recent decades, several experiments have provided detailed observations of the Universe at early and late times have opened the era of the so-called precision cosmology. Current observations have confirmed the accelerated expansion of the Universe. This is explained with the presence of a dark energy component, that according to the data is compatible with a cosmological constant in the Einstein equations.

In this chapter, we review the basic concepts of the Big Bang standard cosmological model and introduce some of its problems, which are mainly solved with cosmic inflation. We then describe the basics of the general relativistic perturbations and finally present the current ΛCDM concordance model and discuss some of the unsolved discrepancies that remain between different observations.

1.1 The Big Bang standard cosmological model

The Big Bang theory [1] was formulated in the 1946 by George Gamow and his collaborators Ralph Alpher and Robert Herman. In order to explain the formation of light elements (the Big Bang nucleosynthesis mechanism), they proposed an initial hot and dense phase of the Universe, followed by a cooling and expanding phase that remains up to the present day [2].

Already before the Big Bang formulation, in 1929, Edwin Hubble had

Este documento incorpora firma electrónica, y es copia auténtica de un documento electrónico archivado por la ULL según la Ley 39/2015.
Su autenticidad puede ser contrastada en la siguiente dirección https://sede.ull.es/validacion/

Identificador del documento: 3764923 Código de verificación: JHlWnlbn

Firmado por:	JOSE RAMON BERMEJO CLIMENT *UNIVERSIDAD DE LA LAGUNA*	Fecha: 01/09/2021 17:41:12
	José Alberto Rubiño Martín *UNIVERSIDAD DE LA LAGUNA*	01/09/2021 17:49:44
	FABIO FINELLI *UNIVERSIDAD DE LA LAGUNA*	02/09/2021 14:12:21

Universidad de La Laguna
Oficina de Sede Electrónica
Entrada
Nº registro: 2021/90989
Nº reg. oficina: OF002/2021/89977
Fecha: 03/09/2021 12:24:13

found a linear relation between the galaxies recession velocity and their distances [3], recently renamed as the Hubble-Lemaître law, suggesting that these objects were moving away with respect to others.

As a consequence of the Big Bang model, Alpher and Herman predicted the existence of a Cosmic Microwave Background (CMB) radiation with a temperature around ~ 5 K [4]. This CMB radiation was later detected in 1965 by Arno Penzias and Robert Woodrow Wilson [5], awarded with the Physics Nobel Prize in 1978. The CMB became then the main proof of the Big Bang model. They also measured a temperature of ~ 3 K for the CMB radiation.

More recently, the accelerated expansion of the Universe has been confirmed by different cosmological observations. Observations of supernovae type Ia (SN Ia) in the late 1990s provided the first evidence of this accelerated expansion [6, 7], due to an unknown constituent that is called *dark energy*. The expansion has been later confirmed by other kind of observations such as the CMB [8,44–46] and Baryon Acoustic Oscillations (BAO) [12]. In the upcoming years, galaxy surveys will have the target of measuring the equation of state of dark energy in order to identify its nature.

In the following, we describe the formalism for modelling an homogeneous and isotropic Universe that evolves with time. Throughout this section we will set the value of the speed of light to be $c = 1$.

1.1.1 The Friedmann-Robertson-Walker metric

One of the pillars of cosmology is the *cosmological principle*. The cosmological principle establishes that the Universe is homogeneous and isotropic at each fixed cosmic time. This assumption is supported by the large scale structure (LSS) observations, that confirm an isotropic distribution of matter at cosmological scales. The CMB observations confirm as well a high degree of isotropy of the Universe at early times.

The Friedmann-Robertson-Walker (FRW) metric [13–15] is the simplest way to describe a Universe following this principle, and it is given by

$$\mathrm{d}s^2 = -\mathrm{d}t^2 + a^2(t)\left[\frac{\mathrm{d}r^2}{1-Kr^2} + r^2\left(\mathrm{d}\theta^2 + \sin^2\theta\mathrm{d}\phi^2\right)\right], \qquad (1.1)$$

where t is the cosmic time, $a(t)$ is the scale factor, (r, θ, ϕ) are the spherical comoving coordinates and K is the spatial curvature. The vaules of K can be 0 for an euclidean geometry (flat Universe), -1 for an hyperbolic

Este documento incorpora firma electrónica, y es copia auténtica de un documento electrónico archivado por la ULL según la Ley 39/2015.
Su autenticidad puede ser contrastada en la siguiente dirección https://sede.ull.es/validacion/

Identificador del documento: 3764923 Código de verificación: JHlWnlbn

Firmado por: JOSE RAMON BERMEJO CLIMENT — Fecha: 01/09/2021 17:41:12
UNIVERSIDAD DE LA LAGUNA

José Alberto Rubiño Martín — 01/09/2021 17:49:44
UNIVERSIDAD DE LA LAGUNA

FABIO FINELLI — 02/09/2021 14:12:21
UNIVERSIDAD DE LA LAGUNA

Universidad de La Laguna
Oficina de Sede Electrónica
Entrada
Nº registro: 2021/90989
Nº reg. oficina: OF002/2021/89977
Fecha: 03/09/2021 12:24:13

geometry (open Universe) and +1 for a hyperspheric geometry (closed Universe).

It is useful to define the *conformal time* as:

$$\mathrm{d}\eta = \frac{dt}{a(t)}\,, \tag{1.2}$$

which allows to rewrite Eq. (1.1) as

$$\mathrm{d}s^2 = a^2(\eta)\left[-\mathrm{d}\eta^2 + \frac{\mathrm{d}r^2}{1-Kr^2} + r^2\left(\mathrm{d}\theta^2 + \sin^2\theta\mathrm{d}\phi^2\right)\right]\,. \tag{1.3}$$

Another useful quantity is the redshift z, related to the scale factor through

$$1 + z = \frac{a_0}{a(t)}\,, \tag{1.4}$$

where a_0 is the present-day value of the scale factor, that is commonly set as $a_0 = 1$.

1.1.2 Cosmological equations of motion

The cosmological equations of motion, also known as the Friedmann-Lemaître equations, describe the evolution of the scale factor $a(t)$ and are derived from the General Relativity theory by Einstein [16]. The Einstein field equations are written as

$$R_{\mu\nu} - \frac{1}{2}Rg_{\mu\nu} + \Lambda g_{\mu\nu} = 8\pi G T_{\mu\nu}\,, \tag{1.5}$$

where $R_{\mu\nu}$ is the Ricci tensor, $g_{\mu\nu}$ is the metric tensor, R is the Ricci scalar, Λ is the cosmological constant and $T_{\mu\nu}$ is the energy-momentum tensor, that accounts for the content of the Universe.

The energy-momentum tensor for a perfect fluid is given by

$$T_{\mu\nu} = Pg_{\mu\nu} + (\rho + P)u_\mu u_\nu\,, \tag{1.6}$$

where ρ is the total energy density of the Universe, P is the total pressure and u_μ,u_ν represent the four-velocity of the fluid. Assuming the FRW metric given by Eq. (1.1), one can derive the Friedmann equations [17,18]:

$$H^2 \equiv \left(\frac{\dot{a}}{a}\right)^2 = \frac{8\pi G}{3}\rho + \frac{\Lambda}{3} - \frac{K}{a^2}\,, \tag{1.7}$$

Este documento incorpora firma electrónica, y es copia auténtica de un documento electrónico archivado por la ULL según la Ley 39/2015.
Su autenticidad puede ser contrastada en la siguiente dirección https://sede.ull.es/validacion/

Identificador del documento: 3764923 Código de verificación: JHlWnlbn

Firmado por:	JOSE RAMON BERMEJO CLIMENT *UNIVERSIDAD DE LA LAGUNA*	Fecha: 01/09/2021 17:41:12
	José Alberto Rubiño Martín *UNIVERSIDAD DE LA LAGUNA*	01/09/2021 17:49:44
	FABIO FINELLI *UNIVERSIDAD DE LA LAGUNA*	02/09/2021 14:12:21

Universidad de La Laguna
Oficina de Sede Electrónica
Entrada
Nº registro: 2021/90989
Nº reg. oficina: OF002/2021/89977
Fecha: 03/09/2021 12:24:13

$$\dot{H} + H^2 \equiv \frac{\ddot{a}}{a} = -\frac{4\pi G}{3}(\rho + 3P) + \frac{\Lambda}{3}\,, \tag{1.8}$$

where the derivatives are defined with respect to the cosmic time t and we have introduced the Hubble parameter H, that defines the expansion rate of the Universe at a given time. At present-day, the Hubble parameter value is known as the Hubble constant H_0, and its value according to the most recent observations from the CMB [46] is $H_0 \sim 67$ km s^{-1} Mpc^{-1}.

We define the critical density as

$$\rho_{\rm cr} = \frac{3H^2}{8\pi G}\,. \tag{1.9}$$

With this, we introduce the energy density of a given component X of the the Universe as

$$\Omega_X = \frac{\rho_X}{\rho_{\rm cr}} = \frac{8\pi G}{3}\rho_X \tag{1.10}$$

It is also useful to rearrange Eq. (1.1) including the curvature in the total energy density of the Universe Ω, hence we define

$$\Omega - 1 = \frac{K}{a^2H^2} = \frac{K}{\dot{a}^2}\,. \tag{1.11}$$

The pressure and the energy density are related through the equation of state:

$$P = w\rho\,, \tag{1.12}$$

and the evolution of the density for a perfect fluid is given by the continuity equation, that can be obtained differentiating with respect to time in Eq. (1.1) and substituting Eq. (1.3) into the previous one:

$$\dot{\rho} = -3H(\rho + P)\,. \tag{1.13}$$

From this equation it is possible to obtain the relation between the scale factor and the energy density for the various components of the Universe factor, depending on the equation of state w. In particular, for radiation, with an equation of state $w = -1/3$, we get $\rho \propto a^{-4}$, and for matter, given by $w = 0$ we obtain $\rho \propto a^{-3}$. For the cosmological constant, associated with an equation of state $w = -1$, the corresponding energy density is given by:

$$\rho_\Lambda = -P_\Lambda = \frac{\Lambda}{8\pi G}\,. \tag{1.14}$$

Este documento incorpora firma electrónica, y es copia auténtica de un documento electrónico archivado por la ULL según la Ley 39/2015.
Su autenticidad puede ser contrastada en la siguiente dirección https://sede.ull.es/validacion/

Identificador del documento: 3764923 Código de verificación: JHlWnlbn

Firmado por: JOSE RAMON BERMEJO CLIMENT — Fecha: 01/09/2021 17:41:12
UNIVERSIDAD DE LA LAGUNA

José Alberto Rubiño Martín — 01/09/2021 17:49:44
UNIVERSIDAD DE LA LAGUNA

FABIO FINELLI — 02/09/2021 14:12:21
UNIVERSIDAD DE LA LAGUNA

Universidad de La Laguna
Oficina de Sede Electrónica
Entrada
Nº registro: 2021/90989
Nº reg. oficina: OF002/2021/89977
Fecha: 03/09/2021 12:24:13

Taking into account Eq. (1.4), the first Friedmann-Lemaître equation for a Universe containing radiation, matter and cosmological constant becomes:

$$H^2(z) = H_0^2[\Omega_{\mathrm{m},0}(1+z)^3 + \Omega_{\mathrm{r},0}(1+z)^4 + \Omega_\Lambda + \Omega_{K,0}(1+z)^2]\,, \quad (1.15)$$

where $\Omega_{\mathrm{m},0}$, $\Omega_{\mathrm{r},0}$, Ω_Λ are the present-day densities of matter, radiation and cosmological constant, and $\Omega_{K,0} = 1-\Omega_{\mathrm{m},0}-\Omega_{\mathrm{r},0}-\Omega_\Lambda$ is the curvature density.

1.2 Problems of the Big Bang and cosmic inflation

Although the standard Big Bang theory was successful in explaining the observed recesion of galaxies and the cosmological formation of light elements, the model presents conceptual problems, since it does not provide an explanation for every observation. Here we describe the most important problems and introduce the cosmic inflation, a theory developed in the early 1980s, as a solution.

1.2.1 The horizon problem

In the stantard Big Bang model we can define a cosmological horizon, which delimits the regions that are in causal connection with others. The radius of casual connection can be calculated from the proper distance travelled by a photon, assuming $\mathrm{d}s^2 = 0$ in the FRW metric:

$$r_H(t) = a(t)\int_0^t \frac{\mathrm{d}t'}{a(t')}\,. \quad (1.16)$$

At the last scattering surface, $z \sim 1100$, that is the time of the formation of the CMB radiation due to the decoupling of photons from other particles, r_H was of the order of 100 Mpc, corresponding to $\sim 1^\circ$ in the angular space. This would mean that the different regions of the CMB separated by this amount of space would have never been in casual connection. However, the observed CMB pattern present a high degree of isotropy that can not be explained by the original Big Bang mechanism. This is called the *horizon problem*.

Este documento incorpora firma electrónica, y es copia auténtica de un documento electrónico archivado por la ULL según la Ley 39/2015.
Su autenticidad puede ser contrastada en la siguiente dirección https://sede.ull.es/validacion/

Identificador del documento: 3764923 Código de verificación: JHlWnlbn

Firmado por: JOSE RAMON BERMEJO CLIMENT — Fecha: 01/09/2021 17:41:12
UNIVERSIDAD DE LA LAGUNA

José Alberto Rubiño Martín — 01/09/2021 17:49:44
UNIVERSIDAD DE LA LAGUNA

FABIO FINELLI — 02/09/2021 14:12:21
UNIVERSIDAD DE LA LAGUNA

Universidad de La Laguna
Oficina de Sede Electrónica
Entrada
Nº registro: 2021/90989
Nº reg. oficina: OF002/2021/89977
Fecha: 03/09/2021 12:24:13

1.2.2 The flatness problem

Observations suggest that our Universe is spatially flat, which means that according to Eq. (1.11), $\Omega = 1$. As an example, the *Planck* 2018 [46] results for the combination of the CMB with Baryon Acoustic Oscillations (BAO) report a curvature density $\Omega_K = 0.001 \pm 0.002$. If so, this parameter remains equal to 1 across all the time. Currently Ω has been measured with a few percent accuracy. Since the quantity $|\Omega - 1|$ grows with time, the density Ω at early times should have been extremely close to 1, requiring a fine tuning.

The flatness problem can be also formulated in the following way: assuming a generic initial value of Ω, we find that almost all initial conditions lead either to a closed Universe that recollapses, or to an open Universe in which Ω becomes smaller, something that is not compatible with observations. The flat Universe is then the statistically less probable option.

1.2.3 The magnetic monopole problem

The Grand Unification Theory (GUT) predicts that when the Universe was $t \sim 10^{-35}$ seconds old and the GUT transition phase occurred, some monodimensional relic defects should have been formed. In particular, magnetic monopoles are very massive particles, of the order of 10^{16} GeV, which should result in a very high density Ω_M for these particles.

Measurements of the matter density today are not compatible with this, and together with the lack of a magnetic monopole detection, suggest that their density is very low.

1.2.4 Perturbations

Cosmological perturbations are primordial inhomogeneities that are the seeds that evolve producing the overdensities observed in the large scale structure, and are also responsible for the anisotropies that we detect in the CMB.

However, the Big Bang original model does not provide a mechanism for the formation of these inhomogeneities.

1.2.5 Cosmic inflation

The theory of inflation was proposed in the early 1980s by Alan Guth [19] and Alexei Starobinsky [20]. The inflation theory was initially formulated to solve the first three problems described before (horizon, flatness and

Este documento incorpora firma electrónica, y es copia auténtica de un documento electrónico archivado por la ULL según la Ley 39/2015.
Su autenticidad puede ser contrastada en la siguiente dirección https://sede.ull.es/validacion/

Identificador del documento: 3764923 Código de verificación: JHlWnlbn

Firmado por:	JOSE RAMON BERMEJO CLIMENT *UNIVERSIDAD DE LA LAGUNA*	Fecha: 01/09/2021 17:41:12
	José Alberto Rubiño Martín *UNIVERSIDAD DE LA LAGUNA*	01/09/2021 17:49:44
	FABIO FINELLI *UNIVERSIDAD DE LA LAGUNA*	02/09/2021 14:12:21

Universidad de La Laguna
Oficina de Sede Electrónica
Entrada
Nº registro: 2021/90989
Nº reg. oficina: OF002/2021/89977
Fecha: 03/09/2021 12:24:13

magnetic monopole); however, it came out later than inflation was also able to explain the formation of primordial density perturbations [21–23].

Inflation is defined as a phase in which the scale factor of the Universe is accelerating ($\ddot{a} > 0$). This, according to Eq. (1.3) and assuming a flat space, implies the following condition for inflation:

$$\rho + 3P < 0\,. \tag{1.17}$$

During inflation, the scale factor grows more rapidly than the horizon of causal connection. Therefore, regions that were causally connected before inflation are pushed outside the Hubble radius r_H. This explains the high degree of isotropy of the CMB, solving the horizon problem.

The flatness problem, instead, is solved by the fact that the density parameter Ω evolves according to Eq. (1.11). Since the scale factor is expected to grow exponentially during inflation, Ω tends exponentially to 1 during inflation, whatever was its initial value.

Last, the magnetic monopole problem is also explained, since the extreme expansion of the scale factor diluted these particles, created before or during inflation, making their contribution negligible and extremely difficult to observe.

Given the condition for inflation given by Eq. (1.17), a simple way to satisfy it would be setting $w = -1$. However, a cosmological constant at the moment of inflation would have last forever, since its density is constant while the density of matter and radiation decreases with the scale factor, and we know that the Universe after inflation was dominated by radiation. We therefore consider an accelerated growth of the scale factor by a scalar field that fills the Universe.

The dynamics of a scalar field ϕ minimally coupled to gravity are defined by the action

$$S_\phi = \int \mathrm{d}^4x\sqrt{-g}\left(-\frac{1}{2}\partial^\mu\phi\partial_\mu\phi - V(\phi)\right) \tag{1.18}$$

where $g \equiv \det(g_{\mu\nu})$ and $V(\phi)$ is the potential of the scalar field. The corresponding energy-momentum tensor is given by

$$T_{\mu\nu} = \partial_\mu\phi\partial_\nu\phi - g_{\mu\nu}\left(\frac{1}{2}\partial^\sigma\phi\partial_\sigma\phi + V(\phi)\right)\,, \tag{1.19}$$

Este documento incorpora firma electrónica, y es copia auténtica de un documento electrónico archivado por la ULL según la Ley 39/2015.
Su autenticidad puede ser contrastada en la siguiente dirección https://sede.ull.es/validacion/

Identificador del documento: 3764923 Código de verificación: JHlWnlbn

Firmado por:	JOSE RAMON BERMEJO CLIMENT *UNIVERSIDAD DE LA LAGUNA*	Fecha: 01/09/2021 17:41:12
	José Alberto Rubiño Martín *UNIVERSIDAD DE LA LAGUNA*	01/09/2021 17:49:44
	FABIO FINELLI *UNIVERSIDAD DE LA LAGUNA*	02/09/2021 14:12:21

Universidad de La Laguna
Oficina de Sede Electrónica
Entrada
Nº registro: 2021/90989
Nº reg. oficina: OF002/2021/89977
Fecha: 03/09/2021 12:24:13

Assuming the FRW metric and a perfect fluid, the form of the density is:

$$\rho = \frac{1}{2}\dot{\phi}^2 + V(\phi)\,, \tag{1.20}$$

and for the pressure:

$$P = \frac{1}{2}\dot{\phi}^2 - V(\phi)\,, \tag{1.21}$$

where it is recognisable the presence of a kinetic and a potential term.

The equation of motion for the scalar field is the Klein-Gordon equation:

$$\ddot{\phi} + 3H\dot{\phi} + \frac{\mathrm{d}V}{\mathrm{d}\phi} = 0\,, \tag{1.22}$$

and the Friedmann-Lemaître equations for a Universe containing a scalar field ϕ become

$$H^2 = \frac{8\pi G}{3}\left(\frac{1}{2}\dot{\phi}^2 + V(\phi)\right)\,, \tag{1.23}$$

$$\dot{H} = -4\pi G\dot{\phi}^2\,. \tag{1.24}$$

In order to satisfy the condition for inflation, it is necessary that

$$\dot{\phi}^2 < V(\phi)\,, \tag{1.25}$$

which means that if the potential energy is larger than the kinetic term we will have inflation. This should be provided by a flat enough potential, then the scalar field is expected to roll slowly.

The simplest model of inflation and its predictions is defined by choosing the form of the potential $V(\phi)$. Several models of inflation have been proposed in the literature. We refer the reader to [24] for a review.

1.3 General relativistic perturbations

We present in this section the formalism of the perturbations that origin the CMB anisotropies and the density inhomogeneities that we see in the large scale structure of the Universe today, in the framework of Einstein's theory of general relativity (GR). We refer the reader to [25] for a deeper review.

Este documento incorpora firma electrónica, y es copia auténtica de un documento electrónico archivado por la ULL según la Ley 39/2015.
Su autenticidad puede ser contrastada en la siguiente dirección https://sede.ull.es/validacion/

Identificador del documento: 3764923 Código de verificación: JHlWnlbn

Firmado por:	JOSE RAMON BERMEJO CLIMENT *UNIVERSIDAD DE LA LAGUNA*	Fecha: 01/09/2021 17:41:12
	José Alberto Rubiño Martín *UNIVERSIDAD DE LA LAGUNA*	01/09/2021 17:49:44
	FABIO FINELLI *UNIVERSIDAD DE LA LAGUNA*	02/09/2021 14:12:21

Universidad de La Laguna
Oficina de Sede Electrónica
Entrada
Nº registro: 2021/90989
Nº reg. oficina: OF002/2021/89977
Fecha: 03/09/2021 12:24:13

1.3.1 Metric perturbations

We consider the metric in terms of the conformal time as in Eq. (1.3). The most general first-order perturbation can be written as:

$$\mathrm{d}s^2 = a^2(\eta)\{-(1+2A)\mathrm{d}\eta^2 - 2B_i\mathrm{d}\eta\mathrm{d}x^i + [(1+2D)\delta_{ij} + 2E_{ij}]\mathrm{d}x^i\mathrm{d}x^j\}\,. \quad (1.26)$$

The last term specifies the spatial metric perturbation $2(D\delta_{ij} + E_{ij})$, where E_{ij} is taken to be traceless. B_i is the *shift function* and A is the *lapse function*, which specifies the relation between η and the proper time τ. To first order we have:

$$\frac{1}{a(\eta)}\frac{\mathrm{d}\tau}{\mathrm{d}\eta} = \sqrt{1+2A} \approx 1 + A\,. \quad (1.27)$$

The coordinate system $x^\nu = (\eta, x^i)$ is a global system that applies throughout spacetime. At each spacetime point we also speficy a locally orthonormal frame (t, r^i), such that the time directions of the global and local systems are lined up to first order, and the spatial directions up to zero order. From Eq. (1.26), this is equivalent to:

$$\mathrm{d}t = a(1+A)\mathrm{d}\eta\,, \quad (1.28)$$

$$\mathrm{d}r^i = a\mathrm{d}x^i\,. \quad (1.29)$$

1.3.2 Energy-momentum tensor perturbations

We now derive the perturbations of the Energy-momentum tensor of Einstein GR equation. In the local reference frame, the fluid velocity is given by $v^i = \mathrm{d}r^i/\mathrm{d}t$. In the global coordinates, the components $u^\mu = \mathrm{d}x^\mu/d\tau$ of the fluid 4-velocity are:

$$au^0 = 1\,, \quad (1.30)$$

$$au^i = v^i \equiv v_i\,. \quad (1.31)$$

For the 3-velocity v^i there is no distinction between lower and upper indices. Instead, for the 4-velocity, we have $u_\mu = g_{\mu\nu}u^\nu$, and we find

$$\frac{1}{a}u_0 = -1\,, \quad (1.32)$$

$$\frac{1}{a}u_i = v_i - B_i\,. \quad (1.33)$$

Este documento incorpora firma electrónica, y es copia auténtica de un documento electrónico archivado por la ULL según la Ley 39/2015.
Su autenticidad puede ser contrastada en la siguiente dirección https://sede.ull.es/validacion/

Identificador del documento: 3764923 Código de verificación: JHlWnlbn

Firmado por:	JOSE RAMON BERMEJO CLIMENT *UNIVERSIDAD DE LA LAGUNA*	Fecha: 01/09/2021 17:41:12
	José Alberto Rubiño Martín *UNIVERSIDAD DE LA LAGUNA*	01/09/2021 17:49:44
	FABIO FINELLI *UNIVERSIDAD DE LA LAGUNA*	02/09/2021 14:12:21

Universidad de La Laguna
Oficina de Sede Electrónica
Entrada
Nº registro: 2021/90989
Nº reg. oficina: OF002/2021/89977
Fecha: 03/09/2021 12:24:13

We now consider the expression of the energy-momentum tensor for a perfect fluid, which reads:

$$T^{\mu}_{\nu} = (\rho + P)u^{\mu}u_{\nu} + P\delta^{\mu}_{\nu} + \Sigma^{\mu}_{\nu}\,, \tag{1.34}$$

where Σ^{μ}_{ν} is the anisotropic stress. Working out up to first order, we have:

$$T^{0}_{0} = -(\rho + \delta\rho)\,, \tag{1.35}$$

$$T^{0}_{i} = (\rho + P)(v_i - B_i)\,, \tag{1.36}$$

$$T^{i}_{0} = -(\rho + P)v^{i}\,, \tag{1.37}$$

$$T^{i}_{j} = (P + \delta P)\delta^{i}_{j} + \Sigma^{i}_{j}\,. \tag{1.38}$$

It is also convenient to define a dimensionless anisotropic stress as $\Pi_{ij} \equiv \Sigma_{ij}/P$. Considering only the scalar mode, we can write:

$$B_i \equiv -\frac{ik_i}{k}B\,, \tag{1.39}$$

$$E_{ij} \equiv \left(-\frac{k_i k_j}{k^2} + \frac{1}{3}\delta_{ij}\right)E\,, \tag{1.40}$$

$$v_i \equiv -\frac{ik_i}{k}V\,, \tag{1.41}$$

$$\Pi_{ij} \equiv \left(-\frac{k_i k_j}{k^2} + \frac{1}{3}\delta_{ij}\right)\Pi\,. \tag{1.42}$$

We consider as well that in the scalar mode:

$$\delta x_i = -i\frac{k^i}{k}\delta x\,. \tag{1.43}$$

If we apply the gauge transformation for a perturbation to the metric, we get the following perturbed quantities:

$$\tilde{A} = A - (\delta\eta)' - aH\delta\eta\,, \tag{1.44}$$

$$\tilde{B} = B + (\delta x)' + k\delta\eta \tag{1.45}$$

,

$$\tilde{D} = D - \frac{k}{3}\delta x - aH\delta\eta\,, \tag{1.46}$$

$$\tilde{E} = E + k\delta x\,. \tag{1.47}$$

Este documento incorpora firma electrónica, y es copia auténtica de un documento electrónico archivado por la ULL según la Ley 39/2015.
Su autenticidad puede ser contrastada en la siguiente dirección https://sede.ull.es/validacion/

Identificador del documento: 3764923 Código de verificación: JHlWnlbn

Firmado por: JOSE RAMON BERMEJO CLIMENT — Fecha: 01/09/2021 17:41:12
UNIVERSIDAD DE LA LAGUNA

José Alberto Rubiño Martín — 01/09/2021 17:49:44
UNIVERSIDAD DE LA LAGUNA

FABIO FINELLI — 02/09/2021 14:12:21
UNIVERSIDAD DE LA LAGUNA

Universidad de La Laguna
Oficina de Sede Electrónica
Entrada
Nº registro: 2021/90989
Nº reg. oficina: OF002/2021/89977
Fecha: 03/09/2021 12:24:13

Applying the gauge transformation to the energy-momentum tensor, we obtain:

$$\tilde{V} = V + (\delta x)' \,, \tag{1.48}$$

$$\tilde{\delta} = \delta + 3(1+w)aH\delta\eta \,, \tag{1.49}$$

$$\delta\tilde{P} = \delta P - \dot{P}\delta\eta \,, \tag{1.50}$$

$$\tilde{\Pi} = \Pi \,. \tag{1.51}$$

In these equations, we have introduced the *density contrast*, defined as $\delta \equiv \delta\rho/\rho$, and we have used the continuity equation for the density ρ and the definition of the equation of state $w \equiv P/\rho$.

1.3.3 Evolution of perturbations

We introduce the *conformal Newtonian gauge*, which is determined by the line element:

$$\mathrm{d}s^2 = a^2(\eta) = \left[-(1+2\Psi)\mathrm{d}\eta^2 + (1-2\Phi)\delta_{ij}\mathrm{d}x^i\mathrm{d}x^j\right] \tag{1.52}$$

This gauge is chosen in a way that $B = E = 0$ vanish, and we call Φ and Ψ the *gravitational potentials*. The other commonly adopted gauge is called the *synchronous gauge*, in which $A = B = 0$.

We use the continuity ($D_\mu T^\mu_0 = 0$) and Euler ($D_\mu T^\mu_i = 0$) equations and find the following first-order perturbations:

$$\dot{\rho} = -(1+w)(kV - 3\dot{\Phi}) + 3aHw\left(\delta - \frac{\delta P}{P}\right) \,, \tag{1.53}$$

$$\dot{V} = -aH(1-3w)V - \frac{\dot{w}}{1+w}V + k\frac{\delta P}{\rho+P} - \frac{2}{3}k\frac{w}{1+w}\Pi + k\Psi \,. \tag{1.54}$$

From the Einstein field equations, we find:

$$\delta + 3\frac{aH}{k}(1+w)V = -\frac{2}{3}\left(\frac{k}{aH}\right)^2\Phi \,, \tag{1.55}$$

$$\Pi = \left(\frac{k}{aH}\right)^2(\Psi - \Phi) \,, \tag{1.56}$$

Este documento incorpora firma electrónica, y es copia auténtica de un documento electrónico archivado por la ULL según la Ley 39/2015.
Su autenticidad puede ser contrastada en la siguiente dirección https://sede.ull.es/validacion/

Identificador del documento: 3764923 Código de verificación: JHlWnlbn

Firmado por:	JOSE RAMON BERMEJO CLIMENT *UNIVERSIDAD DE LA LAGUNA*	Fecha: 01/09/2021 17:41:12
	José Alberto Rubiño Martín *UNIVERSIDAD DE LA LAGUNA*	01/09/2021 17:49:44
	FABIO FINELLI *UNIVERSIDAD DE LA LAGUNA*	02/09/2021 14:12:21

Universidad de La Laguna
Oficina de Sede Electrónica
Entrada
Nº registro: 2021/90989
Nº reg. oficina: OF002/2021/89977
Fecha: 03/09/2021 12:24:13

which are called the *constraint equations*, given that they do not involve time derivatives. On scales well inside the horizon ($k \gg aH$), we expect that the first equation becomes

$$\delta = -\frac{2}{3}\left(\frac{k}{aH}\right)^2 \Phi\,, \tag{1.57}$$

which is called the *Poisson equation*. We expect that when the Universe is matter dominated, $\Phi = \Psi$.

If the cosmic fluid has many components, the total perturbations are:

$$\delta\rho = \sum_i \delta\rho_i\,, \tag{1.58}$$

$$(\rho + P)V = \sum_i (\rho_i + P_i)V_i\,, \tag{1.59}$$

$$\delta P = \sum_i \delta P_i\,, \tag{1.60}$$

$$P\Pi = \sum_i P_i \Pi_i\,. \tag{1.61}$$

Those components that do not exchange energy with their surroundings will satisfy the continuity equation; and those that do not exchange momentum will satisfy the Euler equation.

We consider that the cosmic fluid has four components: cold dark matter (CDM), baryons (B), photons (γ) and neutrinos (ν). Since the cold dark matter does not interact and has no pressure, it will satisfy the continuity and Euler equations:

$$\dot{\delta_c} = -kV_c + 3\dot{\Phi}\,, \tag{1.62}$$

$$\dot{V_c} = -aHV_c + k\Psi\,. \tag{1.63}$$

Photons and baryons will satisfy the continuity equation, since the Thomson scattering does not modify the photon energy:

$$\dot{\delta_\gamma} = -\frac{4}{3}kV_\gamma + 4\dot{\Phi}\,, \tag{1.64}$$

$$\dot{\delta_B} = -kV_B + 3\dot{\Phi}\,. \tag{1.65}$$

Este documento incorpora firma electrónica, y es copia auténtica de un documento electrónico archivado por la ULL según la Ley 39/2015.
Su autenticidad puede ser contrastada en la siguiente dirección https://sede.ull.es/validacion/

Identificador del documento: 3764923 Código de verificación: JHlWnlbn

Firmado por:	JOSE RAMON BERMEJO CLIMENT *UNIVERSIDAD DE LA LAGUNA*	Fecha: 01/09/2021 17:41:12
	José Alberto Rubiño Martín *UNIVERSIDAD DE LA LAGUNA*	01/09/2021 17:49:44
	FABIO FINELLI *UNIVERSIDAD DE LA LAGUNA*	02/09/2021 14:12:21

Universidad de La Laguna
Oficina de Sede Electrónica
Entrada
Nº registro: 2021/90989
Nº reg. oficina: OF002/2021/89977
Fecha: 03/09/2021 12:24:13

We assume that Thomson scattering of photons off electrons prevents completely the photon diffusion (the tight-coupling approximation). Since the electron and proton number density is the same, we find

$$V_B = V_\gamma \,, \tag{1.66}$$

$$\frac{\delta(n_B/n_\gamma)}{n_B/n_\gamma} = \delta_B - \frac{3}{4}\delta_\gamma = \text{constant} \,, \tag{1.67}$$

where n_B and n_γ are the baryon and photon number densities. The Euler equation for the baryon-photon fluid reads:

$$\dot{V}_\gamma = -aH(1-3\tilde{w})V_\gamma - \frac{\tilde{w}}{1+\tilde{w}}V_\gamma + \frac{k}{3}\frac{\rho_\gamma}{\rho_B + (4/3)\rho_\gamma}\rho_\gamma + k\Psi \,. \tag{1.68}$$

The anisotropic stress for the baryon-photon fluid vanishes in the case we ignore the neutrino perturbation, and for the tight-coupling approximation we get $\Phi = \Psi$.

1.4 The ΛCDM concordance model

In this section we describe the characteristics and parameters of the so-called concordance ΛCDM model of the Universe. This model contains six free parameters and is compatible with all the observations from the CMB and LSS probes at present-day. However, the tensions on the value of some of the parameters measured from different cosmological probes has recently become a hot topic in cosmology, opening the question about the need of new physics.

1.4.1 Parameters

In order to describe the evolution of the Universe after the Big Bang nucleosynthesis (BBN), including perturbations, we need various ingredients.

First, we need some kind of non-baryonic matter, which we call cold dark matter (CDM), that has a negligible interaction with itself and other components and more or less a negligible random motion. Second, we need a dark energy component that is time independent, which dominates at low redshift.

The simplest ΛCDM model assumes that the interactions and motion of the CDM are totally negligible, and sets the dark energy to be a cosmological constant. The unperturbed Universe could be then defined with

Este documento incorpora firma electrónica, y es copia auténtica de un documento electrónico archivado por la ULL según la Ley 39/2015.
Su autenticidad puede ser contrastada en la siguiente dirección https://sede.ull.es/validacion/

Identificador del documento: 3764923 Código de verificación: JHlWnlbn

Firmado por:	JOSE RAMON BERMEJO CLIMENT *UNIVERSIDAD DE LA LAGUNA*	Fecha: 01/09/2021 17:41:12
	José Alberto Rubiño Martín *UNIVERSIDAD DE LA LAGUNA*	01/09/2021 17:49:44
	FABIO FINELLI *UNIVERSIDAD DE LA LAGUNA*	02/09/2021 14:12:21

Universidad de La Laguna
Oficina de Sede Electrónica
Entrada
Nº registro: 2021/90989
Nº reg. oficina: OF002/2021/89977
Fecha: 03/09/2021 12:24:13

just three parameters: the Hubble constant H_0, which measures the expansion rate of the Universe, the baryon density $\Omega_{\rm b}$ and the total matter density $\Omega_{\rm m}$ including dark matter.

In practice, to describe the primordial curvature perturbation we need another two parameters, one corresponding to the amplitude (A_s) and another corresponding to the spectral index (n_s). In some cases, the fluctuation amplitudes can be also described with σ_8, that represents the RMS mass fluctuations on the 8 h^{-1} Mpc scale (where $h \equiv H_0/100$ km s^{-1} Mpc^{-1}).

Finally, we need a sixth parameter to characterize the effects of reionization. Reionization is caused by the early formation of objects that emit radiation and are able to ionize the neutral hydrogen, and it has an effect on the CMB since photons interact with these particles. A suitable parameter for characterizing reionization is the optical depth τ, such that $e^{-\tau}$ is the probability that a photon emitted before reionization (but after photon decoupling) rescatters.

1.4.2 Tensions between current cosmological data

Observations from the CMB and LSS probes are fully compatible with the ΛCDM model, without any observation that has favoured any of its extensions in recent years. However, some tensions on the measured value of the parameters from the different cosmological datasets remain, and in some cases have become larger across time due to the increasing precision of cosmological experiments.

One of the main open problems regarding current measurements is the H_0 tension. Observations at low redshift of the Cepheid-calibrated supernovae [26, 27] and strong lensing time-delays [28] suggest a value around $H_0 \sim 74$ km s^{-1} Mpc^{-1}. On the other hand, CMB data [46], together with LSS probes [29–34] and local measurements based on the inverse distance ladder technique [35,36] favour a lower H_0, around 67 km s^{-1} Mpc^{-1}.

We show in Fig. 1.1 the evolution on the past two decades of the measurements of H_0 from the local Universe (supernovae) and from the CMB. In particular, the tension between the last CMB measurement assuming the ΛCDM model ($H_0 = 67.27 \pm 0.60$ s^{-1} Mpc^{-1}) and the SH$_0$ES team measurement ($H_0 = 74.03 \pm 1.42$ km s^{-1} Mpc^{-1}) result in a 4.4σ discrepancy. This disagreement could be due to the presence of uncorrected systematics or be a suggestion of the need of new physics beyond the

Este documento incorpora firma electrónica, y es copia auténtica de un documento electrónico archivado por la ULL según la Ley 39/2015.
Su autenticidad puede ser contrastada en la siguiente dirección https://sede.ull.es/validacion/

Identificador del documento: 3764923 Código de verificación: JHlWnlbn

Firmado por:	JOSE RAMON BERMEJO CLIMENT *UNIVERSIDAD DE LA LAGUNA*	Fecha: 01/09/2021 17:41:12
	José Alberto Rubiño Martín *UNIVERSIDAD DE LA LAGUNA*	01/09/2021 17:49:44
	FABIO FINELLI *UNIVERSIDAD DE LA LAGUNA*	02/09/2021 14:12:21

Universidad de La Laguna
Oficina de Sede Electrónica
Entrada
Nº registro: 2021/90989
Nº reg. oficina: OF002/2021/89977
Fecha: 03/09/2021 12:24:13

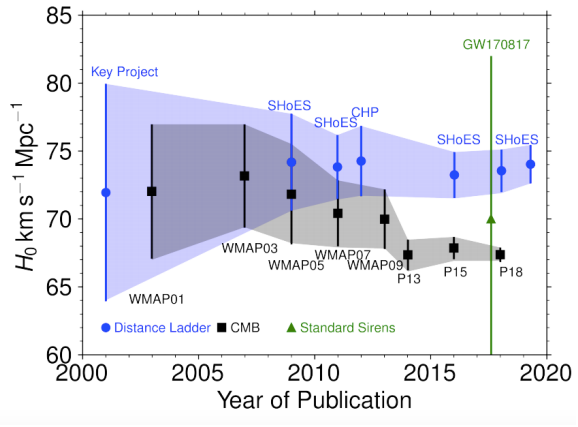

FIGURE 1.1— Evolution of the constraints on H_0 from the CMB and from the distance ladders (supernovae) on the last two decades. Credits: W. Friedmann (see [37])

ΛCDM model.

Another discrepancy between different cosmological datasets is the S_8 tension. Large scale structure observations are able to constrain mainly the total matter density $\Omega_{\rm m}$ and the fluctuation amplitude σ_8 parameters of the ΛCDM model. However, it has been found a difference with respect to the CMB constraints in the ($\Omega_{\rm m}$,σ_8) plane. The last results from the Dark Energy Survey (DES) Year 3 results [38], including the galaxy number counts and weak lensing from $\sim$ 100 million galaxies, report a tension of $\sim 2.3\sigma$ with respect to the *Planck* 2018 data [46] in the S_8 parameter, defined as $S_8 \equiv \sigma_8\sqrt{\Omega_{\rm m}/0.3}$. We show in Fig. 1.2 the differences found in the ($\Omega_{\rm m}$,σ_8) plane considering the cosmic shear information from DES and the CMB data from *Planck*.

Recently, many solutions have been proposed to the H_0 tension, which is the stronger one in statistical terms. These solutions mainly try to extend the cosmological standard model in order to reduce the statistical deviation. In the upcoming years, LSS surveys will measure the matter distribution of the Universe with an unprecedented sensitivity. The analysis of their data and the combination and cross-correlation of these surveys with the CMB information will be crucial to constrain extended models

Este documento incorpora firma electrónica, y es copia auténtica de un documento electrónico archivado por la ULL según la Ley 39/2015.
Su autenticidad puede ser contrastada en la siguiente dirección https://sede.ull.es/validacion/

Identificador del documento: 3764923 Código de verificación: JHlWnlbn

Firmado por:	JOSE RAMON BERMEJO CLIMENT *UNIVERSIDAD DE LA LAGUNA*	Fecha: 01/09/2021 17:41:12
	José Alberto Rubiño Martín *UNIVERSIDAD DE LA LAGUNA*	01/09/2021 17:49:44
	FABIO FINELLI *UNIVERSIDAD DE LA LAGUNA*	02/09/2021 14:12:21

Universidad de La Laguna
Oficina de Sede Electrónica
Entrada
Nº registro: 2021/90989
Nº reg. oficina: OF002/2021/89977
Fecha: 03/09/2021 12:24:13

and to understand whether the H_0 and S_8 tensions are or not a hint of new physics.

Este documento incorpora firma electrónica, y es copia auténtica de un documento electrónico archivado por la ULL según la Ley 39/2015.
Su autenticidad puede ser contrastada en la siguiente dirección https://sede.ull.es/validacion/

Identificador del documento: 3764923 Código de verificación: JHlWnlbn

Firmado por:	JOSE RAMON BERMEJO CLIMENT *UNIVERSIDAD DE LA LAGUNA*	Fecha: 01/09/2021 17:41:12
	José Alberto Rubiño Martín *UNIVERSIDAD DE LA LAGUNA*	01/09/2021 17:49:44
	FABIO FINELLI *UNIVERSIDAD DE LA LAGUNA*	02/09/2021 14:12:21

Universidad de La Laguna
Oficina de Sede Electrónica
Entrada
Nº registro: 2021/90989
Nº reg. oficina: OF002/2021/89977
Fecha: 03/09/2021 12:24:13

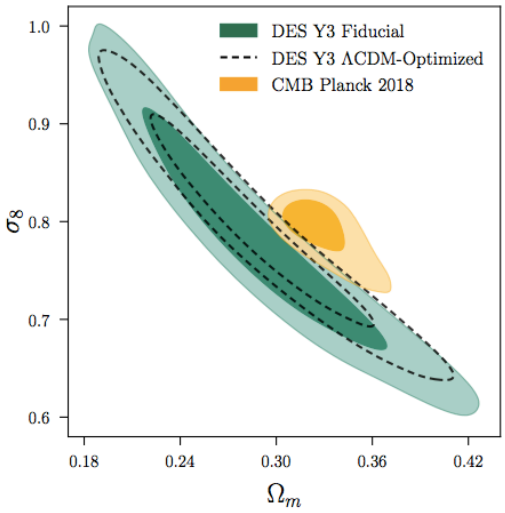

FIGURE 1.2— Posterior distributions on the (σ_8, Ω_m) plane obtained from cosmic shear information from DES and the CMB data from *Planck*. Image from [38]

Este documento incorpora firma electrónica, y es copia auténtica de un documento electrónico archivado por la ULL según la Ley 39/2015.
Su autenticidad puede ser contrastada en la siguiente dirección https://sede.ull.es/validacion/

Identificador del documento: 3764923 Código de verificación: JHlWnlbn

Firmado por:	JOSE RAMON BERMEJO CLIMENT *UNIVERSIDAD DE LA LAGUNA*	Fecha: 01/09/2021 17:41:12
	José Alberto Rubiño Martín *UNIVERSIDAD DE LA LAGUNA*	01/09/2021 17:49:44
	FABIO FINELLI *UNIVERSIDAD DE LA LAGUNA*	02/09/2021 14:12:21

Universidad de La Laguna
Oficina de Sede Electrónica
Entrada
Nº registro: 2021/90989
Nº reg. oficina: OF002/2021/89977
Fecha: 03/09/2021 12:24:13

Este documento incorpora firma electrónica, y es copia auténtica de un documento electrónico archivado por la ULL según la Ley 39/2015.
Su autenticidad puede ser contrastada en la siguiente dirección https://sede.ull.es/validacion/

Identificador del documento: 3764923 Código de verificación: JHlWnlbn

Firmado por:	JOSE RAMON BERMEJO CLIMENT *UNIVERSIDAD DE LA LAGUNA*	Fecha: 01/09/2021 17:41:12
	José Alberto Rubiño Martín *UNIVERSIDAD DE LA LAGUNA*	01/09/2021 17:49:44
	FABIO FINELLI *UNIVERSIDAD DE LA LAGUNA*	02/09/2021 14:12:21

Universidad de La Laguna
Oficina de Sede Electrónica
Entrada
Nº registro: 2021/90989
Nº reg. oficina: OF002/2021/89977
Fecha: 03/09/2021 12:24:13

2

Cosmological observations

Measurements of the cosmic microwave background anisotropies have reached in the last year precision enough to constrain the parameters of the ΛCDM model at sub-percent level, and future CMB experiments will improve our understanding of the Universe. In addition, many future large scale structure surveys will improve the measurements on this parameters and will open the possibility of constraining extended models that currently are not probed by the CMB. The combination of the two probes including their cross-correlation seems crucial for the future precision cosmology.

In this chapter we review the formalism for describing the observations of the CMB anisotropies (including temperature, polarization and lensing) and two of the main large scale structure trancers (galaxy clustering and weak lensing) in the 2D angular space. We introduce as well the cross-correlations between the CMB fiels and LSS probes.

2.1 The cosmic microwave background

The cosmic microwave background radiation is the relic radiation from Big Bang. It is predicted that at $z \sim 1100$, the Universe was cold enough to allow the combination of electrons with atomic nuclei. This process is called recombination, and in consequence the photons decrease the rate of their interaction with baryons, allowing them to propagate through the Universe until nowadays. The surface in which the photons have their last

Este documento incorpora firma electrónica, y es copia auténtica de un documento electrónico archivado por la ULL según la Ley 39/2015.
Su autenticidad puede ser contrastada en la siguiente dirección https://sede.ull.es/validacion/

Identificador del documento: 3764923 Código de verificación: JHlWnlbn

Firmado por:	JOSE RAMON BERMEJO CLIMENT *UNIVERSIDAD DE LA LAGUNA*	Fecha: 01/09/2021 17:41:12
	José Alberto Rubiño Martín *UNIVERSIDAD DE LA LAGUNA*	01/09/2021 17:49:44
	FABIO FINELLI *UNIVERSIDAD DE LA LAGUNA*	02/09/2021 14:12:21

Universidad de La Laguna
Oficina de Sede Electrónica
Entrada
Nº registro: 2021/90989
Nº reg. oficina: OF002/2021/89977
Fecha: 03/09/2021 12:24:13

interaction with electrons is called the *last scattering surface*.

After the first measurements in the 1960s, in 1990 the NASA satellite COsmic Background Explorer (COBE) [39] confirmed the cosmological origin of this radiation, measuring a blackbody spectrum and determining with a very good precision the CMB temperatrue, $T_0 = 2.725 \pm 0.002$ K. COBE detected as well temperature anisotropies at the $\sim 7^\circ$ scale of the order $\Delta T/T \sim 10^{-5}$. These anisotropies are consistent with the inflation predictions and are a snapshot of the cosmological perturbations at the epoch of recombination.

After COBE, there has been an intense activity to improve the CMB observations accuracy and precision, by several satellite, balloon and ground-based experiments. In 2001, the NASA's Wilkinson Microwaves Anisotropy Probe (WMAP) was launched, and it provided many releases for the 1-year, 3-year, 5-year, 7-year and 9-year data [40–43], improving our understanding of the Universe model. After that, ESA's *Planck* satellite improved the precision of the cosmological parameter errors [44–46], measuring a cosmic variance (CV) limited temperature angular power spectra. In the upcoming years, many experiments will have the target of measuring a CV limited E-mode polarization angular power spectra.

We present in the following subsections the formalism for describing the temperature and polarization anisotropies and the CMB lensing deflection field in the spherical harmonic space.

2.1.1 Temperature anisotropies

The CMB temperature anisotropies pattern is the best observable for describing the physics of the early Universe. The temperature measured in a direction $\hat{\mathbf{n}}$ of the sky by an observer at the $(\eta_0, \mathbf{x_0})$ point is:

$$T(\eta_0, \mathbf{x_0}, \hat{\mathbf{n}}) = T(\eta_0)\left[1 + \Theta(\eta_0, \mathbf{x_0}, \hat{\mathbf{n}})\right] , \tag{2.1}$$

where we have introduced the temperature dimensionless field Θ. This field can be expanded in spherical harmonics as:

$$\Theta(\hat{\mathbf{n}}) = \frac{\delta T(\hat{\mathbf{n}})}{T} = \sum_{\ell} \sum_{m=-\ell}^{\ell} a_{\ell m} Y_{\ell m}(\hat{\mathbf{n}}) , \tag{2.2}$$

where $a_{\ell m}$ are the *multipole moments*, defined as

$$a_{\ell m} = \int \mathrm{d}\Omega Y^*_{\ell m}(\hat{\mathbf{n}})\Theta(\hat{\mathbf{n}}) . \tag{2.3}$$

Este documento incorpora firma electrónica, y es copia auténtica de un documento electrónico archivado por la ULL según la Ley 39/2015.
Su autenticidad puede ser contrastada en la siguiente dirección https://sede.ull.es/validacion/

Identificador del documento: 3764923 Código de verificación: JHlWnlbn

Firmado por: JOSE RAMON BERMEJO CLIMENT — Fecha: 01/09/2021 17:41:12
UNIVERSIDAD DE LA LAGUNA

José Alberto Rubiño Martín — 01/09/2021 17:49:44
UNIVERSIDAD DE LA LAGUNA

FABIO FINELLI — 02/09/2021 14:12:21
UNIVERSIDAD DE LA LAGUNA

Universidad de La Laguna
Oficina de Sede Electrónica
Entrada
Nº registro: 2021/90989
Nº reg. oficina: OF002/2021/89977
Fecha: 03/09/2021 12:24:13

We also define the *angular power spectrum* as

$$\delta_{\ell\ell'}\delta_{mm'}C_\ell = \langle a_{\ell m} a^*_{\ell' m'} \rangle \,, \tag{2.4}$$

where the brackets denote the average over an ensemble of realizations of the fluctuations. In an ideal case in which we neglect the noise, the angular power spectrum of the CMB can be obtained as

$$\hat{C}_\ell = \frac{1}{2\ell+1} \sum_{m=-\ell}^{\ell} |a_{\ell m}|^2 \,. \tag{2.5}$$

In this case, $\hat{C}_\ell$ is an unbiased estimator of the true ensemble. However, for an all sky statistical analysis of the CMB, the anisotropies are affected by the *cosmic variance*, which is connected to the fact that we are doing a statistical analysis of one single realization (the only sky that we observe). The number of modes at a given multipole is given by $2\ell+1$, this means that for high multipoles, associated to smaller scales, we will have more information to drawn, while at large scales there will be less information available. In particular, low multipoles are affected by the cosmic variance:

$$\frac{\Delta C_\ell}{C_\ell} = \sqrt{\frac{2}{2\ell+1}} \,. \tag{2.6}$$

The multipole moment can be expressed as well in terms of the primordial power spectrum of curvature perturbations $\mathcal{P}_\mathcal{R}(k)$ as:

$$a_{\ell m} = 4\pi(-i)^\ell \int \frac{\mathrm{d}^3 k}{(2\pi)^3} \Theta_\ell(k) \mathcal{P}_\mathcal{R}(k) Y_{\ell m}(k) \,, \tag{2.7}$$

where $\Theta_\ell(k)$ is the transfer function, that can be obtained as the line-of-sight solution of the Bolztmann equation [47]:

$$\begin{aligned} \Theta_\ell(k) = \left(\Phi + \frac{1}{3}\delta_\gamma \right)\Big|_{\eta_*} j_\ell(k(\eta_0 - \eta_*)) + v_\gamma(\eta_+) j'_\ell(k(\eta_0 - \eta_*)) \\ +2\int_{\eta_*}^{\eta_0} \mathrm{d}\eta \dot{\Phi} j_\ell(k(\eta_0 - \eta)) \,. \end{aligned} \tag{2.8}$$

where η_* represents the conformal time at the last scattering surface ($z \sim 1100$). The angular power spectrum can be expressed now as a function of $\Theta_\ell(k)$:

$$C_\ell = \frac{2}{\pi} \int k^2 \mathrm{d}k \mathcal{P}_\mathcal{R}(k) \Theta^2_\ell(k) \,. \tag{2.9}$$

Este documento incorpora firma electrónica, y es copia auténtica de un documento electrónico archivado por la ULL según la Ley 39/2015.
Su autenticidad puede ser contrastada en la siguiente dirección https://sede.ull.es/validacion/

Identificador del documento: 3764923 Código de verificación: JHlWnlbn

Firmado por:	JOSE RAMON BERMEJO CLIMENT *UNIVERSIDAD DE LA LAGUNA*	Fecha: 01/09/2021 17:41:12
	José Alberto Rubiño Martín *UNIVERSIDAD DE LA LAGUNA*	01/09/2021 17:49:44
	FABIO FINELLI *UNIVERSIDAD DE LA LAGUNA*	02/09/2021 14:12:21

Universidad de La Laguna
Oficina de Sede Electrónica
Entrada
Nº registro: 2021/90989
Nº reg. oficina: OF002/2021/89977
Fecha: 03/09/2021 12:24:13

From the combination of the last two equations, we obtain the following terms, connected to the three terms in $\Theta_\ell(k)$:

- The Sachs-Wolfe (SW) term, which describes the evolution of the primordial perturbations into the the metric and density perturbations described by δ_γ.
- The Doppler term, related to the velocity of photons v_γ.
- The Integrated Sachs-Wolfe (ISW) term, which is an additional contribution due to the variation of the gravitational potentials Φ, Ψ with time. The potentials vary with time when the Universe is not matter dominated, hence the ISW term has a contribution from early times in which the Universe is radiation dominated, and a late time contribution due to the cosmological constant Λ.

Further, we also obtain three cross terms between the above ones, which represent a small contribution.

2.1.2 Polarization anisotropies

It is expected that scattering during recombination genetares linear polarization in the CMB radiation [48]. Furthermore, at large scales, reionization scattering induces also an extra polarization.

The polarization is commonly treated in terms of the Stokes parameters: I is the intensity, Q and U describe the linear polarization and V the circular polarization.

$$(Q \pm iU)(\hat{\mathbf{n}}) = \sum_\ell \sum_{m=-\ell}^{\ell} a^{\pm 2}_{\ell m} Y^{\pm 2}_{\ell m}(\hat{\mathbf{n}})\,. \tag{2.10}$$

It is useful to introduce the following multipole moments for the E-mode and B-mode polarization:

$$a^E_{\ell m} = \frac{1}{2}\left(a^{+2}_{\ell m} + a^{-2}_{\ell m}\right)\,, \tag{2.11}$$

$$a^B_{\ell m} = \frac{1}{2}\left(a^{+2}_{\ell m} - a^{-2}_{\ell m}\right)\,, \tag{2.12}$$

which are associated with the following fields:

$$E(\hat{\mathbf{n}}) = \sum_\ell \sum_{m=-\ell}^{\ell} a^E_{\ell m} Y_{\ell m}(\hat{\mathbf{n}})\,, \tag{2.13}$$

Este documento incorpora firma electrónica, y es copia auténtica de un documento electrónico archivado por la ULL según la Ley 39/2015.
Su autenticidad puede ser contrastada en la siguiente dirección https://sede.ull.es/validacion/

Identificador del documento: 3764923 Código de verificación: JHlWnlbn

Firmado por:	JOSE RAMON BERMEJO CLIMENT *UNIVERSIDAD DE LA LAGUNA*	Fecha: 01/09/2021 17:41:12
	José Alberto Rubiño Martín *UNIVERSIDAD DE LA LAGUNA*	01/09/2021 17:49:44
	FABIO FINELLI *UNIVERSIDAD DE LA LAGUNA*	02/09/2021 14:12:21

Universidad de La Laguna
Oficina de Sede Electrónica
Entrada
Nº registro: 2021/90989
Nº reg. oficina: OF002/2021/89977
Fecha: 03/09/2021 12:24:13

$$B(\hat{\mathbf{n}}) = \sum_{\ell} \sum_{m=-\ell}^{\ell} a^{B}_{\ell m} Y_{\ell m}(\hat{\mathbf{n}})\,. \tag{2.14}$$

Appart from the three autocorrelations of the temperature and polarization anisotropies (TT, EE and BB), we have to consider the cross-correlation between temperature and E-modes, TE. The other two cross-correlations, TB and EB, vanish under parity symmetry.

We can generalize the expression for the angular power spectrum in order to introduce the cross-correlations as:

$$C_{\ell}^{X,Y} = \frac{1}{2\ell+1} \sum_{m=-\ell}^{\ell} \langle a^{X}_{\ell m}{}^{*} a^{Y}_{\ell m} \rangle\,, \tag{2.15}$$

where $X, Y = T, E, B$.

2.1.3 CMB lensing

The CMB weak lensing is originated by the fact that photons from the last scattering surface pass through cosmic structures in their path to us. Due to the gravitational lensing effect, we detect a deflection field $\mathbf{d}$ that maps the shift in the direction of a photon. For the temperature and polarization fields, we have [49–51]:

$$\tilde{\Theta}(\hat{\mathbf{n}}) = \Theta(\hat{\mathbf{n}} + \mathbf{d}\hat{\mathbf{n}})\,, \tag{2.16}$$

$$(\tilde{Q} \pm i\tilde{U})(\hat{\mathbf{n}}) = (Q \pm iU)(\hat{\mathbf{n}} + \mathbf{d}\hat{\mathbf{n}})\,, \tag{2.17}$$

where we denote with the tilde the lensed fields. The deflection field can be written as a gradient of the lensing potential ϕ:

$$\mathbf{d} = \nabla\phi\,. \tag{2.18}$$

The lensing potential for the CMB is defined as [52, 53]:

$$\phi(\hat{\mathbf{n}}) = 2\int_{0}^{z_*} \frac{\mathrm{d}z}{H(z)} \left(\frac{1}{\chi(z)} - \frac{1}{\chi(z*)}\right) \Phi(\hat{\mathbf{n}}, z)\,, \tag{2.19}$$

and it can be expanded in spherical harmonics as

$$\phi(\hat{\mathbf{n}}) = \sum_{\ell} \sum_{m=-\ell}^{\ell} \phi_{\ell m} Y_{\ell m}(\hat{\mathbf{n}})\,. \tag{2.20}$$

Este documento incorpora firma electrónica, y es copia auténtica de un documento electrónico archivado por la ULL según la Ley 39/2015.
Su autenticidad puede ser contrastada en la siguiente dirección https://sede.ull.es/validacion/

Identificador del documento: 3764923 Código de verificación: JHlWnlbn

Firmado por:	JOSE RAMON BERMEJO CLIMENT *UNIVERSIDAD DE LA LAGUNA*	Fecha: 01/09/2021 17:41:12
	José Alberto Rubiño Martín *UNIVERSIDAD DE LA LAGUNA*	01/09/2021 17:49:44
	FABIO FINELLI *UNIVERSIDAD DE LA LAGUNA*	02/09/2021 14:12:21

Universidad de La Laguna
Oficina de Sede Electrónica
Entrada
Nº registro: 2021/90989
Nº reg. oficina: OF002/2021/89977
Fecha: 03/09/2021 12:24:13

The deflection map is defined as:

$$d_{\ell m} = -i\sqrt{\ell(\ell+1)}\phi_{\ell m}\,. \tag{2.21}$$

With this we can define the angular power spectrum of the CMB lensing deflection and of the CMB lensing potential, which are related through:

$$C_\ell^{dd} = \langle d^*_{\ell m} d_{\ell m}\rangle = \ell(\ell+1)C_\ell^{\phi\phi}\,. \tag{2.22}$$

2.2 Large scale structure tracers and their cross-correlations

Several galaxy surveys, using various techniques, have been planned in order to measure the distribution of the large scale structure of the Universe and obtain cosmological implications.

As recent example, we can mention the last release of the Sloan Digital Sky Survey (SDSS), named eBOSS [54], which has measured the spectra of ~ 4 million galaxies. Also in the last years, the Dark Energy Survey (DES) [55] has improved our understanding of the Universe by measuring the galaxy clustering and weak lensing from ~ 100 million galaxies using a photometric survey. DESI [124] is an ongoing spectroscopic survey that will cover $\sim 1/3$ of the sky and measure the spectra of ~ 50 million objects. In the next decade, experiments such as Euclid, Vera C. Rubin Observatory, SPHEREx and SKA will measure the matter distribution of the Universe with even higher depth and precision.

In the following, we present the formalism for treating the two main probes of large scale structure surveys in the harmonic domain: galaxy number counts and weak lensing.

2.2.1 Galaxy number counts

Galaxy number counts, also referred as *galaxy clustering*, trace the distribution of the dark matter of the Universe, which is related to the baryon distribution that we can observe with large spectroscopic or photometric surveys. This probe is usually analyzed in the 3D Fourier space using the matter power spectrum. In this work, instead, we will study the projection into the 2D harmonic domain, which will allow to account for the cross-correlation between galaxy number counts and other fields, such as the CMB or the galaxy weak lensing.

Este documento incorpora firma electrónica, y es copia auténtica de un documento electrónico archivado por la ULL según la Ley 39/2015.
Su autenticidad puede ser contrastada en la siguiente dirección https://sede.ull.es/validacion/

Identificador del documento: 3764923 Código de verificación: JHlWnlbn

Firmado por:	JOSE RAMON BERMEJO CLIMENT *UNIVERSIDAD DE LA LAGUNA*	Fecha: 01/09/2021 17:41:12
	José Alberto Rubiño Martín *UNIVERSIDAD DE LA LAGUNA*	01/09/2021 17:49:44
	FABIO FINELLI *UNIVERSIDAD DE LA LAGUNA*	02/09/2021 14:12:21

Universidad de La Laguna
Oficina de Sede Electrónica
Entrada
Nº registro: 2021/90989
Nº reg. oficina: OF002/2021/89977
Fecha: 03/09/2021 12:24:13

In general, the angular power spectrum of two fields cross-correlation can be calculated as

$$C_\ell^{XY} = 4\pi \int \frac{\mathrm{d}k}{k} \mathcal{P}_\mathcal{R}(k) I_\ell^X(k) I_\ell^Y(k)\,, \tag{2.23}$$

where $\mathcal{P}_\mathcal{R}(k) \equiv k^3 P(k)/(2\pi^2)$ is the dimensionless primordial power spectrum and $I_\ell^X(k)$ is the kernel for the X field for unit primordial power spectrum.

The kernel of the galaxy number counts is given, if we neglect the corrections from redshift space distortions (RSD) and general relativity (GR), by [69]

$$I_\ell^G(k) = \int_0^\infty \frac{\mathrm{d}z}{(2\pi)^{3/2}} \frac{c}{H(z)} \frac{\mathrm{d}N}{\mathrm{d}z}(z) \Delta_k(z) j_\ell(k\chi(z))\,, \tag{2.24}$$

where $\mathrm{d}N/\mathrm{d}z$ is the normalized window function for the redshift distribution of sources, $\chi(z)$ is the conformal distance, and j_ℓ the spherical Bessel functions. Here $\Delta_k(z)$ is the total number counts fluctuation in Newtonian gauge, usually approximated to

$$\Delta_k(z) \simeq b_G(z) \delta_k^{\mathrm{c}}(z)\,, \tag{2.25}$$

where $b_G(z)$ is the galaxy bias and $\delta_k^{\mathrm{c}}(z)$ is the comoving-gauge linear matter density perturbation. The galaxy bias b_G accounts for the fact that the galaxy density is a tracer that is biased with respect to the total matter density fluctuations, which is the quantity that we are interested in measuring.

While lensing and other lightcone effects on the galaxy number counts angular power spectra have a small impact on the uncertainties on cosmological parameters, it will be necessary to model these contributions in order to avoid biases on cosmological parameters such as dark-energy parameters and the total neutrino mass [64, 70–75].

The CMB temperature kernel, when cross-correlated with galaxy counts is given by the ISW contribution

$$I_\ell^{\mathrm{ISW}}(k) = -\int_0^\infty \mathrm{d}z\; e^{-\tau} \left(\frac{\mathrm{d}\Phi}{\mathrm{d}z} + \frac{\mathrm{d}\Psi}{\mathrm{d}z} \right) j_\ell(k\chi(z))\,, \tag{2.26}$$

where τ is the reionization optical depth and Φ, Ψ are the gravitational potentials defined by the metric perturbations.

Este documento incorpora firma electrónica, y es copia auténtica de un documento electrónico archivado por la ULL según la Ley 39/2015.
Su autenticidad puede ser contrastada en la siguiente dirección https://sede.ull.es/validacion/

Identificador del documento: 3764923 Código de verificación: JHlWnlbn

Firmado por:	JOSE RAMON BERMEJO CLIMENT *UNIVERSIDAD DE LA LAGUNA*	Fecha: 01/09/2021 17:41:12
	José Alberto Rubiño Martín *UNIVERSIDAD DE LA LAGUNA*	01/09/2021 17:49:44
	FABIO FINELLI *UNIVERSIDAD DE LA LAGUNA*	02/09/2021 14:12:21

Universidad de La Laguna
Oficina de Sede Electrónica
Entrada
Nº registro: 2021/90989
Nº reg. oficina: OF002/2021/89977
Fecha: 03/09/2021 12:24:13

The CMB lensing potential kernel is given by [76]

$$I_\ell^\phi(k) = \frac{3\Omega_{m,0}H_0^2}{k^2 c}\int_0^\infty \frac{\mathrm{d}z}{(2\pi)^{3/2}}\frac{1+z}{H(z)}\left(\frac{\chi(z_*)-\chi(z)}{\chi(z_*)\chi(z)}\right)\delta_k^{\mathrm{c}}(z) j_\ell(k\chi(z))\,, \tag{2.27}$$

where z_* is the redshift of the last scattering surface ($z_* \simeq 1100$). We discuss in Section 3.3 the effect of the non-linear corrections on the CMB lensing, galaxy and cross-correlation power spectra, which are modelled with `halofit` [67, 77].

We now describe all the RSD and GR contributions to the observed galaxy number counts $\Delta_k(z)$.

Contributions from RSD and general relativity

The observed number counts $\Delta_\ell(k,z)$ can be split in the density term plus various corrections:

$$\Delta_\ell(k,z) = \Delta_\ell^{\mathrm{D}} + \Delta_\ell^{\mathrm{RSD}} + \Delta_\ell^{\mathrm{L}} + \Delta_\ell^{\mathrm{V}} + \Delta_\ell^{\mathrm{TD}} + \Delta_\ell^{\mathrm{ISW}} + \Delta_\ell^{\mathrm{P}}\,. \tag{2.28}$$

The density term Δ_ℓ^{D} is defined as

$$\Delta_\ell^{\mathrm{D}} = b(z)\delta_k^{\mathrm{s}}(z) j_\ell(k\chi) + (b_e - 3)\,\mathcal{H}(z)\frac{v_k}{k} j_\ell(k\chi)\,, \tag{2.29}$$

where $\delta_k^{\mathrm{s}}(z)$ is the synchronous-gauge linear matter density perturbation, $\mathcal{H}$ is the conformal Hubble parameter and b_e is the evolution bias, which is defined as $b_e = \partial[a^3\bar{N}]/\partial \ln a$, here $\bar{N}$ is the number density of background sources. We can rewrite $\Delta_\ell^{\mathrm{D}} = \delta_k^{\mathrm{n}}(z) j_\ell(k\chi)$ if we define the Newtonian-gauge density perturbation as

$$\delta_k^{\mathrm{n}}(z) = b_G(z)\delta_k^{\mathrm{s}}(z) + (b_e - 3)\,\mathcal{H}(z)\frac{v_k}{k}\,, \tag{2.30}$$

where $b_G(z)$ is the galaxy bias and v_k is the Newtonian-gauge velocity of the sources.

The term $\Delta_\ell^{\mathrm{RSD}}$ accounts for the redshift space distortions,

$$\Delta_\ell^{\mathrm{RSD}} = \frac{k v_k}{\mathcal{H}} j_\ell''(k\chi)\,. \tag{2.31}$$

The lensing term Δ_ℓ^{L} accounts for the contribution from the lensing convergence, which is given by

$$\Delta_\ell^{\mathrm{L}}(k,\chi) = \frac{\ell(\ell+1)}{2}(2-5s)\int_0^\chi \mathrm{d}\chi' \frac{\chi-\chi'}{\chi\chi'}\left[\phi_k(\chi') + \psi_k(\chi')\right] j_\ell(k\chi')\,, \tag{2.32}$$

Este documento incorpora firma electrónica, y es copia auténtica de un documento electrónico archivado por la ULL según la Ley 39/2015.
Su autenticidad puede ser contrastada en la siguiente dirección https://sede.ull.es/validacion/

Identificador del documento: 3764923 Código de verificación: JHlWnlbn

Firmado por: JOSE RAMON BERMEJO CLIMENT — Fecha: 01/09/2021 17:41:12
UNIVERSIDAD DE LA LAGUNA

José Alberto Rubiño Martín — 01/09/2021 17:49:44
UNIVERSIDAD DE LA LAGUNA

FABIO FINELLI — 02/09/2021 14:12:21
UNIVERSIDAD DE LA LAGUNA

Universidad de La Laguna
Oficina de Sede Electrónica
Entrada
Nº registro: 2021/90989
Nº reg. oficina: OF002/2021/89977
Fecha: 03/09/2021 12:24:13

where ϕ_k and ψ_k are the metric perturbations in the longitudinal gauge and $s \equiv \partial \log \bar{N}_s / \partial m_*$ is the magnification bias, which accounts for the fact that observed galaxies are magnified by lensing.

The velocity term $\Delta_\ell^{\rm V}$ accounts for the Doppler effect due to peculiar motions and it is expressed as

$$\Delta_\ell^{\rm V} = \left[\frac{2-5s}{\mathcal{H}(z)\chi} + 5s - b_e + \frac{\dot{\mathcal{H}}}{\mathcal{H}^2}\right] v_k j'_\ell(k\chi)\,. \tag{2.33}$$

We consider also the ISW term ($\Delta_\ell^{\rm ISW}$), the time-delay term ($\Delta_\ell^{\rm TD}$) and other local contributions from gravitational potentials ($\Delta_\ell^{\rm P}$), given by

$$\Delta_\ell^{\rm ISW} = \left[\dot{\phi}_k(\chi) + \dot{\psi}_k(\chi)\right] j_\ell(k\chi) \int_0^\chi {\rm d}\chi' \left[\frac{2-5s}{\mathcal{H}\chi'} + 5s - b_e + \frac{\dot{\mathcal{H}}}{\mathcal{H}^2}\right], \tag{2.34}$$

$$\Delta_\ell^{\rm TD} = \left[\phi_k(\chi) + \psi_k(\chi)\right] j_\ell(k\chi) \int_0^\chi {\rm d}\chi' \frac{2-5s}{\chi'}\,, \tag{2.35}$$

$$\Delta_\ell^{\rm P} = \left\{\left[\frac{2-5s}{\mathcal{H}(z)\chi} + 5s - b_e + \frac{\dot{\mathcal{H}}}{\mathcal{H}^2} + 1\right]\psi_k + (5s-2)\phi_k + \frac{\dot{\phi}_k}{\mathcal{H}}(z)\right\} j_\ell(k\chi)\,. \tag{2.36}$$

2.2.2 Galaxy weak lensing

Weak lensing of galaxies, also commonly known as *cosmic shear*, is originated due to the gravitational lensing effect produced on the galaxy shapes by the structures through which their light pass until reaching the observer. Given the nature of this measurement, it can be done only with photometric galaxy surveys.

All the weak lensing quantities can be defined from the lensing potential

$$\phi\left(\hat{\mathbf{n}}, \chi\right) = \frac{2}{c^2}\int_0^\chi {\rm d}\chi' \frac{\chi - \chi'}{\chi\chi'} \Phi\left(\chi'\hat{\mathbf{n}}, \chi'\right)\,, \tag{2.37}$$

where $\Phi\left(\hat{\mathbf{n}}, \chi\right)$ is the gravitational potential. The comoving distance is

$$\chi(z) = \int_0^z \frac{c\,{\rm d}z'}{H(z')}\,. \tag{2.38}$$

Este documento incorpora firma electrónica, y es copia auténtica de un documento electrónico archivado por la ULL según la Ley 39/2015.
Su autenticidad puede ser contrastada en la siguiente dirección https://sede.ull.es/validacion/

Identificador del documento: 3764923 Código de verificación: JHlWnlbn

Firmado por: JOSE RAMON BERMEJO CLIMENT — Fecha: 01/09/2021 17:41:12
UNIVERSIDAD DE LA LAGUNA

José Alberto Rubiño Martín — 01/09/2021 17:49:44
UNIVERSIDAD DE LA LAGUNA

FABIO FINELLI — 02/09/2021 14:12:21
UNIVERSIDAD DE LA LAGUNA

Universidad de La Laguna
Oficina de Sede Electrónica
Entrada
Nº registro: 2021/90989
Nº reg. oficina: OF002/2021/89977
Fecha: 03/09/2021 12:24:13

The observable 2-dimensional galaxy lensing potential, averaged over background sources with a redshift distribution $W_b(\chi)$, is given by

$$\phi_g(\hat{\mathbf{n}}) = \frac{2}{c^2}\int_0^\chi \frac{\mathrm{d}\chi'}{\chi'} q_b(\chi')\,\Phi(\chi'\hat{\mathbf{n}},\chi')\ , \tag{2.39}$$

where $q_b(\chi)$ is the lensing efficiency (for a given background distribution W_b) defined as

$$q_b(\chi) = \int_\chi \mathrm{d}\chi' \frac{\chi'-\chi}{\chi'} W_b(\chi')\ . \tag{2.40}$$

By expanding the gravitational potential in Fourier space and using the plane-wave expansion, we can define the lensing potential kernel as [68]

$$I_\ell^\phi(k) = 2\left(\frac{3\Omega_m H_0^2}{2k^2c^2}\right)\int \frac{\mathrm{d}\chi}{(2\pi)^{3/2}}\frac{q_b(\chi)}{\chi a(\chi)} j_\ell(k\chi)\,\delta(k,\chi)\ , \tag{2.41}$$

where Ω_m is the present-day matter density, H_0 is the Hubble constant, $\delta(k,\chi)$ is the comoving-gauge matter density perturbation, and j_ℓ the spherical Bessel functions.

We introduce also the lensing convergence, defined as

$$\kappa = \nabla^2\phi/2\,. \tag{2.42}$$

The convergence can be expanded in spherical harmonics as

$$\kappa(\hat{\mathbf{n}}) = -\frac{1}{2}\sum_{\ell,m}\ell(\ell+1)\phi_{\ell m}Y_\ell^m(\hat{\mathbf{n}})\ , \tag{2.43}$$

and we can relate the kernel functions of the lensing potential and convergence by

$$I_\ell^\kappa(k) = \frac{\ell(\ell+1)}{2} I_\ell^\phi(k)\,. \tag{2.44}$$

Este documento incorpora firma electrónica, y es copia auténtica de un documento electrónico archivado por la ULL según la Ley 39/2015.
Su autenticidad puede ser contrastada en la siguiente dirección https://sede.ull.es/validacion/

Identificador del documento: 3764923 Código de verificación: JHlWnlbn

Firmado por:	JOSE RAMON BERMEJO CLIMENT *UNIVERSIDAD DE LA LAGUNA*	Fecha: 01/09/2021 17:41:12
	José Alberto Rubiño Martín *UNIVERSIDAD DE LA LAGUNA*	01/09/2021 17:49:44
	FABIO FINELLI *UNIVERSIDAD DE LA LAGUNA*	02/09/2021 14:12:21

Universidad de La Laguna
Oficina de Sede Electrónica
Entrada
Nº registro: 2021/90989
Nº reg. oficina: OF002/2021/89977
Fecha: 03/09/2021 12:24:13

3

Including CMB-LSS cross-correlation in future surveys

In this chapter we present the future CMB and galaxy surveys that we have considered for producing mock data for the different purposes of this work, and then we forecast by a signal-to-noise ratio analysis the amount of information contained in the cross-correlation between the CMB fields and galaxy number counts for the combinations of these surveys. We also explore whether the inclusion of the RSD and first-order general relativity contributions to the angular power spectra of the galaxy number counts affects its auto-correlation and cross-correlation angular power spectra. The chapter is organized as follows: in Sec. 3.1 we describe the experimental specifications of the CMB experiments, in Sec. 3.2 we present the various future galaxy surveys, in Sec. 3.3 we perform the signal-to-noise analysis and in Sec. 3.4 we discuss the impact of the RSD and general relativity contributions.

The results shown in this chapter are part of the work published in Bermejo-Climent et al. (2020) [64] and Bermejo-Climent et al. (2021) [78].

3.1 CMB surveys

As CMB surveys, we use *Planck*-like synthetic data reproducing the *Planck* 2018 results for ΛCDM parameters [46], the ground-based future experiments Simons Observatory (SO) [79] and CMB Stage-4 (S4) [80],

Este documento incorpora firma electrónica, y es copia auténtica de un documento electrónico archivado por la ULL según la Ley 39/2015.
Su autenticidad puede ser contrastada en la siguiente dirección https://sede.ull.es/validacion/

Identificador del documento: 3764923 Código de verificación: JHlWnlbn

Firmado por:	JOSE RAMON BERMEJO CLIMENT *UNIVERSIDAD DE LA LAGUNA*	Fecha: 01/09/2021 17:41:12
	José Alberto Rubiño Martín *UNIVERSIDAD DE LA LAGUNA*	01/09/2021 17:49:44
	FABIO FINELLI *UNIVERSIDAD DE LA LAGUNA*	02/09/2021 14:12:21

Universidad de La Laguna
Oficina de Sede Electrónica
Entrada
Nº registro: 2021/90989
Nº reg. oficina: OF002/2021/89977
Fecha: 03/09/2021 12:24:13

and Lite satellite for the studies of B-mode polarization and Inflation from cosmic background Radiation Detection (LiteBIRD) [81, 82] as the next concept for a space mission dedicated to CMB polarization. As a further step, in some cases we will also consider two concepts of future space missions: Probe of Inflation and Cosmic Origins (PICO) [1] [87] and Polarized Radiation Imaging and Spectroscopy Mission (PRISM)[2] [88].

We consider the multipole coefficients $C_\ell^{TT}, C_\ell^{EE}, C_\ell^{TE}$ as signal for temperature, polarization and temperature-polarization cross-correlation, respectively. As terms for the isotropic noise deconvolved with the instrument beam we consider [83]

$$\mathcal{N}_\ell^X = w_X^{-1} b_\ell^{-2}, \qquad b_\ell = e^{-\ell(\ell+1)\theta^2_{\rm FWHM}/16\ln 2} \tag{3.1}$$

where $X = TT, EE$, $\theta_{\rm FWHM}$ is the full width half maximum (FWHM) of the beam in radians and w_{TT}, w_{EE} are the inverse square of the detector noise level for temperature and polarization in arcmin^{-2} μK^{-2}. For CMB lensing, we use the resulting $\mathcal{N}_\ell^{TT}$ and $\mathcal{N}_\ell^{EE}$ to reconstruct the minimum variance quadratic estimator for the noise $\mathcal{N}_\ell^{\phi\phi}$, combining the TT, EE, BB, TE, TB, EB estimators according to the Hu-Okamoto algorithm [84] and using the publicly available code `quicklens`[3]. We show in Fig. 4.3 the TT and $\phi\phi$ power spectra and the corresponding noise for the experiments considered.

3.1.1 *Planck*

In order to reproduce a realistic simulation of *Planck*-like data we match our specifics in a manner that reproduce the *Planck* 2018 results [46], which account for the entire data processing pipelines, including foreground contamination, systematics and other uncertainties that cannot be represented in our formalism. Therefore we consider only the 143 GHz channel with $w_{TT} = 33$ μK^2 arcmin^2, $w_{EE} = 70.2$ μK^2 arcmin^2 and $\theta_{\rm FWHM} = 7.3$ arcmin and we inflate the noise in polarization, $\mathcal{N}_\ell^{EE}$, for $\ell < 30$ matching the resulting uncertainty of the optical depth in *Planck* 2018 results. We consider the CMB lensing power spectrum $C_\ell^{\phi\phi}$ in the conservative range, i.e. for $8 \leq \ell \leq 400$, and neglect the $T\phi$, $E\phi$ cross-correlations according to the *Planck* real likelihood.

[1] http://pico.umn.edu
[2] https://www.cosmos.esa.int/web/voyage-2050
[3] https://github.com/dhanson/quicklens

Este documento incorpora firma electrónica, y es copia auténtica de un documento electrónico archivado por la ULL según la Ley 39/2015.
Su autenticidad puede ser contrastada en la siguiente dirección https://sede.ull.es/validacion/

Identificador del documento: 3764923 Código de verificación: JHlWnlbn

Firmado por: JOSE RAMON BERMEJO CLIMENT — Fecha: 01/09/2021 17:41:12
UNIVERSIDAD DE LA LAGUNA

José Alberto Rubiño Martín — 01/09/2021 17:49:44
UNIVERSIDAD DE LA LAGUNA

FABIO FINELLI — 02/09/2021 14:12:21
UNIVERSIDAD DE LA LAGUNA

Universidad de La Laguna
Oficina de Sede Electrónica
Entrada
Nº registro: 2021/90989
Nº reg. oficina: OF002/2021/89977
Fecha: 03/09/2021 12:24:13

3.1.2 Simons Observatory

The Simons Observatory [79] will be a set of ground-based telescopes in Atacama, Chile, which is expected to have its first light in 2021. It will cover $\sim 40\%$ of the sky over six frequency bands ranging from 27 to 280 GHz, with a temperature sensitivity from 71 to 54 μK arcmin and a beam from 7.4 to 0.9 arcmin. To obtain $\mathcal{N}_\ell^{TT}$ and $\mathcal{N}_\ell^{EE}$ we combine the noise for the LAT baseline specifications of the six frequency bands given in [79]. We re-adapt the resulting minimum variance lensing noise in order to match the baseline configuration in [79].

We assume $\ell_{\rm max} = 3000$ for all the CMB channels. Since this is a ground-based experiment, we limit the minimum multipole to $\ell_{\rm min} = 40$ and add the *Planck*-like specifications described above for $2 \leq \ell \leq 39$ with $f_{\rm sky} = 0.7$. We also add the *Planck*-like specifications for $40 \leq \ell \leq 1500$ for the remaining sky fraction $f_{\rm sky} = 0.3$ not observed by SO.

3.1.3 LiteBIRD

LiteBIRD [81, 82] is a proposal for a satellite selected by ISAS as a large strategic mission for the Japanese space agency (JAXA), with contributions of USA, Europe and Canada, with planned launch in 2027. Its main goal is the measurement of the CMB polarization anisotropy pattern with an angular resolution down to 18 arcmin and fifteen frequency channels spanning from 34 GHz to 448 GHz, a range optimized for the foreground removal. As instrumental specifications for LiteBIRD, we use the 7 central frequency channels of the configuration described in [81]. We adopt $f_{\rm sky} = 0.7$ and $\ell_{\rm max} = 1350$ as in [85].

3.1.4 CMB-S4

CMB stage-4 [80] describes the next generation CMB ground-based experiment. It will consist in a set of dedicated telescopes in the South Pole and Atacama. For S4 we adopt $w_{TT} = 1$ μK arcmin, $w_{EE} = \sqrt{2}$ μK arcmin, $\theta_{\rm FWHM} = 3$ arcmin and $f_{\rm sky} = 0.4$ as in [86]. Since S4 is ground-based, we use $\ell_{\rm min} = 40$ and $\ell_{\rm max} = 3000$, following [80]. As for SO, we use complementary measurements in CMB temperature, polarization and lensing at large angular scales ($2 \leq \ell \leq 39$) and for the remaining fraction of the sky not observed by S4: given the timeline of CMB S4, for this purpose we use the capabilities of LiteBIRD.

Este documento incorpora firma electrónica, y es copia auténtica de un documento electrónico archivado por la ULL según la Ley 39/2015.
Su autenticidad puede ser contrastada en la siguiente dirección https://sede.ull.es/validacion/

Identificador del documento: 3764923 Código de verificación: JHlWnlbn

Firmado por:	JOSE RAMON BERMEJO CLIMENT *UNIVERSIDAD DE LA LAGUNA*	Fecha: 01/09/2021 17:41:12
	José Alberto Rubiño Martín *UNIVERSIDAD DE LA LAGUNA*	01/09/2021 17:49:44
	FABIO FINELLI *UNIVERSIDAD DE LA LAGUNA*	02/09/2021 14:12:21

Universidad de La Laguna
Oficina de Sede Electrónica
Entrada
Nº registro: 2021/90989
Nº reg. oficina: OF002/2021/89977
Fecha: 03/09/2021 12:24:13

3.1.5 Concepts of future space missions

PICO and PRISM are two concepts for future space missions that would be able to have a very good sensitivity for temperature and polarization at all scales, having a large sky coverage.

As experimental specifications, for PICO we use the 7 channels ranging from 75 to 220 GHz given in [87]. We assume $\ell_{\rm max} = 3000$ and 70% of sky coverage.

For PRISM we sum the 12 channels ranging from 52 to 385 GHz in [88]. We adopt $\ell_{\rm max} = 4000$ and 75% for the sky fraction.

3.2 Future galaxy surveys

For future galaxy surveys we consider the ESA mission Euclid, the ground-based Vera C. Rubin Observatory (LSST), the NASA mission Spectro-Photometer for the History of the Universe, Epoch of Reionization, and Ices Explorer (SPHEREx) and the radio continuum galaxy surveys Evolutionary Map of the Universe (EMU) and Square Kilometer Array in Phase 1 (SKA1).

We parametrize the number density distribution of a galaxy survey $\mathrm{d}N/\mathrm{d}z$ as

$$\frac{\mathrm{d}N}{\mathrm{d}z} \propto f(z) \exp\left[-\left(\frac{z}{z_0}\right)^{\beta}\right] \tag{3.2}$$

where $f(z)$ is a redshift-dependent function and z_0, β are parameters that depend on the galaxy survey. We perform a tomographic analysis dividing the galaxy surveys in several redshift bins. For the Euclid-like, LSST and SPHEREx surveys we assume that the density distribution of a single bin is given by

$$\frac{\mathrm{d}n^i_{\rm gal}}{\mathrm{d}z} = \frac{\mathrm{d}N}{\mathrm{d}z} \int_{z_{\rm min}}^{z_{\rm max}} \mathrm{d}z_m p(z_m|z) \tag{3.3}$$

where $p(z_m|z)$ is the probability density for the measured redshift z_m given the true redshift z of the galaxy, and $z_{\rm min}$, $z_{\rm max}$ are the edges of the redshift bin, respectively. As baseline model for $p(z_m|z)$ we adopt a gaussian characterized by an intrinsic redshift scatter σ_z as [89]

$$p(z_m|z) = \frac{1}{\sqrt{2\pi}\sigma_z} e^{-\frac{1}{2}(z_m - z)^2/\sigma_z^2}\,. \tag{3.4}$$

Este documento incorpora firma electrónica, y es copia auténtica de un documento electrónico archivado por la ULL según la Ley 39/2015.
Su autenticidad puede ser contrastada en la siguiente dirección https://sede.ull.es/validacion/

Identificador del documento: 3764923 Código de verificación: JHlWnlbn

Firmado por: JOSE RAMON BERMEJO CLIMENT — Fecha: 01/09/2021 17:41:12
UNIVERSIDAD DE LA LAGUNA

José Alberto Rubiño Martín — 01/09/2021 17:49:44
UNIVERSIDAD DE LA LAGUNA

FABIO FINELLI — 02/09/2021 14:12:21
UNIVERSIDAD DE LA LAGUNA

Universidad de La Laguna
Oficina de Sede Electrónica
Entrada
Nº registro: 2021/90989
Nº reg. oficina: OF002/2021/89977
Fecha: 03/09/2021 12:24:13

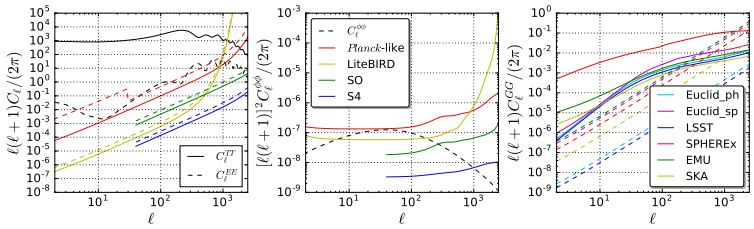

FIGURE 3.1— Left panel: signal and noise for the CMB temperature and polarization for the various CMB surveys considered. The solid lines correspond to the temperature and the dashed lines to polarization. Mid panel: signal and noise for the CMB lensing. The black dashed curve corresponds to the $\phi\phi$ angular power spectra and the solid colored lines to the noise for the various CMB surveys. Right panel: signal and noise for the galaxy number counts. The solid lines represent the GG angular power spectra of the single bin configuration for the 6 surveys, and the dashed lines the corresponding shot noise.

Solving Eq. (3.3) we obtain

$$\frac{\mathrm{d}n_i}{\mathrm{d}z} = \frac{1}{2}\frac{\mathrm{d}N}{\mathrm{d}z}\left[\mathrm{erf}\left(\frac{z_{\rm max}-z}{\sqrt{2}\sigma_z}\right) - \mathrm{erf}\left(\frac{z_{\rm min}-z}{\sqrt{2}\sigma_z}\right)\right] \tag{3.5}$$

where erf is the error function.

For the radio continuum galaxy surveys EMU and SKA1, since there is not a definition of the intrinsic scatter σ_z, we adopt gaussian windows with a dispersion equal to the half width of the bin according to the recipe in [90].

The Poisson shot noise for the galaxy angular correlations between bins is given by

$$\mathcal{N}_\ell^G(z_i, z_j) = \frac{\delta_{ij}}{n^i_{\rm gal}} \tag{3.6}$$

where $n^i_{\rm gal}$ is the number of objects per steradian unit in the i-th bin. We represent in Fig. 4.3 the angular power spectra C_ℓ^{GG} for the single bin configuration of each survey and the corresponding shot noise.

For the galaxy bias redshift evolution, we adopt different functional forms for each survey, including a scale-dependent bias due to the primordial local non-Gaussianity contribution, as defined in Eq. (5.5). We represent in Fig. 3.3 the bias redshift evolution $b_G(z)$ for the four galaxy surveys.

Este documento incorpora firma electrónica, y es copia auténtica de un documento electrónico archivado por la ULL según la Ley 39/2015.
Su autenticidad puede ser contrastada en la siguiente dirección https://sede.ull.es/validacion/

Identificador del documento: 3764923 Código de verificación: JHlWnlbn

Firmado por: JOSE RAMON BERMEJO CLIMENT — Fecha: 01/09/2021 17:41:12
UNIVERSIDAD DE LA LAGUNA

José Alberto Rubiño Martín — 01/09/2021 17:49:44
UNIVERSIDAD DE LA LAGUNA

FABIO FINELLI — 02/09/2021 14:12:21
UNIVERSIDAD DE LA LAGUNA

Universidad de La Laguna
Oficina de Sede Electrónica
Entrada
Nº registro: 2021/90989
Nº reg. oficina: OF002/2021/89977
Fecha: 03/09/2021 12:24:13

3.2.1 Euclid surveys

The European Space Agency (ESA) Cosmic Vision mission Euclid [91] is scheduled to be launched in 2022, with the goal of exploring the dark sector of the Universe. Euclid will measure the galaxy clustering in a spectroscopic survey of tens of millions of Hα emitting galaxies and the cosmic shear in a photometric survey of billions of galaxies. We consider here the galaxy clustering from both surveys.

For the Euclid-like photometric survey (hereafter Euclid-ph-like) we parametrize the number density redshift distribution following Eq. (3.2) with $f(z) = z^2$, $\beta = 3/2$, $z_0 = 0.64$ and the distribution is normalized to account for number density of $\bar{n}_{\rm g} = 30$ sources per arcmin^2. We consider a sky coverage of 15000 deg^2, and a redshift evolution of the bias following $b_G(z) = \sqrt{1+z}$ as in [92]. For the tomographic analysis, we divide the survey in 10 redshift bins with the same number of sources per bin. The redshift accuracy is given by $\sigma_z = 0.05(1+z)$.

The Euclid-like spectroscopic survey (hereafter Euclid-sp-like) will measure the galaxy clustering from ~ 30 million Hα emitters. According to the updated predictions obtained by [93, 94], the Euclid-like wide single-grism survey will reach a flux limit $F_{\rm H\alpha} > 2\times10^{-16}$ erg cm^{-2} s^{-1} and will cover a redshift range $0.9 \leq z \leq 1.8$. The sky coverage is also 15000 deg^2 and the expected number density of objects will be $\bar{n}_{\rm g} \simeq 2000$ sources per deg^2. We fit the number density distribution using the *model 3* data by [93], and assume as galaxy bias redshift evolution $b_G(z) = 0.7+0.7z$ following the fitting for emission line object from [95]. For the tomography, we divide the survey in 9 bins with the same redshift width ($\Delta z = 0.1$), and the redshift accuracy is assumed to be $\sigma_z = 0.001(1+z)$. In Fig. 3.2 we show the normalized dN/dz of both Euclid-like surveys and the binning choice.

3.2.2 Vera C. Rubin Observatory

The Vera C. Rubin Observatory Large Synoptic Survey Telescope, previously known as LSST, will be a 8.4 meter ground-based telescope in Chile that will measure the galaxy clustering and weak lensing with a photometric survey that will cover a 13800 deg^2 area. This survey is expected to observe $\bar{n}_{\rm g} = 48$ sources per arcmin^2, with a linear galaxy bias which evolves with redshift following the equation $b_G(z) = 0.95/D(z)$ [96], where $D(z)$ is the linear growth factor. The number density redshift distribution is parametrized using Eq. (3.2) with $f(z) = z^2$, $\beta = 0.9$ and $z_0 = 0.28$.

Este documento incorpora firma electrónica, y es copia auténtica de un documento electrónico archivado por la ULL según la Ley 39/2015.
Su autenticidad puede ser contrastada en la siguiente dirección https://sede.ull.es/validacion/

Identificador del documento: 3764923 Código de verificación: JHlWnlbn

Firmado por: JOSE RAMON BERMEJO CLIMENT — Fecha: 01/09/2021 17:41:12
UNIVERSIDAD DE LA LAGUNA

José Alberto Rubiño Martín — 01/09/2021 17:49:44
UNIVERSIDAD DE LA LAGUNA

FABIO FINELLI — 02/09/2021 14:12:21
UNIVERSIDAD DE LA LAGUNA

Universidad de La Laguna
Oficina de Sede Electrónica
Entrada
Nº registro: 2021/90989
Nº reg. oficina: OF002/2021/89977
Fecha: 03/09/2021 12:24:13

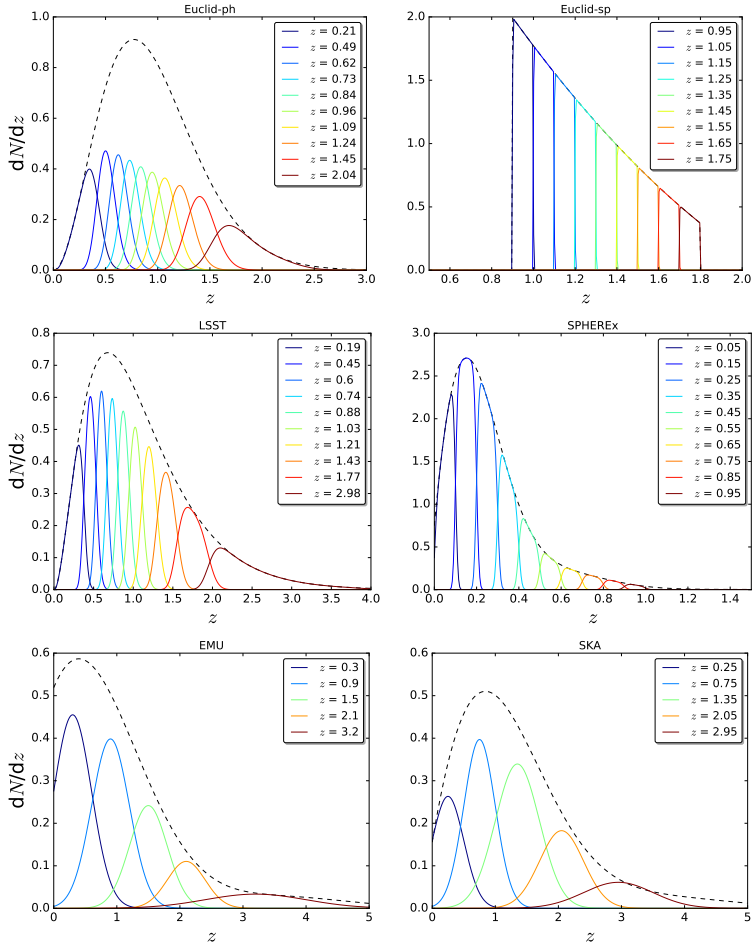

FIGURE 3.2— Normalized number density of objects as a function of the redshift for our six surveys. The black dashed line represents the global density distribution $\mathrm{d}N/\mathrm{d}z$ of the survey and the colored lines represent the corresponding density distribution of the tomographic bins. We show also the central redshift of each bin.

Este documento incorpora firma electrónica, y es copia auténtica de un documento electrónico archivado por la ULL según la Ley 39/2015.
Su autenticidad puede ser contrastada en la siguiente dirección https://sede.ull.es/validacion/

Identificador del documento: 3764923 Código de verificación: JHlWnlbn

Firmado por: JOSE RAMON BERMEJO CLIMENT — Fecha: 01/09/2021 17:41:12
UNIVERSIDAD DE LA LAGUNA

José Alberto Rubiño Martín — 01/09/2021 17:49:44
UNIVERSIDAD DE LA LAGUNA

FABIO FINELLI — 02/09/2021 14:12:21
UNIVERSIDAD DE LA LAGUNA

Universidad de La Laguna
Oficina de Sede Electrónica
Entrada
Nº registro: 2021/90989
Nº reg. oficina: OF002/2021/89977
Fecha: 03/09/2021 12:24:13

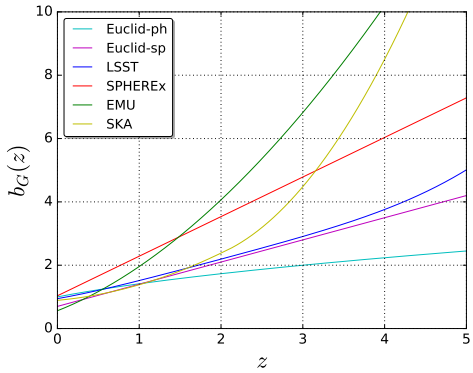

FIGURE 3.3— Redshift evolution of the galaxy bias $b_G(z)$ for the six galaxy surveys considered.

For the tomographic analysis, we divide the survey in 10 redshift bins with the same number of sources per bin. The redshift accuracy is given by $\sigma_z = 0.03(1+z)$. In Fig. 3.2 we show the normalized $\mathrm{d}N/\mathrm{d}z$ of the survey and the binning choice.

In the following, we will refer Vera C. Rubin observatory as LSST.

3.2.3 SPHEREx

SPHEREx is a recently approved NASA space mission that will measure the galaxy clustering using a spectro-photometric technique and covers $\sim 80\%$ of the sky [97]. In this work we assume the specifications of SPHEREx-2, a sample of the survey with low number density of galaxies but high redshift accuracy, this corresponds to ~ 70 million objects and $\sigma_z = 0.008(1+z)$. We fit the number density distribution following Eq. (3.2) and the redshift evolution of the galaxy bias as in [98][4]. For the tomography we divide the survey in 10 redshift bins with $\Delta z = 0.1$. We show in Fig. 3.2 the number density distribution and the binning (note however that for SPHEREx the different flux cuts lead to different configurations).

[4]We wish to thank Olivier Doré and Roland de Putter for making available the SPHEREx specifications to us.

Este documento incorpora firma electrónica, y es copia auténtica de un documento electrónico archivado por la ULL según la Ley 39/2015.
Su autenticidad puede ser contrastada en la siguiente dirección https://sede.ull.es/validacion/

Identificador del documento: 3764923 Código de verificación: JHlWnlbn

Firmado por:	JOSE RAMON BERMEJO CLIMENT *UNIVERSIDAD DE LA LAGUNA*	Fecha: 01/09/2021 17:41:12
	José Alberto Rubiño Martín *UNIVERSIDAD DE LA LAGUNA*	01/09/2021 17:49:44
	FABIO FINELLI *UNIVERSIDAD DE LA LAGUNA*	02/09/2021 14:12:21

Universidad de La Laguna
Oficina de Sede Electrónica
Entrada
Nº registro: 2021/90989
Nº reg. oficina: OF002/2021/89977
Fecha: 03/09/2021 12:24:13

3.2.4 Radio continuum galaxy surveys

Next generation of wide-area radio continuum surveys as SKA and one of its precursors, EMU, will play an important role in our understanding of the cosmology. In addition, wide-area radio continuum surveys will extend to substantially larger areas than many of the forthcoming optical surveys, i.e. $\gtrsim 20,000$ square degrees, and will not be affected by dust. On the other hand, redshift information for individual sources can only be retrieved by the cross-correlation with surveys at other wavelengths.

EMU [99] is an all-sky continuum survey planned for the new Australian SKA Pathfinder (ASKAP). EMU will cover the same area (75% of the sky) as NVSS, but will be 45 times more sensitive, and will have an angular resolution (10 arcsec) five times better. We consider for EMU a flux limit of 100 μJy assuming a 10σ r.m.s. detection threshold over the frequency range 1100-1400 MHz.

The Square Kilometer Array 1 (SKA1) is an international project to build a next generation telescope. We study the SKA1-MID [100] baseline: a dish array based in the Northern Cape province of South Africa. We consider SKA1-MID in Band 1 covering slightly less than half the sky with a flux limit predicted to be at 25 μJy assuming a 10σ r.m.s. detection threshold over the frequency range 350-1050 MHz.

Radio continuum surveys will not provide redshift information, however it will be possible to separate sources by cross-correlating with other catalogues. Hence, we adopt a more conservative choice for the tomography and divide EMU and SKA1 in 5 broad bins in redshift as in [90]. We represent the number density of sources and the binning in Fig. 3.2.

3.3 Signal-to-noise analysis

In this section we calculate the signal-to-noise ratio (SNR) of the cross-correlations of the CMB temperature and lensing[5] with galaxy number counts and study the impact of the tomography on this quantity. In order to explore the dependence of the SNR on the fiducial model, we do the calculations for the following cosmologies:

- A baseline ΛCDM+Σm_ν cosmology, with $\Omega_b h^2 = 0.022383$, $\Omega_c h^2 = 0.12011$, $H_0 = 67.32$ km s^{-1} Mpc^{-1}, $\tau = 0.0543$, $n_s = 0.96605$,

[5] We do not show the SNR of the cross-correlation between CMB polarization and galaxies, EG, since it is small and noise dominated and very far from detection.

Este documento incorpora firma electrónica, y es copia auténtica de un documento electrónico archivado por la ULL según la Ley 39/2015.
Su autenticidad puede ser contrastada en la siguiente dirección https://sede.ull.es/validacion/

Identificador del documento: 3764923 Código de verificación: JHlWnlbn

Firmado por:	JOSE RAMON BERMEJO CLIMENT *UNIVERSIDAD DE LA LAGUNA*	Fecha: 01/09/2021 17:41:12
	José Alberto Rubiño Martín *UNIVERSIDAD DE LA LAGUNA*	01/09/2021 17:49:44
	FABIO FINELLI *UNIVERSIDAD DE LA LAGUNA*	02/09/2021 14:12:21

Universidad de La Laguna
Oficina de Sede Electrónica
Entrada
Nº registro: 2021/90989
Nº reg. oficina: OF002/2021/89977
Fecha: 03/09/2021 12:24:13

$\ln(10^{10}A_s) = 3.0448$ and $\sum m_\nu = 0.06$ eV, consistently with the *Planck* 2018 results [46].

- An alternative cosmology, with a larger departure from $w = -1$ such as $(w_0, w_a) =$ (-0.6, -1), assuming the Chevallier-Polarski-Linder (CPL) parametrization of dark energy, given by the formula [101, 102]:

$$w(z) = w_0 + \frac{z}{1+z} w_a \,. \tag{3.7}$$

We compute the C_ℓ angular power spectra of the CMB temperature, polarization and lensing, of the galaxy number counts power spectra and all the cross-correlations between the different fields using a modified version of the publicly available code `CAMB_sources`[6] [69]. Among our modifications we mention the specifications of each galaxy survey and the possibility of setting a scale-dependent bias.

We also check the importance of non-linear corrections in this analysis. For this, we introduce the cross-correlation coefficient between CMB and galaxies (noted as G) as in [103]

$$r_\ell^{XG} \equiv \frac{C_\ell^{XG}}{\sqrt{C_\ell^{XX} C_\ell^{GG}}} \tag{3.8}$$

where $X \equiv \{T, E, \phi\}$. In Fig. 3.4, we show and compare the cross-correlation coefficients for the six galaxy surveys obtained using linear perturbations only and the same coefficients calculated including non-linear corrections from `halofit`, finding small differences between the two assumptions.

The SNR of the tomographic cross-correlation between a CMB field and galaxies is given by [104]

$$\left(\frac{S}{N}\right)^2 = \sum_{i,j} \sum_{\ell=2}^{\ell_{\rm max}} (2\ell+1) f_{\rm sky}^{XG} C_\ell^{XG}(z_i) [{\rm Cov}_\ell^{-1}]_{ij} C_\ell^{XG}(z_j) \tag{3.9}$$

where the i, j indices stand for the redshift bins, $X \equiv \{T, \phi\}$, $f_{\rm sky}$ is the overlapping sky fraction and ${\rm Cov}_\ell$ is the covariance matrix, defined as

$$[{\rm Cov}_\ell]_{ij} = \bar{C}_\ell^{GG}(z_i, z_j) \bar{C}_\ell^{XX} + C_\ell^{XG}(z_i) C_\ell^{XG}(z_j) \tag{3.10}$$

[6] https://github.com/cmbant/CAMB/tree/CAMB_sources

Este documento incorpora firma electrónica, y es copia auténtica de un documento electrónico archivado por la ULL según la Ley 39/2015.
Su autenticidad puede ser contrastada en la siguiente dirección https://sede.ull.es/validacion/

Identificador del documento: 3764923 Código de verificación: JHlWnlbn

Firmado por:	JOSE RAMON BERMEJO CLIMENT *UNIVERSIDAD DE LA LAGUNA*	Fecha: 01/09/2021 17:41:12
	José Alberto Rubiño Martín *UNIVERSIDAD DE LA LAGUNA*	01/09/2021 17:49:44
	FABIO FINELLI *UNIVERSIDAD DE LA LAGUNA*	02/09/2021 14:12:21

Universidad de La Laguna
Oficina de Sede Electrónica
Entrada
Nº registro: 2021/90989
Nº reg. oficina: OF002/2021/89977
Fecha: 03/09/2021 12:24:13

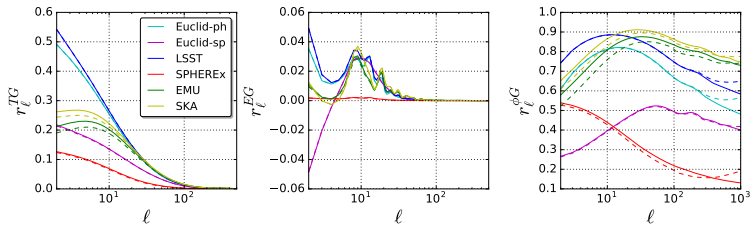

FIGURE 3.4— Cross-correlation coefficients r_ℓ^{TG} (left panel), r_ℓ^{EG} (mid panel) and $r_\ell^{\phi G}$ (right panel) for the six galaxy surveys. The solid lines are obtained using the angular power spectra calculated with linear perturbations only, and the dashed lines include also the non-linear corrections from `halofit`.

TABLE 3.1— Overlapping sky fraction $f_{\rm sky}$ between each pair of CMB and galaxy surveys.

	Euclid-ph-like	Euclid-sp-like	LSST	SPHEREx	EMU	SKA1
Planck	0.36	0.36	0.33	0.7	0.7	0.5
SO	0.25	0.25	0.33	0.4	0.4	0.4
LiteBIRD	0.36	0.36	0.33	0.7	0.7	0.5
S4	0.25	0.25	0.33	0.4	0.4	0.4

where

$$\bar{C}_\ell^{GG}(z_i, z_j) = C_\ell^{GG}(z_i, z_j) + \delta_{ij}\mathcal{N}_\ell^{GG}(z_i) \tag{3.11}$$

and

$$\bar{C}_\ell^{XX} = C_\ell^{XX} + \mathcal{N}_\ell^{XX}\,. \tag{3.12}$$

For the cross-correlation sky fraction $f_{\rm sky}^{XG}$ we assume the common sky area to both CMB and galaxy surveys. We list in Tab. 3.1 the overlapping sky fraction between each pair of CMB and galaxy surveys considered here.

As far as $\ell_{\rm max}$ is concerned in Eq. (3.9), we concentrate on quasi-linear scales in this work. For TG most of the information is concentrated only on linear scales and we cut the sum to $\ell_{\rm max} = 200$. For ϕG we adopt:

$$\ell_{\rm max}^{\phi G} = \sqrt{\ell_{\rm max}^{\phi\phi}(\chi(\bar{z})k_{\rm max} - 1/2)} \tag{3.13}$$

where $\ell_{\rm max}^{\phi\phi} = 1000$, $\chi(\bar{z})$ is the comoving distance at the median redshift $\bar{z}$ of the redshift bin $[105, 106]$ and $k_{\rm max} = 0.1\ h/{\rm Mpc}$.

We calculate the SNR for the TG and ϕG cross-correlations for all the combinations between the CMB and galaxy surveys considered. In order to quantify the impact of the tomography, we consider different

Este documento incorpora firma electrónica, y es copia auténtica de un documento electrónico archivado por la ULL según la Ley 39/2015.
Su autenticidad puede ser contrastada en la siguiente dirección https://sede.ull.es/validacion/

Identificador del documento: 3764923 Código de verificación: JHlWnlbn

Firmado por: JOSE RAMON BERMEJO CLIMENT — Fecha: 01/09/2021 17:41:12
UNIVERSIDAD DE LA LAGUNA

José Alberto Rubiño Martín — 01/09/2021 17:49:44
UNIVERSIDAD DE LA LAGUNA

FABIO FINELLI — 02/09/2021 14:12:21
UNIVERSIDAD DE LA LAGUNA

Universidad de La Laguna
Oficina de Sede Electrónica
Entrada
Nº registro: 2021/90989
Nº reg. oficina: OF002/2021/89977
Fecha: 03/09/2021 12:24:13

TABLE 3.2— TG signal-to-noise for the different combinations of CMB and galaxy surveys. The numbers between parenthesis correspond to the alternative fiducial model for (w_0, w_a).

	Euclid-ph-like		Euclid-sp-like		LSST	
	1 bin	10 bins	1 bin	9 bins	1 bin	10 bins
Planck	3.8 (4.3)	4.0 (4.4)	2.2 (2.5)	2.2 (2.5)	3.8 (4.3)	4.0 (4.4)
Planck+SO	3.8 (4.3)	4.0 (4.4)	2.2 (2.5)	2.2 (2.5)	3.8 (4.3)	4.0 (4.4)
LiteBIRD+S4	3.8 (4.3)	4.0 (4.4)	2.2 (2.5)	2.2 (2.5)	3.8 (4.3)	4.0 (4.4)
	SPHEREx		EMU		SKA1	
	1 bin	10 bins	1 bin	5 bins	1 bin	5 bins
Planck	1.3 (1.4)	4.2 (4.8)	4.3 (4.8)	5.0 (5.6)	4.1 (4.5)	4.6 (5.1)
Planck+SO	1.3 (1.4)	4.4 (5.0)	4.3 (4.8)	5.0 (5.6)	4.1 (4.6)	4.7 (5.2)
LiteBIRD+S4	1.3 (1.4)	4.4 (5.0)	4.3 (4.8)	5.0 (5.6)	4.1 (4.6)	4.7 (5.2)

TABLE 3.3— ϕG signal-to-noise for the different combinations of CMB and galaxy surveys. The numbers between parenthesis correspond to the alternative fiducial model for (w_0, w_a).

	Euclid-ph-like		Euclid-sp-like		LSST	
	1 bin	10 bins	1 bin	9 bins	1 bin	10 bins
Planck	61 (59)	73 (71)	43 (42)	43 (42)	67 (65)	82 (80)
Planck+SO	95 (92)	119 (116)	71 (70)	71 (70)	118 (115)	152 (150)
LiteBIRD+S4	137 (133)	181 (178)	103 (102)	108 (107)	152 (149)	208 (206)
	SPHEREx		EMU		SKA1	
	1 bin	10 bins	1 bin	5 bins	1 bin	5 bins
Planck	21 (20)	54 (52)	80 (79)	88 (87)	87 (85)	93 (92)
Planck+SO	28 (27)	89 (86)	116 (115)	132 (131)	145 (143)	161 (160)
LiteBIRD+S4	38 (37)	138 (133)	175 (174)	216 (215)	201 (200)	239 (238)

configurations with a different number of bins starting from a single bin (i.e. the whole survey) up to the baseline number specified in Sec. 3.2. We list in Tabs. 3.2 and 3.3 the SNR for TG and ϕG, respectively, for the single bin case and the baseline number of bins.

For either the baseline cosmology and the alternative one, we obtain similar SNRs. However, the SNR for TG can increase around $\sim$ 10-15% by assuming the alternative values of (w_0, w_a), demonstrating the capability of the CMB temperature-galaxy cross-correlation to help discriminating among deviations from Λ. Since the CMB temperature anisotropy pattern is signal dominated for the multipoles relevant for the TG cross-correlation already with Planck, the SNR is mostly dependent on the common sky fraction of the CMB map and the galaxy survey. For the baseline fiducial cosmology we find that next photometric surveys from Euclid and LSST will reach a 4σ detection for the ISW, but the radio continuum galaxy

Este documento incorpora firma electrónica, y es copia auténtica de un documento electrónico archivado por la ULL según la Ley 39/2015.
Su autenticidad puede ser contrastada en la siguiente dirección https://sede.ull.es/validacion/

Identificador del documento: 3764923 Código de verificación: JHlWnlbn

Firmado por: JOSE RAMON BERMEJO CLIMENT — Fecha: 01/09/2021 17:41:12
UNIVERSIDAD DE LA LAGUNA

José Alberto Rubiño Martín — 01/09/2021 17:49:44
UNIVERSIDAD DE LA LAGUNA

FABIO FINELLI — 02/09/2021 14:12:21
UNIVERSIDAD DE LA LAGUNA

Universidad de La Laguna
Oficina de Sede Electrónica
Entrada
Nº registro: 2021/90989
Nº reg. oficina: OF002/2021/89977
Fecha: 03/09/2021 12:24:13

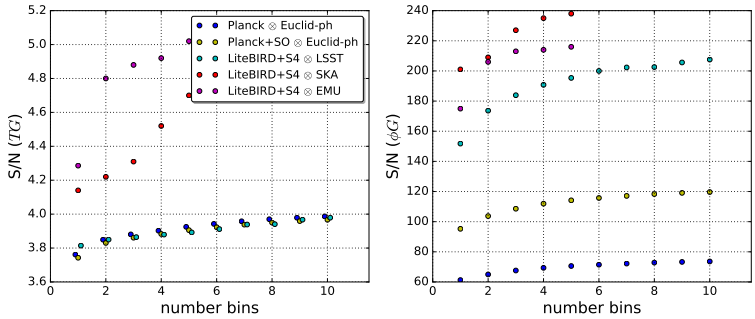

FIGURE 3.5— Signal-to-noise ratio of the TG (left panel) and ϕG (right panel) cross-correlations as a function of the number of bins N. The blue dots correspond to *Planck* $\otimes$ Euclid-ph-like, the yellow dots to *Planck*+SO $\otimes$ Euclid-ph-like, the cyan dots to LiteBIRD+S4 $\otimes$ LSST, the red dots to LiteBIRD+S4 $\otimes$ SKA1 and the purple dots to LiteBIRD+S4 $\otimes$ EMU.

surveys are the most promising in this respect, reaching $\sim 5\sigma$ in the EMU and SKA1 tomographic configurations, consistently with [74]. We get a slightly better ISW detection with EMU as a consequence of its sky fraction, that allows a larger overlap with the CMB, as shown in Tab. 3.1. We also note that SPHEREx is the survey which benefits more from a tomographic approach for the ISW detection.

In the case of ϕG, there is a larger margin of improvement expected with the next CMB polarization experiments with respect to the current $\sim 20\sigma$ detection obtained by *Planck* and NVSS [107]. For all the future galaxy surveys considered we indeed obtain a larger SNR. For ϕG the CMB lensing noise is dominant for *Planck* whereas it decreases significantly for *Planck*+SO and LiteBIRD+S4 as shown in Fig. 4.3. As a consequence, the SNR for ϕG can increase up to a factor $\sim$ 2-3 for LiteBIRD+S4 with respect to *Planck*. Once again, SPHEREx is the survey which benefits more from a tomographic approach also for the CMB lensing-galaxy cross-correlation. We also note that the values for the SNRs obtained for the alternative cosmology are very similar to the fiducial one, albeit slightly smaller.

We show in Fig. 3.5 the behavior of the TG and ϕG SNR as a function of the number of bins N to complement the information contained in Tabs. 3.2 and 3.3. We consider the combinations of *Planck* and

Este documento incorpora firma electrónica, y es copia auténtica de un documento electrónico archivado por la ULL según la Ley 39/2015.
Su autenticidad puede ser contrastada en la siguiente dirección https://sede.ull.es/validacion/

Identificador del documento: 3764923 Código de verificación: JHlWnlbn

Firmado por: JOSE RAMON BERMEJO CLIMENT — Fecha: 01/09/2021 17:41:12
UNIVERSIDAD DE LA LAGUNA

José Alberto Rubiño Martín — 01/09/2021 17:49:44
UNIVERSIDAD DE LA LAGUNA

FABIO FINELLI — 02/09/2021 14:12:21
UNIVERSIDAD DE LA LAGUNA

Universidad de La Laguna
Oficina de Sede Electrónica
Entrada
Nº registro: 2021/90989
Nº reg. oficina: OF002/2021/89977
Fecha: 03/09/2021 12:24:13

Planck+SO with Euclid-like photometric survey, and LiteBIRD+S4 with LSST, EMU and SKA1, and divide the galaxy surveys progressively in different number of bins up to the baseline (10 bins for Euclid-ph-like and LSST and 5 bins for EMU and SKA1). We obtain that the TG SNR for Euclid-ph-like and LSST saturates around $\sim 4\sigma$ independently of the CMB survey chosen, as can be already seen from Tabs. 3.2 and 3.3. This is a consequence of the increasing Poisson shot noise and redshift overlapping between bins when pushing the tomography. For ϕG, we get an improvement of the SNR as a consequence of future better measurement of CMB lensing, and we find as well a saturation when increasing the number of bins for both Euclid-like and LSST: the better SNR reached by LSST compared to the Euclid-like photometric survey is due to the overlap in the scanning strategy of SO and LSST. We finally note that a more aggressive binning scheme than the one adopted here could enhance the scientific capability of EMU and SKA.

3.4 Impact of RSD and general relativity contributions

In this section we evaluate the importance of the contributions from RSD and general relativity to the galaxy counts angular power spectra described in Sec. 2.2.1.

The impact of these contributions is highly dependent on the magnification bias $s(z)$ assumed for each galaxy survey. We give here the details of the functional form of $s(z)$ for each survey.

For the Euclid-like photometric survey, we adopt the $s(z)$ functional form by [108], given by

$$s(z) = 0.12 + 0.21z + 0.07z^2 + 0.10z^3 \,. \tag{3.14}$$

For the Euclid-like spectroscopic survey, we derive and fit the functional form of $s(z)$ using the *model 3* luminosity function by [93]. This is done integrating the luminosity function from a given flux threshold, and then computing the derivative of the number counts with respect to the magnitude by finite differences.

For a flux threshold of $F_{\rm cut} = 2 \times 10^{-16}$ erg s^{-1} cm^{-2} we find

$$s(z) = 0.33 + 0.46z + 0.15z^2 - 0.16z^3 + 0.03z^4 \,. \tag{3.15}$$

Este documento incorpora firma electrónica, y es copia auténtica de un documento electrónico archivado por la ULL según la Ley 39/2015.
Su autenticidad puede ser contrastada en la siguiente dirección https://sede.ull.es/validacion/

Identificador del documento: 3764923 Código de verificación: JHlWnlbn

Firmado por: JOSE RAMON BERMEJO CLIMENT — Fecha: 01/09/2021 17:41:12
UNIVERSIDAD DE LA LAGUNA

José Alberto Rubiño Martín — 01/09/2021 17:49:44
UNIVERSIDAD DE LA LAGUNA

FABIO FINELLI — 02/09/2021 14:12:21
UNIVERSIDAD DE LA LAGUNA

Universidad de La Laguna
Oficina de Sede Electrónica
Entrada
Nº registro: 2021/90989
Nº reg. oficina: OF002/2021/89977
Fecha: 03/09/2021 12:24:13

Note that this fit is valid only for $z \geq 0.6$ since the *model 3* by [93] does not include data for low redshift objects.

For LSST, assuming the luminosity function by [109] and a limiting magnitude $m = 26$, we obtain

$$s(z) = 0.11 + 0.25 - 0.42z^2 + 0.51z^3 - 0.24z^4 + 0.05z^5 \,. \tag{3.16}$$

For EMU we use the luminosity function by luminosity function by [109] and assuming a flux threshold of 20 mJy we get

$$s(z) = 0.29 + 0.61z - 0.36z^2 + 0.08z^3 + 0.008z^4 \,. \tag{3.17}$$

For SKA, we use the the luminosity function [109] and with a flux threshold of 100 mJy in this case, we obtain

$$s(z) = 0.33 - 0.10z + 0.16z^2 - 0.05z^3 + 0.005z^4 \,, \tag{3.18}$$

For SPHEREx, since there is not in the literature a derivation of its magnification bias or an estimation for its luminosity function, we assume a minimal constant value $s(z) = 0.42$.

We now quantify the impact of the contributions defined here on the GG autospectra and the TG, ϕG cross-correlation spectra for the redshift bins of SKA1 and Euclid-ph-like. In Figs. 3.6 and 3.7 we show the relative differences on the spectra obtained for each term, together and independently, with respect to the spectra including the density term only. We obtain that the relative weight of the corrections is larger at higher z and large scales ($\ell \lesssim 100$). The RSD and velocity terms are the most important for the GG spectra, while the lensing contribution has a larger impact on the cross-correlation spectra.

Este documento incorpora firma electrónica, y es copia auténtica de un documento electrónico archivado por la ULL según la Ley 39/2015.
Su autenticidad puede ser contrastada en la siguiente dirección https://sede.ull.es/validacion/

Identificador del documento: 3764923 Código de verificación: JHlWnlbn

Firmado por:	JOSE RAMON BERMEJO CLIMENT *UNIVERSIDAD DE LA LAGUNA*	Fecha: 01/09/2021 17:41:12
	José Alberto Rubiño Martín *UNIVERSIDAD DE LA LAGUNA*	01/09/2021 17:49:44
	FABIO FINELLI *UNIVERSIDAD DE LA LAGUNA*	02/09/2021 14:12:21

Universidad de La Laguna
Oficina de Sede Electrónica
Entrada
Nº registro: 2021/90989
Nº reg. oficina: OF002/2021/89977
Fecha: 03/09/2021 12:24:13

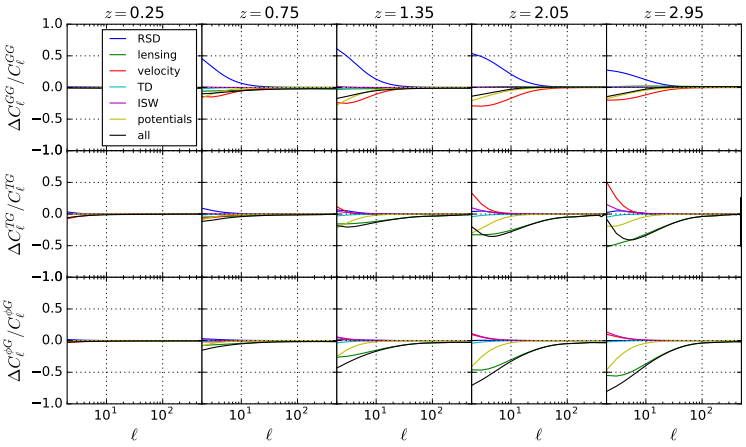

FIGURE 3.6— Relative impact of the contributions to the total number counts with respect to the density-only angular power spectra for the GG autospectra (top panel) and for the TG (mid panel) and ϕG (bottom panel) cross-correlation spectra of the 5 SKA1 redshift bins. The coloured lines correspond to the impact of each single term and the black lines to the sum of all the contributions.

Este documento incorpora firma electrónica, y es copia auténtica de un documento electrónico archivado por la ULL según la Ley 39/2015.
Su autenticidad puede ser contrastada en la siguiente dirección https://sede.ull.es/validacion/

Identificador del documento: 3764923 Código de verificación: JHlWnlbn

Firmado por: JOSE RAMON BERMEJO CLIMENT — Fecha: 01/09/2021 17:41:12
UNIVERSIDAD DE LA LAGUNA

José Alberto Rubiño Martín — 01/09/2021 17:49:44
UNIVERSIDAD DE LA LAGUNA

FABIO FINELLI — 02/09/2021 14:12:21
UNIVERSIDAD DE LA LAGUNA

Universidad de La Laguna
Oficina de Sede Electrónica
Entrada
Nº registro: 2021/90989
Nº reg. oficina: OF002/2021/89977
Fecha: 03/09/2021 12:24:13

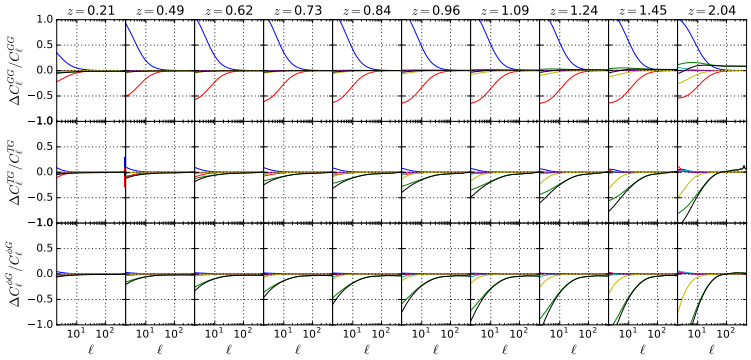

FIGURE 3.7— Relative impact of the contributions to the total number counts with respect to the density-only angular power spectra for the GG autospectra (top panel) and for the TG (mid panel) and ϕG (bottom panel) cross-correlation spectra of the 10 Euclid-ph-like redshift bins. The coloured lines correspond to the impact of each single term and the black lines to the sum of all the contributions.

Este documento incorpora firma electrónica, y es copia auténtica de un documento electrónico archivado por la ULL según la Ley 39/2015.
Su autenticidad puede ser contrastada en la siguiente dirección https://sede.ull.es/validacion/

Identificador del documento: 3764923 Código de verificación: JHlWnlbn

Firmado por: JOSE RAMON BERMEJO CLIMENT — Fecha: 01/09/2021 17:41:12
UNIVERSIDAD DE LA LAGUNA

José Alberto Rubiño Martín — 01/09/2021 17:49:44
UNIVERSIDAD DE LA LAGUNA

FABIO FINELLI — 02/09/2021 14:12:21
UNIVERSIDAD DE LA LAGUNA

Universidad de La Laguna
Oficina de Sede Electrónica
Entrada
Nº registro: 2021/90989
Nº reg. oficina: OF002/2021/89977
Fecha: 03/09/2021 12:24:13

Este documento incorpora firma electrónica, y es copia auténtica de un documento electrónico archivado por la ULL según la Ley 39/2015.
Su autenticidad puede ser contrastada en la siguiente dirección https://sede.ull.es/validacion/

Identificador del documento: 3764923 Código de verificación: JHlWnlbn

Firmado por:	JOSE RAMON BERMEJO CLIMENT *UNIVERSIDAD DE LA LAGUNA*	Fecha: 01/09/2021 17:41:12
	José Alberto Rubiño Martín *UNIVERSIDAD DE LA LAGUNA*	01/09/2021 17:49:44
	FABIO FINELLI *UNIVERSIDAD DE LA LAGUNA*	02/09/2021 14:12:21

Universidad de La Laguna
Oficina de Sede Electrónica
Entrada
Nº registro: 2021/90989
Nº reg. oficina: OF002/2021/89977
Fecha: 03/09/2021 12:24:13

4

Lensing ratios with future galaxy surveys

Weak gravitational lensing is one of the most direct probes of the distribution of dark matter and it is correlated with the intervening process of structure formation. Beyond the full weak lensing analysis, it is also useful to consider the cross-correlation between weak lensing and other fields (such as galaxy clustering) as additional probes and consistency checks.

Ratios between cross-correlations of galaxies and weak lensing at two different source planes in redshift have been proposed as cosmographic distance measurements [110–115] (see Fig. 4.1 for an illustration). The role of these ratio estimators between the weak lensing at two different redshift and a matter tracer as a cosmographic measure becomes extremely transparent under different approximations, such as the Limber and flat sky approximation, and the limit in which the foreground distribution is extremely peaked in redshift.

Being a ratio between two cross-correlation terms with the same lens, this estimator is largely independent on the clustering bias of the lens and weak lensing systematics, but depends on most of the background cosmological parameters. By taking one of the source planes as the CMB last scattering surface, the lever arm of such a lensing ratio estimator becomes somewhat maximal [114, 115].

The scientific potential of the CMB lensing ratio as a cosmographic measurement for the next generation of CMB and LSS experiments has

Este documento incorpora firma electrónica, y es copia auténtica de un documento electrónico archivado por la ULL según la Ley 39/2015.
Su autenticidad puede ser contrastada en la siguiente dirección https://sede.ull.es/validacion/

Identificador del documento: 3764923 Código de verificación: JHlWnlbn

Firmado por:	JOSE RAMON BERMEJO CLIMENT *UNIVERSIDAD DE LA LAGUNA*	Fecha: 01/09/2021 17:41:12
	José Alberto Rubiño Martín *UNIVERSIDAD DE LA LAGUNA*	01/09/2021 17:49:44
	FABIO FINELLI *UNIVERSIDAD DE LA LAGUNA*	02/09/2021 14:12:21

Universidad de La Laguna
Oficina de Sede Electrónica
Entrada
Nº registro: 2021/90989
Nº reg. oficina: OF002/2021/89977
Fecha: 03/09/2021 12:24:13

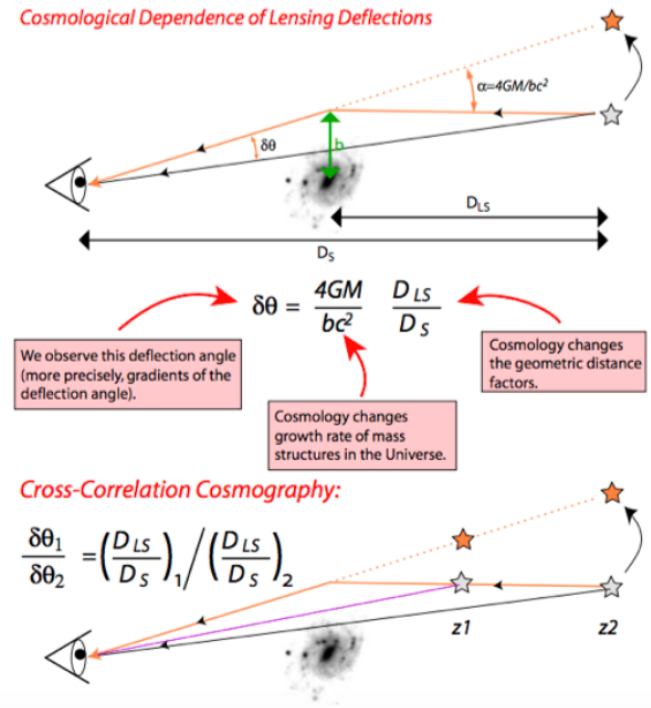

FIGURE 4.1— Illustration of the usefullness of cross-correlation cosmography using two background sources lensed by the same foreground. Credits: G. Bernstein (2004)

Este documento incorpora firma electrónica, y es copia auténtica de un documento electrónico archivado por la ULL según la Ley 39/2015.
Su autenticidad puede ser contrastada en la siguiente dirección https://sede.ull.es/validacion/

Identificador del documento: 3764923 Código de verificación: JHlWnlbn

Firmado por:	JOSE RAMON BERMEJO CLIMENT *UNIVERSIDAD DE LA LAGUNA*	Fecha: 01/09/2021 17:41:12
	José Alberto Rubiño Martín *UNIVERSIDAD DE LA LAGUNA*	01/09/2021 17:49:44
	FABIO FINELLI *UNIVERSIDAD DE LA LAGUNA*	02/09/2021 14:12:21

Universidad de La Laguna
Oficina de Sede Electrónica
Entrada
Nº registro: 2021/90989
Nº reg. oficina: OF002/2021/89977
Fecha: 03/09/2021 12:24:13

been forecast in several papers [115–117]. The estimator for the lensing ratio between CMB lensing/galaxies and galaxy shear/galaxies has already been applied to real data [117, 118]. Miyatake et al. [118] used CMASS [119] and CFHTLens [120] for galaxy lenses and sources, respectively, and CMB lensing from *Planck* 2015 [121]. Prat et al. [117] used galaxy position and lensing from DES Y1 [122] and CMB lensing from a combination of *Planck* 2015 and SPT [123].

In this chapter we study and extend the lensing ratio estimator as introduced by Das and Spergel in [115] (henceforth DS09) and we study its scientific capabilities in the context of future cosmological observations. We show how the approximations in the galaxy and lensing kernel and the finite width in redshift of the lenses density distributions affect to the multipole dependence of the lensing ratio. The inclusion of the lensing magnification contribution in the galaxy number counts introduces a further and larger dependence on the multipoles, which we show that neglecting these effects might lead to bias in the inference of cosmological parameters, and calls for an extension of a lensing ratio estimator which takes into account the dependence on multipoles.

This chapter is organized as follows. After this introduction, we introduce the notation for the CMB lensing/galaxy and galaxy shear/galaxy cross-correlation, respectively, in Section 4.1. In Section 4.2 we introduce the experimental specifications of the CMB anisotropies and galaxy surveys we use in our forecasts. In Section 4.3 we forecast the capabilities of a Euclid-like[1] [91] experiment alone and in combination with galaxy lenses at lower redshift from DESI[2] [124] and SPHEREx[3] [97] in measuring the lensing ratio as originally introduced in DS09. In Section 4.4 we consider the ratio between the CMB lensing/galaxy and galaxy shear/galaxy cross-correlations without approximations and replacing the galaxy density with the galaxy number counts including RSD and lensing magnification contributions and introduce its minimum variance estimator. In Section 4.5 we forecast the expected errors on cosmological parameters by using the novel methodology introduced in Section 4.4.

This chapter contains the main results that have been published in Bermejo-Climent et al. (2020) [64].

[1] https://www.cosmos.esa.int/web/euclid/home
[2] https://www.desi.lbl.gov/
[3] http://spherex.caltech.edu/

Este documento incorpora firma electrónica, y es copia auténtica de un documento electrónico archivado por la ULL según la Ley 39/2015.
Su autenticidad puede ser contrastada en la siguiente dirección https://sede.ull.es/validacion/

Identificador del documento: 3764923 Código de verificación: JHlWnlbn

Firmado por:	JOSE RAMON BERMEJO CLIMENT *UNIVERSIDAD DE LA LAGUNA*	Fecha: 01/09/2021 17:41:12
	José Alberto Rubiño Martín *UNIVERSIDAD DE LA LAGUNA*	01/09/2021 17:49:44
	FABIO FINELLI *UNIVERSIDAD DE LA LAGUNA*	02/09/2021 14:12:21

Universidad de La Laguna
Oficina de Sede Electrónica
Entrada
Nº registro: 2021/90989
Nº reg. oficina: OF002/2021/89977
Fecha: 03/09/2021 12:24:13

4.1 Formalism

In this section we define the quantities involved in the angular power spectra of the cross-correlation between a foreground lens galaxy population and a background weak lensing source that comes from the CMB or from the galaxy shear.

We are interested in the cross-correlation of a foreground galaxy number density field with two different backgrounds as the convergence field from the weak lensing of galaxies and of the CMB.

The angular power spectrum of these cross-correlations can be calculated following Eq. (2.23). The kernel for the galaxy weak lensing is defined in Sec. 2.2.2. In the case of CMB lensing, the source distribution can be approximated by $W_{\rm CMB}(\chi) \simeq \delta_{\rm D}(\chi - \chi_*)$ and the lensing efficiency by

$$q_{\rm CMB}(\chi) \simeq \frac{\chi_* - \chi}{\chi_*}\,, \tag{4.1}$$

where χ_* is the comoving distance at the surface of last scattering, and Eq. (2.41) reduces to

$$I_\ell^{\phi_{\rm CMB}}(k) = 2\left(\frac{3\Omega_m H_0^2}{2k^2c^2}\right)\int \frac{{\rm d}\chi}{(2\pi)^{3/2}}\frac{\chi_* - \chi}{\chi_*\chi}\frac{1}{a(\chi)} j_\ell(k\chi)\,\delta(k,\chi)\,. \tag{4.2}$$

In this chapter we will use the lensing convergence instead of the potential as baseline for obtaining the angular power spectra. The convergence $\kappa = \nabla^2\phi/2$ can be expanded in spherical-harmonics as

$$\kappa(\hat{\mathbf{n}}) = -\frac{1}{2}\sum_{\ell,m}\ell(\ell+1)\phi_{\ell m}Y_\ell^m(\hat{\mathbf{n}})\,, \tag{4.3}$$

and we can relate the two kernel functions by

$$I_\ell^\kappa(k) = \frac{\ell(\ell+1)}{2} I_\ell^\phi(k)\,. \tag{4.4}$$

The 2-dimensional integrate window function for the galaxy number counts is

$$I_\ell^G(k) = \int \frac{{\rm d}\chi}{(2\pi)^{3/2}} W_f(\chi)\Delta_\ell^s(k,\chi) \tag{4.5}$$

where $\Delta_\ell^s(k,\chi)$ is the synchronous gauge source counts Fourier transformed and expanded into multipoles and $W_f(\chi)$ is the foreground redshift

Este documento incorpora firma electrónica, y es copia auténtica de un documento electrónico archivado por la ULL según la Ley 39/2015.
Su autenticidad puede ser contrastada en la siguiente dirección https://sede.ull.es/validacion/

Identificador del documento: 3764923 Código de verificación: JHlWnlbn

Firmado por: JOSE RAMON BERMEJO CLIMENT — Fecha: 01/09/2021 17:41:12
UNIVERSIDAD DE LA LAGUNA

José Alberto Rubiño Martín — 01/09/2021 17:49:44
UNIVERSIDAD DE LA LAGUNA

FABIO FINELLI — 02/09/2021 14:12:21
UNIVERSIDAD DE LA LAGUNA

Universidad de La Laguna
Oficina de Sede Electrónica
Entrada
Nº registro: 2021/90989
Nº reg. oficina: OF002/2021/89977
Fecha: 03/09/2021 12:24:13

distribution of galaxies. We assume that $\Delta^s_\ell(k,\chi)$ is related to the underlying matter density field through a redshift dependent galaxy bias b_g as $\Delta^s_\ell(k,\chi) = b_g(\chi)\delta(k,\chi)j_\ell(k\chi)$.

Finally, we define the lensing ratio as DS09

$$r_\ell \equiv \frac{C_\ell^{\kappa_{\rm CMB}G}}{C_\ell^{\kappa_{\rm gal}G}}\,. \tag{4.6}$$

4.2 Data and specifications

We define here the specifications for the future large scale structure and CMB surveys considered in order to produce the mock signal and noise data. The lensing ratio estimator is based in the cross-correlations between three ingredients: a tracer for the foreground galaxy population, a background of source galaxies traced by a Euclid-like photometric survey; and the CMB lensing background source, for which we consider a *Planck*-like experiment and many future experiments.

We create the mock data for the angular power spectra using `CLASSgal` [125, 126]. The non-linear corrections are modeled as `halofit` with the recipe by [67]. For the fiducial cosmology we assume a ΛCDM+$\sum m_\nu$ model with one massive neutrino consistent with the *Planck* 2018 results [46]. We use $\Omega_b h^2 = 0.022383$, $\Omega_c h^2 = 0.12011$, $H_0 = 67.32$ km s^{-1} Mpc^{-1}, $\tau = 0.0543$, $n_s = 0.96605$, $\ln(10^{10}A_s) = 3.0448$ and $\sum m_\nu = 0.06$ eV.

4.2.1 Galaxy lenses

For the foreground lens population we use a Euclid-like spectroscopic survey and lower redshift populations like DESI and SPHEREx that allow to increase the background number of objects and the distance between the lens and the sources, which come from the Euclid photometric survey. We describe here the specifications of these experiments.

We adopt as baseline for a given lens population narrow slices with $\Delta z = 0.1$. For this, we convolve the number density distribution $\mathrm{d}N/\mathrm{d}z$ with a Gaussian probability distribution for the measured redshift given the redshift accuracy following Eqs. (3.3)-(3.4).

In the harmonic space, the Poisson shot noise for a given foreground population at redshift z_i is obtained as the inverse of the number of objects per steradian,

$$\mathcal{N}^G_\ell(z_i) = \frac{4\pi f_{\rm sky}}{\bar{n}^i_{\rm g}} \tag{4.7}$$

Este documento incorpora firma electrónica, y es copia auténtica de un documento electrónico archivado por la ULL según la Ley 39/2015.
Su autenticidad puede ser contrastada en la siguiente dirección https://sede.ull.es/validacion/

Identificador del documento: 3764923 Código de verificación: JHlWnlbn

Firmado por: JOSE RAMON BERMEJO CLIMENT — Fecha: 01/09/2021 17:41:12
UNIVERSIDAD DE LA LAGUNA

José Alberto Rubiño Martín — 01/09/2021 17:49:44
UNIVERSIDAD DE LA LAGUNA

FABIO FINELLI — 02/09/2021 14:12:21
UNIVERSIDAD DE LA LAGUNA

Universidad de La Laguna
Oficina de Sede Electrónica
Entrada
Nº registro: 2021/90989
Nº reg. oficina: OF002/2021/89977
Fecha: 03/09/2021 12:24:13

where $f_{\rm sky}$ is the sky fraction and $n_{\rm g}^i$ is the total number of galaxies.

Euclid-like spectroscopic survey

For the Euclid spectroscopic survey we follow the specifications described in Sec. 3.2. We represent in Fig. 4.2 the $\mathrm{d}N/\mathrm{d}z$ of the full survey and the selected foreground population for the first redshift bin at $0.9 < z_{\rm lens} < 1$. We will refer hereafter this foreground configuration as Euclid-r1.

Lenses at lower redshift

For the foreground lens populations at lower redshift we consider the ground-based survey Dark Energy Spectroscopic Instrument (DESI) and the recently approved NASA mission SPHEREx.

DESI is an ongoing spectroscopic survey that covers ~ 14000 deg^2 in the sky. Here we consider the lower redshift target objects: the Bright Galaxy Sample (BGS), which will measure ~ 10 million galaxies at $0 < z < 0.4$. We adopt the specifications in [124] for the number density distribution and the bias redshift evolution, which is given by $b_g(z) = 1.34/D(z)$. The redshift accuracy is given by $\sigma_z = 0.001(1+z)$. The overlapping sky fraction with Euclid will be limited to ~ 4000 deg^2.

For SPHEREx we adopt the specifications described in Sec. 3.2. Since this survey will cover $\sim 80\%$ of the sky, there will be full overlap with the background from Euclid and all the CMB experiments. We represent in Fig. 4.2 the $\mathrm{d}N/\mathrm{d}z$ of the full survey and the lens foreground population for a bin at $0.2 < z_{\rm lens} < 0.3$. We will refer hereafter this foreground configuration as SPHEREx-r1.

4.2.2 Galaxy shear sources

The Euclid photometric survey will measure both galaxy clustering and weak lensing from a sample of billions of galaxies. Here we will consider the weak lensing from a given background population. We parametrize the specifications of the survey as described in Sec. 3.2.

We assume that the background population is given by a broad bin that maximizes the number of objects behind the lenses without overlapping with them. For this, we convolve the $\mathrm{d}N/\mathrm{d}z$ of the photometric survey with a Gaussian redshift probability distribution with a dispersion $\sigma_z = 0.05(1+z)$, following Eq. (3.5). We show in Fig. 4.2 the $\mathrm{d}N/\mathrm{d}z$ of the photometric survey and the maximal background source populations for the two foregrounds of the Euclid-r1 and SPHEREx-r1 configurations.

Este documento incorpora firma electrónica, y es copia auténtica de un documento electrónico archivado por la ULL según la Ley 39/2015.
Su autenticidad puede ser contrastada en la siguiente dirección https://sede.ull.es/validacion/

Identificador del documento: 3764923 Código de verificación: JHlWnlbn

Firmado por: JOSE RAMON BERMEJO CLIMENT — Fecha: 01/09/2021 17:41:12
UNIVERSIDAD DE LA LAGUNA

José Alberto Rubiño Martín — 01/09/2021 17:49:44
UNIVERSIDAD DE LA LAGUNA

FABIO FINELLI — 02/09/2021 14:12:21
UNIVERSIDAD DE LA LAGUNA

Universidad de La Laguna
Oficina de Sede Electrónica
Entrada
Nº registro: 2021/90989
Nº reg. oficina: OF002/2021/89977
Fecha: 03/09/2021 12:24:13

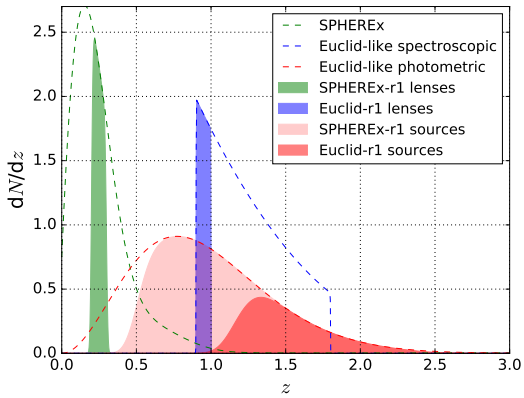

FIGURE 4.2— Survey configuration for the lensing ratio. The green dashed curve represents the normalized $\mathrm{d}N/\mathrm{d}z$ of SPHEREx and the green shaded area corresponds to a bin at $0.2 < z < 0.3$ for the foreground population of the SPHEREx-r1 configuration. The blue dashed curve represents the normalized $\mathrm{d}N/\mathrm{d}z$ of the Euclid-like spectroscopic survey, and the blue shaded area corresponds to the bin at $0.9 < z < 1.0$ that traces the foreground of the Euclid-r1 configuration. The red dashed curve represents the normalized $\mathrm{d}N/\mathrm{d}z$ of the Euclid-like photometric survey, and the pink and red shaded areas correspond to the background of source galaxies beyond the SPHEREx-r1 and Euclid-r1 lenses.

The shear noise for the background population for a redshift bin at z_i is obtained as

$$\mathcal{N}_\ell^{\kappa_{\rm gal}}(z_i) = \sigma_\epsilon^2 \frac{4\pi f_{\rm sky}}{\bar{n}_{\rm g}^i} \tag{4.8}$$

where σ_ϵ is the intrinsic ellipticity RMS, for which we adopt $\sigma_\epsilon = 0.22$, $f_{\rm sky}$ is the sky coverage and $n_{\rm g}^i$ is the number of sources.

4.2.3 CMB lensing source

For the CMB lensing background source we consider as surveys the ESA mission *Planck* [127], the ground-based future experiments SO [79] and CMB-S4, the proposed space mission LiteBIRD, and the two concepts PICO and PRISM. The specifications of these experiments will be also used for temperature and polarization for a quantitative assessment of what the lensing ratio can add to the information of the CMB fields alone.

The specifications and methodology for obtaining the minimum vari-

Este documento incorpora firma electrónica, y es copia auténtica de un documento electrónico archivado por la ULL según la Ley 39/2015.
Su autenticidad puede ser contrastada en la siguiente dirección https://sede.ull.es/validacion/

Identificador del documento: 3764923 Código de verificación: JHlWnlbn

Firmado por:	JOSE RAMON BERMEJO CLIMENT *UNIVERSIDAD DE LA LAGUNA*	Fecha: 01/09/2021 17:41:12
	José Alberto Rubiño Martín *UNIVERSIDAD DE LA LAGUNA*	01/09/2021 17:49:44
	FABIO FINELLI *UNIVERSIDAD DE LA LAGUNA*	02/09/2021 14:12:21

Universidad de La Laguna
Oficina de Sede Electrónica
Entrada
Nº registro: 2021/90989
Nº reg. oficina: OF002/2021/89977
Fecha: 03/09/2021 12:24:13

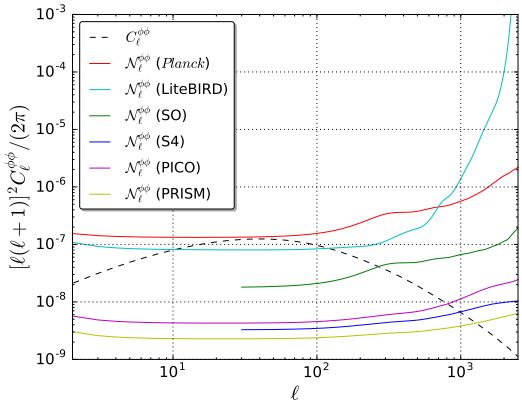

FIGURE 4.3— Signal of the CMB lensing potential data and its noise computed for the experiments considered using the minimum variance estimator.

ance estimator for the CMB lensing noise are those described in Sec. 3.1. We show in Fig. 4.3 the CMB lensing potential noise $\mathcal{N}_\ell^{\phi\phi}$ obtained for the experiments considered in this chapter.

4.3 Cosmographic lensing ratio measurements

In this section we study how under some approximations the lensing ratio r_ℓ can be interpreted as a cosmographic measurement that does not depend on the multipoles, astrophysical uncertainties and perturbations. We then present forecasts for the error on the lensing ratio for this previously introduced limit using the future cosmological surveys mock data described in Section 4.2 and explore how this uncertainty varies with the foreground population redshift $z_{\rm lens}$ and the selected background.

4.3.1 The cosmographic ratio limit

We show here the limit in which the lensing ratio r_ℓ defined in Section 4.1 becomes a geometrical quantity independent of the angular scale, the power spectrum and the galaxy bias. This limit needs to assume the Limber approximation, to select a foreground lens population which is narrow enough in redshift and to neglect the effects on the galaxy number

Este documento incorpora firma electrónica, y es copia auténtica de un documento electrónico archivado por la ULL según la Ley 39/2015.
Su autenticidad puede ser contrastada en la siguiente dirección https://sede.ull.es/validacion/

Identificador del documento: 3764923 Código de verificación: JHlWnlbn

Firmado por: JOSE RAMON BERMEJO CLIMENT — Fecha: 01/09/2021 17:41:12
UNIVERSIDAD DE LA LAGUNA

José Alberto Rubiño Martín — 01/09/2021 17:49:44
UNIVERSIDAD DE LA LAGUNA

FABIO FINELLI — 02/09/2021 14:12:21
UNIVERSIDAD DE LA LAGUNA

Universidad de La Laguna
Oficina de Sede Electrónica
Entrada
Nº registro: 2021/90989
Nº reg. oficina: OF002/2021/89977
Fecha: 03/09/2021 12:24:13

counts from observing on the past light cone.

Limber approximation

In order to speed up the computation of Eq. (2.23), which is time-consuming due to the rapid oscillations of the spherical Bessel function at high multipoles, it is commonly adopted the Limber approximation [128] which is accurate at high-ℓ. It consists in replacing the spherical Bessel function $j_\ell(k\chi)$ with a Dirac delta-function $\delta_{\rm D}$

$$j_\ell(k\chi) \to \sqrt{\frac{\pi}{2(\ell+1/2)}}\delta_{\rm D}\left(\ell+\frac{1}{2}-k\chi\right). \tag{4.9}$$

We can then approximate the kernel functions (2.41)-(4.2)-(4.5) obtaining the following angular power spectra

$$C_\ell^{\phi\phi}(z_i,z_j) = \frac{4}{(\ell+1/2)^4}\left(\frac{3\Omega_{\rm m}H_0^2}{2c^2}\right)^2\int {\rm d}\chi \frac{q_{b_i}(\chi)q_{b_j}(\chi)}{a^2(\chi)}P_\delta\left(\frac{\ell+1/2}{\chi},\chi\right), \tag{4.10}$$

$$C_\ell^{GG}(z_i,z_j) = \int {\rm d}\chi \frac{W_{f_i}(\chi)W_{f_j}(\chi)}{\chi^2}b_g^2(\chi)P_\delta\left(\frac{\ell+1/2}{\chi},\chi\right), \tag{4.11}$$

$$C_\ell^{\phi G}(z_i,z_j) = \frac{2}{(\ell+1/2)^2}\left(\frac{3\Omega_{\rm m}H_0^2}{2c^2}\right)\int {\rm d}\chi \frac{q_{b_i}(\chi)W_{f_j}(\chi)}{a(\chi)\chi}b_g(\chi)P_\delta\left(\frac{\ell+1/2}{\chi},\chi\right), \tag{4.12}$$

for background sources, foreground lenses, and their cross-correlation, where the matter power spectrum is defined as

$$\langle\delta(\mathbf{k},\chi)\delta^*(\mathbf{k}',\chi)\rangle = (2\pi)^3 P_\delta(k,\chi)\delta_{\rm D}(\mathbf{k}-\mathbf{k}'). \tag{4.13}$$

We show in Fig. 4.4 the effect of the Limber approximation in the cross-correlation angular power spectra $C_\ell^{\kappa_{\rm CMB}G}$ and $C_\ell^{\kappa_{\rm gal}G}$ and in the lensing ratio r_ℓ, using the Euclid-r1 configuration. We find that the Limber approximation changes the signal of the denominator $C_\ell^{\kappa_{\rm gal}G}$ and hence the ratio r_ℓ at the lowest multipoles, smoothing the ℓ-dependence that appears when this approximation is not used.

In DS09 it is also considered the flat-sky approximation. In this limit, the sky is approximated by a 2-dimensional plane tangential to the celestial sphere and mathematically expansions in spherical harmonics are replaced by Fourier expansions

$$\sum_{\ell,m}\phi_{\ell,m}Y_\ell^m(\hat{\mathbf{n}}) \to \int \frac{{\rm d}^2\boldsymbol{\theta}}{(2\pi)^2}\phi(\ell)e^{\imath\boldsymbol{\theta}\cdot\hat{\mathbf{n}}}. \tag{4.14}$$

Este documento incorpora firma electrónica, y es copia auténtica de un documento electrónico archivado por la ULL según la Ley 39/2015.
Su autenticidad puede ser contrastada en la siguiente dirección https://sede.ull.es/validacion/

Identificador del documento: 3764923 Código de verificación: JHlWnlbn

Firmado por:	JOSE RAMON BERMEJO CLIMENT *UNIVERSIDAD DE LA LAGUNA*	Fecha: 01/09/2021 17:41:12
	José Alberto Rubiño Martín *UNIVERSIDAD DE LA LAGUNA*	01/09/2021 17:49:44
	FABIO FINELLI *UNIVERSIDAD DE LA LAGUNA*	02/09/2021 14:12:21

Universidad de La Laguna
Oficina de Sede Electrónica
Entrada
Nº registro: 2021/90989
Nº reg. oficina: OF002/2021/89977
Fecha: 03/09/2021 12:24:13

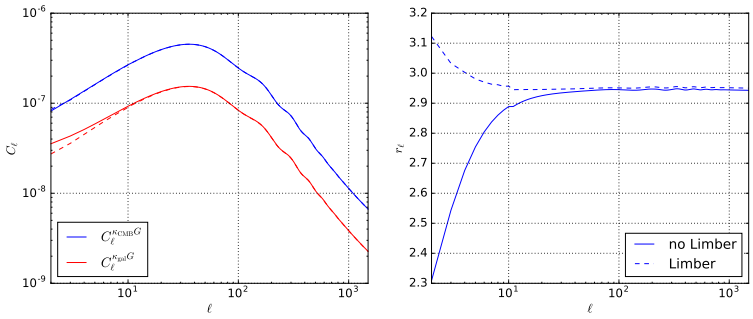

FIGURE 4.4— Impact of the Limber approximation on both lensing-galaxy cross-correlation angular power spectra (left panel) and on the lensing ratio (right panel), using the Euclid-r1 configuration at $z_{\rm lens} = 0.95$

The relation between the convergence and lensing kernel 4.4 is then

$$I_\ell^\kappa(k) \simeq \frac{\ell^2}{2} I_\ell^\phi(k)\,. \tag{4.15}$$

The flat-sky approximation does not affect the *ratio* since the difference in the prefactor $\ell + 1/2 \to \ell$ cancels out.

Narrow foreground

If the redshift distribution of the foreground population is narrow enough in redshift or if we have a redshift accuracy σ_z sufficient to slice the foreground population in narrow redshift bins, we can approximate the foreground redshift distribution as a Dirac delta-function

$$W_f(\chi) \propto \delta_{\rm D}(\chi - \chi_f)\,, \tag{4.16}$$

where χ_f is the peak of the distribution. We then find

$$C_\ell^{\phi G}(z_f, z_b) = \frac{2}{(\ell+1/2)^2}\left(\frac{3\Omega_{\rm m}H_0^2}{2c^2}\right)\frac{b(\chi_f)P_\delta\left(\frac{\ell+1/2}{\chi_f}, \chi_f\right)}{a(\chi_f)\chi_f}\int {\rm d}\chi \frac{\chi-\chi_f}{\chi} W_b(\chi)\,. \tag{4.17}$$

Under these approximations the ratio loses the ℓ-dependence, we obtain a quantity which depends only on background parameters (H_0, Ω_χ, w_0,

Este documento incorpora firma electrónica, y es copia auténtica de un documento electrónico archivado por la ULL según la Ley 39/2015.
Su autenticidad puede ser contrastada en la siguiente dirección https://sede.ull.es/validacion/

Identificador del documento: 3764923 Código de verificación: JHlWnlbn

Firmado por: JOSE RAMON BERMEJO CLIMENT — Fecha: 01/09/2021 17:41:12
UNIVERSIDAD DE LA LAGUNA

José Alberto Rubiño Martín — 01/09/2021 17:49:44
UNIVERSIDAD DE LA LAGUNA

FABIO FINELLI — 02/09/2021 14:12:21
UNIVERSIDAD DE LA LAGUNA

Universidad de La Laguna
Oficina de Sede Electrónica
Entrada
Nº registro: 2021/90989
Nº reg. oficina: OF002/2021/89977
Fecha: 03/09/2021 12:24:13

...), and the clustering bias cancels out, i.e.

$$r = \frac{\chi_* - \chi_f}{\chi_*} \frac{1}{\int \mathrm{d}\chi \frac{\chi - \chi_f}{\chi} W_b(\chi)} \,. \tag{4.18}$$

Finally, if also the background distribution is sufficiently thin we can recover the standard cosmographic expression for the ratio

$$r = \frac{\chi_* - \chi_f}{\chi_b - \chi_f} \frac{\chi_b}{\chi_*} \,, \tag{4.19}$$

where we assumed $W_b(\chi) \propto \delta_{\rm D}(\chi - \chi_b)$.

4.3.2 Forecasts for future experiments

We quantify the accuracy that will be reachable on the lensing ratio measurement for future experiments in the limit in which it can be considered as an ℓ-independent quantity ($r_\ell \simeq r$). For this, we follow the formalism by DS09 in order to compute the error on r.

The log-likelihood is defined as

$$\chi^2(r) = \sum_\ell \frac{Z_\ell^2}{\sigma^2(Z_\ell)} \,, \tag{4.20}$$

where $Z_\ell = C_\ell^{\kappa_{\rm CMB}G} - r C_\ell^{\kappa_{\rm gal}G}$. For the variance of Z_l at a fiducial value of the ratio r_0, we use the extended definition by [117], which accounts for partial overlap in the sky between surveys,

$$\begin{aligned}\sigma^2(Z_\ell) = \frac{1}{(2\ell+1)} \Bigg[& \frac{1}{f_{\rm sky}^{\kappa_{\rm CMB}G}} \left(\bar{C}_\ell^{\kappa_{\rm CMB}\kappa_{\rm CMB}} \bar{C}_\ell^{GG} + (C_\ell^{\kappa_{\rm CMB}G})^2 \right) \\ & + \frac{r_0^2}{f_{\rm sky}^{\kappa_{\rm gal}G}} \left(\bar{C}_\ell^{\kappa_{\rm gal}\kappa_{\rm gal}} \bar{C}_\ell^{GG} + (C_\ell^{\kappa_{\rm gal}G})^2 \right) \\ & - 2 r_0 \frac{f_{\rm sky}^{\kappa_{\rm CMB}\kappa_{\rm gal}G}}{f_{\rm sky}^{\kappa_{\rm CMB}G} f_{\rm sky}^{\kappa_{\rm gal}G}} \left(C_\ell^{\kappa_{\rm CMB}\kappa_{\rm gal}} \bar{C}_\ell^{GG} + C_\ell^{\kappa_{\rm CMB}G} C_\ell^{\kappa_{\rm gal}G} \right) \Bigg] \,, \end{aligned} \tag{4.21}$$

where $\bar{C}_\ell^{XX} = C_\ell^{XX} + \mathcal{N}_\ell^{XX}$ includes the signal and noise power spectra, and the $f_{\rm sky}$ factors account for the overlapping sky fraction between each

Este documento incorpora firma electrónica, y es copia auténtica de un documento electrónico archivado por la ULL según la Ley 39/2015.
Su autenticidad puede ser contrastada en la siguiente dirección https://sede.ull.es/validacion/

Identificador del documento: 3764923 Código de verificación: JHlWnlbn

Firmado por:	JOSE RAMON BERMEJO CLIMENT *UNIVERSIDAD DE LA LAGUNA*	Fecha: 01/09/2021 17:41:12
	José Alberto Rubiño Martín *UNIVERSIDAD DE LA LAGUNA*	01/09/2021 17:49:44
	FABIO FINELLI *UNIVERSIDAD DE LA LAGUNA*	02/09/2021 14:12:21

Universidad de La Laguna
Oficina de Sede Electrónica
Entrada
Nº registro: 2021/90989
Nº reg. oficina: OF002/2021/89977
Fecha: 03/09/2021 12:24:13

pair of probes. We introduce the maximum likelihood estimator for the lensing ratio solving $\partial\chi^2/\partial r = 0$ as DS09

$$\hat{r} = \frac{\sum_\ell C_\ell^{\kappa_{\rm CMB}G} C_\ell^{\kappa_{\rm gal}G}/\sigma^2(Z_\ell)}{\sum_\ell (C_\ell^{\kappa_{\rm gal}G})^2/\sigma^2(Z_\ell)}\,, \tag{4.22}$$

and we then compute the error on $\hat{r}$ as

$$\frac{1}{\sigma^2(\hat{r})} = \frac{1}{2}\frac{\partial^2\chi^2(r)}{\partial r^2} = \sum_\ell \frac{(C_\ell^{\kappa_{\rm gal}G})^2}{\sigma^2(Z_\ell)}\,. \tag{4.23}$$

In Fig. 4.5 we represent $\hat{r}$ and its error as a function of $z_{\rm lens}$ for the 9 possible bins of the Euclid-like spectroscopic survey and three of the CMB experiments considered: *Planck*, *Planck*+SO and PRISM. As suggested in [115, 117], this estimator is specially sensitive to the curvature of the Universe and the equation of state of dark energy. We therefore calculate also $\hat{r}$ for cosmologies beyond ΛCDM shifting w_0 and Ω_k by a given amount.

We find that for post-*Planck* CMB experiments in which the CMB lensing noise will be reduced by a significant amount, the ratio will be measured with better accuracy specially for the lower redshift bins. At higher redshift for the lenses $z_{\rm lens}$, the higher noise of the galaxy surveys gives less precise measurements. For the non-standard cosmologies, we find that $\hat{r}$ is sensitive in particular to the curvature variations.

For the Euclid-like spectroscopic lenses and using the *Planck* CMB lensing, the best measurement will be $\sigma(\hat{r})/\hat{r} = 5.5\%$, corresponding to the Euclid-r1 configuration at $0.9 < z_{\rm lens} < 1.0$. If we take a lower redshift lens at $0.2 < z_{\rm lens} < 0.3$ for DESI and SPHEREx, we get as relative errors 6.7% and 4.3%, respectively. This means that the measurement for DESI will be affected by the small overlapping sky fraction with Euclid, while using SPHEREx as foreground population can relatively improve the lensing ratio measurement. Using post-*Planck* CMB lensing, we get as relative errors 3.2% and 2.3% for SO in combination with the Euclid-r1 and SPHEREx-r1 configurations, respectively. With PRISM, these two measurements improve to 1.4% and 0.7%, respectively.

In Fig. 4.6 we explore the effect of fixing the background galaxy shear sources to the Euclid-like photometric population placed behind the Euclid-like spectroscopic survey (i.e. behind the higher redshift lens on Fig. 4.5). The increase on the distances between the galaxy lens and

Este documento incorpora firma electrónica, y es copia auténtica de un documento electrónico archivado por la ULL según la Ley 39/2015.
Su autenticidad puede ser contrastada en la siguiente dirección https://sede.ull.es/validacion/

Identificador del documento: 3764923 Código de verificación: JHlWnlbn

Firmado por: JOSE RAMON BERMEJO CLIMENT — Fecha: 01/09/2021 17:41:12
UNIVERSIDAD DE LA LAGUNA

José Alberto Rubiño Martín — 01/09/2021 17:49:44
UNIVERSIDAD DE LA LAGUNA

FABIO FINELLI — 02/09/2021 14:12:21
UNIVERSIDAD DE LA LAGUNA

Universidad de La Laguna
Oficina de Sede Electrónica
Entrada
Nº registro: 2021/90989
Nº reg. oficina: OF002/2021/89977
Fecha: 03/09/2021 12:24:13

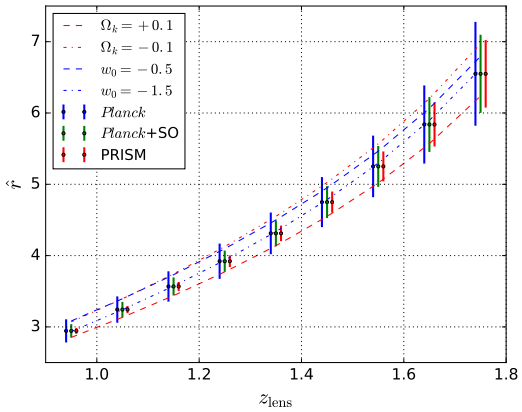

FIGURE 4.5— Forecast measurements of the maximum likelihood estimator for the lensing ratio $\hat{r}$ (4.22) with their errors as a function of the Euclid-like spectroscopic foreground redshift $z_{\rm lens}$ for three CMB experiments: *Planck*, *Planck*+SO and PRISM. The central dots and errorbars correspond to a ΛCDM cosmology while the red and blue dashed curves represent the values of $\hat{r}$ obtained shifting by a certain amount Ω_k and w_0, respectively.

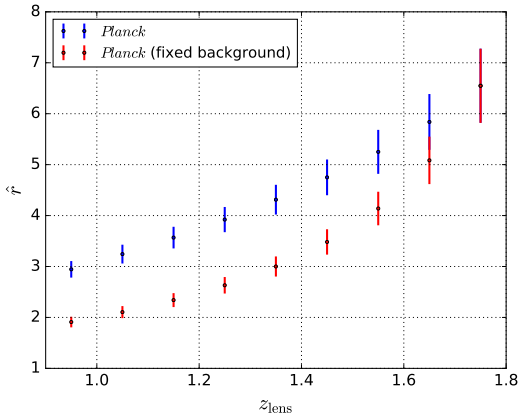

FIGURE 4.6— As for Fig. 4.5 but using *Planck* as CMB lensing background with a variable galaxy background beyond each foreground (blue errorbars) and a fixed galaxy background at $2.0 < z < 2.5$ (red errorbars).

Este documento incorpora firma electrónica, y es copia auténtica de un documento electrónico archivado por la ULL según la Ley 39/2015.
Su autenticidad puede ser contrastada en la siguiente dirección https://sede.ull.es/validacion/

Identificador del documento: 3764923 Código de verificación: JHlWnlbn

Firmado por: JOSE RAMON BERMEJO CLIMENT — Fecha: 01/09/2021 17:41:12
UNIVERSIDAD DE LA LAGUNA

José Alberto Rubiño Martín — 01/09/2021 17:49:44
UNIVERSIDAD DE LA LAGUNA

FABIO FINELLI — 02/09/2021 14:12:21
UNIVERSIDAD DE LA LAGUNA

Universidad de La Laguna
Oficina de Sede Electrónica
Entrada
Nº registro: 2021/90989
Nº reg. oficina: OF002/2021/89977
Fecha: 03/09/2021 12:24:13

source planes shifts the maximum likelihood ratio to lower values and also decreases the absolute error, but we find a very similar relative error in comparison with the variable background case. This also shows that the measurement is not limited by the background noise.

4.4 A generalized lensing ratio estimator

In this section we show how the inclusion of the RSD and lensing magnification contributions to the galaxy number counts has an impact on the angular scale dependence of the lensing ratio r_ℓ and the cosmological information contained on it. We propose the introduction of a multipole dependent estimator to upgrade the formalism by DS09 and consider a more general case beyond assuming that r is constant. We define the signal-to-noise ratio of the $\hat{r}_\ell$ estimator and evaluate the impact of including on the calculation the contributions beyond the density term.

4.4.1 Inclusion of RSD and lensing magnification

Eq. (4.5) assumes only the contribution from the synchronous-gauge galaxy overdensity to the galaxy number counts. Here we quantify the relevance of including other terms to $\Delta^s_\ell(k,\chi)$ given by RSD and lensing magnification (see [69, 129] for details). The RSD and lensing terms are given by Eqs. 2.31-2.32. In this chapter, we consider lensing magnification as the only observational effect on number counts with the density and RSD. We neglect the Doppler, Sachs-Wolfe and other integrated effects (ISW and time-delay) because they are negligible in the calculation of the *ratio*.

In Fig. 4.7 we show the impact of including the RSD term alone and both RSD and lensing contributions together in the cross-correlation angular power spectra $C_\ell^{\kappa_{\rm CMB}G}$ and $C_\ell^{\kappa_{\rm gal}G}$ and in the lensing ratio r_ℓ, adopting the Euclid-r1 configuration.

For the case including only RSD, we find a small correction on the angular power spectra at low multipoles, which results in a slightly higher lensing ratio at $\ell < 10$. When we consider also the lensing magnification, we obtain a larger positive contribution to both $C_\ell^{\kappa_{\rm CMB}G}$ and $C_\ell^{\kappa_{\rm gal}G}$ that is especially strong at large scales but holds also at higher multipoles. This results in a negative $\sim 10\%$ shift for r_ℓ given that the impact of including GR in the denominator $C_\ell^{\kappa_{\rm gal}G}$ is higher. The shape of the lensing ratio becomes less constant with ℓ once the lensing magnification contribution

Este documento incorpora firma electrónica, y es copia auténtica de un documento electrónico archivado por la ULL según la Ley 39/2015.
Su autenticidad puede ser contrastada en la siguiente dirección https://sede.ull.es/validacion/

Identificador del documento: 3764923 Código de verificación: JHlWnlbn

Firmado por: JOSE RAMON BERMEJO CLIMENT — Fecha: 01/09/2021 17:41:12
UNIVERSIDAD DE LA LAGUNA

José Alberto Rubiño Martín — 01/09/2021 17:49:44
UNIVERSIDAD DE LA LAGUNA

FABIO FINELLI — 02/09/2021 14:12:21
UNIVERSIDAD DE LA LAGUNA

Universidad de La Laguna
Oficina de Sede Electrónica
Entrada
Nº registro: 2021/90989
Nº reg. oficina: OF002/2021/89977
Fecha: 03/09/2021 12:24:13

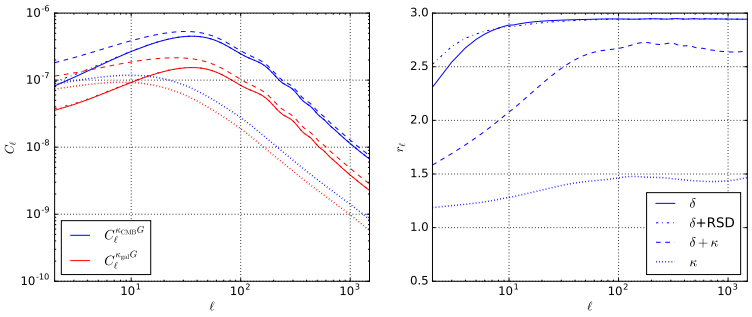

FIGURE 4.7— Impact of the RSD and lensing contributions on the lensing-galaxy cross-correlation angular power spectra (left panel) and on the lensing ratio estimator (right panel) for the Euclid-r1 configuration.

is considered.

We show here how the lensing term induces the ℓ-dependence of the lensing ratio. If we consider the density term and the lensing contribution the kernel of the galaxy number counts becomes

$$I_\ell^G(k) \equiv I_\ell^{G_1}(k) + I_\ell^{G_2}(k) = \int \frac{\mathrm{d}\chi}{(2\pi)^{3/2}} W_f(\chi) \left[\Delta_\ell^s(k,\chi) + \Delta_\ell^{\rm L}(k,\chi)\right] . \tag{4.24}$$

Using the Limber approximation, the first term of the lensing-galaxy cross-correlation is given by Eq. (4.12), and for the second term we find:

$$C_\ell^{\phi G_2}(z_i, z_j) = \frac{\ell(\ell+1)}{(\ell+1/2)^2} \left(\frac{3\Omega_{\rm m} H_0^2}{2c^2}\right) \int \frac{\mathrm{d}\chi}{(2\pi)^3} \frac{q_{b_i}(\chi)}{a(\chi)\chi} \delta\left(\frac{\ell+1/2}{\chi}, \chi\right) (\phi+\psi) \times \int_0^\chi \mathrm{d}\chi' \frac{\chi'-\chi}{\chi'\chi} (2-5s) W_{f_j}(\chi') . \tag{4.25}$$

We note that in this case, the assumption of a narrow foreground would not eliminate the ℓ-dependence of the ratio since the last integral is bound to χ and can not be simplified. We represent in Fig. 4.7 the contribution to the angular power spectra from the lensing magnification term (κ) and their ratio, showing that is not anymore an ℓ-independent quantity. Nonetheless, the ℓ-dependence can be alleviated using a different tracer

Este documento incorpora firma electrónica, y es copia auténtica de un documento electrónico archivado por la ULL según la Ley 39/2015.
Su autenticidad puede ser contrastada en la siguiente dirección https://sede.ull.es/validacion/

Identificador del documento: 3764923 Código de verificación: JHlWnlbn

Firmado por: JOSE RAMON BERMEJO CLIMENT — Fecha: 01/09/2021 17:41:12
UNIVERSIDAD DE LA LAGUNA

José Alberto Rubiño Martín — 01/09/2021 17:49:44
UNIVERSIDAD DE LA LAGUNA

FABIO FINELLI — 02/09/2021 14:12:21
UNIVERSIDAD DE LA LAGUNA

Universidad de La Laguna
Oficina de Sede Electrónica
Entrada
Nº registro: 2021/90989
Nº reg. oficina: OF002/2021/89977
Fecha: 03/09/2021 12:24:13

for the galaxy foreground population which is not affected by the lensing magnification contribution as in [130], where they used as a foreground the SKA HI intensity mapping survey.

4.4.2 Signal-to-noise analysis

We extend here the formalism to compute the error on the lensing ratio by DS09 to consider the angular scale dependence of the ratio. We introduce the signal-to-noise ratio (SNR) of an ℓ-dependent estimator $\hat{r}_\ell$ and compare its value to the ratio studied before.

We start by assuming that different multipoles ℓ are uncorrelated. This is a consequence of neglecting the super-sample covariance and non-Gaussian terms of the covariance matrix of the data, therefore the remaining Gaussian term, which is diagonal in ℓ, is assumed to be dominant at the scales of interest. We then define the log-likelihood of r_ℓ as

$$\chi^2_\ell(r_\ell) = \frac{Z^2_\ell}{\sigma^2_\ell(Z_\ell)}\,, \tag{4.26}$$

where $Z_\ell = C_\ell^{\kappa_{\rm CMB}G} - r_\ell C_\ell^{\kappa_{\rm gal}G}$. For the variance $\sigma_\ell(Z_\ell)$ we extend the definition in Eq. (4.21) replacing r_0 by a multipole dependent fiducial $r_{\ell,0}$

$$\begin{aligned}\sigma^2_\ell(Z_\ell) = \frac{1}{(2\ell+1)} \times \Bigg[& \frac{1}{f_{\rm sky}^{\kappa_{\rm CMB}G}}\left(\bar{C}_\ell^{\kappa_{\rm CMB}\kappa_{\rm CMB}}\bar{C}_\ell^{GG} + (C_\ell^{\kappa_{\rm CMB}G})^2\right) \\ & + \frac{r^2_{\ell,0}}{f_{\rm sky}^{\kappa_{\rm gal}G}}\left(\bar{C}_\ell^{\kappa_{\rm gal}\kappa_{\rm gal}}\bar{C}_\ell^{GG} + (C_\ell^{\kappa_{\rm gal}G})^2\right) \\ & - 2r_{\ell,0}\frac{f_{\rm sky}^{\kappa_{\rm CMB}\kappa_{\rm gal}G}}{f_{\rm sky}^{\kappa_{\rm CMB}G} f_{\rm sky}^{\kappa_{\rm gal}G}}\left(C_\ell^{\kappa_{\rm CMB}\kappa_{\rm gal}}\bar{C}_\ell^{GG} + C_\ell^{\kappa_{\rm CMB}G}C_\ell^{\kappa_{\rm gal}G}\right)\Bigg]\,. \end{aligned} \tag{4.27}$$

The maximum likelihood estimator for the lensing ratio, $\hat{r}_\ell$, is obtained imposing $\partial\chi^2_\ell(r_\ell)/\partial r_\ell = 0$ as

$$\hat{r}_\ell = \frac{C_\ell^{\kappa_{\rm CMB}G}C_\ell^{\kappa_{\rm gal}G}/\sigma^2(Z_\ell)}{(C_\ell^{\kappa_{\rm gal}G})^2/\sigma^2(Z_\ell)} = \frac{C_\ell^{\kappa_{\rm CMB}G}}{C_\ell^{\kappa_{\rm gal}G}}\,, \tag{4.28}$$

which in this case coincides with the definition of the lensing ratio itself. We then estimate the error on $\hat{r}_\ell$ as

$$\frac{1}{\sigma^2_\ell(\hat{r}_\ell)} = \frac{1}{2}\frac{\partial^2\chi^2_\ell(r_\ell)}{\partial r^2_\ell} = \frac{(C_\ell^{\kappa_{\rm gal}G})^2}{\sigma^2_\ell(Z_\ell)}\,, \tag{4.29}$$

Este documento incorpora firma electrónica, y es copia auténtica de un documento electrónico archivado por la ULL según la Ley 39/2015.
Su autenticidad puede ser contrastada en la siguiente dirección https://sede.ull.es/validacion/

Identificador del documento: 3764923 Código de verificación: JHlWnlbn

Firmado por:	JOSE RAMON BERMEJO CLIMENT *UNIVERSIDAD DE LA LAGUNA*	Fecha: 01/09/2021 17:41:12
	José Alberto Rubiño Martín *UNIVERSIDAD DE LA LAGUNA*	01/09/2021 17:49:44
	FABIO FINELLI *UNIVERSIDAD DE LA LAGUNA*	02/09/2021 14:12:21

Universidad de La Laguna
Oficina de Sede Electrónica
Entrada
Nº registro: 2021/90989
Nº reg. oficina: OF002/2021/89977
Fecha: 03/09/2021 12:24:13

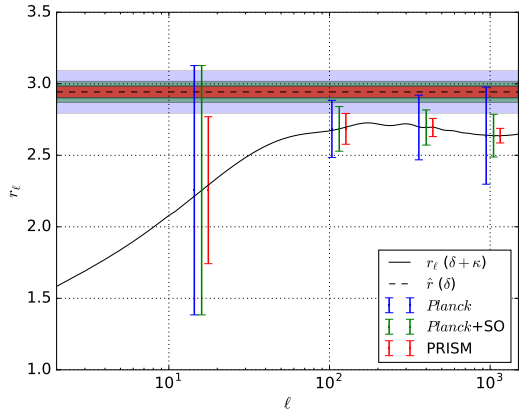

FIGURE 4.8— Lensing ratio and its error measured for the lowest $z_{\rm lens}$ configuration of the Euclid-like spectroscopic survey. The solid black curve represents r_ℓ computed with all the contributions to the galaxy number counts and the dashed line to $\hat{r}$ computed using the density term only. The blue, green and red error bars correspond errors on r_ℓ for *Planck*, *Planck*+SO and PRISM, respectively, in four broad bins - i.e. $(2, 29), (30, 199), (200, 599), (600, 1500)$. The blue, green and red shaded areas represent the 1σ confidence region for $\hat{r}$ calculated for *Planck*, *Planck*+SO and PRISM, respectively.

and with this, we define the SNR of the lensing ratio as the total one as sum over the multipoles since they are uncorrelated, hence

$$\left(\frac{S}{N}\right)^2_{\hat{r}_\ell} = \sum_\ell \frac{\hat{r}_\ell^2}{\sigma_\ell^2(\hat{r}_\ell)} = \sum_\ell \frac{(C_\ell^{\kappa_{\rm CMB}G})^2}{\sigma_\ell^2(Z_\ell)}\,. \tag{4.30}$$

We now assess whether the ℓ-dependence of the lensing ratio will be measurable using the future experiments discussed here. We find that this dependence will be detectable at the level of 1.4σ for *Planck*, 2.2σ for *Planck*+SO and 5.1σ for PRISM by considering unbinned multipoles. We also visualize the importance of the multipole dependence in Fig. 4.8, where we display for the Euclid-r1 configuration the errors on r_ℓ for *Planck*, *Planck*+SO and PRISM, by taking as an example 4 broad bins - see caption for more details. Both the calculation with unbinned multipoles and Fig. 4.8 show how the multipole dependence induced by lensing magnification could be detected with future experiments.

Este documento incorpora firma electrónica, y es copia auténtica de un documento electrónico archivado por la ULL según la Ley 39/2015.
Su autenticidad puede ser contrastada en la siguiente dirección https://sede.ull.es/validacion/

Identificador del documento: 3764923 Código de verificación: JHlWnlbn

Firmado por: JOSE RAMON BERMEJO CLIMENT — Fecha: 01/09/2021 17:41:12
UNIVERSIDAD DE LA LAGUNA

José Alberto Rubiño Martín — 01/09/2021 17:49:44
UNIVERSIDAD DE LA LAGUNA

FABIO FINELLI — 02/09/2021 14:12:21
UNIVERSIDAD DE LA LAGUNA

Universidad de La Laguna
Oficina de Sede Electrónica
Entrada
Nº registro: 2021/90989
Nº reg. oficina: OF002/2021/89977
Fecha: 03/09/2021 12:24:13

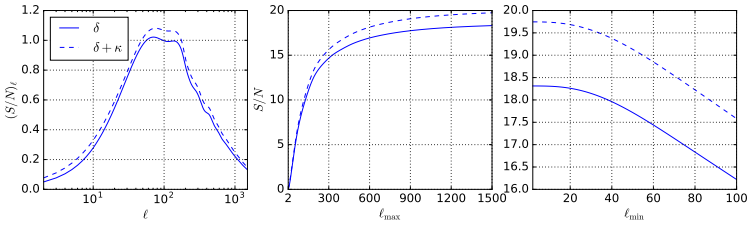

FIGURE 4.9— Contribution of each ℓ to the signal-to-noise of r_ℓ (left panel) and cumulative signal-to-noise as a function of $\ell_{\rm max}$ (center panel) and $\ell_{\rm min}$ (right panel). The solid lines represent the case including only the density term (δ) and the dashed lines correspond to the calculation including also the lensing magnification term ($\delta + \kappa$).

We calculate and show in Fig. 4.9 the SNR of the lensing ratio for the Euclid-r1 configuration as a function of $\ell_{\rm max}$ and $\ell_{\rm min}$, as well as the individual contribution of each multipole to the total amount. We find that the majority of the information of this estimator is around $\ell \sim 100$. We also find that including corrections from general relativity increases the SNR around $\lesssim 10\%$.

In Tab. 4.1 we list the SNR of the lensing ratio measurement for the CMB experiments considered as a function of the lens redshift $z_{\rm lens}$ of each bin. We find that the post-*Planck* CMB lensing will reduce significantly the error on this measurement, reaching up to $\sim 1\%$ with PRISM. We also note the synergies between the Euclid-like survey and the CMB space missions due to the overlapping sky fraction, as an example PICO will be able to measure the lensing ratio with better accuracy than S4 despite having a larger CMB lensing noise. The impact of the lensing correction is stronger at higher $z_{\rm lens}$, allowing to increase the SNR up to a factor $\sim$ 2-3 for the last redshift bin. We have also checked that complementing the ground-based SO and S4 experiments with *Planck* at $\ell < 30$ does not have a significant impact on the SNR.

4.5 Cosmological parameter constraints

We investigate here by a Fisher matrix approach whether the measurement of the lensing ratio can help to constrain cosmological parameters in extended models when it is added to the CMB information.

We define the Fisher matrix of the lensing ratio r_ℓ as

Este documento incorpora firma electrónica, y es copia auténtica de un documento electrónico archivado por la ULL según la Ley 39/2015.
Su autenticidad puede ser contrastada en la siguiente dirección https://sede.ull.es/validacion/

Identificador del documento: 3764923 Código de verificación: JHlWnlbn

Firmado por: JOSE RAMON BERMEJO CLIMENT — Fecha: 01/09/2021 17:41:12
UNIVERSIDAD DE LA LAGUNA

José Alberto Rubiño Martín — 01/09/2021 17:49:44
UNIVERSIDAD DE LA LAGUNA

FABIO FINELLI — 02/09/2021 14:12:21
UNIVERSIDAD DE LA LAGUNA

Universidad de La Laguna
Oficina de Sede Electrónica
Entrada
Nº registro: 2021/90989
Nº reg. oficina: OF002/2021/89977
Fecha: 03/09/2021 12:24:13

$z_{\rm lens}$	*Planck*		LiteBIRD		SO		S4		PICO		PRISM	
	δ	δ+κ	δ	δ+κ	δ	δ+κ	δ	δ+κ	δ	δ+κ	δ	δ+κ
0.95	18	20	23	25	31	34	55	61	60	67	72	81
1.05	18	20	23	25	30	34	51	59	55	64	64	77
1.15	17	19	22	25	28	33	46	56	50	62	56	72
1.25	16	19	20	25	26	33	40	53	43	58	48	67
1.35	15	19	19	24	23	32	35	50	37	55	40	61
1.45	14	19	17	24	21	30	29	46	30	50	32	54
1.55	12	18	15	23	18	28	23	42	24	45	25	48
1.65	11	17	12	22	15	27	18	37	19	40	19	42
1.75	9	16	10	20	12	25	13	32	14	35	14	36

TABLE 4.1— SNR of the lensing ratio for the CMB experiments considered as a function of the foreground redshift $z_{\rm lens}$ for the 9 bins of the Euclid-like spectroscopic survey. We list the SNR calculated using the density term only (δ) and considering also the contribution from lensing magnification (δ+κ).

$$\mathcal{F}^{r_\ell}_{\alpha\beta} \equiv \left\langle \frac{\partial^2 \mathcal{L}}{\partial\theta_\alpha \partial\theta_\beta} \right\rangle = \sum_\ell \frac{\partial r_\ell}{\partial\theta_\alpha} \frac{1}{\sigma^2_\ell(r_\ell)} \frac{\partial r_\ell}{\partial\theta_\beta}\,, \tag{4.31}$$

where θ_α, θ_β are the cosmological parameters. The lensing ratio Fisher matrix is added as uncorrelated to the CMB Fisher matrix [131, 132], which is given by

$$\mathcal{F}^{\rm CMB}_{\alpha\beta} = \sum_\ell \frac{2\ell+1}{2} f^{\rm CMB}_{\rm sky} {\rm Tr}\left[\frac{\partial \mathcal{C}}{\partial\theta_\alpha}\mathcal{C}^{-1}\frac{\partial \mathcal{C}}{\partial\theta_\beta}\mathcal{C}^{-1}\right], \tag{4.32}$$

where $\mathcal{C}$ is the 3x3 covariance matrix of the CMB data including temperature (TT), polarization (EE), lensing ($\phi\phi$) and their cross-correlations.

For the cosmological model, we extend the baseline ΛCDM+$\sum m_\nu$ cosmology to a 9 parameter model where we allow also to vary the dark energy equation of state and the curvature density (w_0CDM+$\sum m_\nu$+Ω_k), since we have shown in Section 4.3 that the lensing ratio is sensitive to the variation of these parameters. We adopt as fiducial values w_0 = -1 and $\Omega_k = 0$.

We show in Fig. 4.10 the 68% and 95% marginalized confidence regions for h, w_0, Ω_k and $\sum m_\nu$ obtained for a *Planck*-like CMB experiment following the Fisher matrix described in Eq. (4.32) and the sum of both r_ℓ and CMB Fisher matrices. We calculate the r_ℓ Fisher matrix for

Este documento incorpora firma electrónica, y es copia auténtica de un documento electrónico archivado por la ULL según la Ley 39/2015.
Su autenticidad puede ser contrastada en la siguiente dirección https://sede.ull.es/validacion/

Identificador del documento: 3764923 Código de verificación: JHlWnlbn

Firmado por: JOSE RAMON BERMEJO CLIMENT — Fecha: 01/09/2021 17:41:12
UNIVERSIDAD DE LA LAGUNA

José Alberto Rubiño Martín — 01/09/2021 17:49:44
UNIVERSIDAD DE LA LAGUNA

FABIO FINELLI — 02/09/2021 14:12:21
UNIVERSIDAD DE LA LAGUNA

Universidad de La Laguna
Oficina de Sede Electrónica
Entrada
Nº registro: 2021/90989
Nº reg. oficina: OF002/2021/89977
Fecha: 03/09/2021 12:24:13

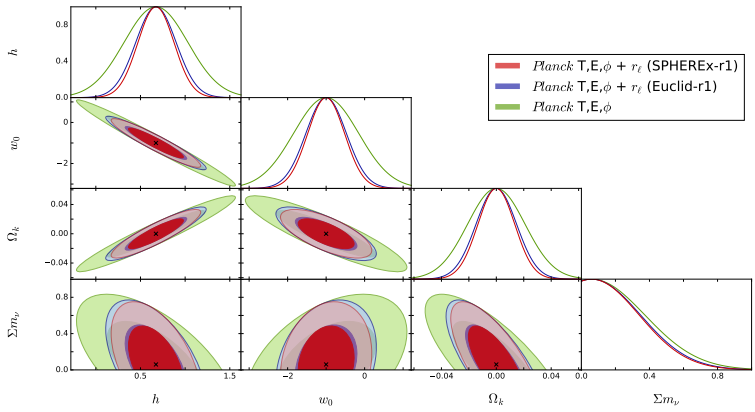

FIGURE 4.10— Marginalized 68% and 95% 2D confidence regions for a w_0CDM+$\sum m_\nu$+Ω_k model obtained by the Fisher matrix of a *Planck*-like experiment including temperature, polarization and lensing (green contours), and adding the Fisher matrix of the lensing ratio obtained using as lens population the first bin of the Euclid-r1 configuration at $0.9 < z_{\rm lens} < 1.0$ (blue contours) and the SPHEREx-r1 at $0.2 < z_{\rm lens} < 0.3$ (red contours). We do not show the other 5 cosmological parameters since they are not sensitive to the addition of lensing ratio to the CMB information.

Este documento incorpora firma electrónica, y es copia auténtica de un documento electrónico archivado por la ULL según la Ley 39/2015.
Su autenticidad puede ser contrastada en la siguiente dirección https://sede.ull.es/validacion/

Identificador del documento: 3764923 Código de verificación: JHlWnlbn

Firmado por:	JOSE RAMON BERMEJO CLIMENT *UNIVERSIDAD DE LA LAGUNA*	Fecha: 01/09/2021 17:41:12
	José Alberto Rubiño Martín *UNIVERSIDAD DE LA LAGUNA*	01/09/2021 17:49:44
	FABIO FINELLI *UNIVERSIDAD DE LA LAGUNA*	02/09/2021 14:12:21

Universidad de La Laguna
Oficina de Sede Electrónica
Entrada
Nº registro: 2021/90989
Nº reg. oficina: OF002/2021/89977
Fecha: 03/09/2021 12:24:13

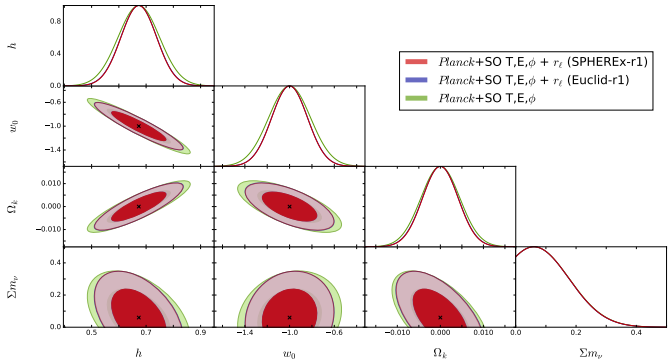

FIGURE 4.11— As for Fig. 4.10 but using *Planck*+SO as CMB experiment.

the Euclid-r1 and SPHEREx-r1 configurations described in Section 4.2. The improvement found by adding the lensing ratio to the CMB information is about $\lesssim 40\%$ for h, w_0 and Ω_k, while the neutrino mass is only marginally improved. For the spatial curvature we get a combined uncertainty of $\sigma(\Omega_k) \sim 0.015$, comparable to the *Planck* 2018 [46] error for a simpler ΛCDM+Ω_k model using CMB temperature and polarization. The constraints from the combination with the lensing ratio obtained with SPHEREx as foreground population are slightly better with respect to the Euclid-like spectroscopic lens.

In Fig. 4.11 we show the same constraints but using *Planck*+SO as CMB experiment. For this case, we find relative improvements around $\sim 15\%$ for h and w_0 and $\sim 10\%$ for Ω_k with respect to the CMB. For the spatial curvature error, we get $\sigma(\Omega_k) \sim 0.004$ for the combination of SO with Euclid-r1 or SPHEREx-r1.

We have shown that the $\hat{r}$ and $\hat{r}_\ell$ estimators -which neglect and include the contribution from lensing magnification, respectively- are different in terms of SNR. We now explore whether neglecting the inclusion of the lensing magnification term can induce a bias in the derived cosmological parameters. Following the formalism by [133], it can be shown the predicted bias in the cosmological parameters due to an uncorrected ef-

Este documento incorpora firma electrónica, y es copia auténtica de un documento electrónico archivado por la ULL según la Ley 39/2015.
Su autenticidad puede ser contrastada en la siguiente dirección https://sede.ull.es/validacion/

Identificador del documento: 3764923 Código de verificación: JHlWnlbn

Firmado por: JOSE RAMON BERMEJO CLIMENT — Fecha: 01/09/2021 17:41:12
UNIVERSIDAD DE LA LAGUNA

José Alberto Rubiño Martín — 01/09/2021 17:49:44
UNIVERSIDAD DE LA LAGUNA

FABIO FINELLI — 02/09/2021 14:12:21
UNIVERSIDAD DE LA LAGUNA

Universidad de La Laguna
Oficina de Sede Electrónica
Entrada
Nº registro: 2021/90989
Nº reg. oficina: OF002/2021/89977
Fecha: 03/09/2021 12:24:13

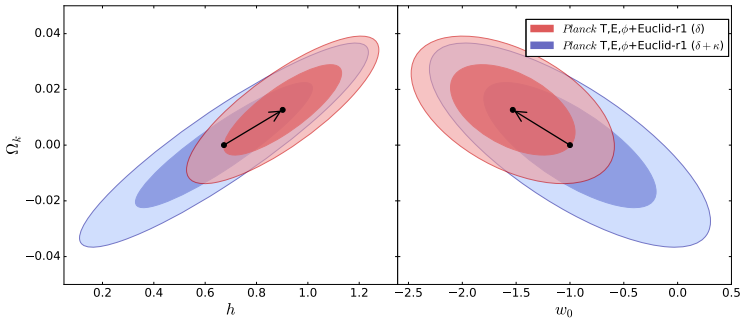

FIGURE 4.12— Predicted bias in the cosmological parameters induced by neglecting the lensing magnification contribution to the galaxy number counts in a combined analysis of the CMB and the lensing ratio, using *Planck* and the Euclid-r1 configuration. The blue contours represent the marginalized 68% and 95% 2D confidence regions for the h-Ω_k and w_0-Ω_k planes obtained considering the lensing contribution ($\delta + \kappa$), while the red contours correspond to the case with the density term only (δ).

fect/systematic is expressed as

$$b_{\theta_\alpha} = (\widetilde{\mathcal{F}}^{-1})_{\alpha\beta} B_\beta \,, \tag{4.33}$$

where $\widetilde{\mathcal{F}}_{\alpha\beta}$ is the Fisher matrix computed by assuming the theoretical signal without the lensing magnification term. The vector B_β is given by

$$B_\beta = \sum_\ell \frac{1}{\sigma^2_\ell(\widetilde{r}_\ell)} (\widetilde{r}_\ell - r_\ell) \frac{\partial \widetilde{r}_\ell}{\partial \theta_\beta} \,, \tag{4.34}$$

where $\widetilde{r}_\ell$ and r_ℓ are the lensing ratios obtained without and with the lensing magnification contribution, respectively.

By our working assumptions, we compute the bias in the cosmological parameters for the combined constraints from *Planck* and the lensing ratio using the Euclid-r1 configuration as an example. We represent the result in Fig. 5.4, where we show the marginalized 68% and 95% 2D confidence regions for the h-Ω_k and w_0-Ω_k planes obtained considering and neglecting the lensing term, and we have shifted the uncorrected contours by the amount given by Eq. (4.33). We get for the bias on the parameters $b_h = 0.23$, $b_{w_0} = -0.53$ and $b_{\Omega_k} = 0.013$, which taking into account the uncertainties from both approaches corresponds to a shift of 0.85σ for h,

Este documento incorpora firma electrónica, y es copia auténtica de un documento electrónico archivado por la ULL según la Ley 39/2015.
Su autenticidad puede ser contrastada en la siguiente dirección https://sede.ull.es/validacion/

Identificador del documento: 3764923 Código de verificación: JHlWnlbn

Firmado por: JOSE RAMON BERMEJO CLIMENT — Fecha: 01/09/2021 17:41:12
UNIVERSIDAD DE LA LAGUNA

José Alberto Rubiño Martín — 01/09/2021 17:49:44
UNIVERSIDAD DE LA LAGUNA

FABIO FINELLI — 02/09/2021 14:12:21
UNIVERSIDAD DE LA LAGUNA

Universidad de La Laguna
Oficina de Sede Electrónica
Entrada
Nº registro: 2021/90989
Nº reg. oficina: OF002/2021/89977
Fecha: 03/09/2021 12:24:13

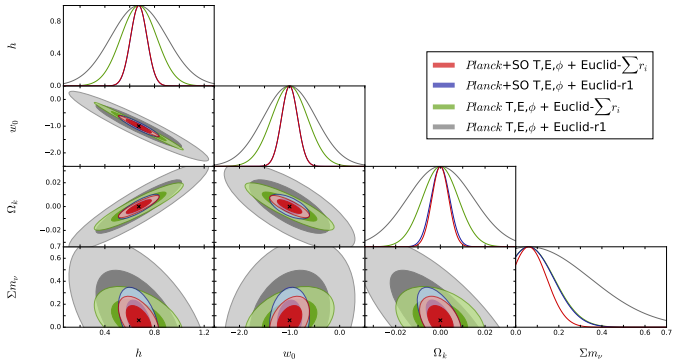

FIGURE 4.13— Marginalized 68% and 95% 2D confidence regions for a w_0CDM+$\sum m_\nu$+Ω_k model forecast by the combination of a *Planck*-like experiment with the Euclid-r1 lensing ratio configuration (grey contours) and the Euclid-$\sum r_i$ tomographic analysis (green contours), and by the combination of *Planck*+SO with the Euclid-r1 configuration (blue contours) and the Euclid-$\sum r_i$ tomographic analysis (red contours).

0.8σ for w_0 and 0.7σ for Ω_k. Whereas the forecast uncertainties by lensing ratio *alone* improve by adding lensing magnification, consistently with the improvement in the SNR shown in Tab. 4.1, it is clear from Fig. 5.4 that the forecast uncertainties in h-Ω_k and w_0-Ω_k in combination with the CMB degrade when taking into account lensing magnification. We interpret this effect as a consequence of introducing an improved lensing ratio which goes beyond its only dependence on distances and on background cosmology and therefore worsten the uncertainties on parameters as h-w_0-Ω_k. Therefore, the neglection of lensing magnification term could overestimate the constraints achievable with lensing ratios using lenses at the typical redshift of a Euclid-like spectroscopic survey, in which this contribution is important, and would lead to a potential bias in the cosmological parameters.

We now explore the possibility of improving the cosmological parameter constraints by combining the 9 possible lensing ratio configurations for Euclid ranging from $z_{\rm lens} = 0.9$ to $z_{\rm lens} = 1.8$ in a joint tomographic measurement, which hereafter we call Euclid-$\sum r_i$. We introduce the covariance of N ratios to take into account that in this combination there

Este documento incorpora firma electrónica, y es copia auténtica de un documento electrónico archivado por la ULL según la Ley 39/2015.
Su autenticidad puede ser contrastada en la siguiente dirección https://sede.ull.es/validacion/

Identificador del documento: 3764923 Código de verificación: JHlWnlbn

Firmado por:	JOSE RAMON BERMEJO CLIMENT *UNIVERSIDAD DE LA LAGUNA*	Fecha: 01/09/2021 17:41:12
	José Alberto Rubiño Martín *UNIVERSIDAD DE LA LAGUNA*	01/09/2021 17:49:44
	FABIO FINELLI *UNIVERSIDAD DE LA LAGUNA*	02/09/2021 14:12:21

Universidad de La Laguna
Oficina de Sede Electrónica
Entrada
Nº registro: 2021/90989
Nº reg. oficina: OF002/2021/89977
Fecha: 03/09/2021 12:24:13

is redshift overlap between the different backgrounds and between some backgrounds and foregrounds. We then rewrite Eq. (4.31) as

$$\mathcal{F}^{r_\ell}_{\alpha\beta} = \sum_\ell \sum_{i,j}^{N} \frac{\partial r^i_\ell}{\partial\theta_\alpha} [\mathrm{Cov}(\hat{r}_\ell)]^{-1}_{ij} \frac{\partial r^j_\ell}{\partial\theta_\beta}\,, \tag{4.35}$$

where the i, j indices run over the ratios and the elements of the covariance matrix $\mathrm{Cov}(\hat{r}_\ell)_{ij}$ are given by

$$\begin{aligned}
\mathrm{Cov}(\hat{r}_\ell)_{ij} = \frac{1}{(2\ell+1)} & \frac{1}{C_\ell^{\kappa^i_{\rm gal}G^i} C_\ell^{\kappa^j_{\rm gal}G^j}} \\
& \times \left[\frac{1}{f_{\rm sky}^{\kappa_{\rm CMB}G}} \left(\bar{C}_\ell^{\kappa_{\rm CMB}\kappa_{\rm CMB}} \bar{C}_\ell^{G^iG^j} + C_\ell^{\kappa_{\rm CMB}G^i} C_\ell^{\kappa_{\rm CMB}G^j} \right) \right. \\
& \quad + \frac{r^i_{\ell,0} r^j_{\ell,0}}{f_{\rm sky}^{\kappa_{\rm gal}G}} \left(\bar{C}_\ell^{\kappa^i_{\rm gal}\kappa^j_{\rm gal}} \bar{C}_\ell^{G^iG^j} + C_\ell^{\kappa^i_{\rm gal}G^j} C_\ell^{\kappa^j_{\rm gal}G^i} \right) \\
& \quad - r^i_{\ell,0} \frac{f_{\rm sky}^{\kappa_{\rm CMB}\kappa_{\rm gal}G}}{f_{\rm sky}^{\kappa_{\rm CMB}G} f_{\rm sky}^{\kappa_{\rm gal}G}} \left(C_\ell^{\kappa_{\rm CMB}\kappa^i_{\rm gal}} \bar{C}_\ell^{G^iG^j} + C_\ell^{\kappa_{\rm CMB}G^i} C_\ell^{\kappa^i_{\rm gal}G^j} \right) \\
& \quad \left. - r^j_{\ell,0} \frac{f_{\rm sky}^{\kappa_{\rm CMB}\kappa_{\rm gal}G}}{f_{\rm sky}^{\kappa_{\rm CMB}G} f_{\rm sky}^{\kappa_{\rm gal}G}} \left(C_\ell^{\kappa_{\rm CMB}\kappa^j_{\rm gal}} \bar{C}_\ell^{G^iG^j} + C_\ell^{\kappa_{\rm CMB}G^j} C_\ell^{\kappa^j_{\rm gal}G^i} \right) \right] .
\end{aligned} \tag{4.36}$$

In Fig. 4.13 we compare the constraints obtained for *Planck* and *Planck*+SO in combination with the Euclid-r1 configuration to their combination with the tomographic Euclid-$\sum r_i$ measurement. For *Planck*, the constraints on h, w_0 and Ω_k are improved around $\sim 40\%$ from the tomography with respect to the single ratio case, this corresponds to a $\sim$ 60-70% improvement with respect to *Planck* alone. We get a joint uncertainty on the spatial curvature of $\sigma(\Omega_k) \sim 0.008$. The neutrino mass is the most benefited parameter from the tomography, reaching up to a $\sim 60\%$ improvement with respect to the single bin case. For *Planck*+SO, the CMB has a higher relative weight but still the error on Ω_k is improved around $\sim 10\%$ with tomography, while the neutrino mass error is improved around $\sim 30\%$.

Este documento incorpora firma electrónica, y es copia auténtica de un documento electrónico archivado por la ULL según la Ley 39/2015.
Su autenticidad puede ser contrastada en la siguiente dirección https://sede.ull.es/validacion/

Identificador del documento: 3764923 Código de verificación: JHlWnlbn

Firmado por:	JOSE RAMON BERMEJO CLIMENT *UNIVERSIDAD DE LA LAGUNA*	Fecha: 01/09/2021 17:41:12
	José Alberto Rubiño Martín *UNIVERSIDAD DE LA LAGUNA*	01/09/2021 17:49:44
	FABIO FINELLI *UNIVERSIDAD DE LA LAGUNA*	02/09/2021 14:12:21

Universidad de La Laguna
Oficina de Sede Electrónica
Entrada
Nº registro: 2021/90989
Nº reg. oficina: OF002/2021/89977
Fecha: 03/09/2021 12:24:13

5

A 2D tomographic approach to CMB and galaxy clustering

We have shown in Sec. 3.3 that the cross-correlation between CMB fields and galaxy surveys carries important cosmological information, and in particular, that the CMB lensing - number counts cross-correlation has a higher signal-to-noise compared to the corresponding one with CMB temperature. In this chapter, we investigate what can the cross-correlation of CMB fields with galaxy number counts add to a joint 2D tomographic analysis of both probes, in terms of constraining parameters for standard and non-standard cosmological models.

First, we describe in Sec. 5.1 the Fisher matrix formalism that we use for forecasting constraints on cosmological parameters. In Sec. 5.2 this analysis is performed for the current concordance ΛCDM model and some of its important extensions such as: (i) the w_0, w_a parametrization for a dark energy component with a parameter of state dependent on the redshift, (ii) a neutrino sector in which $N_{\rm eff}$ and Σm_ν are allowed to vary, (iii) primordial perturbations which allow the running of the spectral index and a local non-Gaussianity parameter which leads to a scale dependence for the galaxy bias. These generalizations beyond the ΛCDM cosmology in the dark energy, neutrino and primordial perturbation sectors are considered either separately, i.e. three different extensions of the concordance cosmology with 2 extra parameters, and jointly, i.e. as an extended cosmological model with 12 parameters (see [134] for a study of a different 12 cosmological parameters model with current data), as an example of

Este documento incorpora firma electrónica, y es copia auténtica de un documento electrónico archivado por la ULL según la Ley 39/2015.
Su autenticidad puede ser contrastada en la siguiente dirección https://sede.ull.es/validacion/

Identificador del documento: 3764923 Código de verificación: JHlWnlbn

Firmado por:	JOSE RAMON BERMEJO CLIMENT *UNIVERSIDAD DE LA LAGUNA*	Fecha: 01/09/2021 17:41:12
	José Alberto Rubiño Martín *UNIVERSIDAD DE LA LAGUNA*	01/09/2021 17:49:44
	FABIO FINELLI *UNIVERSIDAD DE LA LAGUNA*	02/09/2021 14:12:21

Universidad de La Laguna
Oficina de Sede Electrónica
Entrada
Nº registro: 2021/90989
Nº reg. oficina: OF002/2021/89977
Fecha: 03/09/2021 12:24:13

the type of extended cosmologies which could be studied in the future thanks to the improvement in the data and the combination between different kinds of data. Then, in Sec. 5.3 we apply the same methodology to obtain constraints on four non-standard inflationary models that produce deviations (features) from a power-law primordial power spectrum.

In terms of analysis, our study focus on the relevance of including CMB cross-correlation for multipoles where the linear perturbation is sufficiently adequate as in [105]. This conservative cut to linear scales insure scientific validity to our analysis since accurate descriptions on non-linear scales are not available for all the cosmological models we analyze. At the same time it is useful to know how to use the whole cosmological information contained in linear scales, given the necessity to introduce theoretical uncertainties in correctly handling non-linear scales [136].

In Sec. 5.4 we give an outlook on the possible extensions of this methodology, first including an effect on scale dependence of the galaxy bias due to massive neutrinos, and then exploring the capabilities of including the galaxy weak lensing as additional cosmological probe, as well as its cross-correlations with the CMB fields and the galaxy number counts. Finally, in Sec. 5.5 we present the Euclid official forecasts for the combination of all its probes with the CMB, which have been supported by the methodology described in this chapter.

The methodology and results in this chapter reflect mainly the work published in Bermejo-Climent et al. (2021) [78]. Sec. 5.3 shows content that belongs to a paper in preparation, and Sec. 5.5 contains part of the results shown in [135].

5.1 Fisher formalism for cosmological parameter forecasts

We use the Fisher matrix information [137] to forecast cosmological parameters uncertainties. In the Fisher formalism, the likelihood $\mathcal{L}$ is assumed to be a multivariate Gaussian and the minimum errors on the cosmological parameters are given by the diagonal of the inverse of the Fisher matrix as $\sigma_i \geq \sqrt{(\mathcal{F}^{-1})_{ii}}$. The Fisher matrix $\mathcal{F}$ is defined as:

$$\mathcal{F}_{\alpha\beta} = \left\langle \frac{\partial^2 \mathcal{L}}{\partial\theta_\alpha \partial\theta_\beta} \right\rangle = \frac{1}{2}\mathrm{Tr}\left[\frac{\partial \mathcal{C}}{\partial\theta_\alpha}\mathcal{C}^{-1}\frac{\partial \mathcal{C}}{\partial\theta_\beta}\mathcal{C}^{-1} \right], \tag{5.1}$$

where $\mathcal{C}$ is the theoretical covariance matrix and θ_α, θ_β are the cosmological parameters. If we take into account the number of modes given by

Este documento incorpora firma electrónica, y es copia auténtica de un documento electrónico archivado por la ULL según la Ley 39/2015.
Su autenticidad puede ser contrastada en la siguiente dirección https://sede.ull.es/validacion/

Identificador del documento: 3764923 Código de verificación: JHlWnlbn

Firmado por:	JOSE RAMON BERMEJO CLIMENT *UNIVERSIDAD DE LA LAGUNA*	Fecha: 01/09/2021 17:41:12
	José Alberto Rubiño Martín *UNIVERSIDAD DE LA LAGUNA*	01/09/2021 17:49:44
	FABIO FINELLI *UNIVERSIDAD DE LA LAGUNA*	02/09/2021 14:12:21

Universidad de La Laguna
Oficina de Sede Electrónica
Entrada
Nº registro: 2021/90989
Nº reg. oficina: OF002/2021/89977
Fecha: 03/09/2021 12:24:13

$(2\ell+1)f_{\rm sky}/2$, Eq. (5.1) becomes

$$\mathcal{F}_{\alpha\beta} = \sum_{\ell_{\rm min}}^{\ell_{\rm max}} \sum_{abcd} \frac{2\ell+1}{2} f_{\rm sky}^{abcd} \frac{\partial C_\ell^{ab}}{\partial\theta_\alpha} (\mathcal{C}^{-1})^{bc} \frac{\partial C_\ell^{cd}}{\partial\theta_\alpha} (\mathcal{C}^{-1})^{da} \,, \tag{5.2}$$

where $abcd \in \{T, E, \phi, G_1, ..., G_N\}$ [1] and $f_{\rm sky}^{abcd} \equiv \sqrt{f_{\rm sky}^{ab} f_{\rm sky}^{cd}}$ is the effective sky fraction for each pair of channels. The theoretical covariance matrix $\mathcal{C}$ is defined as

$$\mathcal{C} = \begin{bmatrix} \bar{C}_\ell^{TT} & C_\ell^{TE} & C_\ell^{T\phi} & C_\ell^{TG_1} & \dots & C_\ell^{TG_N} \\ C_\ell^{TE} & \bar{C}_\ell^{EE} & C_\ell^{E\phi} & C_\ell^{EG_1} & \dots & C_\ell^{EG_N} \\ C_\ell^{T\phi} & C_\ell^{E\phi} & \bar{C}_\ell^{\phi\phi} & C_\ell^{\phi G_1} & \dots & C_\ell^{\phi G_N} \\ C_\ell^{TG_1} & C_\ell^{EG_1} & C_\ell^{\phi G_1} & \bar{C}_\ell^{G_1G_1} & \dots & C_\ell^{G_1G_N} \\ \vdots & \vdots & \vdots & \vdots & \ddots & \vdots \\ C_\ell^{TG_N} & C_\ell^{EG_N} & C_\ell^{\phi G_N} & C_\ell^{G_1G_N} & \dots & \bar{C}_\ell^{G_NG_N} \end{bmatrix} . \tag{5.3}$$

Concerning the minimum multipole $\ell_{\rm min}$ in Eq. (5.1), we use as baseline $\ell_{\rm min}^{GG} = \ell_{\rm min}^{TG} = \ell_{\rm min}^{\phi G}$. We link $\ell_{\rm min}^{GG}$ to the sky fraction covered by the galaxy survey and we adopt $\ell_{\rm min}^{GG} = 10$ for Euclid-like, $\ell_{\rm min}^{GG} = 20$ for LSST, $\ell_{\rm min}^{GG} = 5$ for SKA. We consider $\ell_{\rm min}^{GG} = 2$ for SPHEREx and EMU since both cover a wider sky fraction. For $\ell_{\rm max}^{\phi G}$ we restrict to quasi-linear scales as discussed in Section 3.3 and we set $\ell_{\rm max}^{GG} = \chi(\bar{z})k_{\rm max} - 1/2$ with $\chi(\bar{z})$ is the comoving distance at the median redshift $\bar{z}$ of the redshift bin $[105, 106]$ and $k_{\rm max} = 0.1$ h/Mpc.

5.2 Constraints on ΛCDM and extensions

In this section we present the forecast constraints on cosmological parameters from the 2D angular tomographic combination of the CMB and galaxy clustering. We describe the cosmological models that we target in Sec. 5.2.1 and we show the results in Sec. 5.2.2.

5.2.1 Cosmological models

We adopt different cosmologies as fiducial models in our analysis. First, we test a ΛCDM cosmology and the w_0CDM model for the dark energy equation of state. We then consider three representative cases for the dark

[1] Note that we consider $C_\ell^{TT}, C_\ell^{TE}, C_\ell^{EE}$ to avoid double counting the lensing contribution as in [138].

Este documento incorpora firma electrónica, y es copia auténtica de un documento electrónico archivado por la ULL según la Ley 39/2015.
Su autenticidad puede ser contrastada en la siguiente dirección https://sede.ull.es/validacion/

Identificador del documento: 3764923 Código de verificación: JHlWnlbn

Firmado por:	JOSE RAMON BERMEJO CLIMENT *UNIVERSIDAD DE LA LAGUNA*	Fecha: 01/09/2021 17:41:12
	José Alberto Rubiño Martín *UNIVERSIDAD DE LA LAGUNA*	01/09/2021 17:49:44
	FABIO FINELLI *UNIVERSIDAD DE LA LAGUNA*	02/09/2021 14:12:21

Universidad de La Laguna
Oficina de Sede Electrónica
Entrada
Nº registro: 2021/90989
Nº reg. oficina: OF002/2021/89977
Fecha: 03/09/2021 12:24:13

energy sector, neutrino physics and physics of the Early Universe, each modelled by a two parameters extension of the baseline ΛCDM cosmology. Finally, we consider as extCDM the 12 parameters cosmological model that considers jointly the three above mentioned extensions.

For the dark energy sector, we use the CPL parametrization [101, 102] of the parameter of state redshift dependence, given by Eq. (3.7).

For the neutrino physics we consider the minimal mass for the normal hierarchy assuming a total neutrino mass of $\Sigma m_\nu = 0.06$ eV in a single neutrino and two massless neutrinos. By allowing $N_{\rm eff}$ to vary, we consider the number of relativistic species (including massless neutrino) as the second free parameter.

For the extensions connected to the physics of the Early Universe we consider a primordial power spectrum given by

$$\mathcal{P}_\mathcal{R}(k) \equiv \frac{k^3}{2\pi^2}|\mathcal{R}_k|^2 = A_s(k/k_*)^{n_s-1+\frac{1}{2}\frac{\mathrm{d}n_s}{\mathrm{d}\ln k}\ln(k/k_*)}\,, \tag{5.4}$$

allowing for a running term $\frac{\mathrm{d}n_s}{\mathrm{d}\ln k} \neq 0$. Moreover, we consider a scale-dependent bias induced by a primordial local non-Gaussianity $f_{\rm NL}^{\rm loc}$ as [139, 140]

$$b(k,z) = b_G(z) + \Delta b(k,z) = b_G(z) + [b_G(z)-1] f_{\rm NL}^{\rm loc}\delta_c \frac{3\Omega_m H_0^2}{c^2 k^2 T(k) D(z)}\,, \tag{5.5}$$

where $b_G(z)$ is the usual linear galaxy bias calculated assuming scale-independent Gaussian initial conditions, δ_c is the critical spherical over-density ($\delta_c \simeq 1.686$ as predicted in [141]), $T(k)$ is the matter transfer function, for which we adopt the analytical expression by [142], and $D(z)$ is the linear growth factor normalized according to the CMB convention.

For the central values of the parameters we adopt a ΛCDM+Σm_ν fiducial model consistent with the *Planck* 2018 results [46]: $\Omega_b h^2 = 0.022383$, $\Omega_c h^2 = 0.12011$, $H_0 = 67.32$ km s^{-1} Mpc^{-1}, $\tau = 0.0543$, $n_s = 0.96605$, $\ln(10^{10}A_s) = 3.0448$, $w_0 = $ -1, $w_a = 0$, $\sum m_\nu = 0.06$ eV, $N_{\rm eff} = 3.046$, $\frac{\mathrm{d}n_s}{\mathrm{d}\ln k} = 0$ and $f_{\rm NL} = 0$.

We include in our analysis nuisance parameters to account for the uncertainties in the number density distribution and galaxy clustering bias of the surveys. We vary the redshift parameter z_0 to consider the uncertainties on the $\mathrm{d}N/\mathrm{d}z$ function, and include a free constant per bin as $b_n(\bar{z}_n)b_G(z)$, where n is the n-th redshift bin, to account for the uncertainties on the galaxy clustering bias function. In the single bin cases, we

Este documento incorpora firma electrónica, y es copia auténtica de un documento electrónico archivado por la ULL según la Ley 39/2015.
Su autenticidad puede ser contrastada en la siguiente dirección https://sede.ull.es/validacion/

Identificador del documento: 3764923 Código de verificación: JHlWnlbn

Firmado por: JOSE RAMON BERMEJO CLIMENT — Fecha: 01/09/2021 17:41:12
UNIVERSIDAD DE LA LAGUNA

José Alberto Rubiño Martín — 01/09/2021 17:49:44
UNIVERSIDAD DE LA LAGUNA

FABIO FINELLI — 02/09/2021 14:12:21
UNIVERSIDAD DE LA LAGUNA

Universidad de La Laguna
Oficina de Sede Electrónica
Entrada
Nº registro: 2021/90989
Nº reg. oficina: OF002/2021/89977
Fecha: 03/09/2021 12:24:13

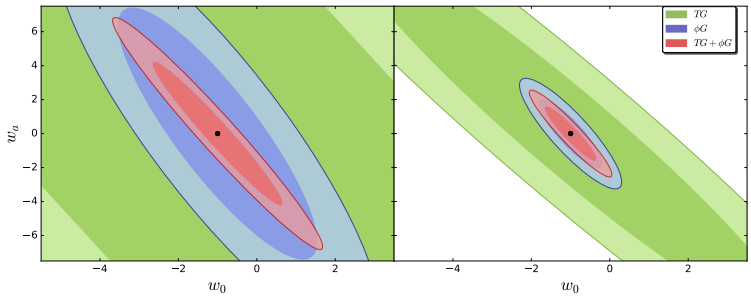

FIGURE 5.1— Marginalized 68% and 95% 2D confidence regions for the constraints from TG, ϕG and the combination of both for the $w_0 w_a$CDM model. The left panels correspond to *Planck* × Euclid-ph-like and the right panels to LiteBIRD+S4 × SKA1. The green contours correspond to the temperature-galaxy cross-correlation constraints (TG) the blue contours to the lensing-galaxy cross-correlation (ϕG) and the red contours to the sum of both ($TG + \phi G$).

also include an extra nuisance parameter that modifies the slope of $b_G(z)$. Hence, we include 3 nuisance parameters for the single bin cases and N+1 nuisance parameters for the N bins tomographic cases.

5.2.2 Joint forecasts on cosmological parameters

In order to quantify the relevance of including the CMB-galaxy cross-correlation for the parameter constraints, we compare the forecast uncertainties using two approaches. The first one is the simple combination of CMB and galaxy clustering (GC) as uncorrelated probes, which we call CMB + GC. In this case, we apply Eq. (5.2) to both probes independently and we add the two resulting Fisher matrices, being equivalent to neglecting the off-diagonal blocks in Eq. (5.3) that account for the CMB-galaxy cross-correlation. In the second approach, which we call CMB × GC, we compute one joint Fisher matrix using the full covariance matrix described by Eq. (5.3) that includes the TG, EG and ϕG correlations. We choose to present the results in this way since the CMB-GC cross-correlation alone would lead to loose constraints on parameters. Fig. 5.1 indeed shows the constraints from TG and ϕG separately and jointly for the dark energy extension for *Planck* × Euclid-ph and LiteBIRD + CMB-S4 × SKA1. The information from ϕG provides better constraints than TG alone, but the combined constraints $TG + \phi G$ are still loose.

Este documento incorpora firma electrónica, y es copia auténtica de un documento electrónico archivado por la ULL según la Ley 39/2015.
Su autenticidad puede ser contrastada en la siguiente dirección https://sede.ull.es/validacion/

Identificador del documento: 3764923 Código de verificación: JHlWnlbn

Firmado por: JOSE RAMON BERMEJO CLIMENT — Fecha: 01/09/2021 17:41:12
UNIVERSIDAD DE LA LAGUNA

José Alberto Rubiño Martín — 01/09/2021 17:49:44
UNIVERSIDAD DE LA LAGUNA

FABIO FINELLI — 02/09/2021 14:12:21
UNIVERSIDAD DE LA LAGUNA

Universidad de La Laguna
Oficina de Sede Electrónica
Entrada
Nº registro: 2021/90989
Nº reg. oficina: OF002/2021/89977
Fecha: 03/09/2021 12:24:13

It is also useful to introduce the Figure of Merit (FoM) to quantify the capability of constraining a pair of parameters (α,β) as [92]

$$\mathrm{FoM}_{\alpha,\beta} = \frac{1}{\sqrt{\det(\mathcal{F}^{-1}_{\alpha,\beta})}}\,, \tag{5.6}$$

where $\mathcal{F}^{-1}_{\alpha,\beta}$ is the 2x2 covariance matrix of the two parameters. More generally, we can define the FoM of N parameters as [143, 144]

$$\mathrm{FoM}_{\alpha_i} = \left[\frac{1}{\det(\mathcal{F}^{-1}_{\alpha_i})}\right]^{1/N}\,, \tag{5.7}$$

where $\mathcal{F}^{-1}_{\alpha_i}$ is the covariance NxN corresponding matrix of the parameters. We use the first definition to calculate the FoM of two parameters; we use the second one for the FoM of the primary cosmological parameters and for the FoM of the bias nuisance parameters of a given model. Note that the FoM defined in [145] can be obtained by $(\cdot)^{N/2}$ the one in Eq. (5.7).

We quantify the relevance of the CMB-GC cross-correlation comparing the parameter constraints obtained with the CMB + GC and CMB × GC approaches described in Sec. 4.5. In order to evaluate the impact of tomography, for each galaxy survey we present results either by using a single redshift bin and the baseline number of bins discussed in Sec. 3.2. We first discuss the ΛCDM model, then w_0CDM, the three two parameters extensions - w_0w_aCDM, ΛCDM + $\{\Sigma m_\nu, N_{\rm eff}\}$, ΛCDM + $\{\mathrm{d}n_s/\mathrm{d}\ln k, f_{\rm NL}\}$ - and then the 12 parameters extCDM model. For each model in the Tabs. of Appendix B, we quote the 68% marginalized uncertainties on cosmological parameters and FoMs, which show the improvement in cosmology and in the characterization of the galaxy clustering bias.

For the ΛCDM model the improvement in the uncertainties in cosmological parameters due to the CMB-GC cross-correlation is maximum for $\Omega_c h^2$, whose uncertainty improves by $\lesssim 20\%$ in the combinations of *Planck* with EMU and SKA1. The uncertainties for the various configurations are displayed in Tab. A.1. Since it has been discussed [103, 146] that CMB-GC cross-correlation can help to constrain fluctuation amplitudes, we also derive the uncertainty on σ_8 for the ΛCDM and the extCDM models using a Jacobian matrix transformation.

For the dark energy extensions, the uncertainties on the parameters of state can be reduced up to a factor $\lesssim 2$ with the inclusion of CMB-GC

Este documento incorpora firma electrónica, y es copia auténtica de un documento electrónico archivado por la ULL según la Ley 39/2015.
Su autenticidad puede ser contrastada en la siguiente dirección https://sede.ull.es/validacion/

Identificador del documento: 3764923 Código de verificación: JHlWnlbn

Firmado por: JOSE RAMON BERMEJO CLIMENT — Fecha: 01/09/2021 17:41:12
UNIVERSIDAD DE LA LAGUNA

José Alberto Rubiño Martín — 01/09/2021 17:49:44
UNIVERSIDAD DE LA LAGUNA

FABIO FINELLI — 02/09/2021 14:12:21
UNIVERSIDAD DE LA LAGUNA

Universidad de La Laguna
Oficina de Sede Electrónica
Entrada
Nº registro: 2021/90989
Nº reg. oficina: OF002/2021/89977
Fecha: 03/09/2021 12:24:13

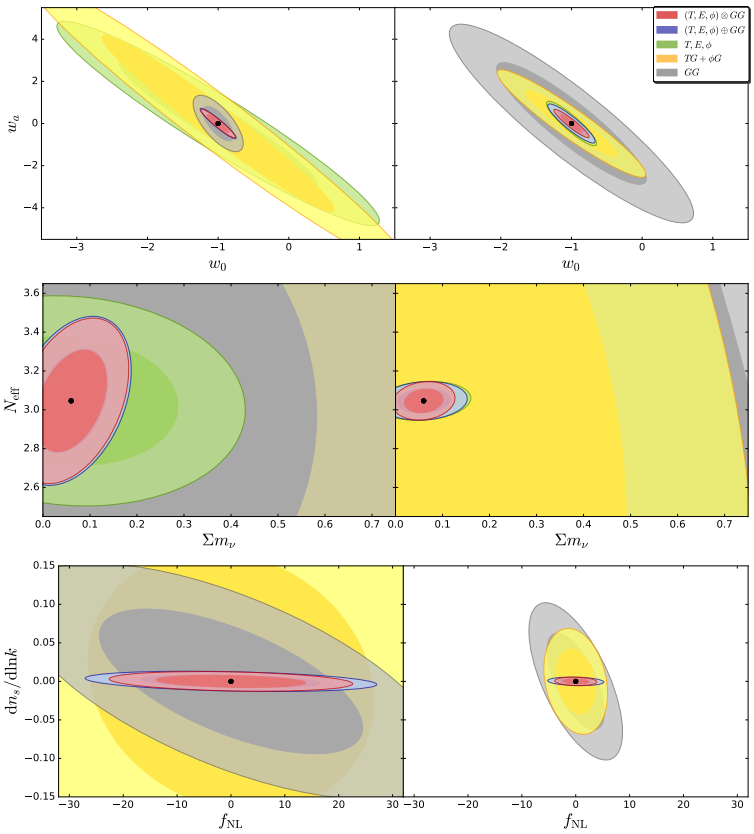

FIGURE 5.2— Marginalized 68% and 95% 2D confidence regions for the constraints from CMB, GC and cross-correlation independently and jointly for the three 2 parameter ΛCDM extensions: dark energy (top), neutrino physics (middle) and primordial universe (bottom). The left panels correspond to *Planck* × Euclid-ph-like and the right panels to LiteBIRD+S4 × SKA1. The green contours correspond to the CMB-only constraints (T, E, ϕ), the yellow contours to the cross-correlation only $(TG, \phi G)$, the grey contours to the galaxy counts (GG), the blue contours to the CMB-GC combination as uncorrelated $(T, E, \phi + GG)$ and the red contours to the combination including cross-correlation $(T, E, \phi \times GG)$. In the bottom panel the green contours are not shown since $f_{\rm NL}$ is not constrained from the CMB information in our analysis.

Este documento incorpora firma electrónica, y es copia auténtica de un documento electrónico archivado por la ULL según la Ley 39/2015.
Su autenticidad puede ser contrastada en la siguiente dirección https://sede.ull.es/validacion/

Identificador del documento: 3764923 Código de verificación: JHlWnlbn

Firmado por: JOSE RAMON BERMEJO CLIMENT — Fecha: 01/09/2021 17:41:12
UNIVERSIDAD DE LA LAGUNA

José Alberto Rubiño Martín — 01/09/2021 17:49:44
UNIVERSIDAD DE LA LAGUNA

FABIO FINELLI — 02/09/2021 14:12:21
UNIVERSIDAD DE LA LAGUNA

Universidad de La Laguna
Oficina de Sede Electrónica
Entrada
Nº registro: 2021/90989
Nº reg. oficina: OF002/2021/89977
Fecha: 03/09/2021 12:24:13

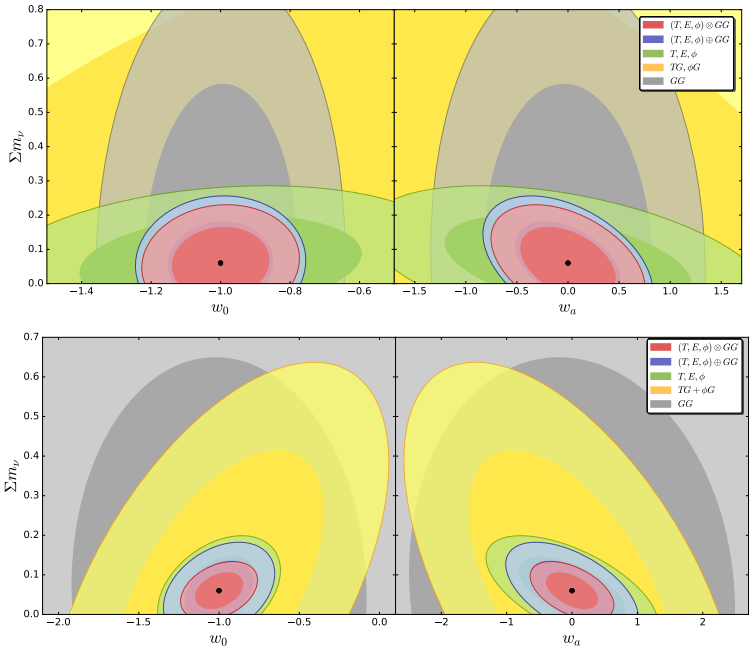

FIGURE 5.3— Marginalized 68% and 95% 2D confidence regions for the joint constraints on Σm_ν and w_0, w_a for a 9 parameters model ($w_0 w_a$CDM+Σm_ν) using the combination of *Planck*+SO and Euclid-ph-like in the top panel and of LiteBIRD+CMB-S4 and SKA1 in the bottom panel. The grey contours correspond to LSS-only constraints (GG), the yellow contours to the cross-correlation only ($TG+\phi$G) the green contours to the CMB-only constraints (T, E, ϕ), the blue contours to the combination of CMB and galaxy clustering as uncorrelated and the red ones to the combination including cross-correlation.

Este documento incorpora firma electrónica, y es copia auténtica de un documento electrónico archivado por la ULL según la Ley 39/2015.
Su autenticidad puede ser contrastada en la siguiente dirección https://sede.ull.es/validacion/

Identificador del documento: 3764923 Código de verificación: JHlWnlbn

Firmado por:	JOSE RAMON BERMEJO CLIMENT *UNIVERSIDAD DE LA LAGUNA*	Fecha: 01/09/2021 17:41:12
	José Alberto Rubiño Martín *UNIVERSIDAD DE LA LAGUNA*	01/09/2021 17:49:44
	FABIO FINELLI *UNIVERSIDAD DE LA LAGUNA*	02/09/2021 14:12:21

Universidad de La Laguna
Oficina de Sede Electrónica
Entrada
Nº registro: 2021/90989
Nº reg. oficina: OF002/2021/89977
Fecha: 03/09/2021 12:24:13

cross-correlation. In the simpler w_0CDM model, we obtain the best uncertainty on the dark energy parameter of state ($\sigma(w_0) \sim 0.025$) with the combination of LiteBIRD+S4 × Euclid-ph-like. CMB-GC cross-correlation can complement those surveys that in the uncorrelated CMB + GC combination do not achieve the best constraints: as an example, for the w_0CDM model the error on w_0 from *Planck*+SO + SKA1 combination is improved by $\sim 40\%$ when adding the cross-correlation. For the w_0w_a model, the LiteBIRD+S4 × Euclid-ph-like combination provides also the best constraints. In some cases, the dark energy FoM can be improved up to a factor $\lesssim 2.5$ with the inclusion of CMB-GC cross-correlation.

For the neutrino sector, while $N_{\rm eff}$ is mainly constrained from CMB as already said, the uncertainty on the neutrino mass can be reduced by CMB-GC cross-correlation up to a factor $\sim 40\%$. We forecast a $\sim 2.5\sigma$ detection ($\sigma(\Sigma m_\nu) \sim 25$ meV) of the neutrino mass from the 2D joint analysis of CMB and GC for the combinations of LiteBIRD+S4 with Euclid-ph-like, LSST and SKA1, and an almost 4σ detection ($\sigma(\Sigma m_\nu) \sim 16$ meV) for the combination of LiteBIRD+S4 with SPHEREx.

For the primordial universe sector, since the CMB-GC cross-correlation impact on the running uncertainty is negligible, we recover similar constraints on $\mathrm{d}n_s/\mathrm{d}\ln k$ to the results from a joint analysis of the CMB and the 3D galaxy power spectra $P(k)$ given in [98, 147]. For $f_{\rm NL}$, the impact of CMB-GC cross-correlation is maximal when using the single bin configuration since $f_{\rm NL}$ is not constrained from the GC autospectra without tomography, as it is also shown in [90]. Considering the full CMB × GC tomographic approach, we forecast an uncertainty $\sigma(f_{\rm NL}) \sim 1.5$ for SKA1 and $\sigma(f_{\rm NL}) \sim 2$ for its precursor EMU. Due to their large $f_{\rm sky}$ and redshift depth, we note that radio continuum surveys will perform better than Euclid-like, LSST and SPHEREx for detecting the scale-dependent bias induced by $f_{\rm NL}$. Let us also note that the minimum multipole $\ell_{\rm min}$ is quite critical for $\sigma(f_{\rm NL})$. In order to quantify the effect of this choice, we compute the Fisher matrix for the tomographic combination of *Planck* and EMU (which has $\ell_{\rm min} = 2$) using instead $\ell_{\rm min} = 20$, as for LSST. We obtain $\sigma(f_{\rm NL}) = 2.8$ for *Planck* × EMU and $\sigma(f_{\rm NL}) = 6.2$ for *Planck* + EMU, which compared to the errors in Tab. A.5 (2.1 and 2.8, respectively) shows a degradation of the constraints, in particular for the galaxy autospectra.

In Fig. 5.2 we compare the constraints from the CMB, GC and their cross-correlation with the errors from the CMB + GC and CMB × GC

Este documento incorpora firma electrónica, y es copia auténtica de un documento electrónico archivado por la ULL según la Ley 39/2015.
Su autenticidad puede ser contrastada en la siguiente dirección https://sede.ull.es/validacion/

Identificador del documento: 3764923 Código de verificación: JHlWnlbn

Firmado por:	JOSE RAMON BERMEJO CLIMENT *UNIVERSIDAD DE LA LAGUNA*	Fecha: 01/09/2021 17:41:12
	José Alberto Rubiño Martín *UNIVERSIDAD DE LA LAGUNA*	01/09/2021 17:49:44
	FABIO FINELLI *UNIVERSIDAD DE LA LAGUNA*	02/09/2021 14:12:21

Universidad de La Laguna
Oficina de Sede Electrónica
Entrada
Nº registro: 2021/90989
Nº reg. oficina: OF002/2021/89977
Fecha: 03/09/2021 12:24:13

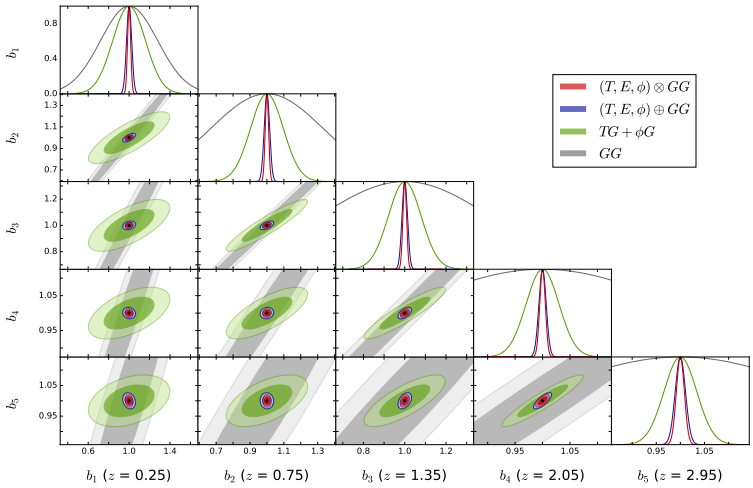

FIGURE 5.4— Marginalized 68% and 95% 2D confidence regions for the joint constraints on the bias nuisance parameters using the combination of LiteBIRD+S4 and SKA1. The grey contours correspond to LSS-only constraints (GG), the green contours to the cross-correlation only ($TG + \phi$G), the blue contours to the combination of CMB and galaxy clustering as uncorrelated and the red ones to the combination including cross-correlation.

Este documento incorpora firma electrónica, y es copia auténtica de un documento electrónico archivado por la ULL según la Ley 39/2015.
Su autenticidad puede ser contrastada en la siguiente dirección https://sede.ull.es/validacion/

Identificador del documento: 3764923 Código de verificación: JHlWnlbn

Firmado por: JOSE RAMON BERMEJO CLIMENT — Fecha: 01/09/2021 17:41:12
UNIVERSIDAD DE LA LAGUNA

José Alberto Rubiño Martín — 01/09/2021 17:49:44
UNIVERSIDAD DE LA LAGUNA

FABIO FINELLI — 02/09/2021 14:12:21
UNIVERSIDAD DE LA LAGUNA

Universidad de La Laguna
Oficina de Sede Electrónica
Entrada
Nº registro: 2021/90989
Nº reg. oficina: OF002/2021/89977
Fecha: 03/09/2021 12:24:13

combinations for the three 2 parameters extensions studied (dark energy, neutrino physics and primordial universe). We consider two different cases: *Planck* × LSST and S4 × SKA1. For the primordial universe extension, we do not show the CMB information since in our analysis $f_{\rm NL}$ is only constrained from the induced scale-dependent bias which enters in the GG, TG and ϕG angular power spectra. The CMB-GC cross-correlation information independently is capable for providing competitive constraints on the local non-Gaussianity parameter: for the best case, when cross-correlating LiteBIRD+S4 with SKA1 we obtain $\sigma(f_{\rm NL}) \sim 2.4$ from $TG + \phi G$.

For the 12 parameters extCDM model, we find that the inclusion of the CMB-GC cross-correlation mainly improves the constraints on H_0, the parameters of state of dark energy, the neutrino mass and $f_{\rm NL}$. Parameters like $N_{\rm eff}$ and $\mathrm{d}n_s/\mathrm{d}\ln k$ are mainly constrained by CMB alone and their uncertainties are only marginally improved by adding galaxy surveys on quasi-linear scales. We derive as well for this model the uncertainties on σ_8 and find that CMB-GC cross-correlation can improve up to a factor $\lesssim$ 2 the constraints on this parameter for the combination of *Planck* with SKA1.

CMB-GC cross-correlation can help in breaking degeneracies which remain in the uncorrelated combination of CMB and GC. It has been shown that the neutrino mass limit is model dependent, and in particular it becomes weaker for cosmologies with extended dark energy models and modified gravity. This degeneracy was first noticed in [148] and then observed in real data analysis such as [149–151]. Here, we forecast the uncertainties on the 9 parameters model w_0w_aCDM+Σm_ν for the combinations of *Planck*+SO with Euclid-ph-like and LiteBIRD+S4 with SKA1. In Fig. 5.3 we show the 68% and 95% confidence regions for the w_0-Σm_ν and w_a-Σm_ν planes obtained from the CMB, GC and cross-correlation information independently and from the uncorrelated CMB + GC and full CMB × GC combinations. The orientation of the $TG + \phi G$ ellipses is found to be different with respect to the GG contours, which helps in reducing the joint uncertainties.

CMB-GC cross-correlation has also the capability of constraining the galaxy bias parameters, in particular for the single bin cases since the GC without tomography does not constrain the bias. In the multiple bin cases, CMB-GC cross-correlation can increase the FoM of the bias parameters up to a factor $\lesssim 2$. We show in Fig. 5.4 th e constraints by the various probes

Este documento incorpora firma electrónica, y es copia auténtica de un documento electrónico archivado por la ULL según la Ley 39/2015.
Su autenticidad puede ser contrastada en la siguiente dirección https://sede.ull.es/validacion/

Identificador del documento: 3764923 Código de verificación: JHlWnlbn

Firmado por:	JOSE RAMON BERMEJO CLIMENT *UNIVERSIDAD DE LA LAGUNA*	Fecha: 01/09/2021 17:41:12
	José Alberto Rubiño Martín *UNIVERSIDAD DE LA LAGUNA*	01/09/2021 17:49:44
	FABIO FINELLI *UNIVERSIDAD DE LA LAGUNA*	02/09/2021 14:12:21

Universidad de La Laguna
Oficina de Sede Electrónica
Entrada
Nº registro: 2021/90989
Nº reg. oficina: OF002/2021/89977
Fecha: 03/09/2021 12:24:13

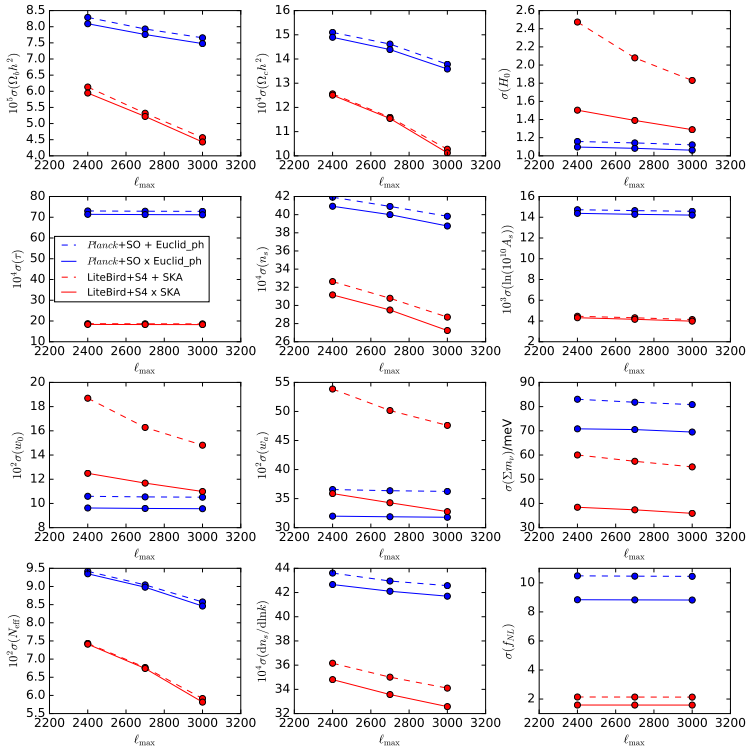

FIGURE 5.5— 68% marginalized constraints on the 12 cosmological parameters of the extCDM model as a function of $\ell_{\rm max}$ of the CMB for the tomographic combinations of *Planck*+SO with Euclid-ph-like and LiteBIRD+S4 with SKA1. The dashed lines correspond to the constraints from CMB + GC and the solid lines to the ones from CMB × GC.

Este documento incorpora firma electrónica, y es copia auténtica de un documento electrónico archivado por la ULL según la Ley 39/2015.
Su autenticidad puede ser contrastada en la siguiente dirección https://sede.ull.es/validacion/

Identificador del documento: 3764923 Código de verificación: JHlWnlbn

Firmado por: JOSE RAMON BERMEJO CLIMENT — Fecha: 01/09/2021 17:41:12
UNIVERSIDAD DE LA LAGUNA

José Alberto Rubiño Martín — 01/09/2021 17:49:44
UNIVERSIDAD DE LA LAGUNA

FABIO FINELLI — 02/09/2021 14:12:21
UNIVERSIDAD DE LA LAGUNA

Universidad de La Laguna
Oficina de Sede Electrónica
Entrada
Nº registro: 2021/90989
Nº reg. oficina: OF002/2021/89977
Fecha: 03/09/2021 12:24:13

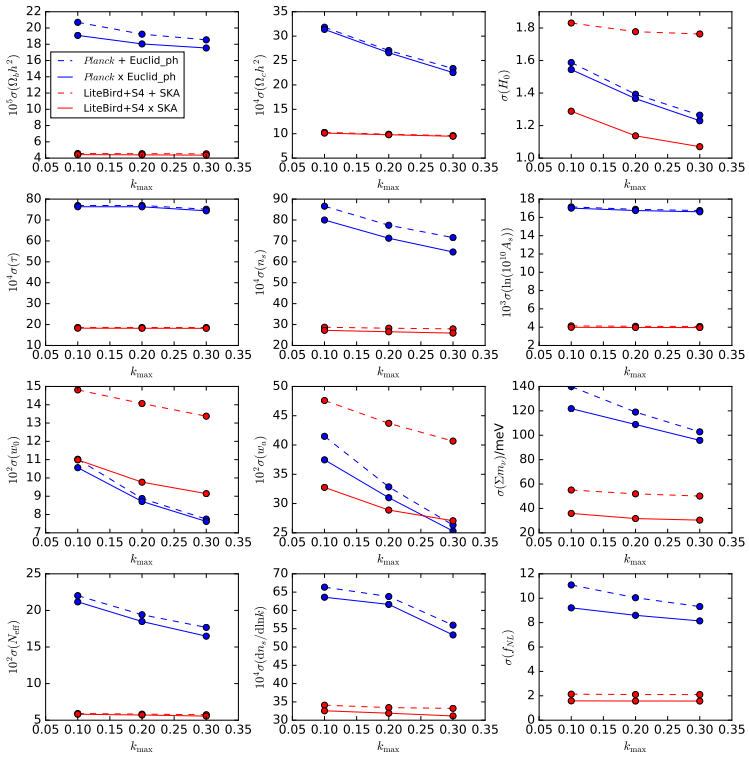

FIGURE 5.6— 68% marginalized constraints on the 12 cosmological parameters of the extCDM model as a function of $k_{\rm max}$ for the tomographic combinations of *Planck* with Euclid-ph-like and LiteBIRD+S4 with SKA1. The dashed lines correspond to the constraints from CMB + GC and the solid lines to the ones from CMB × GC.

Este documento incorpora firma electrónica, y es copia auténtica de un documento electrónico archivado por la ULL según la Ley 39/2015.
Su autenticidad puede ser contrastada en la siguiente dirección https://sede.ull.es/validacion/

Identificador del documento: 3764923 Código de verificación: JHlWnlbn

Firmado por: JOSE RAMON BERMEJO CLIMENT — Fecha: 01/09/2021 17:41:12
UNIVERSIDAD DE LA LAGUNA

José Alberto Rubiño Martín — 01/09/2021 17:49:44
UNIVERSIDAD DE LA LAGUNA

FABIO FINELLI — 02/09/2021 14:12:21
UNIVERSIDAD DE LA LAGUNA

Universidad de La Laguna
Oficina de Sede Electrónica
Entrada
Nº registro: 2021/90989
Nº reg. oficina: OF002/2021/89977
Fecha: 03/09/2021 12:24:13

on the 5 bias parameters for the tomographic combination LiteBIRD+S4 and SKA1.

As discussed in Section 3.1, our *Planck*-like forecasts are obtained by using $\ell_{\rm max} = 1500$ in order to reproduce the Planck 2018 uncertainties for parameters for the baseline cosmology, whereas the high-ℓ likelihood reaches $\ell_{\rm max} = 2500(2000)$ in temperature (polarization) and includes several foregrounds residuals and secondary anisotropies nuisance parameters. We therefore study the impact of a 10% and 20% reduction $\ell_{\rm max}$ for SO/CMB-S4, which means to adopt $\ell^{T,E}_{\rm max} = 2700$, $\ell^{\phi}_{\rm max} = 900$ and $\ell^{T,E}_{\rm max} = 2400$, $\ell^{\phi}_{\rm max} = 800$, respectively. For these two cases, we compute the constraints on the cosmological parameters for the extCDM model using the tomographic combinations of *Planck*+SO with Euclid-ph-like and LiteBIRD+S4 with SKA1. We represent in Fig. 5.5 the constraints as a function of the CMB maximum multipole. It is shown that for some parameters like H_0 and w_0, adopting a more conservative cut in the CMB increases the relative importance of the CMB-GC cross-correlation.

We also explore the behavior of the constraints when using scales smaller than $k_{\rm max} = 0.1\ h/{\rm Mpc}$ in the analysis. We take the tomographic combinations of *Planck* with Euclid-ph-like and S4 with SKA1, and calculate the uncertainties on the extCDM model from CMB + GC and CMB $\times$ GC using $k_{\rm max} = 0.2\ h/{\rm Mpc}$ and $k_{\rm max} = 0.3\ h/{\rm Mpc}$. In Fig. 5.6 we show the errors for the 12 cosmological parameters as function of $k_{\rm max}$. We find improvements with $k_{\rm max}$ for the constraints on majority of the parameters, except for those like τ that are constrained by CMB or $f_{\rm NL}$ which is mainly constrained from large scales. The neutrino mass and the dark energy parameters of state are those that have benefited most from the increase of $k_{\rm max}$.

Let us finally note that we have considered experimental specifications of CMB instruments which have already operated/or in preparation/or funded. We have not studied in depth the concept for a next CMB space mission dedicated to polarization with an angular resolution would allow a CMB lensing reconstruction much better than *Planck* even at low multipoles such as CORE [152, 153] or PICO [154] or PRISM [155]. For the cosmological model with 12 parameters studied here, we have checked that the uncertainties in cosmological parameters improve when combining a PRISM-like experiment with EMU or SPHEREx compared to the combination with LiteBIRD+S4, albeit the relative importance of CMB-GC cross-correlation does not change much with respect to the cases discussed

Este documento incorpora firma electrónica, y es copia auténtica de un documento electrónico archivado por la ULL según la Ley 39/2015.
Su autenticidad puede ser contrastada en la siguiente dirección https://sede.ull.es/validacion/

Identificador del documento: 3764923 Código de verificación: JHlWnlbn

Firmado por: JOSE RAMON BERMEJO CLIMENT — Fecha: 01/09/2021 17:41:12
UNIVERSIDAD DE LA LAGUNA

José Alberto Rubiño Martín — 01/09/2021 17:49:44
UNIVERSIDAD DE LA LAGUNA

FABIO FINELLI — 02/09/2021 14:12:21
UNIVERSIDAD DE LA LAGUNA

Universidad de La Laguna
Oficina de Sede Electrónica
Entrada
Nº registro: 2021/90989
Nº reg. oficina: OF002/2021/89977
Fecha: 03/09/2021 12:24:13

here.

5.3 Constraints on primordial features

The search of primordial features in galaxy surveys has attracted a lot of attention in the recent years. The possibility to complement at low redshift the constraints from CMB anisotropies with the clustering power spectrum from future galaxy surveys has been first explored for scales in the linear regime in the previous section. It has been shown how galaxy surveys could help in finding primordial superimposed oscillations which were otherwise hidden in WMAP or *Planck* data [98, 156] even by restricting to linear scales. More recently, there have been studies of the damping of primordial superimposed oscillations at scales which have gone through non-linear gravitational instability [157–159] in order to exploit all the cosmological information contained in LSS surveys.

In this section we apply our 2D tomographic approach in alternative to the more studied search for features in the clustering power spectrum. There are several reasons to pursue our approach. First, we aim to assess if a 2D tomographic approach can reach a precision similar to the 3D clustering power spectrum in the search of features, how it was shown in [105] for the ΛCDM model. Further, a 2D tomographic approach can incoroprate easily the CMB-LSS cross correlation which can therefore be an additional handle in the search of features largely unexplored in quantitative details.

We describe in Sec. 5.3.1 the four inflationary models that we consider. We then explore in Sec. 5.3.2 the effect of the features models in the angular power spectra of the CMB, galaxy clustering and their cross correlation, and present the forecast constraints on the parameters by our 2D tomographic approach in Sec. 5.3.3.

5.3.1 Deviations from a power law primordial power spectrum

We consider four inflationary models that produce features in the primordial power spectrum, i.e. deviations from a simple power law for the primordial fluctuations given by

$$\mathcal{P}_{\mathcal{R},0}(k) = A_s \left(\frac{k}{k_*}\right)^{n_s-1} . \tag{5.8}$$

Three of our models cause local features at large scales: an exponen-

Este documento incorpora firma electrónica, y es copia auténtica de un documento electrónico archivado por la ULL según la Ley 39/2015.
Su autenticidad puede ser contrastada en la siguiente dirección https://sede.ull.es/validacion/

Identificador del documento: 3764923 Código de verificación: JHlWnlbn

Firmado por:	JOSE RAMON BERMEJO CLIMENT *UNIVERSIDAD DE LA LAGUNA*	Fecha: 01/09/2021 17:41:12
	José Alberto Rubiño Martín *UNIVERSIDAD DE LA LAGUNA*	01/09/2021 17:49:44
	FABIO FINELLI *UNIVERSIDAD DE LA LAGUNA*	02/09/2021 14:12:21

Universidad de La Laguna
Oficina de Sede Electrónica
Entrada
Nº registro: 2021/90989
Nº reg. oficina: OF002/2021/89977
Fecha: 03/09/2021 12:24:13

tial cut-off at large scales (hereafter MI), the so-called Starobinsky model (hereafter MII) and a step in the inflation potential (hereafter MIII); while the fourth model that we consider, the logarithmic super-imposed oscillations (hereafter MIV), produces a global feature in the primordial power spectrum.

Exponential cut-off at large scales

This model, introduced in [160], multiplies the power law primordial power spectrum $\mathcal{P}_{\mathcal{R},0}(k)$ by an exponential cut-off with variable stiffness, following the parametrization

$$\mathcal{P}_{\mathcal{R}}(k) = \mathcal{P}_{\mathcal{R},0}(k)\left\{1 - \exp\left[-\left(\frac{k}{k_c}\right)^{\lambda_c}\right]\right\}, \tag{5.9}$$

where k_c and λ_c are the parameters of the model. These two parameters introduce a suppression of the primordial power spectrum at large scales: k_c is the relevant scale at which the suppression starts and λ_c accounts for its stiffness. This parametrization is motivated by models with a short inflationary stage in which the onset of the slow-roll phase coincides in time with the largest observable scales exiting the Hubble radius. In these scales, the primordial power spectrum is strongly suppressed.

For the fiducial values of the model parameters we take $\log_{10}(k_c) =$ -3.47, as in the bestfit from *Planck* 2015 [161], and $\lambda_c = 3.35$. This last choice for the stiffness is motivated in [160].

Starobinsky model

The so-called Starobinsky model was introduced in [162]. It presents a sharp change (kink) in the slope of the inflaton potential $V(\phi)$ that is given by

$$V(\phi) = \begin{cases} V_0 + A_+(\phi - \phi_0), & \phi \gg \phi_0 \\ V_0 + A_-(\phi - \phi_0), & \phi \ll \phi_0 \end{cases}. \tag{5.10}$$

Under the approximation $|A_+\phi|, |A_-\phi| \ll V_0$, the curvature power spectrum can be analytically derived and expressed as

$$\mathcal{P}_{\mathcal{R}}(k) = \mathcal{P}_{\mathcal{R},0}(k) \times \mathcal{D}(y, \mathcal{A}_{\rm kink}), \tag{5.11}$$

Este documento incorpora firma electrónica, y es copia auténtica de un documento electrónico archivado por la ULL según la Ley 39/2015.
Su autenticidad puede ser contrastada en la siguiente dirección https://sede.ull.es/validacion/

Identificador del documento: 3764923 Código de verificación: JHlWnlbn

Firmado por: JOSE RAMON BERMEJO CLIMENT — Fecha: 01/09/2021 17:41:12
UNIVERSIDAD DE LA LAGUNA

José Alberto Rubiño Martín — 01/09/2021 17:49:44
UNIVERSIDAD DE LA LAGUNA

FABIO FINELLI — 02/09/2021 14:12:21
UNIVERSIDAD DE LA LAGUNA

Universidad de La Laguna
Oficina de Sede Electrónica
Entrada
Nº registro: 2021/90989
Nº reg. oficina: OF002/2021/89977
Fecha: 03/09/2021 12:24:13

$$\begin{aligned}\mathcal{D}(y,\mathcal{A}_{\rm kink}) = 1 &+ \frac{9}{2}\mathcal{A}_{\rm kink}^2\left(\frac{1}{y}+\frac{1}{y^3}\right)^2 \\ &+\frac{3}{2}\mathcal{A}_{\rm kink}\left(4+3\mathcal{A}_{\rm kink}-3\frac{\mathcal{A}_{\rm kink}}{y^4}\right)\frac{1}{y^2}\cos(2y) \\ &+3\mathcal{A}_{\rm kink}\left(1-\frac{1+3\mathcal{A}_{\rm kink}}{y^2}-\frac{3\mathcal{A}_{\rm kink}}{y^4}\right)\frac{1}{y}\sin(2y)\,,\end{aligned} \tag{5.12}$$

where $y \equiv k/k_{\rm kink}$. Here $k_{\rm kink}$ is the scale of the transition and $\mathcal{A}_{\rm kink}$ is the amplitude of the feature, given by $\mathcal{A}_{\rm kink} = (A_+ - A_-)/A_+$. For the fiducial values of the model parameters we take the bestfit from *Planck* 2015 [161]: $\mathcal{A}_{\rm kink} = 0.089$ and $\log_{10}(k_{\rm kink}) = $ -3.05.

Step in the inflaton potential

This model presents a step in the inflationary potential [163] which leads to a localized oscillatory pattern in the primordial power spectrum. The potential is given by

$$V(\phi) = \frac{1}{2}m^2\phi^2\left[1 + c\tanh\left(\frac{\phi-\phi_0}{b}\right)\right]\,, \tag{5.13}$$

where c and d are the height the width of the step, respectively, localized at ϕ_0. An analytic approximation for the primordial power spectrum generated by this potential has been obtained in [164, 165]:

$$\mathcal{P}_{\mathcal{R}}(k) = \exp\left\{\ln\mathcal{P}_{\mathcal{R},0}(k) + \mathcal{D}(y,\mathcal{A}_{\rm st},x_{\rm st})\right\}\,, \tag{5.14}$$

$$\begin{aligned}\mathcal{D}(y,\mathcal{A}_{\rm st},x_{\rm st}) = \frac{\mathcal{A}_{\rm st}}{2y^3}&\left[\left(18y-6y^3\right)\cos(2y)+\left(15y^2-9\right)\sin(2y)\right]\frac{y}{x_{\rm st}}\cosh\left(\frac{y}{x_{\rm st}}\right) \\ &+\ln\left[1+\frac{1}{2}\left(\frac{\pi}{2}(1-n_s)-\frac{3\mathcal{A}_{\rm st}}{y^3}\left[y\cos(y)-\sin(y)\right]\right.\right. \\ &\left.\left.\times\left[3y\cos(y)+\left(2y^2-3\right)\sin(y)\right]\frac{y}{x_{\rm st}}\cosh\left(\frac{y}{x_{\rm st}}\right)\right)^2\right]\end{aligned} \tag{5.15}$$

where $y \equiv k/k_{\rm st}$. Here $k_{\rm st}$ is the scale of the transition, $\mathcal{A}_{\rm st}$ tunes the amplitude of the feature and $x_{\rm st}$ is related to the duration of the slow-roll

Este documento incorpora firma electrónica, y es copia auténtica de un documento electrónico archivado por la ULL según la Ley 39/2015.
Su autenticidad puede ser contrastada en la siguiente dirección https://sede.ull.es/validacion/

Identificador del documento: 3764923 Código de verificación: JHlWnlbn

Firmado por: JOSE RAMON BERMEJO CLIMENT — Fecha: 01/09/2021 17:41:12
UNIVERSIDAD DE LA LAGUNA

José Alberto Rubiño Martín — 01/09/2021 17:49:44
UNIVERSIDAD DE LA LAGUNA

FABIO FINELLI — 02/09/2021 14:12:21
UNIVERSIDAD DE LA LAGUNA

Universidad de La Laguna
Oficina de Sede Electrónica
Entrada
Nº registro: 2021/90989
Nº reg. oficina: OF002/2021/89977
Fecha: 03/09/2021 12:24:13

violation. For the fiducial values of the model parameters we take the bestfit from *Planck* 2018 [166]: $\mathcal{A}_{\rm st} = 0.38$, $\log_{10}(k_{\rm st})$ = -3.09 and $\ln(x_{\rm st})$ = 0.15.

Logarithmic super-imposed oscillations

As an example for a model that leads to a global feature, we consider the case of logarithmic oscillations super-imposed to the primordial power spectrum, which create a pattern given by

$$\mathcal{P}_{\mathcal{R}}(k) = \mathcal{P}_{\mathcal{R},0}(k)\left[1 + \mathcal{A}_{\log}\cos\left(\omega_{\log}\ln\left(\frac{k}{k_*}\right) + \phi_{\log}\right)\right]. \tag{5.16}$$

where $\mathcal{A}_{\log}$ is the amplitude of the oscillations and $\omega_{\log}$, $\phi_{\log}$ describe their frequency and phase, respectively. This pattern can be generated by different mechanisms as axion monodromy inflation [167] and initial quantum states different from Bunch-Davies [168]. More recent developments including drifting oscillations can be found in [169]. For the fiducial values of the model parameters we take the bestfit from *Planck* 2018 [166]: $\mathcal{A}_{\log}$ = 0.014, $\log_{10}(\omega_{\log}) = 1.26$ and $\phi_{\log}/2\pi = 0.07$.

5.3.2 Impact on the angular power spectra

We use and modify the public code `CAMB` [2] [69] to implement the deviations from a power law primordial power spectrum and calculate the angular power spectra of the CMB, galaxy clustering and their cross-correlation. We assume a fiducial cosmology according to the *Planck* 2018 results [46]: $\Omega_b h^2 = 0.022383$, $\Omega_c h^2 = 0.12011$, $H_0 = 67.32$ km s^{-1} Mpc^{-1}, $\tau = 0.0543$, $n_s = 0.96605$ and $\ln(10^{10}A_s) = 3.0448$.

In Fig. 5.7 we show the relative differences with respect to the ΛCDM angular power spectra of the CMB temperature, polarization and lensing for the primordial features models described in Sect. 5.3. We find that the local features produced by models MI-MIII can change up to ∼20% the TT and EE spectra and up to ∼10% the $\phi\phi$ spectra at low ℓ. Instead, the global feature by model MIV introduces small oscillations with respect to the ΛCDM spectra which are stronger at smaller scales.

We now explore how the specifications of the window function such as the median redshift or the bin width affect to the galaxy clustering and cross-correlation angular power spectra for the primordial features models

[2] https://github.com/cmbant/CAMB

Este documento incorpora firma electrónica, y es copia auténtica de un documento electrónico archivado por la ULL según la Ley 39/2015.
Su autenticidad puede ser contrastada en la siguiente dirección https://sede.ull.es/validacion/

Identificador del documento: 3764923 Código de verificación: JHlWnlbn

Firmado por: JOSE RAMON BERMEJO CLIMENT — Fecha: 01/09/2021 17:41:12
UNIVERSIDAD DE LA LAGUNA

José Alberto Rubiño Martín — 01/09/2021 17:49:44
UNIVERSIDAD DE LA LAGUNA

FABIO FINELLI — 02/09/2021 14:12:21
UNIVERSIDAD DE LA LAGUNA

Universidad de La Laguna
Oficina de Sede Electrónica
Entrada
Nº registro: 2021/90989
Nº reg. oficina: OF002/2021/89977
Fecha: 03/09/2021 12:24:13

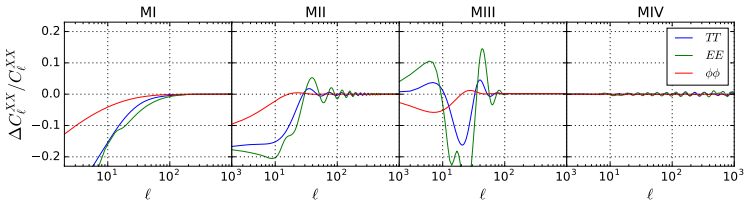

FIGURE 5.7— Relative differences with respect to the ΛCDM angular power spectra of the CMB temperature (blue lines), polarization (green lines) and lensing (red lines) for the four inflationary models.

studied in this section. For this, we take gaussian bins with different central redshifts and widths and compute the relative differences with the ΛCDM angular power spectra in each model. We show in Fig. 5.8 the results as a function of the central redshift and in Fig. 5.9 as a function of the redshift width. We find up to $\sim 20\%$ differences for the local features produced by models MI-MIII, while the global feature given by model MIV the differences are smaller (few percent). For the *GG* autospectra ,we find that for the local, large scale features (models I-III) the differences with respect to ΛCDM are larger when using wider redshift bins, while it does not seem to be a preferred central redshift.

5.3.3 Joint forecasts on features parameters

We now apply the Fisher forecasting formalism for a 2D joint analysis of CMB and galaxy number counts described in Sec. 5.1 to the features models we study. Beyond the six ΛCDM parameters and the features parameters for each model, we include as well as extra cosmological parameters the neutrino mass sum Σm_ν assuming a fiducial mass of 0.06 eV and the normal hierarchy, and the redshift width of reionization, $\Delta z_{\rm re}$, with a fiducial value equal to 0.5.

Regarding the nuisance parameters for the galaxy number counts, as in Sec. 5.2.2 we vary the galaxy bias $b_G(z)$ in each redshift bin. Further, we marginalize as well over a constant parameter s_0, with fiducial value equal to 1, that multiplies the magnification bias redshift dependence function $s(z)$. This choice is motivated by the impact at large scales of three of the features models on the angular power spectra of the galaxy number counts and their cross-correlations, as shown in Figs. 5.8-5.9. Since the relativis-

Este documento incorpora firma electrónica, y es copia auténtica de un documento electrónico archivado por la ULL según la Ley 39/2015.
Su autenticidad puede ser contrastada en la siguiente dirección https://sede.ull.es/validacion/

Identificador del documento: 3764923 Código de verificación: JHlWnlbn

Firmado por: JOSE RAMON BERMEJO CLIMENT — Fecha: 01/09/2021 17:41:12
UNIVERSIDAD DE LA LAGUNA

José Alberto Rubiño Martín — 01/09/2021 17:49:44
UNIVERSIDAD DE LA LAGUNA

FABIO FINELLI — 02/09/2021 14:12:21
UNIVERSIDAD DE LA LAGUNA

Universidad de La Laguna
Oficina de Sede Electrónica
Entrada
Nº registro: 2021/90989
Nº reg. oficina: OF002/2021/89977
Fecha: 03/09/2021 12:24:13

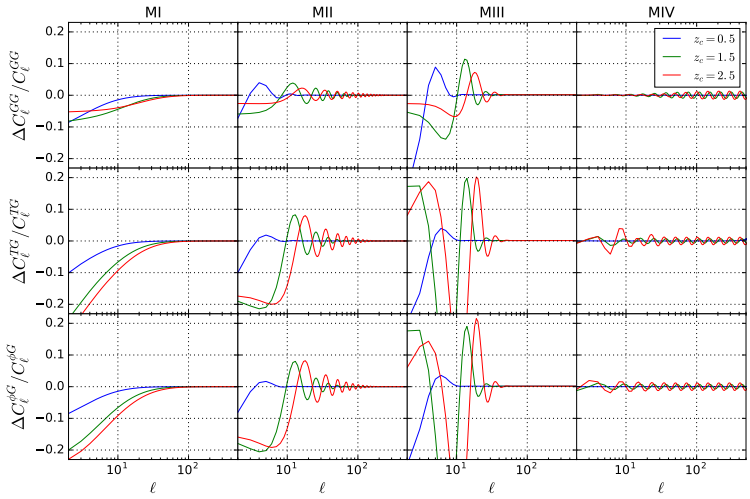

FIGURE 5.8— Relative differences with respect to the ΛCDM angular power spectra of the galaxy autospectra (top panels), temperature-galaxy cross-correlation (mid panels) and lensing-galaxy cross-correlation (bottom panels) for the four inflationary models. We have considered gaussian redshift windows centered at $z_c = 0.5$ (blue lines), $z_c = 1.5$ (green lines) and $z_c = 2.5$ (red lines), with a fixed width $\Delta z = 0.3$.

tic effects depending on the magnification bias also modify these angular power spectra at the lowest multipoles (see Sec. 3.4), we explore in this way the capability of breaking possible degeneracies betweeen the features and magnification bias parameters by the inclusion of cross-correlation.

For the cosmological observations, we consider as CMB surveys *Planck* and the Simons Observatory. In this case, we complement the large scales ($\ell < 40$) and the remaining sky fraction not observed by SO with the LiteBIRD specifications (see Sec. 3.1 for more details). As galaxy surveys, we consider the tomographic configurations of both Euclid photometric and spectroscopic surveys, SKA1 and SPHEREx. In this way, we cover different kinds of surveys in terms of redshift accuracy and coverage in order to understand which one is the most effective for constraining primordial features.

We list the 68% marginalized constraints on the ΛCDM and extra

Este documento incorpora firma electrónica, y es copia auténtica de un documento electrónico archivado por la ULL según la Ley 39/2015.
Su autenticidad puede ser contrastada en la siguiente dirección https://sede.ull.es/validacion/

Identificador del documento: 3764923 Código de verificación: JHlWnlbn

Firmado por: JOSE RAMON BERMEJO CLIMENT — Fecha: 01/09/2021 17:41:12
UNIVERSIDAD DE LA LAGUNA

José Alberto Rubiño Martín — 01/09/2021 17:49:44
UNIVERSIDAD DE LA LAGUNA

FABIO FINELLI — 02/09/2021 14:12:21
UNIVERSIDAD DE LA LAGUNA

Universidad de La Laguna
Oficina de Sede Electrónica
Entrada
Nº registro: 2021/90989
Nº reg. oficina: OF002/2021/89977
Fecha: 03/09/2021 12:24:13

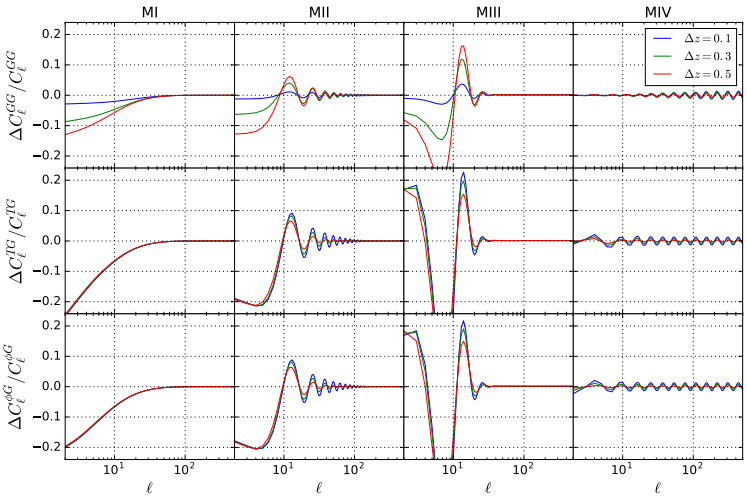

FIGURE 5.9— Relative differences with respect to the ΛCDM angular power spectra of the galaxy autospectra (top panels), temperature-galaxy cross-correlation (mid panels) and lensing-galaxy cross-correlation (bottom panels) for the four inflationary models. We have considered gaussian redshift windows centered at $z_c = 1.5$ with a variable width $\Delta z = 0.1$ (blue lines), $\Delta z = 0.3$ (green lines) and $\Delta z = 0.5$ (red lines).

parameters for the four models in Appendix A. Here, we show as relevant examples the constraints on H_0 and on the extra parameters in Figs. 5.10-5.12 for models I-III from the combination of *Planck* with SKA1, and in Fig. 5.13 for the combination of *Planck* with Euclid-ph.

As a general trend, we find that for the models of features at large scales (MI-MIII), the combination of the CMB with SKA1 provides the best constraints on the features parameters. Beyond this parameters, the cross-correlation between the CMB and galaxy clustering from SKA1 is found to be capable of improving up to a factor $\gtrsim 2$ the constraints on H_0, Σm_ν and on the magnification bias parameter s_0. Instead, for model IV, which depends on smaller scales, we find that the combination of the CMB with both Euclid surveys will provide the best constraints.

The better performance of SKA1 for the features models that depend on large scales can be explained according to the results shown in

Este documento incorpora firma electrónica, y es copia auténtica de un documento electrónico archivado por la ULL según la Ley 39/2015.
Su autenticidad puede ser contrastada en la siguiente dirección https://sede.ull.es/validacion/

Identificador del documento: 3764923 Código de verificación: JHlWnlbn

Firmado por: JOSE RAMON BERMEJO CLIMENT — Fecha: 01/09/2021 17:41:12
UNIVERSIDAD DE LA LAGUNA

José Alberto Rubiño Martín — 01/09/2021 17:49:44
UNIVERSIDAD DE LA LAGUNA

FABIO FINELLI — 02/09/2021 14:12:21
UNIVERSIDAD DE LA LAGUNA

Universidad de La Laguna
Oficina de Sede Electrónica
Entrada
Nº registro: 2021/90989
Nº reg. oficina: OF002/2021/89977
Fecha: 03/09/2021 12:24:13

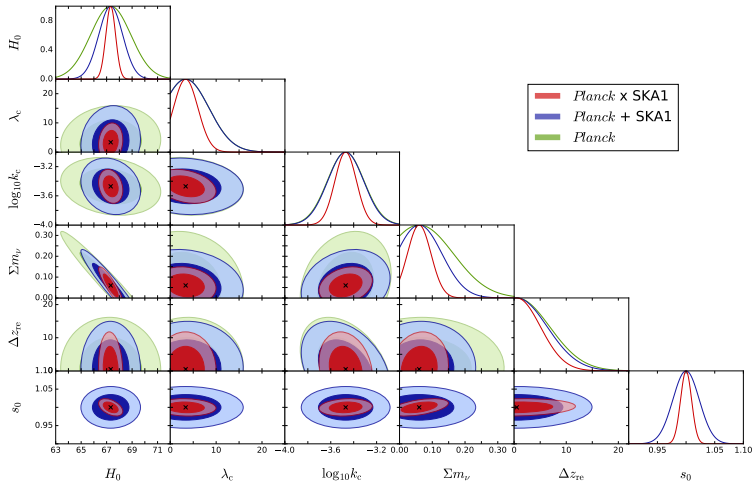

FIGURE 5.10— Marginalized 68% and 95% 2D confidence regions for the constraints on H_0 and the extra parameters of the exponential cutoff at large scales model (MI). The green contours represent the constraints from *Planck* alone, the blue contours represent the uncorrelated combination of *Planck* and SKA1 and the red contours the full combination including cross-correlation. We do not show the contours from SKA1 alone since for this model, the galaxy clustering alone does not constrain the features parameters.

Sec. 5.3.2: in particular, the galaxy number counts autospectra seem to be more sensitive to broader and deeper redshift bins, a condition that is satisfied due to the SKA1 broad redshift coverage.

5.4 Outlook

We give in this section an outlook on possible extensions of our baseline 2D tomographic approach methodology. First, we investigate the impact on the constraints of including a scale-dependent bias induced by the presence of massive neutrinos in Sec. 5.4.1. Then, in Sec. 5.4.2 we explore the capabilities of adding weak lensing as a third additional cosmological probe in a joint likelihood, as well as its cross-correlation with the CMB fields and galaxy number counts.

Este documento incorpora firma electrónica, y es copia auténtica de un documento electrónico archivado por la ULL según la Ley 39/2015.
Su autenticidad puede ser contrastada en la siguiente dirección https://sede.ull.es/validacion/

Identificador del documento: 3764923 Código de verificación: JHlWnlbn

Firmado por:	JOSE RAMON BERMEJO CLIMENT *UNIVERSIDAD DE LA LAGUNA*	Fecha: 01/09/2021 17:41:12
	José Alberto Rubiño Martín *UNIVERSIDAD DE LA LAGUNA*	01/09/2021 17:49:44
	FABIO FINELLI *UNIVERSIDAD DE LA LAGUNA*	02/09/2021 14:12:21

Universidad de La Laguna
Oficina de Sede Electrónica
Entrada
Nº registro: 2021/90989
Nº reg. oficina: OF002/2021/89977
Fecha: 03/09/2021 12:24:13

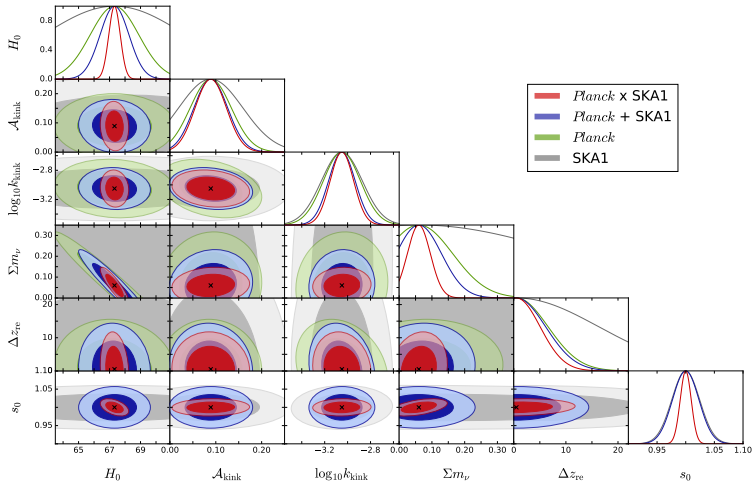

FIGURE 5.11— Marginalized 68% and 95% 2D confidence regions for the constraints on H_0 and the extra parameters of the Starobinsky model (MII). The grey contours represent the constraints from SKA1 alone, the green contours represent the constraints from *Planck* alone, the blue contours represent the uncorrelated combination of *Planck* and SKA1 and the red contours the full combination including cross-correlation.

5.4.1 Scale-dependent bias induced by massive neutrinos

We quantify the impact of a scale dependence of the galaxy bias induced by a neutrino mass, which is an additional effect which has drawn a lot of attention recently [170–173], but has not been considered as a baseline in our 2D tomographic approach to CMB and galaxy clustering.

The presence of massive neutrinos affects the total matter fraction of the Universe, since the linear growth of matter fluctuations is suppressed for scales smaller than the neutrinos free streaming scale [174]. This has an effect on the galaxy bias, introducing a scale dependence. In order to estimate its impact on uncertainties of cosmological parameters, we consider the scale dependence of the galaxy bias as in [175], i.e. as a smooth transition around $k_{\rm nr}$, which is the free streaming scale for the non-relativistic neutrinos. This modelling of the scale-dependent bias is

Este documento incorpora firma electrónica, y es copia auténtica de un documento electrónico archivado por la ULL según la Ley 39/2015.
Su autenticidad puede ser contrastada en la siguiente dirección https://sede.ull.es/validacion/

Identificador del documento: 3764923 Código de verificación: JHlWnlbn

Firmado por:	JOSE RAMON BERMEJO CLIMENT *UNIVERSIDAD DE LA LAGUNA*	Fecha: 01/09/2021 17:41:12
	José Alberto Rubiño Martín *UNIVERSIDAD DE LA LAGUNA*	01/09/2021 17:49:44
	FABIO FINELLI *UNIVERSIDAD DE LA LAGUNA*	02/09/2021 14:12:21

Universidad de La Laguna
Oficina de Sede Electrónica
Entrada
Nº registro: 2021/90989
Nº reg. oficina: OF002/2021/89977
Fecha: 03/09/2021 12:24:13

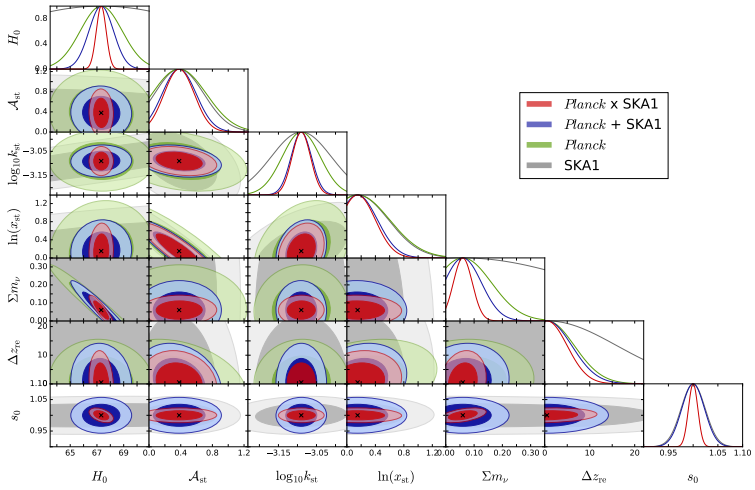

FIGURE 5.12— Marginalized 68% and 95% 2D confidence regions for the constraints on H_0 and the extra parameters of the step in the inflaton potential model (MIII). The grey contours represent the constraints from SKA1 alone, the green contours represent the constraints from *Planck* alone, the blue contours represent the uncorrelated combination of *Planck* and SKA1 and the red contours the full combination including cross-correlation.

expressed as [175]

$$b(k,z) = b_{k\ll k_{\rm nr}}(z) + \frac{b_{k\ll k_{\rm nr}}(z) - b_{k\gg k_{\rm nr}}(z)}{2}\left\{\tanh\left[\ln\left(\frac{k}{k_{\rm nr}}\right)^{\gamma}\right] + 1\right\}, \tag{5.17}$$

where $\gamma = 5$, $k_{\rm nr}$ is given by

$$k_{\rm nr} \approx 0.018\left(\frac{m_\nu}{1{\rm eV}}\right)^{1/2}\sqrt{\Omega_{\rm m}}h\ {\rm Mpc}^{-1}, \tag{5.18}$$

and the values of $b_{k\ll k_{\rm nr}}(z)$ and $b_{k\gg k_{\rm nr}}(z)$ correspond to the two asymptotic regimes of the bias: at k much smaller than $k_{\rm nr}$ we recover the standard ΛCDM galaxy bias, hence $b_{k\ll k_{\rm nr}}(z) \simeq b_G(z)$; while at k larger than $k_{\rm nr}$ the bias corresponds to $b_{k\gg k_{\rm nr}}(z) \simeq b_G(z)(1-f_\nu)$, where $f_\nu = \Omega_\nu/\Omega_{\rm m}$.

In order to take into account surveys of different redshift coverage and depth, we implement the scale-dependent bias and recompute the

Este documento incorpora firma electrónica, y es copia auténtica de un documento electrónico archivado por la ULL según la Ley 39/2015.
Su autenticidad puede ser contrastada en la siguiente dirección https://sede.ull.es/validacion/

Identificador del documento: 3764923 Código de verificación: JHlWnlbn

Firmado por: JOSE RAMON BERMEJO CLIMENT — Fecha: 01/09/2021 17:41:12
UNIVERSIDAD DE LA LAGUNA

José Alberto Rubiño Martín — 01/09/2021 17:49:44
UNIVERSIDAD DE LA LAGUNA

FABIO FINELLI — 02/09/2021 14:12:21
UNIVERSIDAD DE LA LAGUNA

Universidad de La Laguna
Oficina de Sede Electrónica
Entrada
Nº registro: 2021/90989
Nº reg. oficina: OF002/2021/89977
Fecha: 03/09/2021 12:24:13

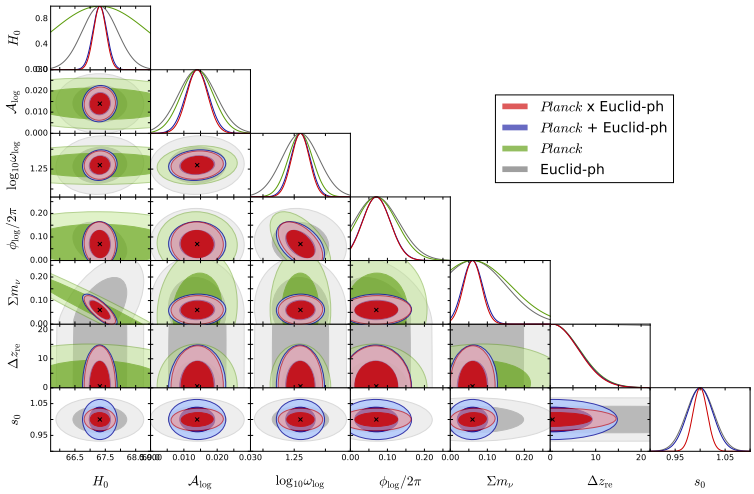

FIGURE 5.13— Marginalized 68% and 95% 2D confidence regions for the constraints on H_0 and the extra parameters of the logarithmic super-imposed oscillations model (MIV). The grey contours represent the constraints from SKA1 alone, the green contours represent the constraints from *Planck* alone, the blue contours represent the uncorrelated combination of *Planck* and SKA1 and the red contours the full combination including cross-correlation.

constraints on the ΛCDM+$\{\Sigma m_\nu, N_{\rm eff}\}$ cosmology for the Euclid-ph-like, SPHEREx and SKA1 surveys using their tomographic configurations. We list in Tab. 5.1 the constraints on the neutrino mass compared to the case neglecting the scale-dependent bias for these three surveys, alone and in their uncorrelated and full combinations with the *Planck*-like CMB survey.

We find tighter constraints in the neutrino mass from galaxy surveys after having introduced the scale-dependent bias. For galaxy clustering only, the error is smaller by less than 1% for SPHEREx, but this difference grows to $\sim 15\%$ for Euclid-ph-like and $\sim 30\%$ for SKA1. This suggests that the effect of the scale-dependent bias is more important for deeper surveys in redshift. When combining (including its cross-correlation) with the *Planck* information, these differences are $\sim 14\%$ ($\sim 10\%$) for SKA1 and $\lesssim 2\%$ for Euclid-ph-like. For the combination with more powerful CMB surveys such as SO and S4, these differences should be even smaller.

Este documento incorpora firma electrónica, y es copia auténtica de un documento electrónico archivado por la ULL según la Ley 39/2015.
Su autenticidad puede ser contrastada en la siguiente dirección https://sede.ull.es/validacion/

Identificador del documento: 3764923 Código de verificación: JHlWnlbn

Firmado por: JOSE RAMON BERMEJO CLIMENT — Fecha: 01/09/2021 17:41:12
UNIVERSIDAD DE LA LAGUNA

José Alberto Rubiño Martín — 01/09/2021 17:49:44
UNIVERSIDAD DE LA LAGUNA

FABIO FINELLI — 02/09/2021 14:12:21
UNIVERSIDAD DE LA LAGUNA

Universidad de La Laguna
Oficina de Sede Electrónica
Entrada
Nº registro: 2021/90989
Nº reg. oficina: OF002/2021/89977
Fecha: 03/09/2021 12:24:13

	Euclid-ph-like	SPHEREx	SKA1
C_ℓ^{GG}	297 (347)	510 (512)	407 (575)
$Planck + C_\ell^{GG}$	67 (68)	61 (61)	92 (107)
$Planck \times C_\ell^{GG}$	72 (73)	55 (55)	77 (85)

TABLE 5.1— Uncertainty on the neutrino mass $\sigma(m_\nu)$ in meV for each galaxy survey and their uncorrelated and full combinations with the *Planck* CMB survey, obtained after the implementation of the scale-dependent bias. The numbers between parenthesis correspond to the uncertainty calculated neglecting the scale-dependent bias.

We therefore conclude that our results in Sect. 5.2.2 based on linear scales are robust to the inclusion of the scale-dependence in the galaxy bias due to neutrino mass, an additional effect which can actually slightly decrease the expected uncertainty on the neutrino mass.

5.4.2 Inclusion of weak lensing

As a further step, we extend our methodology for a 2D tomographic approach to CMB and galaxy clustering to the inclusion of the galaxy weak lensing as additional cosmological probe. Already in Chapter 5, we have introduced the galaxy clustering - weak lensing cross-correlation for the lensing ratio. In this section, we aim to give an outlook on the uncertainties on cosmological parameters that can be reached by a joint tomographic approach to the three probes -CMB, galaxy clustering and weak lensing-, accounting for all the cross-correlations between them.

In the Fisher matrix formalism described in Sec. 5.1, for including the weak lensing we generalize Eq. (5.3) as

$$\mathcal{C} = \begin{bmatrix} \bar{C}_\ell^{TT} & C_\ell^{TE} & C_\ell^{T\phi} & C_\ell^{TG_1} & \dots & C_\ell^{TG_N} & C_\ell^{T\kappa_1} & \dots & C_\ell^{T\kappa_N} \\ C_\ell^{TE} & \bar{C}_\ell^{EE} & C_\ell^{E\phi} & C_\ell^{EG_1} & \dots & C_\ell^{EG_N} & C_\ell^{E\kappa_1} & \dots & C_\ell^{E\kappa_N} \\ C_\ell^{T\phi} & C_\ell^{E\phi} & \bar{C}_\ell^{\phi\phi} & C_\ell^{\phi G_1} & \dots & C_\ell^{\phi G_N} & C_\ell^{\phi\kappa_1} & \dots & C_\ell^{\phi\kappa_N} \\ C_\ell^{TG_1} & C_\ell^{EG_1} & C_\ell^{\phi G_1} & \bar{C}_\ell^{G_1G_1} & \dots & C_\ell^{G_1G_N} & C_\ell^{G_1\kappa_1} & \dots & C_\ell^{G_1\kappa_N} \\ \vdots & \vdots & \vdots & \vdots & \ddots & \vdots & \vdots & \ddots & \vdots \\ C_\ell^{TG_N} & C_\ell^{EG_N} & C_\ell^{\phi G_N} & C_\ell^{G_1G_N} & \dots & \bar{C}_\ell^{G_NG_N} & C_\ell^{G_N\kappa_1} & \dots & C_\ell^{G_N\kappa_N} \\ C_\ell^{T\kappa_1} & C_\ell^{E\kappa_1} & C_\ell^{\phi\kappa_1} & C_\ell^{G_1\kappa_1} & \dots & C_\ell^{G_N\kappa_1} & \bar{C}_\ell^{\kappa_1\kappa_1} & \dots & C_\ell^{\kappa_1\kappa_N} \\ \vdots & \vdots & \vdots & \vdots & \ddots & \vdots & \vdots & \ddots & \vdots \\ C_\ell^{T\kappa_N} & C_\ell^{E\kappa_N} & C_\ell^{\phi\kappa_1} & C_\ell^{G_1\kappa_N} & \dots & C_\ell^{G_N\kappa_N} & C_\ell^{\kappa_1\kappa_N} & \dots & \bar{C}_\ell^{\kappa_N\kappa_N} \end{bmatrix}. \tag{5.19}$$

Este documento incorpora firma electrónica, y es copia auténtica de un documento electrónico archivado por la ULL según la Ley 39/2015.
Su autenticidad puede ser contrastada en la siguiente dirección https://sede.ull.es/validacion/

Identificador del documento: 3764923 Código de verificación: JHlWnlbn

Firmado por: JOSE RAMON BERMEJO CLIMENT — Fecha: 01/09/2021 17:41:12
UNIVERSIDAD DE LA LAGUNA

José Alberto Rubiño Martín — 01/09/2021 17:49:44
UNIVERSIDAD DE LA LAGUNA

FABIO FINELLI — 02/09/2021 14:12:21
UNIVERSIDAD DE LA LAGUNA

Universidad de La Laguna
Oficina de Sede Electrónica
Entrada
Nº registro: 2021/90989
Nº reg. oficina: OF002/2021/89977
Fecha: 03/09/2021 12:24:13

where κ_i stands for the weak lensing convergence angular power spectra for the i-th redshift bin.

We apply this formalism to the Euclid photometric survey, given that from the six future galaxy surveys that we have studied in this thesis, only the two optical photometric surveys (Euclid photometric and LSST) will be able to measure galaxy shapes. Concering the minimum multipole for the weak lensing $\ell^{\kappa}_{\rm min}$, we adopt the same choice that for the number counts (see Sec. 5.1), and for the maximum multipole, we set $\ell^{\kappa}_{\rm max} = 1500$ for the weak lensing autospectra and their cross-correlations with CMB fields and galaxy clustering. Since weak lensing is an important probe at small scales, this is a conservative approach following the Euclid photometric *pessimistic* scenario in [176].

We compute the constraints for the 12 parameter extCDM model including the three probes, using *Planck* as CMB survey. In Fig. 5.14, we first show the improvement on the marginalized constraints on H_0 and the 6 extra parameters of the model by adding the weak lensing as uncorrelated probe to the full CMB and galaxy clustering combination (*Planck* x GCph + WL), and then by accounting also for the cross-correlations between weak lensing and the other two probes (*Planck* x GCph x WL). Just by adding weak lensing, we get a visible improvement in all of these parameters, and in particular, the addition of weak lensing is important for breaking the degeneracy between $N_{\rm eff}$ and $\mathrm{d}n_s/\mathrm{dln}k$. Moreover, the cross-correlations of the Euclid-ph weak lensing with the other two probes is found to be relevant as well.

In order to idenfity the individual relevance of each one of the various cross-correlations between CMB, galaxy clustering and weak lensing probes in our 2D joint tomographic approach, we now compute and show in Fig. 5.15 the marginalized constraints on H_0 and the extra parameters of the extCDM model for the following cases:

- The uncorrelated combination of the three probes without any cross-correlation, labeled as *Planck* + GCph + WL.
- A combination of the three probes including the CMB-GC and CMB-WL cross-correlations and neglecting the GC-WL cross-correlation, labeled as *Planck* x (GCph + WL).
- A combination including only the GC-WL cross-correlation and neglecting the CMB cross-correlations, labeled as *Planck* + (GCph x WL).

Este documento incorpora firma electrónica, y es copia auténtica de un documento electrónico archivado por la ULL según la Ley 39/2015.
Su autenticidad puede ser contrastada en la siguiente dirección https://sede.ull.es/validacion/

Identificador del documento: 3764923 Código de verificación: JHlWnlbn

Firmado por: JOSE RAMON BERMEJO CLIMENT — Fecha: 01/09/2021 17:41:12
UNIVERSIDAD DE LA LAGUNA

José Alberto Rubiño Martín — 01/09/2021 17:49:44
UNIVERSIDAD DE LA LAGUNA

FABIO FINELLI — 02/09/2021 14:12:21
UNIVERSIDAD DE LA LAGUNA

Universidad de La Laguna
Oficina de Sede Electrónica
Entrada
Nº registro: 2021/90989
Nº reg. oficina: OF002/2021/89977
Fecha: 03/09/2021 12:24:13

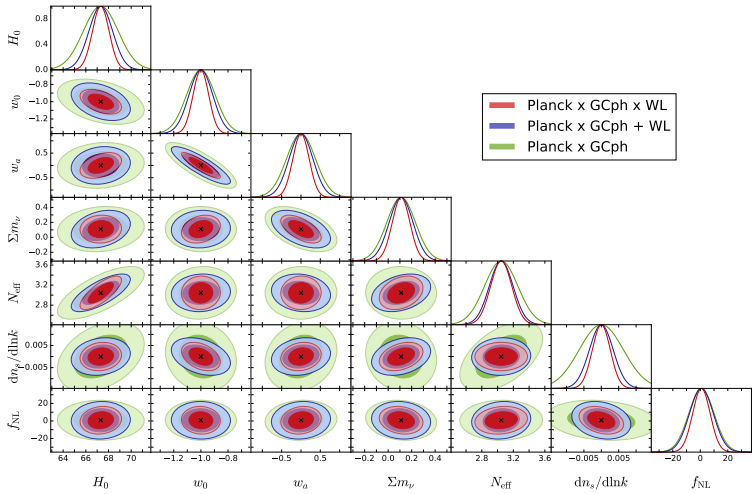

FIGURE 5.14— Marginalized 68% and 95% 2D confidence regions for the constraints on H_0 and the six extra parameters of the extCDM cosmological model. The green contours represent the full combination of the *Planck* CMB fields and the Euclid-ph galaxy clustering, the blue contours represent the addition of Euclid weak lensing as uncorrelated probe to the previous combination, and the red contours represent the full combination of *Planck* with the Euclid photometric galaxy clustering and weak lensing, including all the cross-correlations.

- The full combination of the three probes including all the cross-correlations, labeled as *Planck* x GCph x WL.

For the majority of the parameters, we obtain that the most important contribution in a 2D joint tomographic approach to the three probes is the galaxy clustering - weak lensing cross-correlation, given that the last two cases present very similar results, while the first two cases are as well similar. For $f_{\rm NL}$ instead, the relevance of the addition of the CMB-LSS cross-correlations is comparable to the inclusion of the galaxy clustering - weak lensing cross-correlation, which is compatible with the results shown in Sec. 5.2.2. In the case of Euclid, the importance of including the galaxy clustering - weak lensing cross-correlation in the analysis has been discussed already in the literature (see e.g. [177]).

The analysis shown in this section can be improved in the future with

Este documento incorpora firma electrónica, y es copia auténtica de un documento electrónico archivado por la ULL según la Ley 39/2015.
Su autenticidad puede ser contrastada en la siguiente dirección https://sede.ull.es/validacion/

Identificador del documento: 3764923 Código de verificación: JHlWnlbn

Firmado por: JOSE RAMON BERMEJO CLIMENT — Fecha: 01/09/2021 17:41:12
UNIVERSIDAD DE LA LAGUNA

José Alberto Rubiño Martín — 01/09/2021 17:49:44
UNIVERSIDAD DE LA LAGUNA

FABIO FINELLI — 02/09/2021 14:12:21
UNIVERSIDAD DE LA LAGUNA

Universidad de La Laguna
Oficina de Sede Electrónica
Entrada
Nº registro: 2021/90989
Nº reg. oficina: OF002/2021/89977
Fecha: 03/09/2021 12:24:13

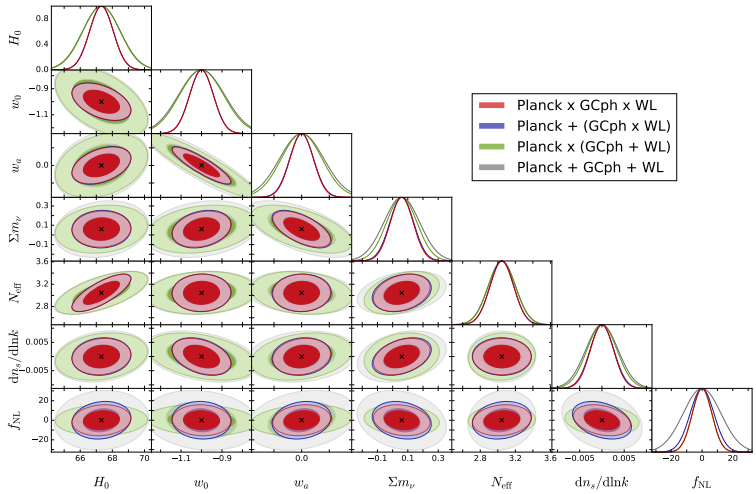

FIGURE 5.15— Marginalized 68% and 95% 2D confidence regions for the constraints on H_0 and the six extra parameters of the extCDM cosmological model by combining *Planck* with the Euclid photometric galaxy clustering and weak lensing probes. The grey contours represent the uncorrelated combination of the three probes without any cross-correlation, the green contours represent the combination of the three probes including the CMB-GC and CMB-WL cross-correlations and neglecting the GC-WL cross-correlation, the blue contours represent the combination including only the GC-WL cross-correlation and neglecting the CMB cross-correlations, and the red contours represent the full combination of *Planck* with the Euclid photometric galaxy clustering and weak lensing, including all the cross-correlations

the addition of weak lensing nuisance parameters related to the intrinsic alignment effects.

5.5 Full Euclid × CMB joint analysis

We have shown in Sec. 5.4.2 an outlook on the combination of the CMB with the galaxy number counts and weak lensing from the Euclid photometric survey. Here, we present forecasts for the combination of all the Euclid probes with the CMB, including also the 3D galaxy power spectra from the Euclid spectroscopic survey. This analysis has been recently shown in [135] and has been supported by the methodology described in this thesis.

Este documento incorpora firma electrónica, y es copia auténtica de un documento electrónico archivado por la ULL según la Ley 39/2015.
Su autenticidad puede ser contrastada en la siguiente dirección https://sede.ull.es/validacion/

Identificador del documento: 3764923 Código de verificación: JHlWnlbn

Firmado por: JOSE RAMON BERMEJO CLIMENT — Fecha: 01/09/2021 17:41:12
UNIVERSIDAD DE LA LAGUNA

José Alberto Rubiño Martín — 01/09/2021 17:49:44
UNIVERSIDAD DE LA LAGUNA

FABIO FINELLI — 02/09/2021 14:12:21
UNIVERSIDAD DE LA LAGUNA

Universidad de La Laguna
Oficina de Sede Electrónica
Entrada
Nº registro: 2021/90989
Nº reg. oficina: OF002/2021/89977
Fecha: 03/09/2021 12:24:13

We take into account all the CMB probes (temperature, polarization and lensing) and all their cross-correlations with Euclid probes in the data vector of the Fisher analysis. This includes those probes which are treated in the 2D angular space (the galaxy clustering from the photometric sample and the weak lensing). Instead, the galaxy clustering from the Euclid spectroscopic sample is treated in the 3D space (see [176] for the details on the methodology) and added as uncorrelated. Since the galaxy clustering from the spectroscopic survey overlaps in redshift with the galaxy clustering from the photometric sample, in the *pessimistic* scenario defined in [135, 176] the photometric clustering is cut for $z > 0.9$, while these galaxies are kept in the *optimistic* case. As CMB specifications, we consider *Planck*, SO and S4 following the specifications described in Sec. 3.1.

For the cosmological models, we consider the ΛCDM model, the w_0w_a parametrization of dark energy described in Sec. 5.2.1, the γ parametrization for modified gravity, and also the non-flat extensions of these models, where the total density Ω of the Universe is allowed to deviate from 1 by varying the $\Omega_{\rm DE,0}$ density parameter for the dark energy together with the matter and baryon densities.

We compare the constraints on the parameters obtained from Euclid alone with the errors once the CMB information and the cross-correlation is added. We find that the addition of CMB probes significantly improves the constraints from Euclid alone on cosmological parameters in all the cosmological cases considered. In most scenarios, $\Omega_{\rm b,0}$ and $\Omega_{\rm DE,0}$ are the parameters that are best improved as a result of the joint analysis.

In the case of $\Omega_{\rm b,0}$ the factor of improvement across the different cosmological models ranges from 1.7 when Planck is added to optimistic Euclid results, up to 9.8 when CMB-S4 data are combined with a more pessimistic scenario for Euclid (with an overall average factor of 5.3). This improvement is likely due to the fact that the shape of the CMB power spectrum and relative amplitudes of the acoustic peaks are highly sensitive to baryon density.

For $\Omega_{\rm DE,0}$ the improvement factor across cosmological models ranges between 3.3 and 13.4 (average 6.2, roughly twice as constraining as the addition of CMB lensing alone), echoing the constraining power of the CMB on curvature.

On the contrary, the Hubble parameter h is among the ones showing the least improvement, with an average factor of improvement of 1.7 (max-

Este documento incorpora firma electrónica, y es copia auténtica de un documento electrónico archivado por la ULL según la Ley 39/2015.
Su autenticidad puede ser contrastada en la siguiente dirección https://sede.ull.es/validacion/

Identificador del documento: 3764923 Código de verificación: JHlWnlbn

Firmado por: JOSE RAMON BERMEJO CLIMENT — Fecha: 01/09/2021 17:41:12
UNIVERSIDAD DE LA LAGUNA

José Alberto Rubiño Martín — 01/09/2021 17:49:44
UNIVERSIDAD DE LA LAGUNA

FABIO FINELLI — 02/09/2021 14:12:21
UNIVERSIDAD DE LA LAGUNA

Universidad de La Laguna
Oficina de Sede Electrónica
Entrada
Nº registro: 2021/90989
Nº reg. oficina: OF002/2021/89977
Fecha: 03/09/2021 12:24:13

imum 3.4). This indicates that the Euclid main probes, galaxy clustering and weak lensing, are already powerful at constraining the background evolution of the Universe, and so CMB data do not add much more information. Moreover, CMB observables depend on h mostly through the location of the acoustic peaks, i.e. the angular size of the sound horizon at recombination, which is an integrated quantity and only directly related to h in the simplest models. Thus, the introduction of additional cosmological parameters – also entering the computation of the angular size – induces degeneracies that further reduce the constraining power of the CMB on h.

Constraints on the other parameters of extensions to the baseline cosmological model, namely w_0, w_a and γ, show a (relatively) moderate improvement with respect to the Euclid-alone constraints, with an average factor of 1.6 (maximum 2.5). The full joint analysis with CMB provides on average an additional improvement factor of 1.4 (maximum 1.9) on these parameter constraints compared to the gains from adding CMB lensing alone.

We illustrate in Fig. 5.16 the improvement on the constraints by adding a SO-like CMB experiment to the Euclid pessimistic datasets, for four selected cosmological models. The results are presented in the form of "radar" plots, which show the ratio of uncertainties given by

$$\frac{\sigma_{\rm after}}{\sigma_{\rm before}}\,, \tag{5.20}$$

referring to the improvement after adding the CMB information and its cross-correlation to Euclid. The distance from the centres of these plots is a visual representation of the 1σ uncertainty on all parameters of our analysis, where a length of one corresponds to the Euclid-only constraints. We observe here once again how adding CMB lensing information (blue lines) affects mostly the nuisance parameters and extended models parameters, whereas the addition of all CMB probes has a more dramatic overall effect on all parameters for all models.

Este documento incorpora firma electrónica, y es copia auténtica de un documento electrónico archivado por la ULL según la Ley 39/2015.
Su autenticidad puede ser contrastada en la siguiente dirección https://sede.ull.es/validacion/

Identificador del documento: 3764923 Código de verificación: JHlWnlbn

Firmado por: JOSE RAMON BERMEJO CLIMENT — Fecha: 01/09/2021 17:41:12
UNIVERSIDAD DE LA LAGUNA

José Alberto Rubiño Martín — 01/09/2021 17:49:44
UNIVERSIDAD DE LA LAGUNA

FABIO FINELLI — 02/09/2021 14:12:21
UNIVERSIDAD DE LA LAGUNA

Universidad de La Laguna
Oficina de Sede Electrónica
Entrada
Nº registro: 2021/90989
Nº reg. oficina: OF002/2021/89977
Fecha: 03/09/2021 12:24:13

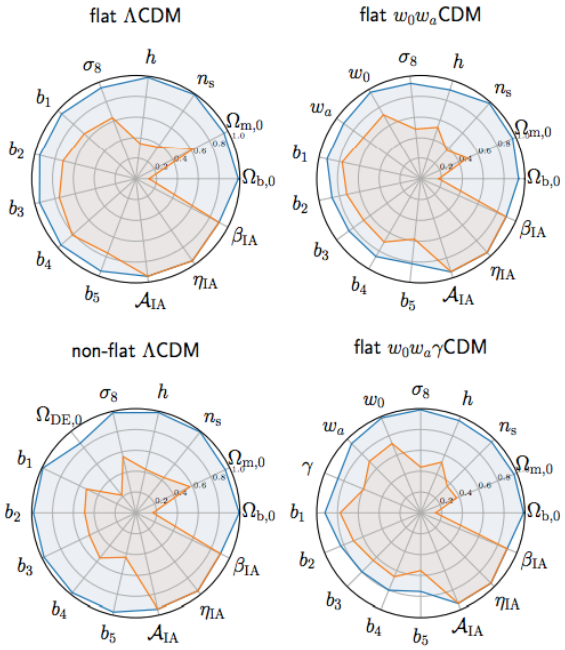

FIGURE 5.16— Ratio of predicted 1σ uncertainties showing how constraints are tightened after adding CMB lensing (blue) or all CMB probes (orange) when compared to the Euclid-only constraints (black outer rim), assuming a pessimistic Euclid scenario and SO-like CMB data, for four selected cosmological models (from top to bottom, left to right: flat ΛCDM; flat w_0w_aCDM; non-flat ΛCDM; and flat $w_0w_a\gamma$CDM)

Este documento incorpora firma electrónica, y es copia auténtica de un documento electrónico archivado por la ULL según la Ley 39/2015.
Su autenticidad puede ser contrastada en la siguiente dirección https://sede.ull.es/validacion/

Identificador del documento: 3764923 Código de verificación: JHlWnlbn

Firmado por:	JOSE RAMON BERMEJO CLIMENT *UNIVERSIDAD DE LA LAGUNA*	Fecha: 01/09/2021 17:41:12
	José Alberto Rubiño Martín *UNIVERSIDAD DE LA LAGUNA*	01/09/2021 17:49:44
	FABIO FINELLI *UNIVERSIDAD DE LA LAGUNA*	02/09/2021 14:12:21

Universidad de La Laguna
Oficina de Sede Electrónica
Entrada
Nº registro: 2021/90989
Nº reg. oficina: OF002/2021/89977
Fecha: 03/09/2021 12:24:13

Conclusions

The upcoming decade will be an exciting period for precision cosmology. Accurate maps of the CMB anisotropies from experiments such as *Planck* have provided information about the early Universe and constraints on the ΛCDM model, and next-generation CMB experiments will improve the sensitivity of this measurements. In addition, various galaxy surveys with different techniques will map the 3D distribution of the dark matter component, providing a complementary probe of the Universe physics at low redshift.

The combination of the two kind of datasets in a joint likelihood will allow to constrain extensions of the ΛCDM concordance model, and to account for the cross-correlation between CMB and LSS as an additional probe. The current challenges in cosmology and the open questions that remain open, such as the H_0 and S_8 tensions, will need to test possible generalizations of the concordance model in order to understand whether new physics are required.

In this thesis, we have developed methodologies for forecasting what we can expect from the combination and cross-correlation of CMB surveys with matter tracers, in the perspective of many upcoming and future cosmological surveys. The main results of this work are summarized in the following:

- By a signal-to-noise ratio anaylsis, we expect to detect the cross-correlation between CMB temperature anisotropies and galaxy number counts, which traces the ISW effect, with $\sim 5\sigma$ significance. In particular, the best measurements of the ISW effect will be possible with upcoming radio continuum surveys such as EMU and SKA thanks to their large sky coverage.

  On the other hand, the cross-correlation between CMB lensing and

Este documento incorpora firma electrónica, y es copia auténtica de un documento electrónico archivado por la ULL según la Ley 39/2015.
Su autenticidad puede ser contrastada en la siguiente dirección https://sede.ull.es/validacion/

Identificador del documento: 3764923 Código de verificación: JHlWnlbn

Firmado por:	JOSE RAMON BERMEJO CLIMENT *UNIVERSIDAD DE LA LAGUNA*	Fecha: 01/09/2021 17:41:12
	José Alberto Rubiño Martín *UNIVERSIDAD DE LA LAGUNA*	01/09/2021 17:49:44
	FABIO FINELLI *UNIVERSIDAD DE LA LAGUNA*	02/09/2021 14:12:21

Universidad de La Laguna
Oficina de Sede Electrónica
Entrada
Nº registro: 2021/90989
Nº reg. oficina: OF002/2021/89977
Fecha: 03/09/2021 12:24:13

galaxy number counts will be detectable at a much higher significance. This amount will be increased with post-*Planck* CMB experiments that will improve the sensitivity of the CMB lensing, such as the Simons Observatory and CMB-S4. Combining CMB-S4 with SKA1, we forecast to measure the CMB lensing - galaxy number counts cross-correlation with more than 200σ significance.

- We have estimated the capabilities of various surveys for measuring the lensing ratio of the CMB lensing - galaxy number counts and galaxy lensing - galaxy number counts cross-correlations. This estimator, which currently has been measured with a uncertainty larger than 10%, will be measured at few percent level using post-*Planck* CMB surveys and a galaxy survey such as Euclid, that will have on board both spectroscopic and photometric instrument for measuring the lenses and the sources, respectively.

  The lensing ratio estimator has been considered in the literature as multipole independent, but in this thesis we have included contributions to the galaxy number counts that were previously neglected, such as lensing magnification. We have obtained that lensing magnification will induce a multipole dependence of the lensing ratio that will be important for future galaxy surveys. In consequence, we have proposed a new estimator to take into account this dependence. Using our new estimator, we have also forecast by a Fisher matrix approach the usefulness of this ratio to break degeneracies present in the CMB information, finding that it can help to constrain extensions of the ΛCDM model in which both the curvature and the dark energy equation of state are allowed to vary.

- We have developed a Fisher matrix code to compute forecasts by a joint 2D tomographic approach to CMB and galaxy number counts, including all the cross-correlations between fields in the harmonic space. We have found that, according to the signal-to-noise analysis results, the CMB lensing - galaxy number counts will be much more powerful than the ISW for reducing the uncertainties on cosmological parameters. In terms of cosmological extended models, we have predicted an improvement of the dark energy FoM up to a factor ~ 2 thanks to the addition of cross-correlation, the detection of the neutrino mass with more than 3σ from the joint analysis of CMB-S4 and SPHEREx, and the measurement of the primordial local non-

Este documento incorpora firma electrónica, y es copia auténtica de un documento electrónico archivado por la ULL según la Ley 39/2015.
Su autenticidad puede ser contrastada en la siguiente dirección https://sede.ull.es/validacion/

Identificador del documento: 3764923 Código de verificación: JHlWnlbn

Firmado por:	JOSE RAMON BERMEJO CLIMENT *UNIVERSIDAD DE LA LAGUNA*	Fecha: 01/09/2021 17:41:12
	José Alberto Rubiño Martín *UNIVERSIDAD DE LA LAGUNA*	01/09/2021 17:49:44
	FABIO FINELLI *UNIVERSIDAD DE LA LAGUNA*	02/09/2021 14:12:21

Universidad de La Laguna
Oficina de Sede Electrónica
Entrada
Nº registro: 2021/90989
Nº reg. oficina: OF002/2021/89977
Fecha: 03/09/2021 12:24:13

Gaussianity $f_{\rm NL}$ with an error around $\sim 1.5-2$ combining the CMB with radio continuum surveys. These results have been obtained just from an analysis limited up to quasi-linear scales.

Further, we have applied our methodology to models of features in the primordial power spectrum originated by some inflationary models. We have presented, for the first time, a joint analysis of the CMB and galaxy clustering for primordial features in the harmonic space, and we have found that the inclusion of cross-correlation is important for helping to constrain some of these models.

We have as well presented an outlook on the extension of our methodology for the inclusion of effects as the scale-dependence of the bias due to the neutrino mass and of additional probes as weak lensing. This methodology has supported also the Euclid official forecasts for the combination of all its probes with the CMB.

The work presented in this thesis can be extended and improved in many directions. First, the inclusion of nuisance parameters that accounts for the intrinsic alignment effect in the weak lensing of galaxies would improve the forecasts on the lensing ratio and on the 2D joint tomographic approach once weak lensing is included. I am currently doing work for including these effects. Regarding the lensing ratio, the development of a new estimator can be also tested with more realistic mock data such as simulations. The 2D tomographic approach that we have developed can be applied as well to other kinds of large scale structure probes beyond galaxy clustering and weak lensing; as an example, we can mention the intensity mapping from radio surveys. Our code and methodology is also useful for forecasting constraints on physical models that have not targeted in this thesis, such as modified gravity.

Este documento incorpora firma electrónica, y es copia auténtica de un documento electrónico archivado por la ULL según la Ley 39/2015.
Su autenticidad puede ser contrastada en la siguiente dirección https://sede.ull.es/validacion/

Identificador del documento: 3764923 Código de verificación: JHlWnlbn

Firmado por:	JOSE RAMON BERMEJO CLIMENT *UNIVERSIDAD DE LA LAGUNA*	Fecha: 01/09/2021 17:41:12
	José Alberto Rubiño Martín *UNIVERSIDAD DE LA LAGUNA*	01/09/2021 17:49:44
	FABIO FINELLI *UNIVERSIDAD DE LA LAGUNA*	02/09/2021 14:12:21

Universidad de La Laguna
Oficina de Sede Electrónica
Entrada
Nº registro: 2021/90989
Nº reg. oficina: OF002/2021/89977
Fecha: 03/09/2021 12:24:13

Este documento incorpora firma electrónica, y es copia auténtica de un documento electrónico archivado por la ULL según la Ley 39/2015.
Su autenticidad puede ser contrastada en la siguiente dirección https://sede.ull.es/validacion/

Identificador del documento: 3764923 Código de verificación: JHlWnlbn

Firmado por:	JOSE RAMON BERMEJO CLIMENT *UNIVERSIDAD DE LA LAGUNA*	Fecha: 01/09/2021 17:41:12
	José Alberto Rubiño Martín *UNIVERSIDAD DE LA LAGUNA*	01/09/2021 17:49:44
	FABIO FINELLI *UNIVERSIDAD DE LA LAGUNA*	02/09/2021 14:12:21

Universidad de La Laguna
Oficina de Sede Electrónica
Entrada
Nº registro: 2021/90989
Nº reg. oficina: OF002/2021/89977
Fecha: 03/09/2021 12:24:13

A

Tables of cosmological parameter constraints

In this appendix we present the 68% marginalized constraints on the parameters for the various cosmological models discussed in Sec. 5.2.2 and Sec. 5.3.3.

We first present the ΛCDM model in Table A.1, the w_0CDM model in Table A.2, the 2 parameters extensions of ΛCDM (dynamical dark energy, neutrino physics and primordial universe) in Tables A.3-A.5, and the 12 parameters extCDM model in Table A.6.

We then show the primordial features models: the exponential cutoff at large scales in Table A.7, the Starobinsky model in Table A.8, the step in the inflaton potential in Table A.9 and the logarithmic super-imposed oscillations in Table A.10.

All the errors are marginalized over the nuisance parameters and correspond to the analysis up to quasi-linear scales with $k_{\rm max} = 0.1\ h/{\rm Mpc}$.

Este documento incorpora firma electrónica, y es copia auténtica de un documento electrónico archivado por la ULL según la Ley 39/2015.
Su autenticidad puede ser contrastada en la siguiente dirección https://sede.ull.es/validacion/

Identificador del documento: 3764923 Código de verificación: JHlWnlbn

Firmado por:	JOSE RAMON BERMEJO CLIMENT *UNIVERSIDAD DE LA LAGUNA*	Fecha: 01/09/2021 17:41:12
	José Alberto Rubiño Martín *UNIVERSIDAD DE LA LAGUNA*	01/09/2021 17:49:44
	FABIO FINELLI *UNIVERSIDAD DE LA LAGUNA*	02/09/2021 14:12:21

Universidad de La Laguna
Oficina de Sede Electrónica
Entrada
Nº registro: 2021/90989
Nº reg. oficina: OF002/2021/89977
Fecha: 03/09/2021 12:24:13

TABLE A.1— 68% marginalized constraints on the parameters of the ΛCDM cosmology obtained from the combination of each pair of CMB and galaxy surveys, in the single bin and tomographic configurations. We show the constraints from the full combination including the CMB-GC cross-correlation (CMB × GC) and, between parenthesis, the constraints from the uncorrelated combination of Fisher matrices (CMB + LSS). We also list FoM of the 6 cosmological parameters. For each survey combination, we mark in boldface the cosmological parameter which benefits most from including the CMB-LSS cross-correlation.

ΛCDM		Euclid-like ph		Euclid-like sp		LSST		SPHEREx		EMU		SKA1	
CMB survey	Parameter	1 bin ×(+)	10 bins ×(+)	1 bin ×(+)	9 bins ×(+)	1 bin ×(+)	10 bins ×(+)	1 bin ×(+)	10 bins ×(+)	1 bin ×(+)	5 bins ×(+)	1 bin ×(+)	5 bins ×(+)
Planck	$10^5\,\sigma(\Omega_b h^2)$	14(14)	11(11)	14(14)	12(12)	14(14)	12(12)	14(14)	12(11)	14(14)	12(13)	14(14)	12(12)
	$10^4\,\sigma(\Omega_c h^2)$	12(12)	**5.8(6.2)**	12(12)	8.5(8.5)	11(11)	**6.8(7.7)**	11(11)	**6.3(7.1)**	11(11)	**8.2(9.9)**	11(11)	**7.5(9.0)**
	$10^2\,\sigma(H_0)$	**56(57)**	26(27)	**56(57)**	38(38)	51(52)	31(34)	52(52)	28(32)	**51(52)**	37(44)	51(52)	34(40)
	$10^4\,\sigma(\tau)$	74(74)	66(67)	74(74)	69(69)	72(72)	67(68)	72(72)	67(67)	72(72)	69(70)	72(72)	67(68)
	$10^4\,\sigma(n_s)$	36(36)	29(29)	36(36)	32(32)	34(35)	30(31)	35(35)	30(30)	35(35)	31(33)	**34(35)**	31(33)
	$10^3\,\sigma(\ln(10^{10}A_s))$	14(14)	13(13)	14(14)	13(13)	13(13)	13(13)	13(13)	13(13)	13(13)	13(13)	13(13)	12(13)
	$10^4\,\sigma(\sigma_8)$	62(63)	50(53)	62(63)	54(54)	**53(55)**	50(53)	55(55)	51(53)	55(55)	48(54)	54(55)	46(52)
	$\mathrm{FoM_{cosmo}}$ / 10^4	15(15)	21(20)	15(15)	18(18)	16(16)	20(19)	16(16)	20(19)	16(16)	19(17)	16(16)	20(18)
	$\mathrm{FoM_{bias}}$ / 10^2	0.21(0.03)	645(619)	0.020(0.005)	35(35)	0.69(0.09)	68(57)	**0.026(0.001)**	47(45)	12(3.4)	117(109)	1.5(0.8)	135(126)
Planck+SO	$10^5\,\sigma(\Omega_b h^2)$	4.7(4.7)	4.5(4.5)	4.7(4.7)	4.6(4.6)	4.7(4.7)	4.5(4.5)	4.7(4.7)	4.5(4.5)	4.7(4.7)	4.6(4.6)	4.7(4.7)	4.6(4.6)
	$10^4\,\sigma(\Omega_c h^2)$	6.2(6.2)	**4.6(4.9)**	6.2(6.2)	5.7(5.7)	6.2(6.2)	**4.8(5.5)**	6.2(6.2)	**4.7(5.2)**	6.2(6.2)	**5.6(6.0)**	6.2(6.2)	**5.1(5.8)**
	$10^2\,\sigma(H_0)$	24(24)	17(18)	24(24)	21(21)	24(24)	18(21)	24(24)	18(20)	24(24)	22(23)	24(24)	20(22)
	$10^4\,\sigma(\tau)$	56(56)	48(49)	56(56)	53(53)	56(56)	49(52)	56(56)	49(51)	56(56)	53(55)	56(56)	51(54)
	$10^4\,\sigma(n_s)$	19(19)	19(19)	19(19)	19(19)	19(19)	19(19)	19(19)	19(19)	19(19)	19(19)	19(19)	19(19)
	$10^3\,\sigma(\ln(10^{10}A_s))$	10(10)	8.5(9.0)	10(10)	9.6(9.6)	10(10)	8.7(9.5)	10(10)	8.8(9.2)	10(10)	9.5(9.9)	10(10)	9.0(9.6)
	$10^4\,\sigma(\sigma_8)$	**30(31)**	29(30)	31(31)	**30(31)**	**30(31)**	28(30)	31(31)	30(30)	31(31)	30(31)	**30(31)**	29(30)
	$\mathrm{FoM_{cosmo}}$ / 10^4	77(77)	86(84)	77(77)	80(80)	77(77)	86(81)	77(77)	83(82)	77(77)	79(78)	77(77)	83(80)
	$\mathrm{FoM_{bias}}$ / 10^2	0.85(0.03)	760(674)	**0.051(0.005)**	38(37)	2.27(0.07)	94(61)	**0.041(0.001)**	52(48)	**24(4)**	146(119)	4.3(1.0)	177(142)
LiteBIRD+S4	$10^5\,\sigma(\Omega_b h^2)$	2.9(2.9)	2.9(2.9)	2.9(2.9)	2.9(2.9)	2.9(2.9)	2.9(2.9)	2.9(2.9)	2.9(2.9)	2.9(2.9)	2.9(2.9)	2.9(2.9)	2.9(2.9)
	$10^4\,\sigma(\Omega_c h^2)$	2.4(2.4)	2.2(2.3)	2.4(2.4)	2.3(2.3)	2.4(2.4)	2.1(2.3)	2.4(2.4)	2.2(2.3)	2.4(2.4)	**2.3(2.4)**	2.4(2.4)	2.2(2.3)
	$10^2\,\sigma(H_0)$	9.1(9.2)	8.3(8.7)	9.2(9.2)	9.0(9.0)	9.1(9.2)	**8.2(8.9)**	9.2(9.2)	**8.5(8.8)**	9.2(9.2)	8.9(9.1)	9.1(9.2)	**8.4(9.0)**
	$10^4\,\sigma(\tau)$	18(18)	17(17)	18(18)	17(17)	18(18)	17(17)	18(18)	17(17)	18(18)	18(18)	18(18)	17(17)
	$10^4\,\sigma(n_s)$	13(13)	13(13)	13(13)	13(13)	13(13)	13(13)	13(13)	13(13)	13(13)	13(13)	13(13)	13(13)
	$10^3\,\sigma(\ln(10^{10}A_s))$	**3.2(3.3)**	3.1(3.2)	3.3(3.3)	3.2(3.2)	**3.2(3.3)**	3.0(3.2)	3.3(3.3)	3.1(3.2)	3.2(3.3)	3.2(3.2)	**3.2(3.3)**	3.1(3.2)
	$10^4\,\sigma(\sigma_8)$	10(10)	10(10)	10(10)	10(10)	10(10)	10(10)	10(10)	10(10)	10(10)	10(10)	10(10)	10(10)
	$\mathrm{FoM_{cosmo}}$ / 10^4	242(242)	252(247)	242(242)	244(244)	242(242)	257(245)	242(242)	245(245)	242(242)	242(242)	242(242)	250(244)
	$\mathrm{FoM_{bias}}$ / 10^2	1.85(0.03)	967(753)	**0.086(0.005)**	**44(42)**	5.39(0.07)	138(67)	**0.054(0.001)**	59(53)	**102(7)**	876(493)	24(1.3)	273(167)

Este documento incorpora firma electrónica, y es copia auténtica de un documento electrónico archivado por la ULL según la Ley 39/2015.
Su autenticidad puede ser contrastada en la siguiente dirección https://sede.ull.es/validacion/

Identificador del documento: 3764923 Código de verificación: JHlWnlbn

Firmado por: JOSE RAMON BERMEJO CLIMENT — Fecha: 01/09/2021 17:41:12
UNIVERSIDAD DE LA LAGUNA

José Alberto Rubiño Martín — 01/09/2021 17:49:44
UNIVERSIDAD DE LA LAGUNA

FABIO FINELLI — 02/09/2021 14:12:21
UNIVERSIDAD DE LA LAGUNA

Universidad de La Laguna
Oficina de Sede Electrónica
Entrada
Nº registro: 2021/90989
Nº reg. oficina: OF002/2021/89977
Fecha: 03/09/2021 12:24:13

TABLE A.2— 68% marginalized constraints on w_0 for the w_0CDM cosmology obtained from the combination of each pair of CMB and galaxy surveys, in the single bin and tomographic configurations. We show the constraints from the full combination including the CMB-GC cross-correlation (CMB × GC) and, between parenthesis, the constraints from the combination of Fisher matrices as uncorrelated (CMB + GC). For each CMB survey, we mark in boldface the galaxy survey for which the error in w_0 has a larger improvement by the inclusion of cross-correlation.

w_0CDM		Euclid-like ph		Euclid-like sp		LSST		SPHEREx		EMU		SKA1	
CMB survey	Parameter	1 bin ×(+)	10 bins ×(+)	1 bin ×(+)	9 bins ×(+)	1 bin ×(+)	10 bins ×(+)	1 bin ×(+)	10 bins ×(+)	1 bin ×(+)	5 bins ×(+)	1 bin ×(+)	5 bins ×(+)
Planck	$10^2\,\sigma(w_0)$	27(31)	4.0(4.4)	25(31)	12(12)	24(28)	7.1(8.4)	27(28)	5.3(5.8)	22(28)	**8.5(15)**	16(27)	8.2(14)
Planck+SO	$10^2\,\sigma(w_0)$	11(11)	3.3(3.6)	11(11)	7.9(8.2)	11(11)	5.0(6.6)	11(11)	4.0(4.3)	11(11)	6.2(9.4)	9.2(11)	**5.3(9.0)**
LiteBIRD+S4	$10^2\,\sigma(w_0)$	6.1(6.1)	2.5(2.8)	6.1(6.1)	5.2(5.2)	6.0(6.1)	3.3(4.6)	6.1(6.1)	2.8(3.2)	6.1(6.1)	4.2(5.7)	5.4(6.1)	**3.6(5.5)**

TABLE A.3— 68% marginalized constraints on w_0 and w_a for the w_0w_aCDM cosmology obtained from the combination of each pair of CMB and galaxy surveys, in the single bin and tomographic configurations. We show the constraints from the full combination including the CMB-GC cross-correlation (CMB × GC) and, between parenthesis, the constraints from the combination of Fisher matrices as uncorrelated (CMB + GC). We also list the FoM of the two extra parameters. For each survey combination, we mark in boldface the cosmological parameter which benefits most from including the CMB-LSS cross-correlation. We mark as well the FoM which is most improved by cross-correlation.

w_0w_aCDM		Euclid-like ph		Euclid-like sp		LSST		SPHEREx		EMU		SKA1	
CMB survey	Parameter	1 bin ×(+)	10 bins ×(+)	1 bin ×(+)	9 bins ×(+)	1 bin ×(+)	10 bins ×(+)	1 bin ×(+)	10 bins ×(+)	1 bin ×(+)	5 bins ×(+)	1 bin ×(+)	5 bins ×(+)
Planck	$10^2\,\sigma(w_0)$	**72(92)**	**10(11)**	**84(92)**	**69(77)**	**75(91)**	**30(37)**	84(92)	**18(20)**	**74(89)**	**32(46)**	**63(77)**	**27(47)**
	$10^2\,\sigma(w_a)$	166(197)	32(34)	188(197)	149(160)	169(194)	72(86)	**176(195)**	38(41)	168(190)	80(106)	155(175)	67(105)
	FoM	2.2(1.6)	79(67)	2.2(1.7)	5.7(5.2)	2.4(1.8)	20(14)	2.1(1.8)	50(42)	2.7(1.9)	15(6.4)	4.0(2.1)	**18(6.9)**
Planck+SO	$10^2\,\sigma(w_0)$	25(26)	**9.4(10)**	26(26)	**24(25)**	25(26)	**17(22)**	26(26)	**14(16)**	26(26)	20(23)	**25(26)**	**15(23)**
	$10^2\,\sigma(w_a)$	**68(71)**	28(32)	71(71)	58(59)	**68(71)**	42(53)	**70(71)**	30(33)	**70(71)**	**53(61)**	70(71)	42(59)
	FoM	13(13)	108(89)	13(13)	22(21)	13(13)	47(28)	13(13)	82(69)	13(13)	30(17)	16(13)	45(19)
LiteBIRD+S4	$10^2\,\sigma(w_0)$	14(14)	7.7(8.7)	14(14)	13(13)	14(14)	**10(13)**	14(14)	10(11)	14(14)	**12(14)**	14(14)	10(13)
	$10^2\,\sigma(w_a)$	**41(43)**	**22(26)**	43(43)	35(35)	40(43)	26(33)	**42(43)**	**22(25)**	**41(43)**	34(39)	**41(43)**	**27(37)**
	FoM	40(38)	183(140)	38(38)	56(54)	42(38)	118(65)	39(39)	162(126)	40(38)	70(45)	45(39)	104(49)

Este documento incorpora firma electrónica, y es copia auténtica de un documento electrónico archivado por la ULL según la Ley 39/2015.
Su autenticidad puede ser contrastada en la siguiente dirección https://sede.ull.es/validacion/

Identificador del documento: 3764923 Código de verificación: JHlWnlbn

Firmado por: JOSE RAMON BERMEJO CLIMENT — Fecha: 01/09/2021 17:41:12
UNIVERSIDAD DE LA LAGUNA

José Alberto Rubiño Martín — 01/09/2021 17:49:44
UNIVERSIDAD DE LA LAGUNA

FABIO FINELLI — 02/09/2021 14:12:21
UNIVERSIDAD DE LA LAGUNA

Universidad de La Laguna
Oficina de Sede Electrónica
Entrada
Nº registro: 2021/90989
Nº reg. oficina: OF002/2021/89977
Fecha: 03/09/2021 12:24:13

TABLE A.4— 68% marginalized constraints on Σm_ν and $N_{\rm eff}$ for the ΛCDM+$\{\Sigma m_\nu, N_{\rm eff}\}$ cosmology obtained from the combination of each pair of CMB and galaxy surveys, in the single bin and tomographic configurations. We show the constraints from the full combination including the CMB-GC cross-correlation (CMB × GC) and, between parenthesis, the constraints from the combination of Fisher matrices as uncorrelated (CMB + GC). We also list the FoM of the two extra parameters. For each survey combination, we mark in boldface the cosmological parameter which benefits most from including the CMB-LSS cross-correlation.

ΛCDM+$\{\Sigma m_\nu, N_{\rm eff}\}$		Euclid-like ph		Euclid-like sp		LSST		SPHEREx		EMU		SKA1	
CMB survey	Parameter	1 bin	10 bins	1 bin	9 bins	1 bin	10 bins	1 bin	10 bins	1 bin	5 bins	1 bin	5 bins
		×(+)	×(+)	×(+)	×(+)	×(+)	×(+)	×(+)	×(+)	×(+)	×(+)	×(+)	×(+)
Planck	$\sigma(\Sigma m_\nu)$/meV	**163(173)**	**68(73)**	**166(171)**	103(103)	**143(149)**	**80(88)**	149(149)	**55(61)**	**140(149)**	**101(132)**	**135(149)**	**85(107)**
	$10^2\ \sigma(N_{\rm eff})$	22(22)	18(18)	22(22)	20(20)	22(22)	19(19)	22(22)	20(20)	21(22)	20(21)	21(22)	19(20)
	FoM	28(26)	85(77)	28(27)	47(47)	33(31)	67(59)	31(31)	92(82)	34(31)	50(36)	35(31)	62(47)
Planck+SO	$\sigma(\Sigma m_\nu)$/meV	74(74)	**48(50)**	74(74)	65(65)	74(74)	**51(60)**	74(74)	**31(43)**	74(74)	**62(72)**	74(74)	**55(68)**
	$10^2\ \sigma(N_{\rm eff})$	6.3(6.3)	6.2(6.2)	6.3(6.3)	6.2(6.2)	6.3(6.3)	6.2(6.2)	6.3(6.3)	6.2(6.2)	6.3(6.3)	6.3(6.3)	6.3(6.3)	6.2(6.2)
	FoM	215(215)	347(325)	216(216)	247(247)	215(215)	320(271)	215(215)	518(376)	215(215)	258(223)	215(215)	298(238)
LiteBIRD+S4	$\sigma(\Sigma m_\nu)$/meV	40(40)	**24(28)**	40(40)	36(36)	40(40)	**25(34)**	40(40)	**16(26)**	40(40)	**33(39)**	40(40)	**27(37)**
	$10^2\ \sigma(N_{\rm eff})$	4.0(4.0)	4.0(4.0)	4.0(4.0)	4.0(4.0)	4.0(4.0)	3.9(4.0)	4.0(4.0)	4.0(4.0)	4.0(4.0)	4.0(4.0)	4.0(4.0)	4.0(4.0)
	FoM	618(618)	1054(893)	619(619)	693(693)	619(619)	1047(744)	620(620)	1525(963)	619(619)	751(639)	619(619)	944(674)

TABLE A.5— 68% marginalized constraints on $dn_s/d\ln k$ and $f_{\rm NL}$ for the ΛCDM+$\{dn_s/d\ln k, f_{\rm NL}\}$ cosmology obtained from the combination of each pair of CMB and galaxy surveys, in the single bin and tomographic configurations. We show the constraints from the full combination including the CMB-GC cross-correlation (CMB × GC) and, between parenthesis, the constraints from the combination of Fisher matrices as uncorrelated (CMB + GC). We also list the FoM of the two extra parameters. For each survey combination, we mark in boldface the cosmological parameter which benefits most from including the CMB-LSS cross-correlation.

ΛCDM+$\{dn_s/d\ln k, f_{\rm NL}\}$		Euclid-like ph		Euclid-like sp		LSST		SPHEREx		EMU		SKA1	
CMB survey	Parameter	1 bin	10 bins	1 bin	9 bins	1 bin	10 bins	1 bin	10 bins	1 bin	5 bins	1 bin	5 bins
		×(+)	×(+)	×(+)	×(+)	×(+)	×(+)	×(+)	×(+)	×(+)	×(+)	×(+)	×(+)
Planck	$10^4\ \sigma(dn_s/d\ln k)$	59(60)	53(55)	60(60)	57(58)	59(60)	53(57)	60(60)	56(57)	60(60)	56(57)	59(60)	53(55)
	$\sigma(f_{\rm NL})$	**49(146)**	**9.1(11)**	**35(46)**	**15(16)**	**22(319)**	**4.6(9.9)**	**627(1443)**	**10(11)**	**16(277)**	**2.1(2.8)**	**15(119)**	**1.7(2.2)**
	FoM	3.5(1.1)	21(18)	4.8(3.6)	12(11)	7.7(0.5)	41(19)	0.3(0.1)	18(17)	11(1)	86(65)	11(1)	111(85)
Planck+SO	$10^4\ \sigma(dn_s/d\ln k)$	31(31)	30(30)	31(31)	31(31)	31(31)	30(31)	31(31)	31(31)	31(31)	31(31)	31(31)	30(30)
	$\sigma(f_{\rm NL})$	**47(146)**	**8.7(10)**	**33(46)**	**14(15)**	**22(319)**	**4.5(9.3)**	**618(1443)**	**9.8(10)**	**15(277)**	**2.1(2.7)**	**14(120)**	**1.7(2.1)**
	FoM	6.7(2.2)	39(33)	9.4(7.0)	24(22)	14.6(1.0)	74(36)	0.5(0.2)	34(24)	21(1.2)	156(122)	22(2.7)	201(159)
LiteBIRD+S4	$10^4\ \sigma(dn_s/d\ln k)$	23(23)	22(23)	23(23)	23(23)	23(23)	22(23)	23(23)	23(23)	23(23)	23(23)	23(23)	22(22)
	$\sigma(f_{\rm NL})$	**42(146)**	**8.2(9.9)**	**31(46)**	**13(14)**	**19(319)**	**4.1(9.0)**	**568(1443)**	**9.4(9.8)**	**12(207)**	**2.0(2.7)**	**11(120)**	**1.6(2.1)**
	FoM	10(3.0)	55(46)	14(9.5)	34(32)	23(1.4)	113(50)	0.8(0.3)	47(46)	34(1.6)	224(166)	39(3.6)	287(214)

Este documento incorpora firma electrónica, y es copia auténtica de un documento electrónico archivado por la ULL según la Ley 39/2015.
Su autenticidad puede ser contrastada en la siguiente dirección https://sede.ull.es/validacion/

Identificador del documento: 3764923 Código de verificación: JHlWnlbn

Firmado por: JOSE RAMON BERMEJO CLIMENT — Fecha: 01/09/2021 17:41:12
UNIVERSIDAD DE LA LAGUNA

José Alberto Rubiño Martín — 01/09/2021 17:49:44
UNIVERSIDAD DE LA LAGUNA

FABIO FINELLI — 02/09/2021 14:12:21
UNIVERSIDAD DE LA LAGUNA

Universidad de La Laguna
Oficina de Sede Electrónica
Entrada
Nº registro: 2021/90989
Nº reg. oficina: OF002/2021/89977
Fecha: 03/09/2021 12:24:13

TABLE A.6— 68% marginalized constraints on the 12 parameters of the extCDM cosmology obtained from the combination of each pair of CMB and galaxy surveys, in the single bin and tomographic configurations. We show the constraints from the full combination including the CMB-GC cross-correlation (CMB × GC) and, between parenthesis, the constraints from the uncorrelated combination of Fisher matrices (CMB + LSS). We also list the derived uncertainties on σ_8, and the FoMs of the 12 cosmological parameters and the bias nuisance parameters. For each survey combination, we mark in boldface the cosmological parameter which benefits most from including the CMB-LSS cross-correlation.

extCDM		Euclid-like ph		Euclid-like sp		LSST		SPHEREx		EMU		SKA1	
CMB survey	Parameter	1 bin ×(+)	10 bins ×(+)	1 bin ×(+)	9 bins ×(+)	1 bin ×(+)	10 bins ×(+)	1 bin ×(+)	10 bins ×(+)	1 bin ×(+)	5 bins ×(+)	1 bin ×(+)	5 bins ×(+)
Planck	$10^5\,\sigma(\Omega_b h^2)$	25(25)	19(20)	25(25)	22(22)	24(25)	19(21)	25(25)	19(22)	24(25)	21(23)	24(25)	19(21)
	$10^4\,\sigma(\Omega_c h^2)$	39(39)	31(31)	39(39)	37(37)	39(39)	35(35)	39(39)	36(36)	39(39)	37(38)	39(39)	36(36)
	$\sigma(H_0)$	11(14)	1.5(1.6)	12(14)	**9.1(10)**	11(14)	3.8(4.7)	14(14)	2.7(3.0)	11(14)	**3.9(6.4)**	7.8(13)	**3.6(6.6)**
	$10^4\,\sigma(\tau)$	79(79)	76(76)	79(79)	77(77)	79(79)	76(77)	79(79)	76(77)	79(79)	77(77)	78(79)	76(77)
	$10^3\,\sigma(\ln(10^{10}A_s))$	109(110)	80(86)	109(110)	97(97)	109(110)	83(91)	109(110)	87(96)	108(110)	91(103)	108(110)	85(95)
	$10^4\,\sigma(n_s)$	18(18)	17(17)	18(18)	17(17)	18(18)	17(17)	18(18)	17(17)	18(18)	17(17)	18(18)	17(17)
	$10^2\,\sigma(w_0)$	77(94)	11(11)	88(95)	72(79)	80(94)	33(40)	88(94)	19(20)	80(93)	33(48)	68(93)	29(50)
	$10^2\,\sigma(w_a)$	202(214)	37(41)	211(214)	164(172)	198(211)	86(106)	193(211)	43(50)	190(208)	62(92)	174(210)	71(113)
	$\sigma(\Sigma m_\nu)/\mathrm{meV}$	229(265)	122(139)	218(263)	181(181)	192(223)	128(164)	221(224)	**87(178)**	179(223)	129(187)	170(222)	109(143)
	$10^2\,\sigma(N_{\rm eff})$	27(27)	21(22)	27(27)	25(25)	27(27)	23(24)	27(27)	24(25)	27(27)	25(26)	27(27)	23(24)
	$10^4\,\sigma(\mathrm{d}n_s/\mathrm{d}\ln k)$	75(76)	64(66)	74(76)	70(70)	74(75)	65(69)	75(75)	67(69)	75(75)	68(71)	74(75)	66(69)
	$\sigma(f_{\rm NL})$	**49(146)**	**9.2(11)**	**35(46)**	16(17)	**22(320)**	**4.7(10)**	**645(1443)**	10(10)	**16(282)**	2.2(2.9)	**16(139)**	1.7(2.3)
	$10^3\,\sigma(\sigma_8)$	96(121)	16(17)	103(121)	80(88)	96(117)	35(44)	113(117)	25(27)	95(116)	36(57)	69(115)	33(59)
	$\mathrm{FoM}_{\rm cosmo}\ /\ 10^2$	8(6)	29(26)	9(8)	14(14)	10(6)	24(18)	5(4)	26(22)	11(6)	25(18)	12(7)	29(21)
	$\mathrm{FoM}_{\rm bias}\ /\ 10^2$	0.11(0.02)	439(405)	0.011(0.004)	22(22)	0.3(0.02)	43(32)	0.017(0.001)	35(30)	1.9(0.7)	55(35)	0.4(0.2)	60(37)
Planck+SO	$10^5\,\sigma(\Omega_b h^2)$	7.9(7.9)	7.5(7.7)	7.9(7.9)	7.9(7.9)	7.9(7.9)	7.5(7.8)	7.9(7.9)	7.6(7.8)	7.9(7.9)	7.7(7.9)	7.9(7.9)	7.4(7.8)
	$10^4\,\sigma(\Omega_c h^2)$	15(15)	14(14)	15(15)	15(15)	15(15)	14(14)	15(15)	14(14)	15(15)	14(14)	15(15)	14(14)
	$\sigma(H_0)$	3.7(3.7)	1.1(1.1)	3.6(3.7)	3.3(3.3)	3.6(3.7)	2.0(2.7)	3.7(3.7)	1.9(2.2)	3.7(3.7)	**2.3(3.2)**	3.1(3.7)	**1.9(3.2)**
	$10^4\,\sigma(\tau)$	75(75)	71(72)	75(75)	73(74)	75(75)	71(73)	75(75)	68(72)	75(75)	73(75)	75(75)	72(74)
	$10^4\,\sigma(n_s)$	41(41)	39(39)	41(41)	40(40)	41(41)	38(40)	41(41)	39(40)	41(41)	40(40)	41(41)	38(40)
	$10^3\,\sigma(\ln(10^{10}A_s))$	15(15)	14(14)	15(15)	14(14)	15(15)	14(14)	15(15)	13(14)	15(15)	15(15)	15(15)	14(15)
	$10^2\,\sigma(w_0)$	26(27)	9.6(10)	27(27)	26(26)	26(27)	18(22)	27(27)	14(15)	27(27)	20(24)	26(27)	16(24)
	$10^2\,\sigma(w_a)$	75(80)	32(36)	80(80)	67(68)	75(80)	51(62)	79(80)	34(38)	78(80)	58(69)	78(80)	47(67)
	$\sigma(\Sigma m_\nu)/\mathrm{meV}$	90(92)	**69(80)**	92(92)	88(89)	89(92)	71(87)	92(92)	**44(86)**	92(92)	78(89)	90(92)	68(85)
	$10^2\,\sigma(N_{\rm eff})$	8.9(8.9)	8.5(8.6)	8.9(8.9)	8.8(8.8)	8.9(8.9)	8.5(8.8)	8.9(8.9)	8.8(8.8)	8.9(8.9)	8.8(8.8)	8.9(8.9)	8.5(8.7)
	$10^4\,\sigma(\mathrm{d}n_s/\mathrm{d}\ln k)$	44(44)	42(42)	44(44)	43(43)	44(44)	42(43)	44(44)	43(43)	44(44)	43(43)	44(44)	42(43)
	$\sigma(f_{\rm NL})$	**47(145)**	8.8(10)	**33(45)**	**14(15)**	**22(319)**	**4.5(6.5)**	**622(1443)**	10(10)	**15(278)**	2.1(2.8)	**14(121)**	1.7(2.2)
	$10^3\,\sigma(\sigma_8)$	31(31)	9(10)	31(31)	28(29)	31(31)	19(24)	31(31)	17(18)	31(31)	20(28)	27(31)	17(28)
	$\mathrm{FoM}_{\rm cosmo}\ /\ 10^2$	40(33)	87(79)	42(41)	55(55)	46(29)	84(64)	26(23)	85(74)	48(30)	83(70)	51(35)	98(76)
	$\mathrm{FoM}_{\rm bias}\ /\ 10^2$	0.50(0.02)	589(504)	0.034(0.004)	29(28)	1.09(0.02)	72(43)	0.028(0.001)	40(35)	7.0(1.2)	92(65)	1.6(0.4)	108(68)
LiteBIRD+S4	$10^5\,\sigma(\Omega_b h^2)$	4.6(4.6)	4.4(4.5)	4.6(4.6)	4.6(4.6)	4.6(4.6)	4.4(4.6)	4.6(4.6)	4.5(4.6)	4.6(4.6)	4.4(4.6)	4.6(4.6)	4.4(4.6)
	$10^4\,\sigma(\Omega_c h^2)$	10(10)	9.9(9.9)	10(10)	10(10)	10(10)	10(10)	10(10)	9.8(10)	10(10)	10(10)	10(10)	10(10)
	$\sigma(H_0)$	2.0(2.0)	0.9(1.0)	2.0(2.0)	1.8(1.8)	2.0(2.0)	1.3(1.7)	2.0(2.0)	1.4(1.5)	2.0(2.0)	1.5(1.9)	1.8(2.0)	1.3(1.8)
	$10^4\,\sigma(\tau)$	18(18)	18(18)	18(18)	18(18)	18(18)	18(18)	18(18)	18(18)	18(18)	18(18)	18(18)	18(18)
	$10^4\,\sigma(n_s)$	29(29)	27(28)	29(29)	28(28)	29(29)	26(28)	29(29)	28(28)	29(29)	28(28)	29(29)	27(28)
	$10^3\,\sigma(\ln(10^{10}A_s))$	4.1(4.2)	4.0(4.1)	4.2(4.2)	4.1(4.1)	4.1(4.2)	4.0(4.1)	4.2(4.2)	3.8(4.1)	4.2(4.2)	4.1(4.2)	4.1(4.2)	4.0(4.1)
	$10^2\,\sigma(w_0)$	15(15)	8.2(9.2)	15(15)	14(14)	15(15)	12(14)	15(15)	11(11)	15(15)	13(14)	15(15)	11(14)
	$10^2\,\sigma(w_a)$	48(52)	27(32)	53(53)	45(46)	46(53)	34(43)	52(52)	27(30)	50(53)	41(49)	50(53)	33(47)
	$\sigma(\Sigma m_\nu)/\mathrm{meV}$	54(66)	**38(51)**	57(57)	54(56)	53(57)	37(54)	58(56)	**28(51)**	56(57)	46(56)	55(57)	**36(55)**
	$10^2\,\sigma(N_{\rm eff})$	5.9(5.9)	5.8(5.9)	5.9(5.9)	5.9(5.9)	5.9(5.9)	5.7(5.9)	5.9(5.9)	5.9(5.9)	5.9(5.9)	5.9(5.9)	5.9(5.9)	5.8(5.9)
	$10^4\,\sigma(\mathrm{d}n_s/\mathrm{d}\ln k)$	34(34)	33(33)	34(34)	34(34)	34(34)	32(34)	34(34)	33(33)	34(34)	34(34)	34(34)	33(34)
	$\sigma(f_{\rm NL})$	**42(145)**	8.3(10)	**31(45)**	**14(15)**	**19(319)**	**4.1(9.2)**	**569(1443)**	9.7(10)	**13(277)**	**2.0(2.7)**	**11(119)**	1.6(2.1)
	$10^3\,\sigma(\sigma_8)$	17(17)	7(8)	17(17)	15(16)	17(17)	12(14)	17(17)	11(13)	17(17)	13(16)	15(17)	11(15)
	$\mathrm{FoM}_{\rm cosmo}\ /\ 10^2$	109(88)	203(177)	112(106)	139(138)	128(77)	216(155)	69(60)	199(172)	132(79)	207(177)	139(90)	245(189)
	$\mathrm{FoM}_{\rm bias}\ /\ 10^2$	0.93(0.02)	759(563)	0.059(0.005)	33(32)	2.03(0.02)	108(49)	0.038(0.001)	45(39)	12(1.3)	132(83)	4.1(0.4)	172(92)

Este documento incorpora firma electrónica, y es copia auténtica de un documento electrónico archivado por la ULL según la Ley 39/2015.
Su autenticidad puede ser contrastada en la siguiente dirección https://sede.ull.es/validacion/

Identificador del documento: 3764923 Código de verificación: JHlWnlbn

Firmado por: JOSE RAMON BERMEJO CLIMENT — Fecha: 01/09/2021 17:41:12
UNIVERSIDAD DE LA LAGUNA

José Alberto Rubiño Martín — 01/09/2021 17:49:44
UNIVERSIDAD DE LA LAGUNA

FABIO FINELLI — 02/09/2021 14:12:21
UNIVERSIDAD DE LA LAGUNA

Universidad de La Laguna
Oficina de Sede Electrónica
Entrada
Nº registro: 2021/90989
Nº reg. oficina: OF002/2021/89977
Fecha: 03/09/2021 12:24:13

TABLE A.7— 68% marginalized constraints on the parameters of the exponential cut at large scales model of primordial features, obtained from the CMB and from the combination of each pair of CMB and galaxy surveys in their tomographic configurations. We show the constraints from the uncorrelated combination of Fisher matrices (CMB + GC), and the full combination including the CMB-GC cross-correlation (CMB × GC).

	Parameter	CMB	Euclid-ph		Euclid-sp		SKA1		SPHEREx	
			+ GC	× GC	+ GC	× GC	+ GC	× GC	+ GC	× GC
Planck	$10^5\ \sigma(\Omega_b h^2)$	17	11	11	12	12	13	11	12	12
	$10^4\ \sigma(\Omega_c h^2)$	15	3.6	3.3	7.9	6.8	8.6	4.0	7.0	6.0
	$\sigma(H_0)$	1.6	0.23	0.21	0.75	0.65	0.94	0.38	0.68	0.5
	$10^4\ \sigma(\tau)$	75	63	56	74	72	72	61	74	71
	$10^4\ \sigma(n_s)$	44	26	25	31	30	36	29	31	29
	$10^3\ \sigma(\ln(10^{10}A_s))$	15	12	10	14	14	14	11	14	13
	$\sigma(\lambda_c)$	5.1	5.0	4.2	5.1	4.9	5.1	2.7	5.1	4.6
	$10^2\ \sigma(\log_{10}k_c)$	16	14	12	14	14	16	9.4	14	13
	$\sigma(\Sigma m_\nu)$/meV	105	29	26	55	51	70	36	54	42
	$\sigma(\Delta z_{\rm re})$	6.3	1.3	0.28	2.0	0.78	5.8	4.5	0.68	0.45
	$10^3\ \sigma(s_0)$	-	26	17	52	41	23	9.6	93	67
LiteBIRD+SO	$10^5\ \sigma(\Omega_b h^2)$	14	4.3	4.3	4.5	4.5	12	4.2	4.4	4.4
	$10^4\ \sigma(\Omega_c h^2)$	10.0	2.0	1.9	4.8	4.7	7.4	3.5	4.8	4.2
	$\sigma(H_0)$	1.1	0.19	0.17	0.49	0.47	0.79	0.34	0.48	0.41
	$10^4\ \sigma(\tau)$	21	19	18	20	19	20	17	19	18
	$10^4\ \sigma(n_s)$	35	15	15	18	18	32	17	18	18
	$10^3\ \sigma(\ln(10^{10}A_s))$	4.6	3.7	3.5	4.1	4.0	4.4	3.4	4.0	3.8
	$\sigma(\lambda_c)$	4.3	4.3	3.8	4.3	4.2	4.3	2.3	4.3	4.0
	$10^2\ \sigma(\log_{10}k_c)$	11	10	9.0	11	10	11	7.4	10	9.9
	$\sigma(\Sigma m_\nu)$/meV	66	14	13	33	32	50	23	32	28
	$\sigma(\Delta z_{\rm re})$	1.5	0.92	0.24	1.2	0.64	1.1	0.15	0.57	0.39
	$10^3\ \sigma(s_0)$	-	26	16	52	35	23	12	92	69

Este documento incorpora firma electrónica, y es copia auténtica de un documento electrónico archivado por la ULL según la Ley 39/2015.
Su autenticidad puede ser contrastada en la siguiente dirección https://sede.ull.es/validacion/

Identificador del documento: 3764923 Código de verificación: JHlWnlbn

Firmado por: JOSE RAMON BERMEJO CLIMENT — Fecha: 01/09/2021 17:41:12
UNIVERSIDAD DE LA LAGUNA

José Alberto Rubiño Martín — 01/09/2021 17:49:44
UNIVERSIDAD DE LA LAGUNA

FABIO FINELLI — 02/09/2021 14:12:21
UNIVERSIDAD DE LA LAGUNA

Universidad de La Laguna
Oficina de Sede Electrónica
Entrada
Nº registro: 2021/90989
Nº reg. oficina: OF002/2021/89977
Fecha: 03/09/2021 12:24:13

TABLE A.8— 68% marginalized constraints on the parameters of the Starobinsky model of primordial features, obtained from the CMB and from the combination of each pair of CMB and galaxy surveys in their tomographic configurations. We show the constraints from the uncorrelated combination of Fisher matrices (CMB + GC), and the full combination including the CMB-GC cross-correlation (CMB × GC).

	Parameter	CMB	Euclid-ph		Euclid-sp		SKA1		SPHEREx	
			+ GC	× GC	+ GC	× GC	+ GC	× GC	+ GC	× GC
Planck	$10^5\ \sigma(\Omega_b h^2)$	17	11	11	12	12	13	11	12	11
	$10^4\ \sigma(\Omega_c h^2)$	15	3.4	3.2	6.6	6.1	8.6	4.1	7.1	5.1
	$\sigma(H_0)$	1.6	0.23	0.21	0.65	0.58	0.93	0.37	0.66	0.47
	$10^4\ \sigma(\tau)$	78	61	56	75	74	74	62	71	66
	$10^4\ \sigma(n_s)$	44	28	27	33	32	36	29	33	31
	$10^3\ \sigma(\ln(10^{10}A_s))$	15	11	10	14	14	14	11	13	12
	$10^3\ \sigma(\mathcal{A}_{\rm kink})$	45	40	38	39	39	37	34	41	40
	$10^2\ \sigma(\log_{10}k_{\rm kink})$	16	13	12	13	13	12	10	14	13
	$\sigma(\Sigma m_\nu)$/meV	104	28	26	53	48	69	35	50	41
	$\sigma(\Delta z_{\rm re})$	6.1	5.9	5.7	6.0	5.9	5.6	4.5	6.0	5.9
	$10^3\ \sigma(s_0)$	-	26	14	52	24	23	9.6	92	67
LiteBIRD+SO	$10^5\ \sigma(\Omega_b h^2)$	4.7	4.2	4.2	4.4	4.4	4.4	4.2	4.4	4.3
	$10^4\ \sigma(\Omega_c h^2)$	6.5	2.1	1.9	4.7	4.4	5.5	2.9	4.8	3.9
	$\sigma(H_0)$	0.65	0.19	0.16	0.46	0.43	0.55	0.28	0.47	0.38
	$10^4\ \sigma(\tau)$	22	21	19	22	21	22	18	22	20
	$10^4\ \sigma(n_s)$	19	15	15	17	18	18	16	18	18
	$10^3\ \sigma(\ln(10^{10}A_s))$	4.6	4.1	3.6	4.4	4.3	4.4	3.6	4.4	4.1
	$10^3\ \sigma(\mathcal{A}_{\rm kink})$	32	31	30	30	30	29	28	31	31
	$10^2\ \sigma(\log_{10}k_{\rm kink})$	9.8	9.0	8.4	9.1	9.1	8.4	8.0	9.2	9.1
	$\sigma(\Sigma m_\nu)$/meV	43	15	13	32	29	37	19	32	26
	$\sigma(\Delta z_{\rm re})$	1.6	1.5	1.1	1.5	1.5	1.5	1.0	1.6	1.3
	$10^3\ \sigma(s_0)$	-	26	13	52	20	23	8.5	92	68

Este documento incorpora firma electrónica, y es copia auténtica de un documento electrónico archivado por la ULL según la Ley 39/2015.
Su autenticidad puede ser contrastada en la siguiente dirección https://sede.ull.es/validacion/

Identificador del documento: 3764923 Código de verificación: JHlWnlbn

Firmado por: JOSE RAMON BERMEJO CLIMENT — Fecha: 01/09/2021 17:41:12
UNIVERSIDAD DE LA LAGUNA

José Alberto Rubiño Martín — 01/09/2021 17:49:44
UNIVERSIDAD DE LA LAGUNA

FABIO FINELLI — 02/09/2021 14:12:21
UNIVERSIDAD DE LA LAGUNA

Universidad de La Laguna
Oficina de Sede Electrónica
Entrada
Nº registro: 2021/90989
Nº reg. oficina: OF002/2021/89977
Fecha: 03/09/2021 12:24:13

TABLE A.9— 68% marginalized constraints on the parameters of the step in the inflaton potential model of primordial features, obtained from the CMB and from the combination of each pair of CMB and galaxy surveys in their tomographic configurations. We show the constraints from the uncorrelated combination of Fisher matrices (CMB + GC), and the full combination including the CMB-GC cross-correlation (CMB × GC).

	Parameter	CMB	Euclid-ph		Euclid-sp		SKA1		SPHEREx	
			+ GC	× GC	+ GC	× GC	+ GC	× GC	+ GC	× GC
Planck	$10^5\ \sigma(\Omega_b h^2)$	17	11	11	12	12	13	11	12	11
	$10^4\ \sigma(\Omega_c h^2)$	15	3.3	3.1	6.5	6.0	8.5	4.0	7.0	5.0
	$\sigma(H_0)$	1.6	0.23	0.21	0.65	0.57	0.92	0.37	0.66	0.47
	$10^4\ \sigma(\tau)$	69	56	52	67	66	65	56	64	59
	$10^4\ \sigma(n_s)$	44	27	27	32	31	35	29	33	31
	$10^3\ \sigma(\ln(10^{10}A_s))$	13	11	9.6	13	12	13	10	12	11
	$10^2\ \sigma(\mathcal{A}_{\rm st})$	34	32	27	33	33	22	19	31	29
	$10^3\ \sigma(\log_{10}k_{\rm st})$	50	42	38	46	45	27	24	43	42
	$10^2\ \sigma(\ln x_{\rm st})$	45	38	33	40	40	28	25	39	36
	$\sigma(\Sigma m_\nu)$/meV	102	27	24	50	46	66	34	49	40
	$\sigma(\Delta z_{\rm re})$	6.1	5.9	5.6	6.0	5.9	5.5	4.5	6.0	5.8
	$10^3\ \sigma(s_0)$	-	26	14	52	24	23	9.5	92	66
LiteBIRD+SO	$10^5\ \sigma(\Omega_b h^2)$	4.7	4.2	4.2	4.4	4.4	4.4	4.2	4.4	4.3
	$10^4\ \sigma(\Omega_c h^2)$	6.5	2.0	1.9	4.7	4.4	5.5	2.9	4.8	3.8
	$\sigma(H_0)$	0.65	0.18	0.16	0.46	0.43	0.55	0.28	0.47	0.37
	$10^4\ \sigma(\tau)$	19	19	17	19	19	19	17	19	18
	$10^4\ \sigma(n_s)$	19	15	15	18	18	19	16	18	18
	$10^3\ \sigma(\ln(10^{10}A_s))$	4.0	3.7	3.3	3.9	3.8	3.9	3.3	3.8	3.6
	$10^2\ \sigma(\mathcal{A}_{\rm st})$	17	16	15	16	16	14	13	16	16
	$10^3\ \sigma(\log_{10}k_{\rm st})$	22	21	21	21	22	18	17	21	21
	$10^2\ \sigma(\ln x_{\rm st})$	24	22	21	24	24	20	19	23	23
	$\sigma(\Sigma m_\nu)$/meV	43	14	12	31	29	37	19	32	25
	$\sigma(\Delta z_{\rm re})$	1.7	1.7	1.1	1.7	1.6	1.6	1.1	1.7	1.4
	$10^3\ \sigma(s_0)$	-	26	13	52	20	23	8.5	92	64

Este documento incorpora firma electrónica, y es copia auténtica de un documento electrónico archivado por la ULL según la Ley 39/2015.
Su autenticidad puede ser contrastada en la siguiente dirección https://sede.ull.es/validacion/

Identificador del documento: 3764923 Código de verificación: JHlWnlbn

Firmado por: JOSE RAMON BERMEJO CLIMENT — Fecha: 01/09/2021 17:41:12
UNIVERSIDAD DE LA LAGUNA

José Alberto Rubiño Martín — 01/09/2021 17:49:44
UNIVERSIDAD DE LA LAGUNA

FABIO FINELLI — 02/09/2021 14:12:21
UNIVERSIDAD DE LA LAGUNA

Universidad de La Laguna
Oficina de Sede Electrónica
Entrada
Nº registro: 2021/90989
Nº reg. oficina: OF002/2021/89977
Fecha: 03/09/2021 12:24:13

TABLE A.10— 68% marginalized constraints on the parameters of the logarithmic superimposed oscillations model of primordial features, obtained from the CMB and from the combination of each pair of CMB and galaxy surveys in their tomographic configurations. We show the constraints from the uncorrelated combination of Fisher matrices (CMB + GC), and the full combination including the CMB-GC cross-correlation (CMB × GC).

	Parameter	CMB	Euclid-ph		Euclid-sp		SKA1		SPHEREx	
			+ GC	× GC	+ GC	× GC	+ GC	× GC	+ GC	× GC
Planck	$10^5\ \sigma(\Omega_b h^2)$	17	11	11	12	12	13	11	12	11
	$10^4\ \sigma(\Omega_c h^2)$	15	3.3	3.1	6.5	5.9	8.7	4.0	7.1	5.0
	$\sigma(H_0)$	1.6	0.23	0.21	0.64	0.56	0.94	0.37	0.68	0.47
	$10^4\ \sigma(\tau)$	70	57	53	68	67	67	57	65	61
	$10^4\ \sigma(n_s)$	44	28	27	33	32	36	29	34	32
	$10^3\ \sigma(\ln(10^{10}A_s))$	14	11	9.6	13	13	13	11	12	11
	$10^4\ \sigma(\mathcal{A}_{\log})$	48	35	32	35	33	42	38	41	40
	$10^3\ \sigma(\log_{10}\omega_{\log})$	20	16	14	15	14	17	16	17	16
	$10^3\ \sigma(\phi_{\log}/2\pi)$	55	38	38	37	37	45	43	45	44
	$\sigma(\Sigma m_\nu)$/meV	103	27	25	51	45	68	34	49	40
	$\sigma(\Delta z_{\rm re})$	5.9	5.8	5.6	5.8	5.8	5.5	4.4	5.8	5.8
	$10^3\ \sigma(s_0)$	-	25	14	49	22	23	9.6	92	67
LiteBIRD+SO	$10^5\ \sigma(\Omega_b h^2)$	4.7	4.2	4.2	4.4	4.4	4.5	4.2	4.4	4.4
	$10^4\ \sigma(\Omega_c h^2)$	6.5	2.1	1.9	4.6	4.3	5.6	2.9	4.8	4.0
	$\sigma(H_0)$	0.65	0.19	0.16	0.46	0.42	0.55	0.28	0.48	0.38
	$10^4\ \sigma(\tau)$	19	19	17	19	19	19	16	19	18
	$10^4\ \sigma(n_s)$	19	15	15	17	18	19	16	18	18
	$10^3\ \sigma(\ln(10^{10}A_s))$	4.1	3.7	3.2	3.9	3.8	4.0	3.3	3.9	3.6
	$10^4\ \sigma(\mathcal{A}_{\log})$	18	17	17	17	17	18	18	18	18
	$10^3\ \sigma(\log_{10}\omega_{\log})$	11	9.3	9.3	9.0	9.0	9.8	9.8	9.9	9.9
	$10^3\ \sigma(\phi_{\log}/2\pi)$	35	30	30	29	29	32	32	33	33
	$\sigma(\Sigma m_\nu)$/meV	43	14	12	31	28	37	19	32	26
	$\sigma(\Delta z_{\rm re})$	1.5	1.5	1.0	1.5	1.4	1.5	0.99	1.5	1.2
	$10^3\ \sigma(s_0)$	-	25	13	49	19	23	8.5	92	68

Este documento incorpora firma electrónica, y es copia auténtica de un documento electrónico archivado por la ULL según la Ley 39/2015.
Su autenticidad puede ser contrastada en la siguiente dirección https://sede.ull.es/validacion/

Identificador del documento: 3764923 Código de verificación: JHlWnlbn

Firmado por: JOSE RAMON BERMEJO CLIMENT — Fecha: 01/09/2021 17:41:12
UNIVERSIDAD DE LA LAGUNA

José Alberto Rubiño Martín — 01/09/2021 17:49:44
UNIVERSIDAD DE LA LAGUNA

FABIO FINELLI — 02/09/2021 14:12:21
UNIVERSIDAD DE LA LAGUNA

Universidad de La Laguna
Oficina de Sede Electrónica
Entrada
Nº registro: 2021/90989
Nº reg. oficina: OF002/2021/89977
Fecha: 03/09/2021 12:24:13

Este documento incorpora firma electrónica, y es copia auténtica de un documento electrónico archivado por la ULL según la Ley 39/2015.
Su autenticidad puede ser contrastada en la siguiente dirección https://sede.ull.es/validacion/

Identificador del documento: 3764923 Código de verificación: JHlWnlbn

Firmado por:	JOSE RAMON BERMEJO CLIMENT *UNIVERSIDAD DE LA LAGUNA*	Fecha: 01/09/2021 17:41:12
	José Alberto Rubiño Martín *UNIVERSIDAD DE LA LAGUNA*	01/09/2021 17:49:44
	FABIO FINELLI *UNIVERSIDAD DE LA LAGUNA*	02/09/2021 14:12:21

Universidad de La Laguna
Oficina de Sede Electrónica
Entrada
Nº registro: 2021/90989
Nº reg. oficina: OF002/2021/89977
Fecha: 03/09/2021 12:24:13

Publication list

The following articles, all of then leaded or co-authored by J. R. Bermejo-Climent, have been prepared during this thesis. They contain some of the results described in this thesis.

- **J. R. Bermejo-Climent**, M. Ballardini, F. Finelli and V. F. Cardone, "Measuring lensing ratios with future cosmological surveys," Phys. Rev. D **102**, no.2, 023502 (2020) doi:10.1103/PhysRevD.102.023502 [arXiv:1911.11766 [astro-ph.CO]].
- **J. R. Bermejo-Climent**, M. Ballardini, F. Finelli, D. Paoletti, R. Maartens, J. A. Rubiño-Martín and L. Valenziano, "Cosmological parameter forecasts by a joint 2D tomographic approach to CMB and galaxy clustering," Phys. Rev. D **103**, no.10, 103502 (2021) doi:10.1103/PhysRevD.103.103502 [arXiv:2106.05267 [astro-ph.CO]].
- **J. R. Bermejo-Climent**, M. Ballardini, F. Finelli and L. Moscardini, "Probing primordial features with 2D angular tomography of the CMB and future galaxy surveys," in preparation.
- S. Ilić, N. Aghanim, C. Baccigalupi, **J. R. Bermejo-Climent** *et al.* [Euclid], "*Euclid* preparation: XV. Forecasting cosmological constraints for the *Euclid* and CMB joint analysis," (2021) [arXiv:2106.08346 [astro-ph.CO]].
- J. Delabrouille *et al.* "Microwave Spectro-Polarimetry of Matter and Radiation across Space and Time," (2019) [arXiv:1909.01591 [astro-ph.CO]].

Este documento incorpora firma electrónica, y es copia auténtica de un documento electrónico archivado por la ULL según la Ley 39/2015.
Su autenticidad puede ser contrastada en la siguiente dirección https://sede.ull.es/validacion/

Identificador del documento: 3764923 Código de verificación: JHlWnlbn

Firmado por:	JOSE RAMON BERMEJO CLIMENT *UNIVERSIDAD DE LA LAGUNA*	Fecha: 01/09/2021 17:41:12
	José Alberto Rubiño Martín *UNIVERSIDAD DE LA LAGUNA*	01/09/2021 17:49:44
	FABIO FINELLI *UNIVERSIDAD DE LA LAGUNA*	02/09/2021 14:12:21

Universidad de La Laguna
Oficina de Sede Electrónica
Entrada
Nº registro: 2021/90989
Nº reg. oficina: OF002/2021/89977
Fecha: 03/09/2021 12:24:13

Este documento incorpora firma electrónica, y es copia auténtica de un documento electrónico archivado por la ULL según la Ley 39/2015.
Su autenticidad puede ser contrastada en la siguiente dirección https://sede.ull.es/validacion/

Identificador del documento: 3764923 Código de verificación: JHlWnlbn

Firmado por:	JOSE RAMON BERMEJO CLIMENT *UNIVERSIDAD DE LA LAGUNA*	Fecha: 01/09/2021 17:41:12
	José Alberto Rubiño Martín *UNIVERSIDAD DE LA LAGUNA*	01/09/2021 17:49:44
	FABIO FINELLI *UNIVERSIDAD DE LA LAGUNA*	02/09/2021 14:12:21

Universidad de La Laguna
Oficina de Sede Electrónica
Entrada
Nº registro: 2021/90989
Nº reg. oficina: OF002/2021/89977
Fecha: 03/09/2021 12:24:13

Bibliography

[1] G. Gamow, "Expanding universe and the origin of elements," Phys. Rev. **70**, 572-573 (1946) doi:10.1103/PhysRev7.0.572

[2] R. A. Alpher, H. Bethe and G. Gamow, "The origin of chemical elements," Phys. Rev. **73**, 803-804 (1948) doi:10.1103/PhysRev.73.803

[3] E. Hubble, "A relation between distance and radial velocity among extra-galactic nebulae," Proc. Nat. Acad. Sci. **15**, 168-173 (1929) doi:10.1073/pnas.15.3.168

[4] R. A. Alpher and R. C. Herman, "Remarks on the Evolution of the Expanding Universe," Phys. Rev. **75**, no.7, 1089-1095 (1949) doi:10.1103/physrev.75.1089

[5] A. A. Penzias and R. W. Wilson, "A Measurement of excess antenna temperature at 4080-Mc/s," Astrophys. J. **142**, 419-421 (1965) doi:10.1086/148307

[6] A. G. Riess *et al.* [Supernova Search Team], "Observational evidence from supernovae for an accelerating universe and a cosmological constant," Astron. J. **116**, 1009-1038 (1998) doi:10.1086/300499 [arXiv:astro-ph/9805201 [astro-ph]].

[7] S. Perlmutter *et al.* [Supernova Cosmology Project], "Measurements of Ω and Λ from 42 high redshift supernovae," Astrophys. J. **517**, 565-586 (1999) doi:10.1086/307221 [arXiv:astro-ph/9812133 [astro-ph]].

[8] D. N. Spergel *et al.* [WMAP], "First year Wilkinson Microwave Anisotropy Probe (WMAP) observations: Determination of cosmological parameters," Astrophys. J. Suppl. **148**, 175-194 (2003) doi:10.1086/377226 [arXiv:astro-ph/0302209 [astro-ph]].

Este documento incorpora firma electrónica, y es copia auténtica de un documento electrónico archivado por la ULL según la Ley 39/2015.
Su autenticidad puede ser contrastada en la siguiente dirección https://sede.ull.es/validacion/

Identificador del documento: 3764923 Código de verificación: JHlWnlbn

Firmado por:	JOSE RAMON BERMEJO CLIMENT *UNIVERSIDAD DE LA LAGUNA*	Fecha: 01/09/2021 17:41:12
	José Alberto Rubiño Martín *UNIVERSIDAD DE LA LAGUNA*	01/09/2021 17:49:44
	FABIO FINELLI *UNIVERSIDAD DE LA LAGUNA*	02/09/2021 14:12:21

Universidad de La Laguna
Oficina de Sede Electrónica
Entrada
Nº registro: 2021/90989
Nº reg. oficina: OF002/2021/89977
Fecha: 03/09/2021 12:24:13

[9] P. A. R. Ade *et al.* [Planck], "Planck 2013 results. XVI. Cosmological parameters," Astron. Astrophys. **571**, A16 (2014) doi:10.1051/0004-6361/201321591 [arXiv:1303.5076 [astro-ph.CO]].

[10] P. A. R. Ade *et al.* [Planck], "Planck 2015 results. XIII. Cosmological parameters," Astron. Astrophys. **594**, A13 (2016) doi:10.1051/0004-6361/201525830 [arXiv:1502.01589 [astro-ph.CO]].

[11] N. Aghanim *et al.* [Planck], "Planck 2018 results. VI. Cosmological parameters," Astron. Astrophys. **641**, A6 (2020) doi:10.1051/0004-6361/201833910 [arXiv:1807.06209 [astro-ph.CO]].

[12] D. J. Eisenstein *et al.* [SDSS], "Detection of the Baryon Acoustic Peak in the Large-Scale Correlation Function of SDSS Luminous Red Galaxies," Astrophys. J. **633**, 560-574 (2005) doi:10.1086/466512 [arXiv:astro-ph/0501171 [astro-ph]].

[13] H. P. Robertson, "Kinematics and World-Structure," Astrophys. J. **82**, 284-301 (1935) doi:10.1086/143681

[14] H. P. Robertson, "Kinematics and World-Structure. 2," Astrophys. J. **83**, 187-201 (1935) doi:10.1086/143716

[15] H. P. Robertson, "Kinematics and World-Structure. 3," Astrophys. J. **83**, 257-271 (1936) doi:10.1086/143726

[16] A. Einstein, "Cosmological Considerations in the General Theory of Relativity," Sitzungsber. Preuss. Akad. Wiss. Berlin (Math. Phys.) **1917**, 142-152 (1917)

[17] A. Friedman, "On the Curvature of space," Z. Phys. **10**, 377-386 (1922) doi:10.1007/BF01332580

[18] G. Lemaitre, "A Homogeneous Universe of Constant Mass and Growing Radius Accounting for the Radial Velocity of Extragalactic Nebulae," Annales Soc. Sci. Bruxelles A **47**, 49-59 (1927) doi:10.1007/s10714-013-1548-3

[19] A. H. Guth, "The Inflationary Universe: A Possible Solution to the Horizon and Flatness Problems," Phys. Rev. D **23**, 347-356 (1981) doi:10.1103/PhysRevD.23.347

Este documento incorpora firma electrónica, y es copia auténtica de un documento electrónico archivado por la ULL según la Ley 39/2015.
Su autenticidad puede ser contrastada en la siguiente dirección https://sede.ull.es/validacion/

Identificador del documento: 3764923 Código de verificación: JHlWnlbn

Firmado por:	JOSE RAMON BERMEJO CLIMENT *UNIVERSIDAD DE LA LAGUNA*	Fecha: 01/09/2021 17:41:12
	José Alberto Rubiño Martín *UNIVERSIDAD DE LA LAGUNA*	01/09/2021 17:49:44
	FABIO FINELLI *UNIVERSIDAD DE LA LAGUNA*	02/09/2021 14:12:21

Universidad de La Laguna
Oficina de Sede Electrónica
Entrada
Nº registro: 2021/90989
Nº reg. oficina: OF002/2021/89977
Fecha: 03/09/2021 12:24:13

[20] A. A. Starobinsky, "A New Type of Isotropic Cosmological Models Without Singularity," Phys. Lett. B **91**, 99-102 (1980) doi:10.1016/0370-2693(80)90670-X

[21] A. A. Starobinsky, "Dynamics of Phase Transition in the New Inflationary Universe Scenario and Generation of Perturbations," Phys. Lett. B **117**, 175-178 (1982) doi:10.1016/0370-2693(82)90541-X

[22] A. H. Guth and S. Y. Pi, "The Quantum Mechanics of the Scalar Field in the New Inflationary Universe," Phys. Rev. D **32**, 1899-1920 (1985) doi:10.1103/PhysRevD.32.1899

[23] J. M. Bardeen, P. J. Steinhardt and M. S. Turner, "Spontaneous Creation of Almost Scale - Free Density Perturbations in an Inflationary Universe," Phys. Rev. D **28**, 679 (1983) doi:10.1103/PhysRevD.28.679

[24] D. Langlois, "Lectures on inflation and cosmological perturbations," Lect. Notes Phys. **800**, 1-57 (2010) doi:10.1007/978-3-642-10598-2_1 [arXiv:1001.5259 [astro-ph.CO]].

[25] D. H. Lyth and A. R. Liddle, "The primordial density perturbation: Cosmology, inflation and the origin of structure" (2009).

[26] A. G. Riess, S. Casertano, W. Yuan, L. M. Macri and D. Scolnic, "Large Magellanic Cloud Cepheid Standards Provide a 1% Foundation for the Determination of the Hubble Constant and Stronger Evidence for Physics beyond ΛCDM," Astrophys. J. **876**, no.1, 85 (2019) doi:10.3847/1538-4357/ab1422 [arXiv:1903.07603 [astro-ph.CO]].

[27] M. J. Reid, D. W. Pesce and A. G. Riess, "An Improved Distance to NGC 4258 and its Implications for the Hubble Constant," Astrophys. J. Lett. **886**, no.2, L27 (2019) doi:10.3847/2041-8213/ab552d [arXiv:1908.05625 [astro-ph.GA]].

[28] K. C. Wong, S. H. Suyu, G. C. F. Chen, C. E. Rusu, M. Millon, D. Sluse, V. Bonvin, C. D. Fassnacht, S. Taubenberger and M. W. Auger, *et al.* "H0LiCOW – XIII. A 2.4 per cent measurement of H0 from lensed quasars: 5.3σ tension between early- and late-Universe probes," Mon. Not. Roy. Astron. Soc. **498**, no.1, 1420-1439 (2020) doi:10.1093/mnras/stz3094 [arXiv:1907.04869 [astro-ph.CO]].

Este documento incorpora firma electrónica, y es copia auténtica de un documento electrónico archivado por la ULL según la Ley 39/2015.
Su autenticidad puede ser contrastada en la siguiente dirección https://sede.ull.es/validacion/

Identificador del documento: 3764923 Código de verificación: JHlWnlbn

Firmado por:	JOSE RAMON BERMEJO CLIMENT *UNIVERSIDAD DE LA LAGUNA*	Fecha: 01/09/2021 17:41:12
	José Alberto Rubiño Martín *UNIVERSIDAD DE LA LAGUNA*	01/09/2021 17:49:44
	FABIO FINELLI *UNIVERSIDAD DE LA LAGUNA*	02/09/2021 14:12:21

Universidad de La Laguna
Oficina de Sede Electrónica
Entrada
Nº registro: 2021/90989
Nº reg. oficina: OF002/2021/89977
Fecha: 03/09/2021 12:24:13

[29] T. M. C. Abbott *et al.* [DES], "Dark Energy Survey Year 1 Results: A Precise H0 Estimate from DES Y1, BAO, and D/H Data," Mon. Not. Roy. Astron. Soc. **480**, no.3, 3879-3888 (2018) doi:10.1093/mnras/sty1939 [arXiv:1711.00403 [astro-ph.CO]].

[30] A. Cuceu, J. Farr, P. Lemos and A. Font-Ribera, "Baryon Acoustic Oscillations and the Hubble Constant: Past, Present and Future," JCAP **10**, 044 (2019) doi:10.1088/1475-7516/2019/10/044 [arXiv:1906.11628 [astro-ph.CO]].

[31] N. Schöneberg, J. Lesgourgues and D. C. Hooper, "The BAO+BBN take on the Hubble tension," JCAP **10**, 029 (2019) doi:10.1088/1475-7516/2019/10/029 [arXiv:1907.11594 [astro-ph.CO]].

[32] M. M. Ivanov, M. Simonović and M. Zaldarriaga, "Cosmological Parameters from the BOSS Galaxy Power Spectrum," JCAP **05**, 042 (2020) doi:10.1088/1475-7516/2020/05/042 [arXiv:1909.05277 [astro-ph.CO]].

[33] T. Colas, G. D'amico, L. Senatore, P. Zhang and F. Beutler, "Efficient Cosmological Analysis of the SDSS/BOSS data from the Effective Field Theory of Large-Scale Structure," JCAP **06**, 001 (2020) doi:10.1088/1475-7516/2020/06/001 [arXiv:1909.07951 [astro-ph.CO]].

[34] O. H. E. Philcox, M. M. Ivanov, M. Simonović and M. Zaldarriaga, "Combining Full-Shape and BAO Analyses of Galaxy Power Spectra: A 1.6\% CMB-independent constraint on H_0," JCAP **05**, 032 (2020) doi:10.1088/1475-7516/2020/05/032 [arXiv:2002.04035 [astro-ph.CO]].

[35] É. Aubourg, S. Bailey, J. E. Bautista, F. Beutler, V. Bhardwaj, D. Bizyaev, M. Blanton, M. Blomqvist, A. S. Bolton and J. Bovy, *et al.* "Cosmological implications of baryon acoustic oscillation measurements," Phys. Rev. D **92**, no.12, 123516 (2015) doi:10.1103/PhysRevD.92.123516 [arXiv:1411.1074 [astro-ph.CO]].

[36] P. Lemos, E. Lee, G. Efstathiou and S. Gratton, "Model independent $H(z)$ reconstruction using the cosmic inverse distance ladder," Mon. Not. Roy. Astron. Soc. **483**, no.4, 4803-4810 (2019) doi:10.1093/mnras/sty3082 [arXiv:1806.06781 [astro-ph.CO]].

Este documento incorpora firma electrónica, y es copia auténtica de un documento electrónico archivado por la ULL según la Ley 39/2015.
Su autenticidad puede ser contrastada en la siguiente dirección https://sede.ull.es/validacion/

Identificador del documento: 3764923 Código de verificación: JHlWnlbn

Firmado por: JOSE RAMON BERMEJO CLIMENT — Fecha: 01/09/2021 17:41:12
UNIVERSIDAD DE LA LAGUNA

José Alberto Rubiño Martín — 01/09/2021 17:49:44
UNIVERSIDAD DE LA LAGUNA

FABIO FINELLI — 02/09/2021 14:12:21
UNIVERSIDAD DE LA LAGUNA

Universidad de La Laguna
Oficina de Sede Electrónica
Entrada
Nº registro: 2021/90989
Nº reg. oficina: OF002/2021/89977
Fecha: 03/09/2021 12:24:13

[37] W. L. Freedman, "Cosmology at a Crossroads," Nature Astron. **1**, 0121 (2017) doi:10.1038/s41550-017-0121 [arXiv:1706.02739 [astro-ph.CO]].

[38] L. F. Secco *et al.* [DES], "Dark Energy Survey Year 3 Results: Cosmology from Cosmic Shear and Robustness to Modeling Uncertainty," [arXiv:2105.13544 [astro-ph.CO]].

[39] J. C. Mather, E. S. Cheng, R. A. Shafer, C. L. Bennett, N. W. Boggess, E. Dwek, M. G. Hauser, T. Kelsall, S. H. Moseley, Jr. and R. F. Silverberg, *et al.* "A Preliminary measurement of the Cosmic Microwave Background spectrum by the Cosmic Background Explorer (COBE) satellite," Astrophys. J. Lett. **354**, L37-L40 (1990) doi:10.1086/185717

[40] D. N. Spergel *et al.* [WMAP], "Wilkinson Microwave Anisotropy Probe (WMAP) three year results: implications for cosmology," Astrophys. J. Suppl. **170**, 377 (2007) doi:10.1086/513700 [arXiv:astro-ph/0603449 [astro-ph]].

[41] E. Komatsu *et al.* [WMAP], "Five-Year Wilkinson Microwave Anisotropy Probe (WMAP) Observations: Cosmological Interpretation," Astrophys. J. Suppl. **180**, 330-376 (2009) doi:10.1088/0067-0049/180/2/330 [arXiv:0803.0547 [astro-ph]].

[42] E. Komatsu *et al.* [WMAP], "Seven-Year Wilkinson Microwave Anisotropy Probe (WMAP) Observations: Cosmological Interpretation," Astrophys. J. Suppl. **192**, 18 (2011) doi:10.1088/0067-0049/192/2/18 [arXiv:1001.4538 [astro-ph.CO]].

[43] G. Hinshaw *et al.* [WMAP], "Nine-Year Wilkinson Microwave Anisotropy Probe (WMAP) Observations: Cosmological Parameter Results," Astrophys. J. Suppl. **208**, 19 (2013) doi:10.1088/0067-0049/208/2/19 [arXiv:1212.5226 [astro-ph.CO]].

[44] P. A. R. Ade *et al.* [Planck], "Planck 2013 results. XVI. Cosmological parameters," Astron. Astrophys. **571**, A16 (2014) doi:10.1051/0004-6361/201321591 [arXiv:1303.5076 [astro-ph.CO]].

[45] P. A. R. Ade *et al.* [Planck], "Planck 2015 results. XIII. Cosmological parameters," Astron. Astrophys. **594**, A13 (2016) doi:10.1051/0004-6361/201525830 [arXiv:1502.01589 [astro-ph.CO]].

Este documento incorpora firma electrónica, y es copia auténtica de un documento electrónico archivado por la ULL según la Ley 39/2015.
Su autenticidad puede ser contrastada en la siguiente dirección https://sede.ull.es/validacion/

Identificador del documento: 3764923 Código de verificación: JHlWnlbn

Firmado por: JOSE RAMON BERMEJO CLIMENT — Fecha: 01/09/2021 17:41:12
UNIVERSIDAD DE LA LAGUNA

José Alberto Rubiño Martín — 01/09/2021 17:49:44
UNIVERSIDAD DE LA LAGUNA

FABIO FINELLI — 02/09/2021 14:12:21
UNIVERSIDAD DE LA LAGUNA

Universidad de La Laguna
Oficina de Sede Electrónica
Entrada
Nº registro: 2021/90989
Nº reg. oficina: OF002/2021/89977
Fecha: 03/09/2021 12:24:13

[46] N. Aghanim *et al.* [Planck], "Planck 2018 results. VI. Cosmological parameters," Astron. Astrophys. **641**, A6 (2020) doi:10.1051/0004-6361/201833910 [arXiv:1807.06209 [astro-ph.CO]].

[47] U. Seljak and M. Zaldarriaga, "A Line of sight integration approach to cosmic microwave background anisotropies," Astrophys. J. **469**, 437-444 (1996) doi:10.1086/177793 [arXiv:astro-ph/9603033 [astro-ph]].

[48] W. Hu and M. J. White, "A CMB polarization primer," New Astron. **2**, 323 (1997) doi:10.1016/S1384-1076(97)00022-5 [arXiv:astro-ph/9706147 [astro-ph]].

[49] K. Tomita and K. Watanabe, "Gravitational Lens Effect on the Cosmic Background Radiation Due to Nonlinear Inhomogeneities," Prog. Theor. Phys. **82**, 563 (1989) doi:10.1143/PTP.82.563

[50] F. Bernardeau, "Weak lensing detection in CMB maps," Astron. Astrophys. **324**, 15-26 (1997) [arXiv:astro-ph/9611012 [astro-ph]].

[51] M. Zaldarriaga and U. Seljak, "Gravitational lensing effect on cosmic microwave background polarization," Phys. Rev. D **58**, 023003 (1998) doi:10.1103/PhysRevD.58.023003 [arXiv:astro-ph/9803150 [astro-ph]].

[52] C. M. Hirata and U. Seljak, "Reconstruction of lensing from the cosmic microwave background polarization," Phys. Rev. D **68**, 083002 (2003) doi:10.1103/PhysRevD.68.083002 [arXiv:astro-ph/0306354 [astro-ph]].

[53] A. Lewis and A. Challinor, "Weak gravitational lensing of the CMB," Phys. Rept. **429**, 1-65 (2006) doi:10.1016/j.physrep.2006.03.002 [arXiv:astro-ph/0601594 [astro-ph]].

[54] R. Ahumada *et al.* [SDSS-IV], "The 16th Data Release of the Sloan Digital Sky Surveys: First Release from the APOGEE-2 Southern Survey and Full Release of eBOSS Spectra," Astrophys. J. Suppl. **249**, no.1, 3 (2020) doi:10.3847/1538-4365/ab929e [arXiv:1912.02905 [astro-ph.GA]].

[55] J. DeRose *et al.* [DES], "Dark Energy Survey Year 3 results: cosmology from combined galaxy clustering and lensing – validation on cosmological simulations," [arXiv:2105.13547 [astro-ph.CO]].

Este documento incorpora firma electrónica, y es copia auténtica de un documento electrónico archivado por la ULL según la Ley 39/2015.
Su autenticidad puede ser contrastada en la siguiente dirección https://sede.ull.es/validacion/

Identificador del documento: 3764923 Código de verificación: JHlWnlbn

Firmado por: JOSE RAMON BERMEJO CLIMENT — Fecha: 01/09/2021 17:41:12
UNIVERSIDAD DE LA LAGUNA

José Alberto Rubiño Martín — 01/09/2021 17:49:44
UNIVERSIDAD DE LA LAGUNA

FABIO FINELLI — 02/09/2021 14:12:21
UNIVERSIDAD DE LA LAGUNA

Universidad de La Laguna
Oficina de Sede Electrónica
Entrada
Nº registro: 2021/90989
Nº reg. oficina: OF002/2021/89977
Fecha: 03/09/2021 12:24:13

[56] A. Aghamousa *et al.* [DESI], "The DESI Experiment Part I: Science,Targeting, and Survey Design," [arXiv:1611.00036 [astro-ph.IM]].

[57] A. Challinor and A. Lewis, "The linear power spectrum of observed source number counts," Phys. Rev. D **84**, 043516 (2011) doi:10.1103/PhysRevD.84.043516 [arXiv:1105.5292 [astro-ph.CO]].

[58] C. Duncan, B. Joachimi, A. Heavens, C. Heymans and H. Hildebrandt, "On the complementarity of galaxy clustering with cosmic shear and flux magnification," Mon. Not. Roy. Astron. Soc. **437**, no.3, 2471-2487 (2014) doi:10.1093/mnras/stt2060 [arXiv:1306.6870 [astro-ph.CO]].

[59] S. Camera, M. G. Santos and R. Maartens, "Probing primordial non-Gaussianity with SKA galaxy redshift surveys: a fully relativistic analysis," Mon. Not. Roy. Astron. Soc. **448**, no.2, 1035-1043 (2015) [erratum: Mon. Not. Roy. Astron. Soc. **467**, no.2, 1505-1506 (2017)] doi:10.1093/mnras/stv040 [arXiv:1409.8286 [astro-ph.CO]].

[60] W. Cardona, R. Durrer, M. Kunz and F. Montanari, "Lensing convergence and the neutrino mass scale in galaxy redshift surveys," Phys. Rev. D **94**, no.4, 043007 (2016) doi:10.1103/PhysRevD.94.043007 [arXiv:1603.06481 [astro-ph.CO]].

[61] C. S. Lorenz, D. Alonso and P. G. Ferreira, "Impact of relativistic effects on cosmological parameter estimation," Phys. Rev. D **97**, no.2, 023537 (2018) doi:10.1103/PhysRevD.97.023537 [arXiv:1710.02477 [astro-ph.CO]].

[62] M. Ballardini and R. Maartens, "Measuring ISW with next-generation radio surveys," Mon. Not. Roy. Astron. Soc. **485**, 1339 (2019) doi:10.1093/mnras/stz480 [arXiv:1812.01636 [astro-ph.CO]].

[63] K. Tanidis, S. Camera and D. Parkinson, "Developing a unified pipeline for large-scale structure data analysis with angular power spectra – II. A case study for magnification bias and radio continuum surveys," Mon. Not. Roy. Astron. Soc. **491**, no.4, 4869-4883 (2020) doi:10.1093/mnras/stz3394 [arXiv:1909.10539 [astro-ph.CO]].

[64] J. R. Bermejo-Climent, M. Ballardini, F. Finelli and V. F. Cardone, "Measuring lensing ratios with future cosmological surveys," Phys.

Este documento incorpora firma electrónica, y es copia auténtica de un documento electrónico archivado por la ULL según la Ley 39/2015.
Su autenticidad puede ser contrastada en la siguiente dirección https://sede.ull.es/validacion/

Identificador del documento: 3764923 Código de verificación: JHlWnlbn

Firmado por:	JOSE RAMON BERMEJO CLIMENT *UNIVERSIDAD DE LA LAGUNA*	Fecha: 01/09/2021 17:41:12
	José Alberto Rubiño Martín *UNIVERSIDAD DE LA LAGUNA*	01/09/2021 17:49:44
	FABIO FINELLI *UNIVERSIDAD DE LA LAGUNA*	02/09/2021 14:12:21

Universidad de La Laguna
Oficina de Sede Electrónica
Entrada
Nº registro: 2021/90989
Nº reg. oficina: OF002/2021/89977
Fecha: 03/09/2021 12:24:13

Rev. D **102**, no.2, 023502 (2020) doi:10.1103/PhysRevD.102.023502 [arXiv:1911.11766 [astro-ph.CO]].

[65] B. Jain and U. Seljak, "Cosmological model predictions for weak lensing: Linear and nonlinear regimes," Astrophys. J. **484**, 560 (1997) doi:10.1086/304372 [arXiv:astro-ph/9611077 [astro-ph]].

[66] S. Bird, M. Viel and M. G. Haehnelt, "Massive Neutrinos and the Non-linear Matter Power Spectrum," Mon. Not. Roy. Astron. Soc. **420**, 2551-2561 (2012) doi:10.1111/j.1365-2966.2011.20222.x [arXiv:1109.4416 [astro-ph.CO]].

[67] R. Takahashi, M. Sato, T. Nishimichi, A. Taruya and M. Oguri, "Revising the Halofit Model for the Nonlinear Matter Power Spectrum," Astrophys. J. **761**, 152 (2012) doi:10.1088/0004-637X/761/2/152 [arXiv:1208.2701 [astro-ph.CO]].

[68] B. Jain and U. Seljak, "Cosmological model predictions for weak lensing: Linear and nonlinear regimes," Astrophys. J. **484**, 560 (1997) doi:10.1086/304372 [arXiv:astro-ph/9611077 [astro-ph]].

[69] A. Challinor and A. Lewis, "The linear power spectrum of observed source number counts," Phys. Rev. D **84**, 043516 (2011) doi:10.1103/PhysRevD.84.043516 [arXiv:1105.5292 [astro-ph.CO]].

[70] C. Duncan, B. Joachimi, A. Heavens, C. Heymans and H. Hildebrandt, "On the complementarity of galaxy clustering with cosmic shear and flux magnification," Mon. Not. Roy. Astron. Soc. **437**, no.3, 2471-2487 (2014) doi:10.1093/mnras/stt2060 [arXiv:1306.6870 [astro-ph.CO]].

[71] S. Camera, M. G. Santos and R. Maartens, "Probing primordial non-Gaussianity with SKA galaxy redshift surveys: a fully relativistic analysis," Mon. Not. Roy. Astron. Soc. **448**, no.2, 1035-1043 (2015) [erratum: Mon. Not. Roy. Astron. Soc. **467**, no.2, 1505-1506 (2017)] doi:10.1093/mnras/stv040 [arXiv:1409.8286 [astro-ph.CO]].

[72] W. Cardona, R. Durrer, M. Kunz and F. Montanari, "Lensing convergence and the neutrino mass scale in galaxy redshift surveys," Phys. Rev. D **94**, no.4, 043007 (2016) doi:10.1103/PhysRevD.94.043007 [arXiv:1603.06481 [astro-ph.CO]].

Este documento incorpora firma electrónica, y es copia auténtica de un documento electrónico archivado por la ULL según la Ley 39/2015.
Su autenticidad puede ser contrastada en la siguiente dirección https://sede.ull.es/validacion/

Identificador del documento: 3764923 Código de verificación: JHlWnlbn

Firmado por:	JOSE RAMON BERMEJO CLIMENT *UNIVERSIDAD DE LA LAGUNA*	Fecha: 01/09/2021 17:41:12
	José Alberto Rubiño Martín *UNIVERSIDAD DE LA LAGUNA*	01/09/2021 17:49:44
	FABIO FINELLI *UNIVERSIDAD DE LA LAGUNA*	02/09/2021 14:12:21

Universidad de La Laguna
Oficina de Sede Electrónica
Entrada
Nº registro: 2021/90989
Nº reg. oficina: OF002/2021/89977
Fecha: 03/09/2021 12:24:13

[73] C. S. Lorenz, D. Alonso and P. G. Ferreira, "Impact of relativistic effects on cosmological parameter estimation," Phys. Rev. D **97**, no.2, 023537 (2018) doi:10.1103/PhysRevD.97.023537 [arXiv:1710.02477 [astro-ph.CO]].

[74] M. Ballardini and R. Maartens, "Measuring ISW with next-generation radio surveys," Mon. Not. Roy. Astron. Soc. **485**, 1339 (2019) doi:10.1093/mnras/stz480 [arXiv:1812.01636 [astro-ph.CO]].

[75] K. Tanidis, S. Camera and D. Parkinson, "Developing a unified pipeline for large-scale structure data analysis with angular power spectra – II. A case study for magnification bias and radio continuum surveys," Mon. Not. Roy. Astron. Soc. **491**, no.4, 4869-4883 (2020) doi:10.1093/mnras/stz3394 [arXiv:1909.10539 [astro-ph.CO]].

[76] B. Jain and U. Seljak, "Cosmological model predictions for weak lensing: Linear and nonlinear regimes," Astrophys. J. **484**, 560 (1997) doi:10.1086/304372 [arXiv:astro-ph/9611077 [astro-ph]].

[77] S. Bird, M. Viel and M. G. Haehnelt, "Massive Neutrinos and the Non-linear Matter Power Spectrum," Mon. Not. Roy. Astron. Soc. **420**, 2551-2561 (2012) doi:10.1111/j.1365-2966.2011.20222.x [arXiv:1109.4416 [astro-ph.CO]].

[78] J. R. Bermejo-Climent, M. Ballardini, F. Finelli, D. Paoletti, R. Maartens, J. A. Rubiño-Martín and L. Valenziano, "Cosmological parameter forecasts by a joint 2D tomographic approach to CMB and galaxy clustering," Phys. Rev. D **103**, no.10, 103502 (2021) doi:10.1103/PhysRevD.103.103502 [arXiv:2106.05267 [astro-ph.CO]].

[79] P. Ade *et al.* [Simons Observatory], "The Simons Observatory: Science goals and forecasts," JCAP **02**, 056 (2019) doi:10.1088/1475-7516/2019/02/056 [arXiv:1808.07445 [astro-ph.CO]].

[80] K. N. Abazajian *et al.* [CMB-S4], "CMB-S4 Science Book, First Edition," [arXiv:1610.02743 [astro-ph.CO]].

[81] M. Hazumi, P. A. R. Ade, Y. Akiba, D. Alonso, K. Arnold, J. Aumont, C. Baccigalupi, D. Barron, S. Basak and S. Beckman, *et al.* "LiteBIRD: A Satellite for the Studies of B-Mode Polarization and Inflation from Cosmic Background Radiation Detection," J. Low Temp. Phys. **194**, no.5-6, 443-452 (2019) doi:10.1007/s10909-019-02150-5

Este documento incorpora firma electrónica, y es copia auténtica de un documento electrónico archivado por la ULL según la Ley 39/2015.
Su autenticidad puede ser contrastada en la siguiente dirección https://sede.ull.es/validacion/

Identificador del documento: 3764923 Código de verificación: JHlWnlbn

Firmado por: JOSE RAMON BERMEJO CLIMENT — Fecha: 01/09/2021 17:41:12
UNIVERSIDAD DE LA LAGUNA

José Alberto Rubiño Martín — 01/09/2021 17:49:44
UNIVERSIDAD DE LA LAGUNA

FABIO FINELLI — 02/09/2021 14:12:21
UNIVERSIDAD DE LA LAGUNA

Universidad de La Laguna
Oficina de Sede Electrónica
Entrada
Nº registro: 2021/90989
Nº reg. oficina: OF002/2021/89977
Fecha: 03/09/2021 12:24:13

[82] H. Sugai, P. A. R. Ade, Y. Akiba, D. Alonso, K. Arnold, J. Aumont, J. Austermann, C. Baccigalupi, A. J. Banday and R. Banerji, *et al.* "Updated Design of the CMB Polarization Experiment Satellite LiteBIRD," J. Low. Temp. Phys. **199**, no.3-4, 1107-1117 (2020) doi:10.1007/s10909-019-02329-w [arXiv:2001.01724 [astro-ph.IM]].

[83] L. Knox, "Determination of inflationary observables by cosmic microwave background anisotropy experiments," Phys. Rev. D **52**, 4307-4318 (1995) doi:10.1103/PhysRevD.52.4307 [arXiv:astro-ph/9504054 [astro-ph]].

[84] T. Okamoto and W. Hu, "CMB lensing reconstruction on the full sky," Phys. Rev. D **67**, 083002 (2003) doi:10.1103/PhysRevD.67.083002 [arXiv:astro-ph/0301031 [astro-ph]].

[85] D. Paoletti and F. Finelli, "Constraints on primordial magnetic fields from magnetically-induced perturbations: current status and future perspectives with LiteBIRD and future ground based experiments," JCAP **11**, 028 (2019) doi:10.1088/1475-7516/2019/11/028 [arXiv:1910.07456 [astro-ph.CO]].

[86] R. Allison, P. Caucal, E. Calabrese, J. Dunkley and T. Louis, "Towards a cosmological neutrino mass detection," Phys. Rev. D **92**, no.12, 123535 (2015) doi:10.1103/PhysRevD.92.123535 [arXiv:1509.07471 [astro-ph.CO]].

[87] S. Hanany *et al.* [NASA PICO], "PICO: Probe of Inflation and Cosmic Origins," [arXiv:1902.10541 [astro-ph.IM]].

[88] J. Delabrouille, M. H. Abitbol, N. Aghanim, Y. Ali-Haïmoud, D. Alonso, M. Alvarez, A. J. Banday, J. G. Bartlett, J. Baselmans and K. Basu, *et al.* "Microwave Spectro-Polarimetry of Matter and Radiation across Space and Time," [arXiv:1909.01591 [astro-ph.CO]].

[89] Z. M. Ma, W. Hu and D. Huterer, "Effect of photometric redshift uncertainties on weak lensing tomography," Astrophys. J. **636**, 21-29 (2005) doi:10.1086/497068 [arXiv:astro-ph/0506614 [astro-ph]].

[90] J. L. Bernal, A. Raccanelli, E. D. Kovetz, D. Parkinson, R. P. Norris, G. Danforth and C. Schmitt, "Probing ΛCDM cosmology with the Evolutionary Map of the Universe survey," JCAP **02**, 030 (2019) doi:10.1088/1475-7516/2019/02/030 [arXiv:1810.06672 [astro-ph.CO]].

Este documento incorpora firma electrónica, y es copia auténtica de un documento electrónico archivado por la ULL según la Ley 39/2015.
Su autenticidad puede ser contrastada en la siguiente dirección https://sede.ull.es/validacion/

Identificador del documento: 3764923 Código de verificación: JHlWnlbn

Firmado por:	JOSE RAMON BERMEJO CLIMENT *UNIVERSIDAD DE LA LAGUNA*	Fecha: 01/09/2021 17:41:12
	José Alberto Rubiño Martín *UNIVERSIDAD DE LA LAGUNA*	01/09/2021 17:49:44
	FABIO FINELLI *UNIVERSIDAD DE LA LAGUNA*	02/09/2021 14:12:21

Universidad de La Laguna
Oficina de Sede Electrónica
Entrada
Nº registro: 2021/90989
Nº reg. oficina: OF002/2021/89977
Fecha: 03/09/2021 12:24:13

[91] R. Laureijs *et al.* [EUCLID], "Euclid Definition Study Report," [arXiv:1110.3193 [astro-ph.CO]].

[92] L. Amendola *et al.* [Euclid Theory Working Group], "Cosmology and fundamental physics with the Euclid satellite," Living Rev. Rel. **16**, 6 (2013) doi:10.12942/lrr-2013-6 [arXiv:1206.1225 [astro-ph.CO]].

[93] L. Pozzetti, C. M. Hirata, J. E. Geach, A. Cimatti, C. Baugh, O. Cucciati, A. Merson, P. Norberg and D. Shi, "Modelling the number density of Hα emitters for future spectroscopic near-IR space missions," Astron. Astrophys. **590**, A3 (2016) doi:10.1051/0004-6361/201527081 [arXiv:1603.01453 [astro-ph.GA]].

[94] A. Merson, Y. Wang, A. Benson, A. Faisst, D. Masters, A. Kiessling and J. Rhodes, "Predicting Hα emission-line galaxy counts for future galaxy redshift surveys," Mon. Not. Roy. Astron. Soc. **474**, no.1, 177-196 (2018) doi:10.1093/mnras/stx2649 [arXiv:1710.00833 [astro-ph.GA]].

[95] A. Merson, A. Smith, A. Benson, Y. Wang and C. M. Baugh, "Linear bias forecasts for emission line cosmological surveys," Mon. Not. Roy. Astron. Soc. **486**, no.4, 5737-5765 (2019) doi:10.1093/mnras/stz1204 [arXiv:1903.02030 [astro-ph.CO]].

[96] D. Alonso *et al.* [LSST Dark Energy Science], "The LSST Dark Energy Science Collaboration (DESC) Science Requirements Document," [arXiv:1809.01669 [astro-ph.CO]].

[97] O. Doré, J. Bock, P. Capak, R. de Putter, T. Eifler, C. Hirata, P. Korngut, E. Krause, D. Masters and A. Raccanelli, *et al.* "Cosmology with the SPHEREX All-Sky Spectral Survey," [arXiv:1412.4872 [astro-ph.CO]].

[98] M. Ballardini, F. Finelli, C. Fedeli and L. Moscardini, "Probing primordial features with future galaxy surveys," JCAP **10**, 041 (2016) [erratum: JCAP **04**, E01 (2018)] doi:10.1088/1475-7516/2016/10/041 [arXiv:1606.03747 [astro-ph.CO]].

[99] R. P. Norris, A. M. Hopkins, J. Afonso, S. Brown, J. J. Condon, L. Dunne, I. Feain, R. Hollow, M. Jarvis and M. Johnston-Hollitt, *et al.* "EMU: Evolutionary Map of the Universe," Publ. Astron. Soc. Austral. **28**, 215 (2011) doi:10.1071/AS11021 [arXiv:1106.3219 [astro-ph.CO]].

Este documento incorpora firma electrónica, y es copia auténtica de un documento electrónico archivado por la ULL según la Ley 39/2015.
Su autenticidad puede ser contrastada en la siguiente dirección https://sede.ull.es/validacion/

Identificador del documento: 3764923 Código de verificación: JHlWnlbn

Firmado por:	JOSE RAMON BERMEJO CLIMENT *UNIVERSIDAD DE LA LAGUNA*	Fecha: 01/09/2021 17:41:12
	José Alberto Rubiño Martín *UNIVERSIDAD DE LA LAGUNA*	01/09/2021 17:49:44
	FABIO FINELLI *UNIVERSIDAD DE LA LAGUNA*	02/09/2021 14:12:21

Universidad de La Laguna
Oficina de Sede Electrónica
Entrada
Nº registro: 2021/90989
Nº reg. oficina: OF002/2021/89977
Fecha: 03/09/2021 12:24:13

[100] D. J. Bacon *et al.* [SKA], "Cosmology with Phase 1 of the Square Kilometre Array: Red Book 2018: Technical specifications and performance forecasts," Publ. Astron. Soc. Austral. **37**, e007 (2020) doi:10.1017/pasa.2019.51 [arXiv:1811.02743 [astro-ph.CO]].

[101] M. Chevallier and D. Polarski, "Accelerating universes with scaling dark matter," Int. J. Mod. Phys. D **10**, 213-224 (2001) doi:10.1142/S0218271801000822 [arXiv:gr-qc/0009008 [gr-qc]].

[102] E. V. Linder, "Exploring the expansion history of the universe," Phys. Rev. Lett. **90**, 091301 (2003) doi:10.1103/PhysRevLett.90.091301 [arXiv:astro-ph/0208512 [astro-ph]].

[103] M. Schmittfull and U. Seljak, "Parameter constraints from cross-correlation of CMB lensing with galaxy clustering," Phys. Rev. D **97**, no.12, 123540 (2018) doi:10.1103/PhysRevD.97.123540 [arXiv:1710.09465 [astro-ph.CO]].

[104] M. LoVerde, L. Hui and E. Gaztanaga, "Magnification-Temperature Correlation: The Dark Side of ISW Measurements," Phys. Rev. D **75**, 043519 (2007) doi:10.1103/PhysRevD.75.043519 [arXiv:astro-ph/0611539 [astro-ph]].

[105] J. Asorey, M. Crocce, E. Gaztanaga and A. Lewis, "Recovering 3D clustering information with angular correlations," Mon. Not. Roy. Astron. Soc. **427**, 1891 (2012) doi:10.1111/j.1365-2966.2012.21972.x [arXiv:1207.6487 [astro-ph.CO]].

[106] A. Loureiro, B. Moraes, F. B. Abdalla, A. Cuceu, M. McLeod, L. Whiteway, S. T. Balan, A. Benoit-Lévy, O. Lahav and M. Manera, *et al.* "Cosmological measurements from angular power spectra analysis of BOSS DR12 tomography," Mon. Not. Roy. Astron. Soc. **485**, no.1, 326-355 (2019) doi:10.1093/mnras/stz191 [arXiv:1809.07204 [astro-ph.CO]].

[107] P. A. R. Ade *et al.* [Planck], "Planck 2013 results. XVII. Gravitational lensing by large-scale structure," Astron. Astrophys. **571**, A17 (2014) doi:10.1051/0004-6361/201321543 [arXiv:1303.5077 [astro-ph.CO]].

[108] J. Fonseca, S. Camera, M. Santos and R. Maartens, "Hunting down horizon-scale effects with multi-wavelength surveys," Astro-

Este documento incorpora firma electrónica, y es copia auténtica de un documento electrónico archivado por la ULL según la Ley 39/2015.
Su autenticidad puede ser contrastada en la siguiente dirección https://sede.ull.es/validacion/

Identificador del documento: 3764923 Código de verificación: JHlWnlbn

Firmado por: JOSE RAMON BERMEJO CLIMENT — Fecha: 01/09/2021 17:41:12
UNIVERSIDAD DE LA LAGUNA

José Alberto Rubiño Martín — 01/09/2021 17:49:44
UNIVERSIDAD DE LA LAGUNA

FABIO FINELLI — 02/09/2021 14:12:21
UNIVERSIDAD DE LA LAGUNA

Universidad de La Laguna
Oficina de Sede Electrónica
Entrada
Nº registro: 2021/90989
Nº reg. oficina: OF002/2021/89977
Fecha: 03/09/2021 12:24:13

phys. J. Lett. **812**, no.2, L22 (2015) doi:10.1088/2041-8205/812/2/L22 [arXiv:1507.04605 [astro-ph.CO]].

[109] D. Alonso, P. Bull, P. G. Ferreira, R. Maartens and M. Santos, "Ultra large-scale cosmology in next-generation experiments with single tracers," Astrophys. J. **814**, no.2, 145 (2015) doi:10.1088/0004-637X/814/2/145 [arXiv:1505.07596 [astro-ph.CO]].

[110] B. Jain and A. Taylor, "Cross-correlation tomography: measuring dark energy evolution with weak lensing," Phys. Rev. Lett. **91**, 141302 (2003) doi:10.1103/PhysRevLett.91.141302 [arXiv:astro-ph/0306046 [astro-ph]].

[111] G. M. Bernstein and B. Jain, "Dark energy constraints from weak lensing cross - correlation cosmography," Astrophys. J. **600**, 17-25 (2004) doi:10.1086/379768 [arXiv:astro-ph/0309332 [astro-ph]].

[112] J. Zhang, L. Hui and A. Stebbins, "Isolating geometry in weak lensing measurements," Astrophys. J. **635**, 806-820 (2005) doi:10.1086/497676 [arXiv:astro-ph/0312348 [astro-ph]].

[113] G. Bernstein, "Metric tests for curvature from weak lensing and baryon acoustic oscillations," Astrophys. J. **637**, 598-607 (2006) doi:10.1086/498079 [arXiv:astro-ph/0503276 [astro-ph]].

[114] W. Hu, D. E. Holz and C. Vale, "CMB Cluster Lensing: Cosmography with the Longest Lever Arm," Phys. Rev. D **76**, 127301 (2007) doi:10.1103/PhysRevD.76.127301 [arXiv:0708.4391 [astro-ph]].

[115] S. Das and D. N. Spergel, "Measuring Distance Ratios with CMB-Galaxy Lensing Cross-correlations," Phys. Rev. D **79**, 043509 (2009) doi:10.1103/PhysRevD.79.043509 [arXiv:0810.3931 [astro-ph]].

[116] P. Ade *et al.* [Simons Observatory], "The Simons Observatory: Science goals and forecasts," JCAP **02**, 056 (2019) doi:10.1088/1475-7516/2019/02/056 [arXiv:1808.07445 [astro-ph.CO]].

[117] J. Prat *et al.* [DES and SPT], "Cosmological lensing ratios with DES Y1, SPT and Planck," Mon. Not. Roy. Astron. Soc. **487**, no.1, 1363-1379 (2019) doi:10.1093/mnras/stz1309 [arXiv:1810.02212 [astro-ph.CO]].

Este documento incorpora firma electrónica, y es copia auténtica de un documento electrónico archivado por la ULL según la Ley 39/2015.
Su autenticidad puede ser contrastada en la siguiente dirección https://sede.ull.es/validacion/

Identificador del documento: 3764923 Código de verificación: JHlWnlbn

Firmado por:	JOSE RAMON BERMEJO CLIMENT *UNIVERSIDAD DE LA LAGUNA*	Fecha: 01/09/2021 17:41:12
	José Alberto Rubiño Martín *UNIVERSIDAD DE LA LAGUNA*	01/09/2021 17:49:44
	FABIO FINELLI *UNIVERSIDAD DE LA LAGUNA*	02/09/2021 14:12:21

Universidad de La Laguna
Oficina de Sede Electrónica
Entrada
Nº registro: 2021/90989
Nº reg. oficina: OF002/2021/89977
Fecha: 03/09/2021 12:24:13

[118] H. Miyatake, M. S. Madhavacheril, N. Sehgal, A. Slosar, D. N. Spergel, B. Sherwin and A. van Engelen, "Measurement of a Cosmographic Distance Ratio with Galaxy and Cosmic Microwave Background Lensing," Phys. Rev. Lett. **118**, no.16, 161301 (2017) doi:10.1103/PhysRevLett.118.161301 [arXiv:1605.05337 [astro-ph.CO]].

[119] M. White, M. Blanton, A. Bolton, D. Schlegel, J. Tinker, A. Berlind, L. da Costa, E. Kazin, Y. T. Lin and M. Maia, *et al.* "The clustering of massive galaxies at z˜0.5 from the first semester of BOSS data," Astrophys. J. **728**, 126 (2011) doi:10.1088/0004-637X/728/2/126 [arXiv:1010.4915 [astro-ph.CO]].

[120] T. Erben, H. Hildebrandt, L. Miller, L. van Waerbeke, C. Heymans, H. Hoekstra, T. D. Kitching, Y. Mellier, J. Benjamin and C. Blake, *et al.* "CFHTLenS: The Canada-France-Hawaii Telescope Lensing Survey - Imaging Data and Catalogue Products," Mon. Not. Roy. Astron. Soc. **433**, 2545 (2013) doi:10.1093/mnras/stt928 [arXiv:1210.8156 [astro-ph.CO]].

[121] P. A. R. Ade *et al.* [Planck], "Planck 2015 results. XV. Gravitational lensing," Astron. Astrophys. **594**, A15 (2016) doi:10.1051/0004-6361/201525941 [arXiv:1502.01591 [astro-ph.CO]].

[122] T. M. C. Abbott *et al.* [DES], "Dark Energy Survey year 1 results: Cosmological constraints from galaxy clustering and weak lensing," Phys. Rev. D **98**, no.4, 043526 (2018) doi:10.1103/PhysRevD.98.043526 [arXiv:1708.01530 [astro-ph.CO]].

[123] Y. Omori, R. Chown, G. Simard, K. T. Story, K. Aylor, E. J. Baxter, B. A. Benson, L. E. Bleem, J. E. Carlstrom and C. L. Chang, *et al.* "A 2500 deg^2 CMB Lensing Map from Combined South Pole Telescope and Planck Data," Astrophys. J. **849**, no.2, 124 (2017) doi:10.3847/1538-4357/aa8d1d [arXiv:1705.00743 [astro-ph.CO]].

[124] A. Aghamousa *et al.* [DESI], "The DESI Experiment Part I: Science,Targeting, and Survey Design," [arXiv:1611.00036 [astro-ph.IM]].

[125] D. Blas, J. Lesgourgues and T. Tram, "The Cosmic Linear Anisotropy Solving System (CLASS) II: Approximation schemes," JCAP **07**, 034 (2011) doi:10.1088/1475-7516/2011/07/034 [arXiv:1104.2933 [astro-ph.CO]].

Este documento incorpora firma electrónica, y es copia auténtica de un documento electrónico archivado por la ULL según la Ley 39/2015.
Su autenticidad puede ser contrastada en la siguiente dirección https://sede.ull.es/validacion/

Identificador del documento: 3764923 Código de verificación: JHlWnlbn

Firmado por: JOSE RAMON BERMEJO CLIMENT — Fecha: 01/09/2021 17:41:12
UNIVERSIDAD DE LA LAGUNA

José Alberto Rubiño Martín — 01/09/2021 17:49:44
UNIVERSIDAD DE LA LAGUNA

FABIO FINELLI — 02/09/2021 14:12:21
UNIVERSIDAD DE LA LAGUNA

Universidad de La Laguna
Oficina de Sede Electrónica
Entrada
Nº registro: 2021/90989
Nº reg. oficina: OF002/2021/89977
Fecha: 03/09/2021 12:24:13

[126] E. Di Dio, F. Montanari, J. Lesgourgues and R. Durrer, "The CLASSgal code for Relativistic Cosmological Large Scale Structure," JCAP **11**, 044 (2013) doi:10.1088/1475-7516/2013/11/044 [arXiv:1307.1459 [astro-ph.CO]].

[127] N. Aghanim *et al.* [Planck], "Planck 2018 results. I. Overview and the cosmological legacy of Planck," Astron. Astrophys. **641**, A1 (2020) doi:10.1051/0004-6361/201833880 [arXiv:1807.06205 [astro-ph.CO]].

[128] D. N. Limber, "The Analysis of Counts of the Extragalactic Nebulae in Terms of a Fluctuating Density Field. II," Astrophys. J. **119**, 655 (1954) doi:10.1086/145870

[129] M. Ballardini and R. Maartens, "Measuring ISW with next-generation radio surveys," Mon. Not. Roy. Astron. Soc. **485**, 1339 (2019) doi:10.1093/mnras/stz480 [arXiv:1812.01636 [astro-ph.CO]].

[130] A. Pourtsidou, D. Bacon and R. Crittenden, "Cross-correlation cosmography with intensity mapping of the neutral hydrogen 21 cm emission," Phys. Rev. D **92**, no.10, 103506 (2015) doi:10.1103/PhysRevD.92.103506 [arXiv:1506.02615 [astro-ph.CO]].

[131] G. Jungman, M. Kamionkowski, A. Kosowsky and D. N. Spergel, "Cosmological parameter determination with microwave background maps," Phys. Rev. D **54**, 1332-1344 (1996) doi:10.1103/PhysRevD.54.1332 [arXiv:astro-ph/9512139 [astro-ph]].

[132] D. J. Eisenstein, W. Hu and M. Tegmark, "Cosmic complementarity: Joint parameter estimation from CMB experiments and redshift surveys," Astrophys. J. **518**, 2-23 (1999) doi:10.1086/307261 [arXiv:astro-ph/9807130 [astro-ph]].

[133] T. D. Kitching, A. Amara, F. B. Abdalla, B. Joachimi and A. Refregier, "Cosmological Systematics Beyond Nuisance Parameters : Form Filling Functions," Mon. Not. Roy. Astron. Soc. **399**, 2107 (2009) doi:10.1111/j.1365-2966.2009.15408.x [arXiv:0812.1966 [astro-ph]].

[134] E. Di Valentino, A. Melchiorri and J. Silk, "Reconciling Planck with the local value of H_0 in extended parameter space," Phys. Lett. B **761**, 242-246 (2016) doi:10.1016/j.physletb.2016.08.043 [arXiv:1606.00634 [astro-ph.CO]].

Este documento incorpora firma electrónica, y es copia auténtica de un documento electrónico archivado por la ULL según la Ley 39/2015.
Su autenticidad puede ser contrastada en la siguiente dirección https://sede.ull.es/validacion/

Identificador del documento: 3764923 Código de verificación: JHlWnlbn

Firmado por:	JOSE RAMON BERMEJO CLIMENT *UNIVERSIDAD DE LA LAGUNA*	Fecha: 01/09/2021 17:41:12
	José Alberto Rubiño Martín *UNIVERSIDAD DE LA LAGUNA*	01/09/2021 17:49:44
	FABIO FINELLI *UNIVERSIDAD DE LA LAGUNA*	02/09/2021 14:12:21

Universidad de La Laguna
Oficina de Sede Electrónica
Entrada
Nº registro: 2021/90989
Nº reg. oficina: OF002/2021/89977
Fecha: 03/09/2021 12:24:13

[135] S. Ilić *et al.* [Euclid], "*Euclid* preparation: XV. Forecasting cosmological constraints for the *Euclid* and CMB joint analysis," [arXiv:2106.08346 [astro-ph.CO]].

[136] T. Baldauf, M. Mirbabayi, M. Simonović and M. Zaldarriaga, "LSS constraints with controlled theoretical uncertainties," [arXiv:1602.00674 [astro-ph.CO]].

[137] M. Tegmark, A. Taylor and A. Heavens, "Karhunen-Loeve eigenvalue problems in cosmology: How should we tackle large data sets?," Astrophys. J. **480**, 22 (1997) doi:10.1086/303939 [arXiv:astro-ph/9603021 [astro-ph]].

[138] J. Errard, S. M. Feeney, H. V. Peiris and A. H. Jaffe, "Robust forecasts on fundamental physics from the foreground-obscured, gravitationally-lensed CMB polarization," JCAP **03**, 052 (2016) doi:10.1088/1475-7516/2016/03/052 [arXiv:1509.06770 [astro-ph.CO]].

[139] N. Dalal, O. Dore, D. Huterer and A. Shirokov, "The imprints of primordial non-gaussianities on large-scale structure: scale dependent bias and abundance of virialized objects," Phys. Rev. D **77**, 123514 (2008) doi:10.1103/PhysRevD.77.123514 [arXiv:0710.4560 [astro-ph]].

[140] S. Matarrese and L. Verde, "The effect of primordial non-Gaussianity on halo bias," Astrophys. J. Lett. **677**, L77-L80 (2008) doi:10.1086/587840 [arXiv:0801.4826 [astro-ph]].

[141] J. E. Gunn and J. R. Gott, III, "On the Infall of Matter into Clusters of Galaxies and Some Effects on Their Evolution," Astrophys. J. **176**, 1-19 (1972) doi:10.1086/151605

[142] D. J. Eisenstein and W. Hu, "Power spectra for cold dark matter and its variants," Astrophys. J. **511**, 5 (1997) doi:10.1086/306640 [arXiv:astro-ph/9710252 [astro-ph]].

[143] A. Alarcon, M. Eriksen and E. Gaztañaga, "Cosmological constraints from multiple tracers in spectroscopic surveys," Mon. Not. Roy. Astron. Soc. **473**, no.2, 1444-1460 (2018) doi:10.1093/mnras/stx2446 [arXiv:1609.08510 [astro-ph.CO]].

[144] D. Alonso, E. Bellini, P. G. Ferreira and M. Zumalacárregui, "Observational future of cosmological scalar-tensor theories," Phys.

Este documento incorpora firma electrónica, y es copia auténtica de un documento electrónico archivado por la ULL según la Ley 39/2015.
Su autenticidad puede ser contrastada en la siguiente dirección https://sede.ull.es/validacion/

Identificador del documento: 3764923 Código de verificación: JHlWnlbn

Firmado por:	JOSE RAMON BERMEJO CLIMENT *UNIVERSIDAD DE LA LAGUNA*	Fecha: 01/09/2021 17:41:12
	José Alberto Rubiño Martín *UNIVERSIDAD DE LA LAGUNA*	01/09/2021 17:49:44
	FABIO FINELLI *UNIVERSIDAD DE LA LAGUNA*	02/09/2021 14:12:21

Universidad de La Laguna
Oficina de Sede Electrónica
Entrada
Nº registro: 2021/90989
Nº reg. oficina: OF002/2021/89977
Fecha: 03/09/2021 12:24:13

Rev. D **95**, no.6, 063502 (2017) doi:10.1103/PhysRevD.95.063502 [arXiv:1610.09290 [astro-ph.CO]].

[145] E. Di Valentino *et al.* [CORE], "Exploring cosmic origins with CORE: Cosmological parameters," JCAP **04**, 017 (2018) doi:10.1088/1475-7516/2018/04/017 [arXiv:1612.00021 [astro-ph.CO]].

[146] R. Pearson and O. Zahn, "Cosmology from cross correlation of CMB lensing and galaxy surveys," Phys. Rev. D **89**, no.4, 043516 (2014) doi:10.1103/PhysRevD.89.043516 [arXiv:1311.0905 [astro-ph.CO]].

[147] J. B. Muñoz, E. D. Kovetz, A. Raccanelli, M. Kamionkowski and J. Silk, "Towards a measurement of the spectral runnings," JCAP **05**, 032 (2017) doi:10.1088/1475-7516/2017/05/032 [arXiv:1611.05883 [astro-ph.CO]].

[148] S. Hannestad, "Neutrino masses and the dark energy equation of state - Relaxing the cosmological neutrino mass bound," Phys. Rev. Lett. **95**, 221301 (2005) doi:10.1103/PhysRevLett.95.221301 [arXiv:astro-ph/0505551 [astro-ph]].

[149] S. Vagnozzi, E. Giusarma, O. Mena, K. Freese, M. Gerbino, S. Ho and M. Lattanzi, "Unveiling ν secrets with cosmological data: neutrino masses and mass hierarchy," Phys. Rev. D **96**, no.12, 123503 (2017) doi:10.1103/PhysRevD.96.123503 [arXiv:1701.08172 [astro-ph.CO]].

[150] S. Roy Choudhury and S. Hannestad, "Updated results on neutrino mass and mass hierarchy from cosmology with Planck 2018 likelihoods," JCAP **07**, 037 (2020) doi:10.1088/1475-7516/2020/07/037 [arXiv:1907.12598 [astro-ph.CO]].

[151] M. Ballardini, M. Braglia, F. Finelli, D. Paoletti, A. A. Starobinsky and C. Umiltà, "Scalar-tensor theories of gravity, neutrino physics, and the H_0 tension," JCAP **10**, 044 (2020) doi:10.1088/1475-7516/2020/10/044 [arXiv:2004.14349 [astro-ph.CO]].

[152] J. Delabrouille *et al.* [CORE], "Exploring cosmic origins with CORE: Survey requirements and mission design," JCAP **04**, 014 (2018) doi:10.1088/1475-7516/2018/04/014 [arXiv:1706.04516 [astro-ph.IM]].

[153] P. de Bernardis *et al.* [CORE], "Exploring cosmic origins with CORE: The instrument," JCAP **04**, 015 (2018) doi:10.1088/1475-7516/2018/04/015 [arXiv:1705.02170 [astro-ph.IM]].

Este documento incorpora firma electrónica, y es copia auténtica de un documento electrónico archivado por la ULL según la Ley 39/2015.
Su autenticidad puede ser contrastada en la siguiente dirección https://sede.ull.es/validacion/

Identificador del documento: 3764923 Código de verificación: JHlWnlbn

Firmado por:	JOSE RAMON BERMEJO CLIMENT *UNIVERSIDAD DE LA LAGUNA*	Fecha: 01/09/2021 17:41:12
	José Alberto Rubiño Martín *UNIVERSIDAD DE LA LAGUNA*	01/09/2021 17:49:44
	FABIO FINELLI *UNIVERSIDAD DE LA LAGUNA*	02/09/2021 14:12:21

Universidad de La Laguna
Oficina de Sede Electrónica
Entrada
Nº registro: 2021/90989
Nº reg. oficina: OF002/2021/89977
Fecha: 03/09/2021 12:24:13

[154] S. Hanany *et al.* [NASA PICO], "PICO: Probe of Inflation and Cosmic Origins," [arXiv:1902.10541 [astro-ph.IM]].

[155] J. Delabrouille, M. H. Abitbol, N. Aghanim, Y. Ali-Haïmoud, D. Alonso, M. Alvarez, A. J. Banday, J. G. Bartlett, J. Baselmans and K. Basu, *et al.* "Microwave Spectro-Polarimetry of Matter and Radiation across Space and Time," [arXiv:1909.01591 [astro-ph.CO]].

[156] M. Ballardini, F. Finelli, R. Maartens and L. Moscardini, "Probing primordial features with next-generation photometric and radio surveys," JCAP **04**, 044 (2018) doi:10.1088/1475-7516/2018/04/044 [arXiv:1712.07425 [astro-ph.CO]].

[157] Z. Vlah, U. Seljak, M. Y. Chu and Y. Feng, "Perturbation theory, effective field theory, and oscillations in the power spectrum," JCAP **03**, 057 (2016) doi:10.1088/1475-7516/2016/03/057 [arXiv:1509.02120 [astro-ph.CO]].

[158] F. Beutler, M. Biagetti, D. Green, A. Slosar and B. Wallisch, "Primordial Features from Linear to Nonlinear Scales," Phys. Rev. Res. **1**, no.3, 033209 (2019) doi:10.1103/PhysRevResearch.1.033209 [arXiv:1906.08758 [astro-ph.CO]].

[159] M. Ballardini, R. Murgia, M. Baldi, F. Finelli and M. Viel, "Nonlinear damping of superimposed primordial oscillations on the matter power spectrum in galaxy surveys," JCAP **04**, no.04, 030 (2020) doi:10.1088/1475-7516/2020/04/030 [arXiv:1912.12499 [astro-ph.CO]].

[160] C. R. Contaldi, M. Peloso, L. Kofman and A. D. Linde, "Suppressing the lower multipoles in the CMB anisotropies," JCAP **07**, 002 (2003) doi:10.1088/1475-7516/2003/07/002 [arXiv:astro-ph/0303636 [astro-ph]].

[161] P. A. R. Ade *et al.* [Planck], "Planck 2015 results. XX. Constraints on inflation," Astron. Astrophys. **594**, A20 (2016) doi:10.1051/0004-6361/201525898 [arXiv:1502.02114 [astro-ph.CO]].

[162] A. A. Starobinsky, "Spectrum of adiabatic perturbations in the universe when there are singularities in the inflation potential," JETP Lett. **55**, 489-494 (1992)

Este documento incorpora firma electrónica, y es copia auténtica de un documento electrónico archivado por la ULL según la Ley 39/2015.
Su autenticidad puede ser contrastada en la siguiente dirección https://sede.ull.es/validacion/

Identificador del documento: 3764923 Código de verificación: JHlWnlbn

Firmado por:	JOSE RAMON BERMEJO CLIMENT *UNIVERSIDAD DE LA LAGUNA*	Fecha: 01/09/2021 17:41:12
	José Alberto Rubiño Martín *UNIVERSIDAD DE LA LAGUNA*	01/09/2021 17:49:44
	FABIO FINELLI *UNIVERSIDAD DE LA LAGUNA*	02/09/2021 14:12:21

Universidad de La Laguna
Oficina de Sede Electrónica
Entrada
Nº registro: 2021/90989
Nº reg. oficina: OF002/2021/89977
Fecha: 03/09/2021 12:24:13

[163] J. A. Adams, B. Cresswell and R. Easther, "Inflationary perturbations from a potential with a step," Phys. Rev. D **64**, 123514 (2001) doi:10.1103/PhysRevD.64.123514 [arXiv:astro-ph/0102236 [astro-ph]].

[164] C. Dvorkin and W. Hu, "Generalized Slow Roll for Large Power Spectrum Features," Phys. Rev. D **81**, 023518 (2010) doi:10.1103/PhysRevD.81.023518 [arXiv:0910.2237 [astro-ph.CO]].

[165] V. Miranda and W. Hu, "Inflationary Steps in the Planck Data," Phys. Rev. D **89**, no.8, 083529 (2014) doi:10.1103/PhysRevD.89.083529 [arXiv:1312.0946 [astro-ph.CO]].

[166] Y. Akrami *et al.* [Planck], "Planck 2018 results. X. Constraints on inflation," Astron. Astrophys. **641**, A10 (2020) doi:10.1051/0004-6361/201833887 [arXiv:1807.06211 [astro-ph.CO]].

[167] R. Flauger, L. McAllister, E. Pajer, A. Westphal and G. Xu, "Oscillations in the CMB from Axion Monodromy Inflation," JCAP **06**, 009 (2010) doi:10.1088/1475-7516/2010/06/009 [arXiv:0907.2916 [hep-th]].

[168] J. Martin and R. Brandenberger, "On the dependence of the spectra of fluctuations in inflationary cosmology on transPlanckian physics," Phys. Rev. D **68**, 063513 (2003) doi:10.1103/PhysRevD.68.063513 [arXiv:hep-th/0305161 [hep-th]].

[169] R. Flauger, L. McAllister, E. Silverstein and A. Westphal, "Drifting Oscillations in Axion Monodromy," JCAP **10**, 055 (2017) doi:10.1088/1475-7516/2017/10/055 [arXiv:1412.1814 [hep-th]].

[170] M. LoVerde, "Halo bias in mixed dark matter cosmologies," Phys. Rev. D **90**, no.8, 083530 (2014) doi:10.1103/PhysRevD.90.083530 [arXiv:1405.4855 [astro-ph.CO]].

[171] A. Raccanelli, L. Verde and F. Villaescusa-Navarro, "Biases from neutrino bias: to worry or not to worry?," Mon. Not. Roy. Astron. Soc. **483**, no.1, 734-743 (2019) doi:10.1093/mnras/sty2162 [arXiv:1704.07837 [astro-ph.CO]].

[172] S. Vagnozzi, T. Brinckmann, M. Archidiacono, K. Freese, M. Gerbino, J. Lesgourgues and T. Sprenger, "Bias due to neutrinos must not uncorrect'd go," JCAP **09**, 001 (2018) doi:10.1088/1475-7516/2018/09/001 [arXiv:1807.04672 [astro-ph.CO]].

Este documento incorpora firma electrónica, y es copia auténtica de un documento electrónico archivado por la ULL según la Ley 39/2015.
Su autenticidad puede ser contrastada en la siguiente dirección https://sede.ull.es/validacion/

Identificador del documento: 3764923 Código de verificación: JHlWnlbn

Firmado por:	JOSE RAMON BERMEJO CLIMENT *UNIVERSIDAD DE LA LAGUNA*	Fecha: 01/09/2021 17:41:12
	José Alberto Rubiño Martín *UNIVERSIDAD DE LA LAGUNA*	01/09/2021 17:49:44
	FABIO FINELLI *UNIVERSIDAD DE LA LAGUNA*	02/09/2021 14:12:21

Universidad de La Laguna
Oficina de Sede Electrónica
Entrada
Nº registro: 2021/90989
Nº reg. oficina: OF002/2021/89977
Fecha: 03/09/2021 12:24:13

[173] C. T. Chiang, M. LoVerde and F. Villaescusa-Navarro, "First detection of scale-dependent linear halo bias in N-body simulations with massive neutrinos," Phys. Rev. Lett. **122**, no.4, 041302 (2019) doi:10.1103/PhysRevLett.122.041302 [arXiv:1811.12412 [astro-ph.CO]].

[174] J. Lesgourgues and S. Pastor, "Massive neutrinos and cosmology," Phys. Rept. **429**, 307-379 (2006) doi:10.1016/j.physrep.2006.04.001 [arXiv:astro-ph/0603494 [astro-ph]].

[175] K. Tanidis and S. Camera, "Developing a unified pipeline for large-scale structure data analysis with angular power spectra – III. Implementing the multitracer technique to constrain neutrino masses," Mon. Not. Roy. Astron. Soc. **502**, no.2, 2952-2960 (2021) doi:10.1093/mnras/staa3536 [arXiv:2009.05584 [astro-ph.CO]].

[176] A. Blanchard *et al.* [Euclid], "Euclid preparation: VII. Forecast validation for Euclid cosmological probes," Astron. Astrophys. **642**, A191 (2020) doi:10.1051/0004-6361/202038071 [arXiv:1910.09273 [astro-ph.CO]].

[177] I. Tutusaus *et al.* [EUCLID], "*Euclid*: The importance of galaxy clustering and weak lensing cross-correlations within the photometric *Euclid* survey," Astron. Astrophys. **643**, A70 (2020) doi:10.1051/0004-6361/202038313 [arXiv:2005.00055 [astro-ph.CO]].

Este documento incorpora firma electrónica, y es copia auténtica de un documento electrónico archivado por la ULL según la Ley 39/2015.
Su autenticidad puede ser contrastada en la siguiente dirección https://sede.ull.es/validacion/

Identificador del documento: 3764923 Código de verificación: JHlWnlbn

Firmado por:	JOSE RAMON BERMEJO CLIMENT *UNIVERSIDAD DE LA LAGUNA*	Fecha: 01/09/2021 17:41:12
	José Alberto Rubiño Martín *UNIVERSIDAD DE LA LAGUNA*	01/09/2021 17:49:44
	FABIO FINELLI *UNIVERSIDAD DE LA LAGUNA*	02/09/2021 14:12:21

Universidad de La Laguna
Oficina de Sede Electrónica
Entrada
Nº registro: 2021/90989
Nº reg. oficina: OF002/2021/89977
Fecha: 03/09/2021 12:24:13

Acknowledgements

I gratefully acknowledge the financial support from an INAF fellowship under the international agreement with IAC.

This thesis would not have been possible without the collaboration of many people.

First of all, I would like to thank my advisors. To Fabio, for proposing this thesis and having been always available for discussing, proposing new ideas and in general being the main support for beginning my scientific career. Thanks also for your help in all the non academic stuff. To Alberto, for being the link with La Laguna during this years and having collaborated a lot to the final shape of this thesis.

I would like also to acknowledge Mario, who has worked close to me during these four years, becoming almost another advisor of this thesis. It has been a pleasure to work with you, developing all these projects without your help would not have been the same. Thank you also for hosting me in Cape Town and giving me a beautiful tour of the city.

During this years, working at INAF OAS Bologna, I have coincided with other people that have collaborated to this thesis. An acknowledgment goes to Dhiraj, which has closely worked with me in some projects; and to Daniela, who has supported as well some of my works. Thanks also to Matteo, who has been my office mate for almost the whole PhD, in particular for collaborating to our feeding with many kilograms of Parmiggiano.

An acknowledgement goes also to those people from other institutions that have collaborated directly with my work, in particular to Vincenzo Cardone, who was very helpful recieving me in Rome. Thanks also to Roy Maartens for meeting me in South Africa and for the useful discussions.

In the personal plane, I have to thank my family for having always

Este documento incorpora firma electrónica, y es copia auténtica de un documento electrónico archivado por la ULL según la Ley 39/2015.
Su autenticidad puede ser contrastada en la siguiente dirección https://sede.ull.es/validacion/

Identificador del documento: 3764923 Código de verificación: JHlWnlbn

Firmado por:	JOSE RAMON BERMEJO CLIMENT *UNIVERSIDAD DE LA LAGUNA*	Fecha: 01/09/2021 17:41:12
	José Alberto Rubiño Martín *UNIVERSIDAD DE LA LAGUNA*	01/09/2021 17:49:44
	FABIO FINELLI *UNIVERSIDAD DE LA LAGUNA*	02/09/2021 14:12:21

Universidad de La Laguna
Oficina de Sede Electrónica
Entrada
Nº registro: 2021/90989
Nº reg. oficina: OF002/2021/89977
Fecha: 03/09/2021 12:24:13

supported my academic career. Further, being this four years in Bologna marks an epoch of my life, in which I have met many friends that have made much easier my period here. I have to thank specially Alex, during your two years here we consolidated a good friendship that started in Tenerife. Also a special thank goes to Teo for becoming my main partner of Bologna's social life, for showing me the deepest places of Poland the year you were there, etc. This years I have also met people that have been always a support, even with a pandemic in the middle. A big thank to Xavi, Jorge and Javi for the classic barbecues in your terrace and for many trips around the country. Thanks also to Dani, Cristian, Cynthia, Francesco, Ivana, Paula, Miguel, Gosia, Sara, Fabio, Silvia, Jesús... and many others that I might be forgetting right now but you know you have been important for me.

Este documento incorpora firma electrónica, y es copia auténtica de un documento electrónico archivado por la ULL según la Ley 39/2015.
Su autenticidad puede ser contrastada en la siguiente dirección https://sede.ull.es/validacion/

Identificador del documento: 3764923 Código de verificación: JHlWnlbn

Firmado por:	JOSE RAMON BERMEJO CLIMENT *UNIVERSIDAD DE LA LAGUNA*	Fecha: 01/09/2021 17:41:12
	José Alberto Rubiño Martín *UNIVERSIDAD DE LA LAGUNA*	01/09/2021 17:49:44
	FABIO FINELLI *UNIVERSIDAD DE LA LAGUNA*	02/09/2021 14:12:21